# Mechanisms of Longevity Regulation and Extension in Yeast and Mechanisms Underlying the Anti-Tumor Effect of Lithocholic Acid in Human Neuroblastoma Cells

Alexander A. Goldberg

A Thesis

in

The Department

of

Biology

Presented in Partial Fulfillment of the Requirements

For the Degree of Doctor of Philosophy at

Concordia University

Montreal, Quebec, Canada

June 2011

**CONCORDIA UNIVERSITY**

**SCHOOL OF GRADUATE STUDIES**

This is to certify that the thesis prepared

By: **Alexander A. Goldberg**

Entitled: **Mechanisms of Longevity Regulation and Extension in Yeast and Mechanisms Underlying the Anti-Tumor Effect of Lithocholic Acid in Human Neuroblastoma Cells**

and submitted in partial fulfillment of the requirements for the degree of

DOCTOR OF PHILOSOPHY (Biology)

complies with the regulations of the University and meets the accepted standards with respect to originality and quality.

Signed by the final examining committee:

Dr. A. Chapman Chair

Dr. D. Thomas External Examiner

Dr. R. Michel Examiner

Dr. C. Bachewich Examiner

Dr. R. Storms Examiner

Dr. V. Titorenko Thesis Supervisor

Approved by Dr. S. Dayanandan
Chair of Department or Graduate Program Director

June 3rd, 2011 Dr. B. Lewis
Dean of Faculty

## ABSTRACT

Mechanisms of Longevity Regulation and Extension in Yeast and Mechanisms Underlying the Anti-Tumor Effect of Lithocholic Acid in Human Neuroblastoma Cells

Alexander A. Goldberg, Ph.D.

Aging of multicellular and unicellular eukaryotic organisms is a multifactorial biological phenomenon that has various causes and affects a plethora of cellular activities. I employ the yeast *Saccharomyces cerevisiae* as a model to study the basic biology and molecular mechanisms of cellular aging in multicellular eukaryotes. The use of this budding yeast as an advantageous model organism in aging research greatly contributed to the current understanding of the molecular and cellular mechanisms underlying longevity regulation in evolutionarily distant eukaryotic organisms, thereby convincingly demonstrating that longevity signaling pathways and mechanisms of their modulation by dietary and pharmacological interventions are conserved across phyla.

To address the inherent complexity of aging from a systems perspective and to build an integrative spatiotemporal model of aging process, I investigated the effect of caloric restriction (CR), a low-calorie dietary regimen, on the metabolic history of chronologically aging yeast. CR has been shown not only to exhibit a robust longevity-extending effect in evolutionarily distant organisms ranging from yeast to rhesus monkeys, but also to improve health by attenuating age-related pathologies and delaying the onset of age-related diseases across phyla. I examined how CR influences the age-related dynamics of changes in the intracellular levels of numerous proteins and

metabolites, carbohydrate metabolism, interorganellar metabolic flow, concentration of reactive oxygen species (ROS), mitochondrial morphology, essential oxidation-reduction processes in mitochondria, mitochondrial proteome, frequency of mitochondrial DNA mutations, dynamics of mitochondrial nucleoid, susceptibility to mitochondria-controlled apoptosis, and stress resistance.

Based on my comparison of the metabolic histories of long-lived CR yeast and short-lived non-CR yeast, I concluded that yeast define their long-term viability by designing a diet-specific pattern of metabolism and organelle dynamics prior to reproductive maturation. My data imply that longevity in chronologically aging yeast is programmed by the level of metabolic capacity and organelle organization they developed, in a diet-specific fashion, prior to entry into a non-proliferative state. Therefore, chronological aging in yeast is the final step of a developmental program progressing through a series of checkpoints.

I designed a chemical genetic screen for small molecules that increase the chronological life span (CLS) of yeast under CR by targeting lipid metabolism and modulating housekeeping longevity pathways that regulate longevity irrespective of the number of available calories. My screen identifies lithocholic acid (LCA) as one of such molecules. My evaluation of the life-extending efficacy of LCA in wild-type (WT) strain on a high- or low-calorie diet revealed that this compound extends yeast CLS irrespective of the number of available calories. I found that the extent to which LCA extends longevity is highest under CR conditions, when the pro-aging processes modulated by the adaptable target of rapamycin (TOR) and cAMP/protein kinase A (cAMP/PKA) signaling pathways are suppressed and the anti-aging processes are activated. Furthermore, the life-

extending efficacy of LCA in CR yeast significantly exceeded that in yeast on a high-calorie diet, in which the adaptable TOR and cAMP/PKA pathways greatly activate the pro-aging processes and suppress the anti-aging processes. Altogether, my findings suggest that, consistent with its sought-after effect on a longevity signaling network, LCA mostly targets certain housekeeping longevity assurance pathways that do not overlap (or only partially overlap) with the adaptable TOR and cAMP/PKA pathways modulated by calorie availability.

Consistent with my assumption that LCA extends longevity not by modulating the adaptable TOR pathway, I found that lack of Tor1p does not impair the life-extending efficacy of LCA under CR. I also revealed that, LCA extends longevity of the *tor1Δ* mutant strain to a very similar degree under CR and non-CR conditions. Thus, by eliminating a master regulator of this key adaptable pathway that shortens the CLS of yeast on a high-calorie diet, the *tor1Δ* mutation abolished the dependence of the anti-aging efficacy of LCA on the number of available calories.

My findings revealed two mechanisms underlying the life-extending effect of LCA in chronologically aging yeast. One mechanism operates in a calorie availability-independent fashion and involves the LCA-governed modulation of housekeeping longevity assurance pathways that do not overlap with the adaptable TOR and cAMP/PKA pathways. The other mechanism extends yeast longevity under non-CR conditions and consists in LCA-driven unmasking of the previously unknown anti-aging potential of PKA. I provide evidence that LCA modulates housekeeping longevity assurance pathways by 1) attenuating mitochondrial fragmentation, a hallmark event of age-related cell death; 2) altering oxidation-reduction processes in mitochondria,

including oxygen consumption, the maintenance of membrane potential, and reactive oxygen species production; 3) enhancing resistance to oxidative and thermal stresses; 4) suppressing mitochondria-controlled apoptosis; and 5) enhancing stability of nuclear and mitochondrial DNA.

Yeast do not synthesize LCA or any other bile acids produced by mammals. Therefore, I propose that bile acids released into the environment by mammals may act as interspecies chemical signals providing longevity benefits to yeast and, perhaps, other species within an ecosystem. I hypothesize that, because bile acids are known to be mildly toxic compounds, they may create selective pressure for the evolution of yeast species that can respond to the bile acids-induced mild cellular damage by developing the most efficient stress protective mechanisms. It is likely that such mechanisms may provide effective protection of yeast against molecular and cellular damage accumulated with age. Thus, I propose that yeast species that have been selected for the most effective mechanisms providing protection against bile acids may evolve the most effective anti-aging mechanisms that are sensitive to regulation by bile acids. I extend my hypothesis on longevity regulation by bile acids by suggesting a hypothesis of the xenohormetic, hormetic and cytostatic selective forces driving the evolution of longevity regulation mechanisms at the ecosystemic level.

To verify my hypothesis empirically, I carried out the LCA-driven multistep selection of long-lived yeast species under laboratory conditions. I found that a lasting exposure of wild-type yeast to LCA results in selection of yeast species that live longer in the absence of this bile acid than their ancestor. My data enabled to rank different

concentrations of LCA with respect to the efficiency with which they cause the appearance of long-lived yeast species.

Aging is one of the major risk factors in the onset and incidence of cancer, and cancer is considered as one of the numerous age-associated diseases whose onset can be delayed and incidence reduced by anti-aging interventions. The interplay between aging and cancer is intricate as these two complex and dynamic biological phenomena have both convergent and divergent underlying mechanisms. One of the major objectives of my thesis was to examine if LCA, a novel anti-aging compound that I identified in a high-throughput chemical genetic screen, also exhibits an anti-tumor effect in cultured human cancer cells by activating certain anti-cancer processes that may (or may not) play an essential role in cellular aging. As a model system for addressing this important question (and if LCA indeed displays an anti-tumor effect, for establishing the mechanism underlying such effect), I choose several cell lines of the human neuroblastoma (NB) tumor.

My findings provide strong evidence that LCA exhibits a potent anti-tumor effect in cultured human NB cells by: 1) activating both intrinsic (mitochondrial) and extrinsic (death receptor) pathways of apoptotic death in these cells; 2) sensitizing them to hydrogen peroxide-induced apoptotic death; and 3) preventing growth and proliferation of their neighbouring NB cells in the culture. Importantly, my findings also imply that LCA does not display any of these deleterious effects in human neurons and, therefore, is a selective anti-tumor compound. Moreover, my mass spectrometry-based measurement of intracellular and extracellular levels of exogenously added LCA revealed that this bile acid does not enter cultured NB cells. Thus, LCA prevents proliferation of human NB

cells and selectively kills these cancer cells by binding to their surface and then initiating intracellular signaling cascades that not only impair their growth and division, but also cause their apoptotic death. The demonstrated inability of LCA to enter cultured human NB cells suggests that this potent and selective anti-cancer compound is unlikely to display undesirable side effects in non-cancerous human neurons. My findings suggest a mechanism underlying a potent and selective anti-tumor effect of LCA in human NB cancer cells.

**Acknowledgements**

I am grateful to my supervisor, Dr. Vladimir Titorenko, for his guidance and support during the years I spent in his laboratory. I would like to thank the members of my committee, Dr. Patrick Gulick and Dr. Reginald Storms, for their valuable suggestions during the course of my graduate research and studies.

Many thanks to all of my current and former lab-mates Adam Beach, Tatiana Boukh-Viner, Simon Bourque, Michelle Tali Burstein, Subrata Chowdhury, Asya Glebov, Tong Guo, Christopher Gregg, Tatiana Iouk, Olivia Koupaki, Pavlo Kyryakov, Oleh Petriv, Vincent Richard, Bahador Abadi, Daniel Aguirre, Zineea Ahmed, Riad Akkari, Alex Alexandrian, Samira Ansary, Sadaf Anwar, Mohammad Sharif Askari, Zeinab Aziz, Kabongo Balufu, Alpana Bangur, Farhana Banu, Quesny Jean Baptiste, Carmen Bayly, Gabriella Bazdikian, Guillaume Beaudoin, Matthieu Bedard, Moria Belanger, Adrian Buensuceso, Stephanie Bramwell, Aman Brar, Andre Cerracchio, Andrew Chang, Steve Chausse, Eileen Colella, Thaisa Cotton, David Cyr, Julie Cyr, Mark Dass, Rosa De Fenza, Gabrielle Depres, Cassandra Di Tomasso, Ozlem Doygun, Supria Mohan Dubey, Lucia Farisello, Fernando Fiscina, Victor Germanov, Colin Goldfinch, Alejandra Gomez Perez, Alexandra Greco, Sandra Haile, Karen Hung Yeung San, Saeeda Hasan, Ahmed Hossain, Mara Inniss, Chidiebere Michael Iro, Mylène Juneau, Wael Kalaji, Narges Kalantari, Simin Kargari, Mulanda Kayembe, Sukhdeep Kenth, Hyun Young Kim, Petko Komsalov, Shogher Kouyoumjian, Karine Lalonde, Melanie Larche, Clemence Larroche, Jeffrey MacKenzie Lee, Sabrina Lo, Michael A. London, Samira Lorne, Lawrence Ma, Gayane Machkalyan, Lydia Makoroka, Naveed Malik, Cynthia Mancinelli, Patrick Marcoux, Haider Mashhedi, Dale Mc Naught,

Hannah Meltzer, Svetlana Milijevic, Gianni Montanaro, Janine Morcos, Ramandeep Mudhar, Rasesh Nagar, Andrew Naimi, Parisa Namitabar, Florentina Negoita, Phuong Nguyen, Yves Nimbona, Mehdi Noei, Reza Noei, Jordan O'Byrne, Derek O'Flaherty, Aloysius Oluoha, David Papadopoli, Christian Parent-Robitaille, Bhavini Patel, Mital Patel, Sabrina Piccioni, Premala Premanathan, Peter Quashie, Nishant Ramlal, Sonia Rampersad, Savitri Rampersad, Parvin Ranjbar, Joel Richard, Stephanie Russo, Tarek Sabri, Abdelhak Saddiki, Mohammad Hassan Salah, Karen Hung Yeung San, Eric Scazzosi, Sandra Scharaw, Christine Schäfers, Elyse Schmidt, Nadia Sheikh, Arash B. Shokouhi, Cristina Sison, Jerani Sivayogan, Rhoda Sollazzo, Jonathan Solomon, Saamala Subramaniam, Nader Toban, Victor Uscatescu, Andrew Victor, Lisiana Vigliotti, Laura Whelton and Vivianne Wong for their friendship and support.

I am grateful to my parents for their invaluable support.

## Table of Contents

## List of Figures and Tables

**List of Abbreviations**

ACO, aconitase; AMPK/TOR, AMP-activated protein kinase/target of rapamycin; cAMP/PKA, cAMP/protein kinase A; C/EBPα, CCAAT/enhancer-binding protein; CCO, cytochrome c oxidase; CFU, colony forming units; CNS, central nervous system; CL, cardiolipin; CLS, chronological life span; CR, caloric restriction; DAG, diacylglycerols; DHAP, dihydroxyacetone phosphate; DHR, dihydrorhodamine 123; DR, dietary restriction; EE, ergosteryl esters; ESI/MS, electrospray ionization mass spectrometry; ER, endoplasmic reticulum; ERG, ergosterol; FA-CoA, CoA esters of fatty acids; FFA, free fatty acids; FoxO, Forkhead box type O; GC/MS, gas chromatography followed by mass spectrometry; HPLC, high performance liquid chromatography; IGF-1, insulin/insulin-like growth factor 1; LBs, lipid bodies; LCA, lithocholic acid; LOD, limit of detection; LOQ, limit of quantitation; LPA, lysophosphatidic acid; MCA, metabolic control analysis; NB, neuroblastoma; PA, phosphatidic acid; PC, phosphatidylcholine; PE, phosphatidylethanolamine; PI, phosphatidylinositol; PI3K, phosphatidylinositol-3-kinase; PKC, protein kinase C; PMBC, peripheral blood mononuclear cells; rDNA, ribosomal DNA; ROS, reactive oxygen species; RLS, replicative life span; SD, standard deviation; SDH, succinate dehydrogenase; TAG, triacylglycerols; TLC, thin-layer chromatography; TORC1, TOR complex 1; WAT, white adipose tissue.

# 1 Introduction

## 1.1 Biological aging: A "passive" lifelong accumulation of unrepaired cellular and molecular damage or an "active" process progressing through a series of checkpoints and governed by a limited number of "master" regulators?

Aging of multicellular and unicellular eukaryotic organisms is a multifactorial biological phenomenon that has various causes and affects a plethora of cellular activities [1 - 16]. At the organismal level, aging can be defined as the progressive decline in the ability of an organism to resist stress, repair damage and battle disease [2, 5, 10 - 14], whereas demographically aging manifests itself as an exponential increase in the mortality rate with the age of the cohort [2, 3, 7, 10, 12 - 15].

There are two contradictory views of biological aging. In one view, aging of multicellular and unicellular eukaryotic organisms is due to a "passive" lifelong build-up of unrepaired damage to cellular macromolecules and organelles [1 - 3, 12 - 14, 17]. Progressive, age-related accumulation of such damage impairs normal functioning of the entire organism, thereby increasing a risk of disease and death [2, 11 - 15]. Thus, in this view, aging is merely a result of the time-dependent, unavoidable accumulation of unrepaired cellular and molecular damage [1 - 3, 12, 17]. However, a growing body of evidence supports the view that aging is the final step of a developmental program. In this alternative view, aging is an "active" process, in which a limited number of "master" regulators orchestrate numerous cellular processes in space and time [18 - 29]. Each of these processes can be considered as a functional module integrated with other modules into a longevity network [4, 10, 24 - 29]. The synergistic action of individual modules

could establish the rate of aging. Furthermore, the relative impact of each module on the rate of aging in a particular organism or cell type could differ at various stages of its lifetime and could also vary in different organisms and cell types [18 - 24]. In this conceptual framework, the longevity network could progress through a series of checkpoints [19 - 21, 24]. At each of these checkpoints, a distinct set of master regulators senses the functional states of critical modules comprising the network. Based on this information and considering the input of some environmental cues (such as caloric and dietary intake, environmental stresses, endocrine factors etc.), master regulators modulate certain processes within monitored modules in order to limit the age-related accumulation of molecular and cellular damage [18 - 21, 24 - 29]. The resulting changes in the dynamics of individual modules comprising the network and in its general configuration are critically important for specifying the rate of aging during late adulthood [18 - 24].

One of the major objectives of my thesis was to test the validity of the above hypothesis that aging is the final step of a developmental program, in which a limited number of "master" regulators orchestrate numerous longevity-defining cellular processes in space and time, and to define the molecular mechanisms underlying such program in chronologically aging yeast.

## 1.2 A signaling network regulates longevity by integrating three signaling pathways that govern numerous longevity-defining cellular processes

The view of biological aging as the final step of a developmental program, in which numerous cellular processes are governed by a limited set of signaling proteins integrated into signaling pathways and networks, has been supported by the identification

of single-gene mutations that extend life span. Although these mutations target only a limited number of genes regulating longevity in such evolutionarily distant organisms as yeast, worms, flies and mice, they affect a plethora of cellular processes [4, 5, 10, 13, 25, 26, 30 - 34]. This wide array of longevity-defining cellular processes - which across phyla are governed by a limited number of signaling proteins integrated into longevity signaling pathways and networks - includes oxidative metabolism in mitochondria, lipid and carbohydrate metabolism, $NAD^+$ homeostasis, amino acid biosynthesis and degradation, ammonium and amino acid uptake, ribosome biogenesis and translation, proteasomal protein degradation, nuclear DNA replication, chromatin assembly and maintenance, actin organization, apoptosis, necrosis, autophagy, protein folding, stress response, signal transduction, cell cycle, and cell growth [4, 7, 8, 10, 24 - 32, 35, 36]. The functional states of all these numerous longevity-defining processes and their spatiotemporal organization are modulated by only a few nutrient- and energy-sensing signaling pathways that are conserved across phyla and include the AMP-activated protein kinase/target of rapamycin (AMPK/TOR), cAMP/protein kinase A (cAMP/PKA) and insulin/insulin-like growth factor 1 (IGF-1) pathways (Figure 1.1) [4, 10, 25 – 27, 30, 35].

The AMPK/TOR pathway regulates longevity in yeast, worms, fruit flies and mammals by acting as an intracellular sensor for the nutrient and energy status (Figure 1.1) [37 - 42]. In response to the high AMP:ATP ratio characteristic of a low level of nutrients or energy within a cell, AMPK is activated to phosphorylate and inhibit TOR protein kinase associated with several other proteins into the TOR complex 1 (TORC1) [37 - 42]. The resulting inhibition of TORC1 triggers global changes in cell physiology

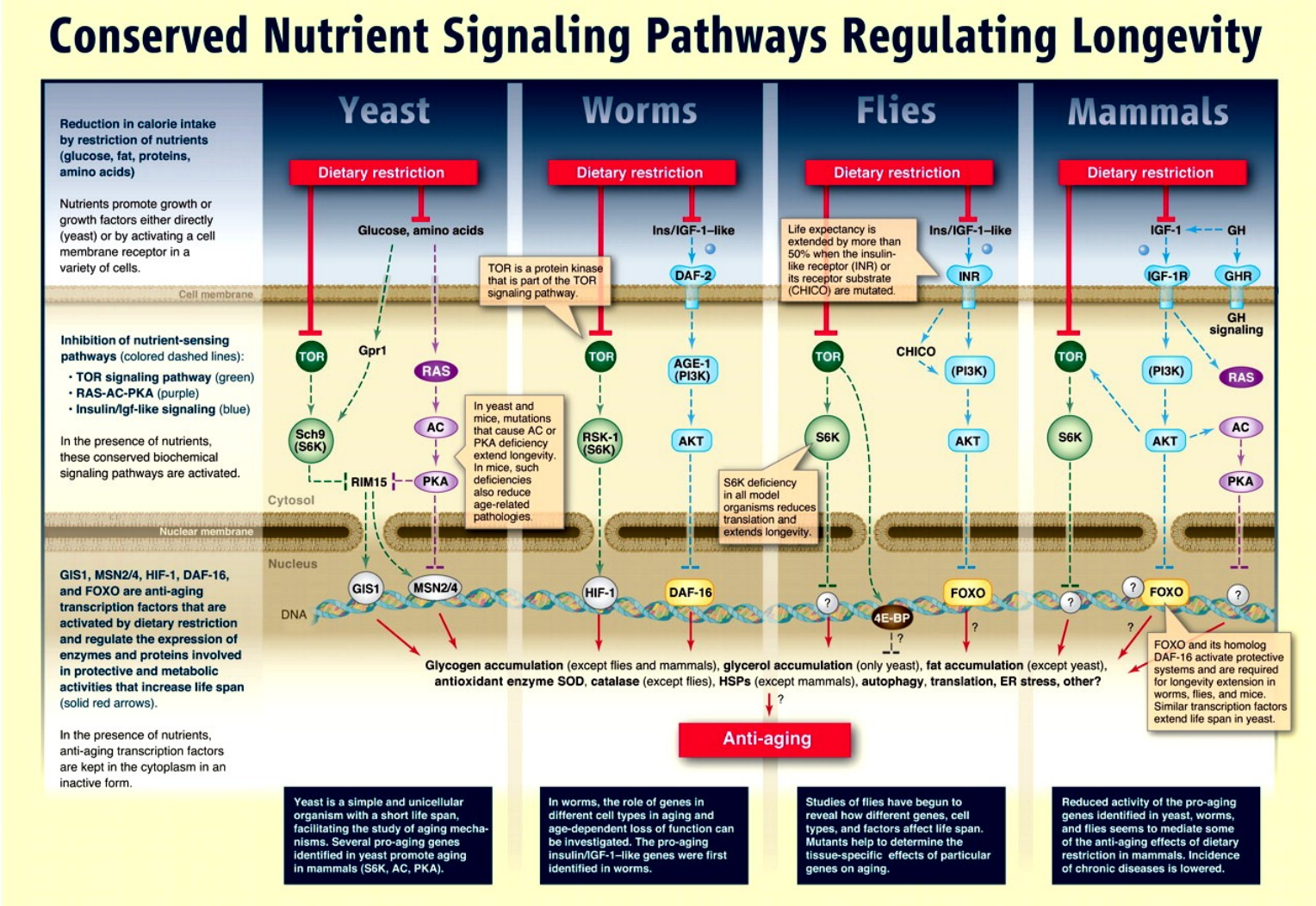


**Figure 1.1.** The functional states of numerous longevity-defining processes and their spatiotemporal organization are modulated by only a few nutrient- and energy-sensing signaling pathways that are conserved across phyla and include the AMP-activated protein kinase/target of rapamycin (AMPK/TOR), cAMP/protein kinase A (cAMP/PKA) and insulin/insulin-like growth factor 1 (IGF-1) pathways (see text in section 1.2 for details). Reproduced from Fontana, L., Partridge, L. and Longo, V.D. (2010). Extending healthy life span - from yeast to humans. *Science* 328:321-326.

by 1) slowing down the energy-consuming processes of cellular growth, ribosome biogenesis and protein translation; 2) initiating a pro-longevity translational program by causing a switch from cap-dependent to cap-independent translation; 3) activating nutrient- and energy-producing autophagy aimed at the removal of damaged

macromolecules and organelles; 4) accelerating mitochondrial translation of oxidative phosphorylation subunits; and 5) causing global changes in mitochondrial gene expression pattern [37, 43 - 45]. The life-extending inhibition of TORC1 can be also achieved in an AMPK-independent manner, in response to low intracellular levels of amino acids [39, 41, 46 - 49]. Moreover, following its phosphorylation by the LKB1 protein kinase under low nutrient or energy conditions within a cell, AMPK extends the life span of worms in a TORC1-independent fashion by slowing down hydrolysis of the neutral lipids triacylglycerols (TAG) [50].

The cAMP/PKA pathway regulates longevity in mice and yeast (Figure 1.1). In mice, this signaling pathway accelerates aging if activated by cAMP produced by AC5, a highly abundant in the heart and brain isoform of adenylate cyclase [51]. Lack of AC5 attenuates cAMP/PKA signaling in mice, thereby reducing the inhibitory effect of PKA on the Raf/MEK/ERK protein kinase cascade [51]. The resulting activation of the protein kinase ERK extends longevity and delays age-related degenerative processes in the heart and bone, likely by elevating the level of the reactive oxygen species (ROS) scavenging enzyme manganese superoxide dismutase, increasing the resistance of mice to oxidative stress and attenuating apoptotic cell death [51]. The essential role for cAMP/PKA in regulating longevity and modulating physiological processes underlying healthy aging in mice has been recently confirmed by observations that lack of either a catalytic subunit of PKA or its regulatory subunit extends life span and improves health by attenuating age-related pathologies [52 - 53].

In yeast cells, the cAMP/PKA pathway is attenuated in response to glucose deprivation, which inhibits such activators of adenylate cyclase Cyr1p as the G protein-

coupled receptor Gpr1p, Gα protein Gpa2p and two small GTP-binding proteins, Ras1p and Ras2p (Figure 1.1) [54, 55]. The attenuation of cAMP/PKA signaling in glucose-deprived yeast cells impairs the ability of cytosolic PKA to phosphorylate the following three proteins in the cytosol: 1) the protein kinase Rim15p (thereby restoring the kinase activity of Rim15p inhibited by PKA-dependent phosphorylation); and 2) the stress response transcription factors Msn2p and Msn4p (thereby enabling the import of their unphosphorylated forms into the nucleus) [56 - 58]. After being imported into the nucleus, Msn2p and Msn4p collaborate with a nuclear pool of Rim15p in activating transcription of numerous pro-longevity genes involved in carbohydrate metabolism, the tricarboxylic acid cycle, trehalose biosynthesis, proteolysis, stress protection, ROS detoxification and cell growth regulation [59 - 62]. The establishment of such global pro-longevity transcriptional pattern ultimately extends both the chronological and replicative life spans of yeast [56, 63, 64]. It should be stressed that, akin to the Raf/MEK/ERK signaling cascade in mammals (see above) [51], its homologous Ste11p/Ste7p/Kss1p protein kinase cascade in yeast is attenuated by PKA and, if active, promotes longevity of chronologically aging yeast [65]. This pro-longevity effect of the Ste11p/Ste7p/Kss1p cascade in yeast under conditions of attenuated cAMP/PKA signaling is synergistic with the pro-longevity action of the nuclear forms of Msn2p, Msn4p and Rim15p not subjected to phosphorylation by cytosolic PKA [65].

Unlike the AMPK/TOR and cAMP/PKA signaling pathways regulating longevity by acting as sensors of the intracellular nutrient and energy status, the insulin/IGF-1 signaling pathway regulates longevity in worms, fruit flies and mice by responding to an endocrine signal that monitors the nutritional status of the whole organism (Figure 1.1)

[66]. In response to an insulin-like ligand, the insulin/IGF-1 pathway activates a phosphatidylinositol-3-kinase and a cascade of protein kinases, ultimately causing phosphorylation of a Forkhead box type O (FoxO) family transcription factor and its sequestration in the cytosol [67, 68]. In worms, fruit flies and mice, reduced signaling through the insulin/IGF-1 pathway extends longevity by inhibiting phosphorylation of their FoxO transcription factors (DAF-16, dFOXO and FoxO1, respectively), thereby enabling their import into the nucleus [69]. Following their nuclear import, these transcription factors activate or repress transcription of numerous longevity-defining genes involved in metabolism, detoxification, apoptosis, stress response, transcription, translation, signaling and development to ultimately establish a global pro-longevity transcriptional pattern [70, 71].

Because in evolutionarily distant organisms the AMPK/TOR, cAMP/PKA and insulin/IGF-1 signaling pathways share several protein kinases and adaptor proteins, they converge into a network regulating longevity in yeast, worms, fruit flies and mammals [4, 35 - 38]. Growing evidence supports the view that this longevity regulation network also includes several proteins that currently are not viewed as being in any of these signaling pathways, including 1) Rtg2p in yeast; 2) CLK-1, ISP-1, JNK, MST-1, PHA-4, Rictor/TORC2/SGK-1, SIR-2.1, SKN-1 and SMK-1 in worms; 3) dSir2 and JNK in fruit flies; and 4) MCLK, $P66^{Shc}$, SIRT1, SIRT6, and SIRT7 in mammals [4, 36, 72 - 74]. It should be stressed that this longevity regulation network responds to the age-related partial mitochondrial dysfunction and is modulated by mitochondrially produced ROS [36, 37, 73, 75]. By sensing the nutritional status of the whole organism as well as the intracellular nutrient and energy status, functional state of mitochondria, and

concentration of ROS produced in mitochondria, the longevity network regulates life span across species by coordinating information flow along its convergent, divergent and multiply branched signaling pathways.

One of the major objectives of my thesis was to examine if lithocholic acid, a novel anti-aging compound that I identified in a high-throughput chemical genetic screen, extends longevity of chronologically aging yeast by attenuating the pro-aging AMPK/TOR and/or cAMP/PKA signaling pathways.

## 1.3 Some dietary regimens can extend longevity and improve health by attenuating age-related pathologies

Because nutrient intake modulates the organismal and intracellular nutrient and energy status, it plays an important role in defining both life span and health span [7, 76 - 78]. Two dietary regimens - known as caloric restriction (CR) and dietary restriction (DR) - have been shown not only to exhibit a robust longevity-extending effect in evolutionarily distant organisms ranging from yeast to rhesus monkeys, but also to improve health by attenuating age-related pathologies and delaying the onset of age-related diseases across phyla (Table 1.1) [76 - 83]. A CR dietary regimen reduces only calorie intake, but does not compromise the supply of amino acids, vitamins and other nutrients [77 - 80]. In contrast, a DR diet reduces the intake of nutrients (but not necessarily of calories) by limiting food supply without causing malnutrition [76, 81 - 83].

A “TOR-centric” model of longevity regulation considers AMPK/TOR as the only signaling pathway underlying all life-extending and health-improving effects of CR

**Table 1.1.** Caloric restriction (CR) and dietary restriction (DR) exhibit a robust longevity-extending effect in evolutionarily distant organisms ranging from yeast to rhesus monkeys and improve health by attenuating age-related pathologies and delaying the onset of age-related diseases across phyla. Adapted from Fontana, L., Partridge, L. and Longo, V.D. (2010). Extending healthy life span - from yeast to humans. *Science* 328:321-326 with modifications.

| **Organism** | **Life-span increase by CR or DR** | **Health improvement by CR or DR** |
|---|---|---|
| Yeast | 3-fold (chronological life span) | Extended reproductive period |
| Worms | 2- to 3-fold | Resistance to misexpressed toxic proteins |
| Fruit flies | 2-fold | None reported |
| Mice | 30-50% | Protection against cancer, diabetes, atherosclerosis, cardiomyopathy, autoimmune, kidney and respiratory diseases; reduced neurodegeneration |
| Rhesus monkeys | Tend noted | Prevention of obesity; protection against cancer, diabetes and cardiovascular disease |
| Humans | Not tested | Prevention of obesity, diabetes, hypertension; reduced risk factors for cancer and cardiovascular disease |

and DR [84 - 89]. According to this model, TORC1 - a core protein complex governing the AMPK/TOR pathway - performs three global functions, all of which are pivotal to the beneficial effects of CR and DR on longevity and health span. First, it integrates the flow of information on the organismal and intracellular nutrient and energy status from AMPK (a protein kinase in the AMPK/TOR pathway), PKA (a protein kinase in the cAMP/PKA pathway), PKB/AKT (a protein kinase in the insulin/IGF-1 pathway), ERK1/2 (a protein kinase in the Raf/MEK/ERK signaling cascade) and $P66^{Shc}$ (a mitochondria-confined

sensor of the redox status within this organelle) [84 - 86]. Second, it functions (independently of AMPK) as a sensor of the intracellular levels of amino acids [84 - 86]. Third, by gathering and processing the information on the organismal and intracellular nutrient, energy and redox status and amino acid availability, it operates as a control center that governs numerous longevity-related processes independently of sirtuins [84 - 86]. The validity of the TOR-centric model for TORC1-orchestrated modulation of the life-extending effects of CR and DR has been confirmed in worms and replicatively aging yeast. In fact, DR is unable to extend longevity of worms with reduced TOR signaling [88, 89]. Furthermore, lack of key components of the TOR signaling pathway eliminates the beneficial effect of CR on the replicative life span of yeast [87].

It seems that, although the TOR pathway alone mediates the longevity benefit associated with CR in replicatively aging yeast, the life-extending effect of this dietary regimen in chronologically aging yeast relies on a signaling network in which the protein kinase Rim15p operates as a nutritional integrator of the TOR and cAMP/PKA pathways and which also includes some other, yet to be identified signaling pathways that are not converged on Rim15p [35]. Furthermore, because the AMPK/TOR, cAMP/PKA and insulin/IGF-1 pathways in worms, fruit flies and mammals are known to converge into a complex network regulating their longevity (see above) [4, 7, 36 - 38], it is likely that these three divergent and multiply branched signaling pathways equally contribute to the life-extending effects of CR and DR in these organisms [4, 90 - 99]. The emerging concept of a signaling network (rather than the AMPK/TOR pathway alone) that mediates the longevity benefit associated with CR and DR by coordinating information flow along its convergent, divergent and multiply branched signaling pathways has been

recently supported by studies in worms. In fact, the life-extending efficacies of different DR regimens in these organisms depend on both independent and overlapping signaling pathways [100].

One of the major objectives of my thesis was to identify small molecules that can extend longevity of chronologically aging yeast even under CR conditions, under which a pro-aging signaling network that integrates the TOR and cAMP/PKA pathways is greatly attenuated or even entirely inactivated. I thought that the availability of such anti-aging compounds would provide a potent chemical biological tool for defining what I call "housekeeping" longevity assurance pathways. I coined this term to emphasize that these pathways: 1) modulate longevity irrespective of the extracellular and intracellular nutrient and energy status – in contrast to TOR and cAMP/PKA, the two longevity signaling pathways that are "adaptable" by nature because they define yeast chronological life span only in response to certain changes in such status; and 2) do not overlap (or only partially overlap) with the adaptable TOR and cAMP/PKA pathways that in yeast are under the stringent control of calorie availability.

## 1.4 Certain pharmacological interventions can delay aging by beneficially influencing age-related pathologies

CR and DR are not the only interventions known to extend longevity in evolutionarily distant organisms. Aging can be slowed down, health improved, age-related pathologies attenuated and the onset of age-related diseases delayed also by certain small molecules, many of which exhibit the beneficial effects on longevity and health span in organisms across phyla (Table 1.2). Many of these longevity- and health

**Table 1.2.** Known anti-aging compounds, their abilities to increase life span in different organisms (under caloric or dietary restriction [CR or DR, respectively], on a standard diet or fed a high-calorie diet), and the mechanisms of their anti-aging action.

| **Compound** | **Increases life span*** | | **Mechanism** |
|---|---|---|---|
| | **CR/DR** | **Standard or high-calorie diet** | |
| Caffeine | Not tested (NT) | + (yeast, CLS) [101] | By inhibiting TORC1, modulates unspecified longevity-related processes [101] governed by the TOR pathway [37, 102] |
| $Li^+$ | + (nematodes**) [103] | + (nematodes) [103] | By altering transcription of genes involved in histone methylation, nucleosome composition and chromatin structure, modulates unspecified longevity-related processes [103] known to be influenced by age-related chromatin reorganization [104] |
| Lipoic acid, propyl gallate, trolox and taxifolin | NT | + (nematodes [105] (all); fruit flies [106] (lipoic acid)) | Antioxidants that may increase life span by detoxifying free radicals and/or enhancing resistance to age-related oxidative stress [105, 106] |
| Metformin, buformin and phenformin | - (nematodes**) [107] | + (nematodes [107]; mice [108]) | Type 2 diabetes therapeutics that - by activating LKB1/AMPK signaling and thereby inhibiting TORC1 [38, 109] - modulate unspecified longevity-related processes [107, 108] known to be governed by the TOR pathway [37, 38, 102] |

| | | | |
|---|---|---|---|
| Methionine sulfoximine | NT | + (yeast, CLS) [110] | By inhibiting glutamine synthetase and reducing both intracellular glutamine level and TORC1-signaling [111], increases life span - perhaps by activating gluconeogenesis and enhancing stress resistance [110] |
| Mianserin | - (nematodes) [112] | + (nematodes) [112] | A serotonin receptor antagonist used as an antidepressant in humans; may increase life span by inhibiting neurotransmission related to food sensing, thereby mimicking a DR-like physiological state [112]*** |
| Rapamycin | + (fruit flies) [113] | + (yeast, CLS [101, 110, 114] and RLS [115]; fruit flies [113]; mice [116]; rodent fibroblasts, human epithelium and fibrosarcoma cells - all RLS [110]) | By inhibiting TORC1 (yeast and fruit flies) [101, 102, 113, 114] and mTORC1 (mammals) [38, 102, 116], increases life span by activating macroautophagy (yeast and fruit flies) [113, 118] and inhibiting cap-dependent protein translation (fruit flies and mice) [113, 116] as well as - perhaps - by promoting gluconeogenesis (yeast) [110], enhancing stress resistance (yeast) [110, 115], and increasing neutral lipid levels (fruit flies) [113] |
| Resveratrol | - (yeast, RLS [119]; fruit flies [120]; | + (yeast, RLS [119] but not CLS [119]; | Increases life span by modulating a number |

| | | | |
|---|---|---|---|
| | mice [121]) | nematodes [120]; fruit flies [120]; fishes [122]; mice [121, 124]; human fibroblasts, RLS [123])**** | of longevity-related processes (*e.g.*, by altering transcription of numerous genes involved in key longevity pathways, stimulating p53 deacetylation, increasing insulin sensitivity and mitochondrial number, reducing IGF-1 levels, activating AMPK and PGC-1α, promoting ER stress response, repressing transcription of PPAR-γ, inhibiting adipocyte differentiation, accelerating storage fat mobilization, inhibiting mTORC1, and activating autophagy [119, 121, 123 - 131]; its life-extending ability in yeast, nematodes and fruit flies depends on Sir2p - a member of the conserved sirtuin family of $NAD^+$-dependent protein deacetylases/mono-ADP-ribosyltransferases [119, 120, 125]***** |
| SkQ1 | NT | + (fungi, daphnias, fruit flies, mice) [132] | By being specifically targeted to mitochondria, acts as an antioxidant that may increase life span by preventing oxidative damage to proteins and lipids (*i.e.*, cardiolipin), altering mitochondrial |

| | | | |
|---|---|---|---|
| | | | morphology, reducing hydrogen peroxide-induced apoptosis and necrosis, and/or slowing down the age-related phosphorylation of histone H2AX [132] |
| Sodium nitroprusside | NT | + (human PBMC,RLS) [133] | By activating expression of the human sirtuin SIRT1 and thereby increasing the extent of SIRT1-dependent histone H4 lysine 16 deacetylation, may cause the development of an anti-aging pattern of transcription of numerous genes involved in longevity regulation [133] |
| Spermidine | NT | + (yeast, CLS; nematodes; fruit flies; human PBMC, RLS) [134] | By inhibiting histone acetyltransferases and promoting histone H3 deacetylation, increases life span by activating transcription of numerous autophagy-related genes; the resulting induction of autophagy suppresses age-related necrotic cell death [134] |
| Valproic acid | NT | + (nematodes) [135] | Is used as a mood stabilizer and an anticonvulsant in humans; may increase life span by promoting nuclear localization of the DAF-16 forkhead transcription factor, thereby reducing the pro-aging effect of the insulin/IGF-1 |

| | | | |
|---|---|---|---|
| | | | signaling pathway [135] |
| LY294002 | NT | + (human fibrosarcoma cells, RLS) [136] | An inhibitor of phosphatidylinositol-3-kinase that – by reducing mTORC1 signaling [37, 102] – modulates unspecified longevity-related processes [136] known to be governed by the TOR pathway [37, 38, 102] |
| U0126 | NT | + (human fibrosarcoma cells, RLS) [136] | An inhibitor of the protein kinase MEK that – by reducing mTORC1 signaling [37, 102] – modulates unspecified longevity-related processes [136] known to be governed by the TOR pathway [37, 38, 102] |

* Mean, median and/or maximum life spans.

** Nematodes carrying mutations that mimic DR under non-DR conditions [103, 105].

*** The ability of mianserin to increase nematode life span can only be seen in liquid media [112], whereas in solid media the compound reduces life span [137].

**** Increases the replicative life span of yeast grown under non-CR conditions [119] only in one out of four different yeast strain backgrounds [138]; one group has been unable to reproduce the life span extension by resveratrol in nematodes and fruit flies [139]; increases the life of mice only if fed a high-calorie diet, but not a standard diet [121, 124].

***** Although the life-extending ability of resveratrol in yeast, nematodes and fruit flies depends on Sir2p [119, 120, 125], it is currently debated whether this anti-aging compound binds to Sir2p (or SIRT1, a mammalian sirtuin) in vivo and/or activates Sir2p or SIRT1 in living cells [126, 138 - 142]; importantly, resveratrol has been shown to inhibit or activate many proteins other than sirtuins by interacting with them [143, 144].

**Abbreviations:** AMPK, the AMP-activated serine/threonine protein kinase; CLS, chronological life span; IGF-1, insulin-like growth factor 1; LKB1, a serine/threonine protein kinase that phosphorylates and activates AMPK; mTORC1, the mammalian target of rapamycin complex 1; NT, not tested; PBMC, peripheral blood mononuclear cells; PGC-1α, peroxisome proliferator-activated receptor-γ co-activator 1α; RLS, replicative life span; TORC1, the yeast target of rapamycin complex 1.

span-extending pharmacological interventions target the AMPK/TOR signaling pathway known to modulate longevity in response to the intracellular nutrient and energy status. Metformin, a type 2 diabetes therapeutics that activates AMPK, extends longevity in worms and mice by reducing TORC1 signaling (Table 1.2) [107, 108]. Methionine sulfoximine, a glutamine synthetase inhibitor that attenuates TORC1 signaling by decreasing the intracellular concentration of the TORC1 activator glutamine, extends the chronological life span of yeast (Table 1.2) [110, 111]. LY294002 and U0126, which lower TORC1 signaling by inhibiting upstream TORC1 activators PI3K and MEK (respectively), increase the replicative life span of cultured human fibrosarcoma cells (Table 1.2) [136]. By acting through FKBP12 to inhibit TORC1, the macrocyclic lactone rapamycin extends 1) longevity in fruit flies and mice [113, 116]; 2) the replicative life spans of cultured rodent fibroblasts, human epithelium cells and human fibrosarcoma cells [117]; and 3) the replicative and chronological life spans of yeast (Table 1.2) [56, 110, 114]. Caffeine, a xanthine alkaloid, increases the chronological life span of yeast by reducing the catalytic activity of Tor1p (Table 1.2) [101].

Some anti-aging compounds extend longevity by targeting the insulin/IGF-1 pathway, which monitors the nutritional status of the whole organism. By modulating an upstream step in this signaling pathway, the serotonin receptor antagonist mianserin (which is used as an antidepressant in humans) increases life span in worms, likely by inhibiting neurotransmission related to food sensing and mimicking a DR-like physiological state (Table 1.2) [112]. A downstream step in this signaling pathway is a target of valproic acid (a mood stabilizer and an anticonvulsant in humans), which

extends longevity in worms by promoting the translocation of the pro-longevity FoxO transcriptional factor DAF-16 into the nucleus (Table 1.2) [135].

Some anti-aging small molecules extend longevity, improve health and attenuate age-related pathologies by modulating longevity-defining processes controlled by proteins that are not viewed as components of the AMPK/TOR, cAMP/PKA and insulin/IGF-1 signaling pathways but are dynamically integrated into a longevity regulation network (see section 1.2 in this chapter of my thesis) they govern. One of these longevity-extending molecules is resveratrol, a small polyphenol produced by plants (Table 1.2). Although the demonstrated by *in vitro* studies ability of resveratrol to activate the protein deacetylase activities of the sirtuins Sir2p (yeast), SIR-2.1 (worms), dSir2 (fruit flies) and SIRT1 (mammals) [131, 145] is disputed [142, 146], it has been shown to modulate activities of many other longevity-related proteins by interacting with them [143, 144] – thereby influencing a plethora of longevity-defining processes [119, 121, 124 - 127, 129]. It is likely that the resveratrol-driven modulation of activities of numerous longevity-defining proteins and processes they govern underlies the observed ability of this small polyphenol molecule 1) to extend the replicative (but not chronological) life span of yeast [119]; 2) to increase the replicative life span of cultured human fibroblasts [123]; and 3) to extend longevity of worms, fruit flies, fishes and mice [120 - 122, 124] (Table 1.2).

Akin to resveratrol, sodium nitroprusside exhibits a potent anti-aging effect by promoting sirtuin-dependent protein deacetylation. Unlike resveratrol, sodium nitroprusside activates expression of the gene encoding sirtuin SIRT1 [133]. The resulting enhancement of SIRT1-driven deacetylation of lysine 16 in histone H4 may

underlie the observed establishment of an anti-aging pattern of transcription and the concomitant replicative life span extension in cultured human peripheral blood mononuclear cells (PMBC) (Table 1.2) [133]

The reduction of the extent of histone acetylation is a longevity-extending process that can be promoted not only by sodium nitroprusside, but also by spermidine. This natural polyamine has been shown to inhibit histone acetyltransferases and promote histone H3 deacetylation - thereby activating transcription of numerous autophagy-related genes, suppressing age-related necrotic cell death and ultimately extending the chronological life span of yeast, the replicative life span of cultured human PMBC, and longevity of worms and fruit flies (Table 1.2) [131, 134]. Of note, histone modification is also a target of another longevity-extending compound, $Li^+$. The ability of this alkali metal ion to cause the age-related chromatin reorganization by altering transcription of genes involved in histone methylation, nucleosome composition and chromatin structure may underlie its beneficial properties as a mood stabilizer in humans and an anti-aging compound in worms (Table 1.2) [103].

Considering the essential role of mitochondria in longevity regulation across phyla [36, 73, 75, 147], it is not surprisingly that several anti-aging compounds extend longevity by influencing longevity-defining processes confined to or governed by these organelles. SkQ1, a plastoquinone derivate, is specifically sorted to mitochondria and operates as an antioxidant that attenuates oxidative damage to mitochondrial proteins and lipids, changes mitochondrial morphology, and impairs mitochondria-controlled forms of apoptotic and necrotic cell death caused by an excessive accumulation of mitochondria-produced hydrogen peroxide (Table 1.2) [132]. By influencing these longevity-defining

processes confined to mitochondria, SkQ1 not only extends longevity in fungi, daphnias, fruit flies and mice, but also improves health and delays the onset of age-related diseases in mice [132]. Furthermore, longevity in worms and fruit flies can be extended by the thermal stress mimetics lipoic acid, propyl gallate, trolox and taxifolin, all of which may delay aging by detoxifying free radicals and enhancing resistance to age-related oxidative stress (Table 1.2) [106, 105].

It should be stressed that all anti-aging compounds known prior to my study are so-called "CR mimetics" and "DR mimetics" because they: 1) similar to CR and DR dietary regimens, increase life span and/or health span under non-CR or non-DR conditions; 2) unlike CR and DR diets, do not restrict caloric and nutrient intake; and 3) mimic life-extending and health-improving effects of CR and DR on metabolic pathways, physiological processes, stress response and gene expression (Table 1.2) [148 - 150]. Furthermore, as detailed in Table 1.2, almost all longevity-extending compounds known prior to my study target the AMPK/TOR and insulin/IGF-1 pathways and impact the sirtuin-governed protein deacetylation module of the longevity signaling network integrating these pathways. As I mentioned in sections 1.2 and 1.3, this network defines longevity only in response to the organismal and intracellular nutrient and energy status. Moreover, such CR mimetics and DR mimetics as resveratrol, metformin and mianserin beneficially influence life span and health span only under non-CR or non-DR conditions, but do not extend longevity or improve health if the supply of calories or nutrients is limited (Table 1.2) [107, 112, 119 - 121]. Therefore, I coined the term "adaptable" to define the AMPK/TOR, cAMP/PKA and insulin/IGF-1 signaling pathways and sirtuin-governed protein deacetylation module - because they all are

integrated into the longevity regulation network targeted by the currently known anti-aging CR mimetics and DR mimetics. The term "adaptable" emphasizes the fact that all these pathways and the sirtuin-governed module exhibit the beneficial effects on longevity and attenuate age-related pathologies only in response to certain changes in the extracellular and intracellular nutrient and energy status of an organism. It should be stressed, however, that recent studies in worms and fruit flies revealed that $Li^+$ and rapamycin (respectively) can extend life span even under DR conditions – although their longevity-extending efficacy under such nutrient-limited conditions is significantly lower than that under non-CR conditions (Table 1.2) [103, 113]. Based on these findings, I thought that some longevity assurance pathways could be "constitutive" or "housekeeping" by nature, assuming that they 1) modulate longevity irrespective of the extracellular and intracellular nutrient and energy status – in contrast to the adaptable AMPK/TOR, cAMP/PKA and insulin/IGF-1 signaling pathways and sirtuin-governed protein deacetylation module; and 2) do not overlap (or only partially overlap) with the adaptable pathways that are under the stringent control of calorie and nutrient availability.

One of the major objectives of my thesis was therefore to identify such housekeeping longevity pathway(s) operating in chronologically aging yeast. To attain this objective, I carried out a chemical genetic screen for anti-aging small molecules that can extend longevity even under CR conditions. I thought that, because under CR conditions the adaptable pro-aging pathways would be fully suppressed and the adaptable anti-aging pathways would be fully activated, a small molecule that can further increase

yeast chronological life span could target the housekeeping longevity pathway(s) that I was trying to identify.

## 1.5 Yeast as a valuable model system for unveiling mechanisms of cellular aging in multicellular eukaryotes

The budding yeast *Saccharomyces cerevisiae* is a valuable model for studying the basic biology of aging and revealing longevity regulation mechanisms in multicellular eukaryotes [6, 34, 152]. There are two different paradigms of aging of this unicellular eukaryote amenable to comprehensive biochemical, genetic, cell biological, chemical biological and system biological analyses. In the replicative aging paradigm, yeast aging is defined by the maximum number of daughter cells that a mother cell can produce before becoming senescent (Figure 1.2) [6, 31]. Replicative aging in yeast mimics aging of dividing ("mitotic") cells in a multicellular eukaryotic organism [6, 31]. In the chronological aging paradigm, yeast aging is defined by the length of time during which a cell remains viable following entry into a non-proliferative state (Figure 1.2) [6, 63, 152]. Chronological aging in yeast is an advantageous model for studying aging of non-dividing ("post-mitotic") cells in a multicellular eukaryotic organism [6, 63, 152]. Yeast chronological aging is assessed using a simple clonogenic assay, which measures the percentage of yeast cells that remain viable at different time points following the entry of a cell population into the non-proliferative stationary phase [63]. A CR diet, which in yeast can be imposed by reducing the initial glucose concentration in a growth medium from 2% to 0.5% or lower, decelerates both replicative and chronological aging of yeast [6, 35, 63, 151].

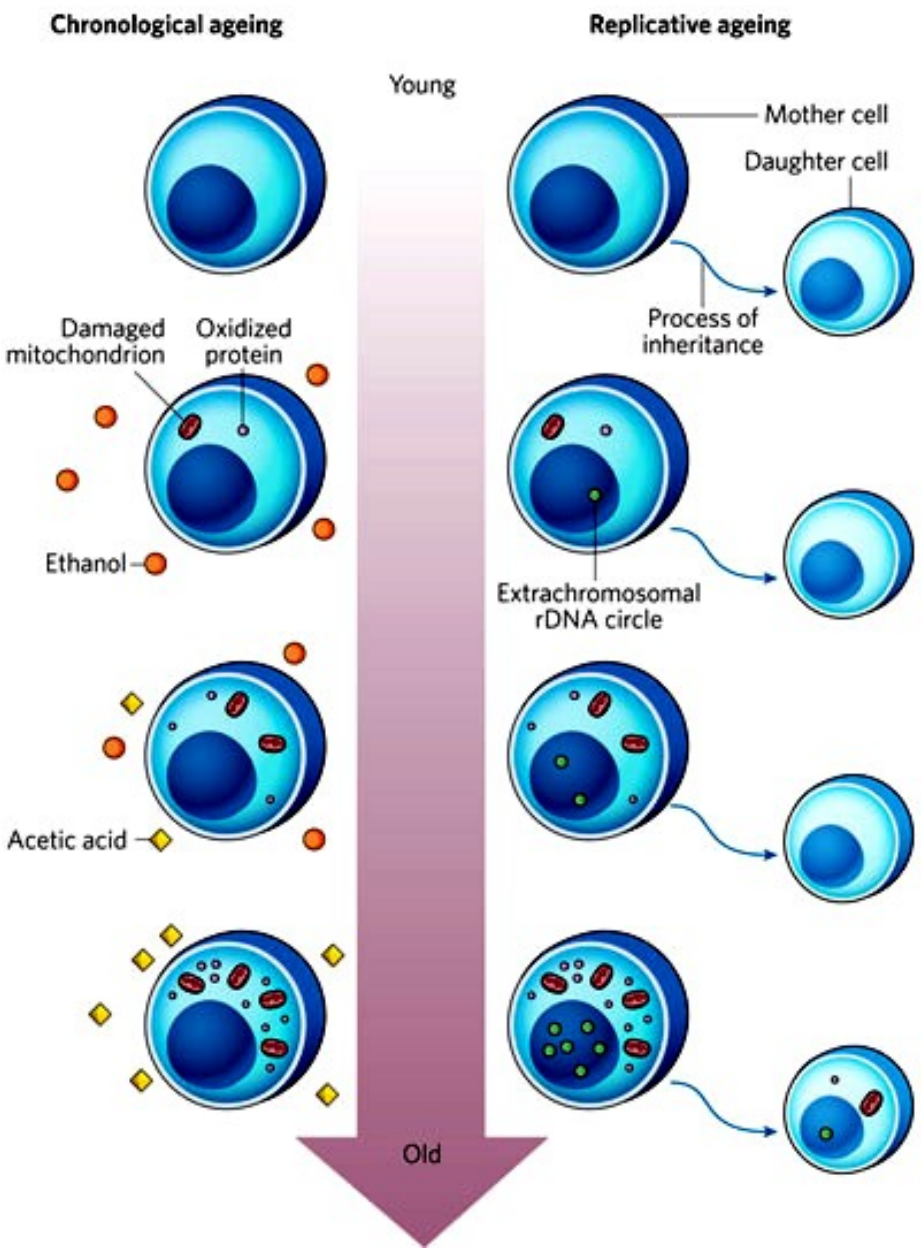


**Figure 1.3.** Two different paradigms of yeast aging. In the replicative aging paradigm, yeast aging is defined by the maximum number of daughter cells that a mother cell can produce before becoming senescent. Replicative aging in yeast mimics aging of dividing ("mitotic") cells in a multicellular eukaryotic organism. In the chronological aging paradigm, yeast aging is defined by the length of time during which a cell remains viable following entry into a non-proliferative state. Chronological aging in yeast is an advantageous model for studying aging of non-dividing ("post-mitotic") cells in a multicellular eukaryotic organism. Yeast chronological aging is assessed using a simple clonogenic assay, which measures the percentage of yeast cells that remain viable at different time points following the entry of a cell population into the non-proliferative stationary phase. (See text in section 1.5 for details). Reproduced from [151].

As I mentioned in sections 1.2, 1.3 and 1.4 of my thesis, longevity signaling pathways and mechanisms of their modulation by dietary and pharmacological interventions are conserved across phyla. It should be stressed that the use of yeast as an advantageous model organism in aging research greatly contributed to the current understanding of the molecular and cellular mechanisms underlying longevity regulation in evolutionarily distant eukaryotic organisms. Due to the relatively short and easily monitored replicative and chronological life spans of this genetically and biochemically manipulable unicellular eukaryote with annotated genome, it has been successfully used to 1) identify numerous novel longevity genes, all of which have been later implicated in regulating longevity of multicellular eukaryotic organisms; 2) establish the chemical nature of molecular damage that causes aging and accelerates the onset of age-related diseases across phyla; and 3) identify several longevity-extending small molecules, all of which have been later shown to slow down aging, improve health, attenuate age-related pathologies and delay the onset of age-related diseases in eukaryotic organisms across phyla [6, 7, 31, 79, 134, 151 - 153].

## 1.6 Cancer as an age-associated disease whose onset can be delayed and incidence reduced by anti-aging interventions: The complex interplay between aging and cancer through convergent and divergent mechanisms

Because of a multi-step nature of the tumorigenesis process whose progression and completion requires an extended period of time, incidence rates of almost all cancers increase with age [154 - 156]. Therefore, aging is considered as one of the major risk factors in the onset and incidence of cancer, whereas cancer is believed to be one of the

numerous diseases associated with aging [157 - 162]. In the commonly accepted paradigm of the relationship between aging and cancer, due to their co-evolution these two complex and dynamic biological processes share common aetiology (*i.e.*, an age-related progressive accumulation of cellular damage) and have coalescent underlying mechanisms [157 - 159]. In this paradigm: 1) some genetic interventions that accelerate the age-related accumulation of cellular damage (or hasten some other common aetiologies of aging and cancer) and target some of the common mechanisms underlying aging and cancer are expected to exhibit both pro-aging and pro-cancer effects; and 2) some genetic, pharmacological and/or dietary interventions that reduce the age-related accumulation of cellular damage (or attenuate some other common aetiologies of aging and cancer) and target some of the common mechanisms underlying aging and cancer are expected to exhibit both anti-aging and anti-cancer effects [157 - 159]. A body of evidence supports the validity of this hypothesis.

In fact, some protein components of a longevity-defining signaling network centered at the mTORC1 complex of the pro-aging AMPK/TOR pathway have been shown to function as oncogenes (*i.e.*, PI3K, Akt and eIF4E – two of which (PI3K and Akt) activate mTORC1, whereas eIF4E is activated by mTORC1 to promote protein synthesis and cell growth) (Figure 1.4) [39, 156 - 165]. In contrast, other proteins integrated into this longevity-defining signaling network are known to be tumor suppressors (*i.e.*, PTEN, LKB1, TSC1 and TSC2 – all of which are mTORC1 inhibitors) (Figure 1.4) [39, 156 - 165]. Accordingly, inherited mutations inactivating the tumor suppressor protein components LKB1, TSC1 and TSC2 of this signaling network hyperactivate mTORC1 (Figure 1.4), thereby promoting cell growth and cell cycle

progression and ultimately resulting in the dominantly inherited benign cancer syndromes of the phakomatose group - which includes the Cowden's syndrome, neurofibromatosis type 1, tuberous sclerosis complex syndrome and Peutz-Jeghers syndrome [39, 156, 161, 163, 164]. Furthermore, somatic mutations in the gene encoding tumor suppressor protein LKB1 hyperactivate mTORC1, thereby promoting cell growth and cell cycle progression (Figure 1.4), and are common for up to 40% of all sporadic non-small cell lung cancers [163, 164]. Moreover, by hyperactivating mTORC1 and promoting cell growth and cell cycle progression (Figure 1.4), mutations in the gene for tumor suppressor protein PTEN cause glioblastoma and metastatic renal cell carcinoma [156, 161, 163, 164].

It should be stressed that by inhibiting (directly or indirectly) mTORC1 and thereby attenuating the pro-aging AMPK/TOR pathway, certain FDA-approved pharmacological interventions exhibit both anti-aging and anti-cancer effects (Figure 1.4). By attenuating the AMPK/TOR pathway that promotes both aging and tumorigenesis, these pharmaceuticals: 1) slow down glycolysis, ribosome biogenesis, protein translation in the cytosol, mitochondrial ROS production, cell growth and cell cycle progression; 2) increase the efficiency of respiration, ROS detoxification and translation of oxidative phosphorylation subunits in mitochondria; 3) activate nutrient- and energy-producing autophagy aimed at the removal of damaged macromolecules and organelles; and 4) enhance stress response [37, 39, 43 - 45]. In fact, both the direct inhibition of mTORC1 by rapamycin and its analogues as well as the indirect (through the activation of the mTORC1 inhibitors LKB1 and AMPK) inhibition of mTORC1 by metformin and its analogues phenformin and Abbott A769662 (Figure 1.4) have been shown to i) inhibit the growth of several types of tumor cells in culture and xenograft

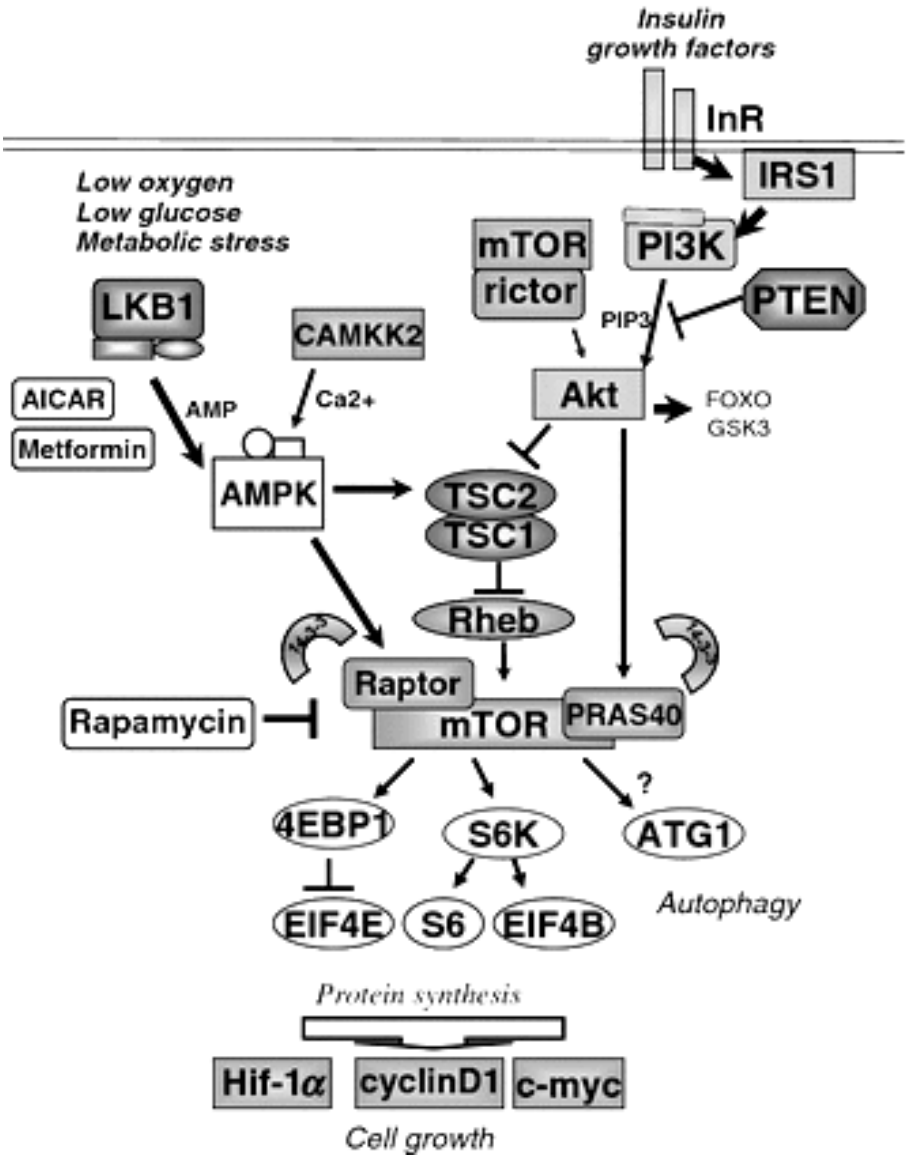


**Figure 1.4.** A longevity-defining signaling network that is centered at the mTORC1 complex of the pro-aging and pro-cancer AMPK/TOR pathway in mammalian cells. By attenuating the AMPK/TOR pathway that promotes both aging and tumorigenesis, the tumor suppressors PTEN, LKB1, TSC1 and TSC2, as well as the FDA-approved pharmaceuticals rapamycin and metformin (and their analogues): 1) slow down glycolysis, ribosome biogenesis, protein translation in the cytosol, mitochondrial ROS production, cell growth and cell cycle progression; 2) increase the efficiency of respiration, ROS detoxification and translation of oxidative phosphorylation subunits in mitochondria; 3) activate nutrient- and energy-producing autophagy aimed at the removal of damaged macromolecules and organelles; and 4) enhance stress response. The PI3K, Akt and eIF4E protein components of the pro-aging and pro-cancer signaling network centered at the mTORC1 complex function as oncogenes. PI3K and Akt activate mTORC1, whereas eIF4E is activated by mTORC1 to promote protein synthesis and cell growth. Reproduced from [38].

mouse models; ii) delay the onset or lower incidence of tumors in transgenic and carcinogen-treated mouse cancer models; and even iii) cure some types of the pre-existing human tumors in pre-clinical trials and clinical settings [160 - 164, 166 - 192].

Certain genetic, pharmacological and dietary interventions exhibit both anti-aging and anti-cancer effects by attenuating two other pro-aging signaling pathways, cAMP/PKA and insulin/IGF-1. Some of these interventions slow down only one of these two pathways, whereas others decelerate both of them or, additionally, also the pro-aging AMPK/TOR pathway and/or the sirtuin-governed protein deacetylation module of the longevity signaling network integrating all these pro-aging signaling pathways. These interventions include disruption of PKA in mice [193], growth hormone receptor and/or IGF-1 deficiencies in mice and humans [194, 195], resveratrol in mice and humans (both in cultured cells and in pre-clinical trials) (reviewed in [161, 162, 196 - 198]), as well as a CR or DR dietary regimen [10, 161, 162, 199 - 208].

Noteworthy, a growing body of evidence supports the view the interplay between aging and cancer is more complex than only sharing common aetiology and having convergent underlying mechanisms (as the commonly accepted paradigm of the relationship between aging and cancer asserts). Indeed, in some situations aging and cancer have antagonistic aetiologies and divergent underlying mechanisms [157 - 159, 209 - 223]. In these situations, the age-dependent accumulation of DNA damage and mutations in normal somatic cells (especially in adult stem and progenitor cells) triggers telomere shortening and/or a gradual rise in the expression of the *INK4a/ARF* locus [157 - 159, 211, 217 - 219, 222]. (The *INK4a/ARF* locus is known to encode two tumor suppressor proteins, namely 1) the p16INK4a protein inhibitor of the cyclin D-dependent

protein kinases CDK4 and CDK6, both of which have been shown to target RB1 and other tumor suppressor members of the retinoblastoma protein family; and 2) the p14ARF/p19ARF protein inhibitor of Mdm2/Hdm2, which has been shown to operate as an oncogene destabilizing tumor suppressor protein p53 [157 - 159, 210, 217, 218]). Both telomere shortening and transcriptional activation of the *INK4a/ARF* locus in normal somatic cells reduce their proliferative potential, thereby promoting cellular senescence, causing a decline in tissue regeneration and repair, impairing tissue homeostasis, and ultimately accelerating cellular and organismal aging [157 - 159, 210, 217 - 219, 223]. Unlike their pro-aging effects in normal somatic cells, both telomere shortening and enhanced expression of *INK4a/ARF* have been shown to exhibit potent anti-cancer effects by reducing the proliferative potential of tumor cells, thereby causing their senescence and preventing their indefinite proliferation [157 - 159, 209 - 223]. Hence, a genetic, pharmacological or dietary anti-cancer intervention that can limit the excessive proliferation of tumor cells by, for instance, inhibiting telomerase or activating expression of *INK4a/ARF* has been predicted to have a pro-aging effect on the cellular and organismal levels [157 - 159, 210, 211, 213, 215 - 218, 221, 223]. Unlike several mentioned above examples of genetic, pharmacological and/or dietary interventions that exhibit both anti-aging and anti-cancer effects by attenuating some common aetiologies of aging and cancer and targeting some of their common underlying mechanisms, the hypothesis on the envisioned pro-aging effect of those anti-cancer interventions that promote cellular senescence by causing telomere shortening and/or activating expression of *INK4a/ARF* remains to be validated.

One of the major objectives of my thesis was to examine if lithocholic acid, a novel anti-aging compound that I identified in a high-throughput chemical genetic screen, also exhibits an anti-tumor effect in cultured human cancer cells by activating certain anti-cancer processes that may (or may not) play an essential role in cellular aging. Of note, my studies described in this thesis revealed that lithocholic acid extends longevity of chronologically aging yeast not by attenuating the pro-aging AMPK/TOR and/or cAMP/PKA signaling pathways - both of which, as mentioned above in this section, have been shown to operate as pro-cancer signaling pathways in mice and humans. Therefore, I thought that an anti-tumor (if any) effect of this bile acid could be due to its ability to modulate some cellular processes whose potential essential role in the tumorigenesis process on the cellular level has not been appreciated so far. As a model for examining if lithocholic acid exhibits an anti-tumor effect in cultured human cancer cells (and if so, for establishing the mechanism underlying such effect), I choose several cell lines of the human neuroblastoma (NB) tumor.

NB is the most commonly diagnosed extracranial solid tumor among children, accounting for approximately 600 new cases diagnosed annually in the US alone [224 - 226]. All NB originate from primordial neuroblast cells that eventually differentiate into the adrenal medulla and early sympathetic nervous system [225, 227 - 229]. In over 70% of all cases studied so far, NB metastasize to other tissues, including bone, bone marrow, lymph nodes, the liver as well as the leptomeningeal and parenchymal regions of the central nervous system (CNS) [224 - 229]. Although most patients diagnosed with non-metastasizing NB have been reported to be cured, less than 40% of those with cancerous migration to other tissues survive despite rigorous chemotherapeutic and surgical

treatment [225]. Noteworthy, even though metastasis of NB to the CNS is rare, it usually coincides with recurrent high-risk cases and accounts for 1 to 16% of all patients with NB recurrence with an often fatal prognosis [226]. These high-risk NB cases regularly contain various genetic abnormalities, most notably 1) amplification of the MYCN gene [230 - 232], a transcription factor known for its role in growth, cell metabolism and division [233]; and 2) deletion of the short arm of chromosome 1p [234], which greatly reduces expression of numerous tumour-suppressing genes [235 - 238]. One of the main challenges of combating high-risk recurring NB is the use of non-toxic agents that not only prevent tumor metastasis, but also eliminate the primary tumor. Currently, NB is treated with a combination of the following seven chemotherapeutic drugs and their derivatives: doxorubicin, cisplatin, cyclophosphamide, topotecan, the epipodophyllotoxins etoposide and teniposide, and vincristine [239 - 240]. These chemotherapeutic compounds are known to induce DNA strand intercalation (doxorubicin, cisplatin, cyclophosphamide and topotecan), DNA strand breaks (epipodophyllotoxins) or mitotic inhibition (vincristine), all of which cause apoptotic death of malignant cancer cells [241 - 245]. In addition, all these anti-NB drugs have been shown to stimulate the release of significant amount of ROS from the major site of their production in mitochondria [241 - 245].

## 1.7 Thesis outline and contributions of colleagues

Chapter 2 describes how I used a combination of functional genetic, cell biological, electron and fluorescence microscopical, proteomic, lipidomic, and metabolomic analyses to investigate the effect of CR, a low-calorie dietary regimen, on

the metabolic history of chronologically aging yeast. I examined how CR influences the age-related dynamics of changes in the intracellular levels of numerous proteins and metabolites, carbohydrate metabolism, interorganellar metabolic flow, concentration of ROS, mitochondrial morphology, essential oxidation-reduction processes in mitochondria, mitochondrial proteome, frequency of mitochondrial DNA mutations, dynamics of mitochondrial nucleoid, susceptibility to mitochondria-controlled apoptosis, and stress resistance. As my comparison of the metabolic histories of long-lived CR yeast and short-lived non-CR yeast revealed, yeast define their long-term viability by designing a diet-specific pattern of metabolism and organelle dynamics prior to reproductive maturation. My data imply that longevity in chronologically aging yeast is programmed by the level of metabolic capacity and organelle organization they developed, in a diet-specific fashion, prior to entry into a non-proliferative state. Therefore, my conclusion is that chronological aging in yeast is the final step of a developmental program progressing through a series of checkpoints.

Chapter 3 describes how I designed a chemical genetic screen for small molecules that increase the chronological life span of yeast under CR by targeting lipid metabolism and modulating housekeeping longevity pathways that regulate longevity irrespective of the number of available calories. My screen identifies lithocholic acid (LCA) as one of such molecules. My evaluation of the life-extending efficacy of LCA in yeast cells on a high- or low-calorie diet revealed that this compound extends yeast chronological life span irrespective of the number of available calories. I found that the extent to which LCA extends longevity is highest under CR conditions, when the pro-aging processes modulated by the adaptable TOR and cAMP/PKA pathways are suppressed and the anti-

aging processes are activated. Furthermore, the life-extending efficacy of LCA in CR yeast significantly exceeded that in yeast on a high-calorie diet, in which the adaptable TOR and cAMP/PKA pathways greatly activate the pro-aging processes and suppress the anti-aging processes. These findings imply that, consistent with its sought-after effect on a longevity signaling network, LCA mostly targets certain housekeeping longevity assurance pathways that do not overlap (or only partially overlap) with the adaptable TOR and cAMP/PKA pathways modulated by calorie availability. Moreover, my findings presented in chapter 3 revealed two mechanisms underlying the life-extending effect of LCA in chronologically aging yeast. One mechanism operates in a calorie availability-independent fashion and involves the LCA-governed modulation of housekeeping longevity assurance pathways. The other mechanism extends yeast longevity under non-CR conditions and consists in LCA-driven unmasking of the previously unknown anti-aging potential of PKA.

Chapter 4 describes how by fusing the "xenohormesis" hypothesis [119, 343, 344], the "anti-aging side effect" hypothesis [349] and my hypothesis on longevity regulation by bile acids and rapamycin within ecosystems, I put forward a unified hypothesis of the xenohormetic, hormetic and cytostatic selective forces driving the evolution of longevity regulation mechanisms at the ecosystemic level. In my unified hypothesis, organisms from all domains of life (*i.e.*, bacteria, fungi, plants and animals) within an ecosystem are able to synthesize chemical compounds that 1) are produced and then released into the environment permanently or only in response to deteriorating environmental conditions, increased population density of competitors and/or predators, or changes in food availability and its nutrient and/or caloric content; 2) are mildly toxic

compounds that trigger a hormetic response in an organism that senses them or, alternatively, are not toxic for any organism within the ecosystem and do not cause a hormetic response; 3) are cytostatic compounds that attenuate the TOR-governed signaling network (*e.g.*, rapamycin and resveratrol) or, alternatively, do not modulate this growth-promoting network (*e.g.*, LCA and other bile acid); and 4) extend longevity of organisms that can sense these compounds, thereby increasing their chances of survival and creating selective force aimed at maintaining the ability of organisms composing the ecosystem to respond to these compounds by undergoing specific life-extending changes to their physiology. My hypothesis implies that the evolution of longevity regulation mechanisms in each group of the organisms composing an ecosystem is driven by the ability of this group of organisms to undergo specific life-extending physiological changes in response to a compendium of "critical" chemical compounds that are permanently or transiently released to the ecosystem by other groups of organisms. Chapter 4 also describes how I verified my hypothesis empirically by carrying out the LCA-driven multistep selection of long-lived yeast species under laboratory conditions. I found that a lasting exposure of wild-type yeast to LCA results in selection of yeast species that live longer in the absence of this bile acid than their ancestor. My data enabled to rank different concentrations of LCA with respect to the efficiency with which they cause the appearance of long-lived yeast species. Because the lowest used concentration of LCA resulted in the highest frequency of long-lived species appearance, I believe that it is unlikely that the life-extending mutations they carry are due to mutagenic action of this bile acid. In chapter 4, I outlined the most critical questions needed to be addressed empirically in the near future to test the validity of other aspects

of my hypothesis on the ecosystemic evolution of longevity regulation mechanisms.

Chapter 5 describes how, by examining the effect of the novel anti-aging compound LCA in cultured human neuroblastoma (NB) cancer cells, I found that this bile acid exhibits a potent anti-tumor effect in NB cells by: 1) activating both intrinsic (mitochondrial) and extrinsic (death receptor) pathways of apoptotic death in these cells; 2) sensitizing them to hydrogen peroxide-induced apoptotic death; and 3) preventing growth and proliferation of their neighbouring NB cells in the culture. Importantly, LCA does not display any of these deleterious effects in human neurons and, therefore, is a selective anti-tumor compound. My mass spectrometry-based measurement of intracellular and extracellular levels of exogenously added LCA revealed that this bile acid does not enter cultured NB cells. I therefore concluded that LCA prevents proliferation of human NB cells and selectively kills these cancer cells by binding to their surface and then initiating intracellular signaling cascades that not only impair their growth and division, but also cause their apoptotic death. The demonstrated inability of LCA to enter cultured human NB cells suggests that this potent and selective anti-cancer compound is unlikely to display undesirable side effects in non-cancerous human neurons. My findings described in chapter 5 suggest a mechanism underlying a potent and selective anti-tumor effect of LCA in cultured human NB cells. In this mechanism, LCA first binds to the G-protein-coupled receptor TGR5, the only known receptor for bile acids in the plasma membrane. In response to such binding, TGR5 and its associated protein partners: 1) transmit the signal from the plasma membrane to the mitochondrial surface to activate mitochondrial outer membrane permeabilization (MOMP); 2) activate, perhaps by a mechanism similar to the one involved in activation of the extrinsic (death

receptor) pathway of apoptosis through ligation of death receptors in the plasma membrane, the initiator caspase-8; and 3) inhibit the inflammatory caspase-1. The LCA/TGR5-induced MOMP results in efflux of cytochrome c from mitochondria, thereby causing apoptosome formation and initiator caspase-9 activation. The proteolytic cleavage of pro-caspase-3 by the enzymatically active caspase-9 elevates caspase-3 activity, thereby enabling the caspase-3-driven cleavage of pro-caspase-6 and activation of the downstream executioner caspase-6. Together, activated caspase-3 and caspase-6 (and perhaps other executioner caspases that are necessary for the proper execution of the LCA-driven, mitochondria-mediated apoptotic program) complete the demolition phase of the program by cleaving their respective protein substrates and producing the morphological features characteristic of apoptotic cell death. In LCA-exposed NB cells, the proteolytic cleavage of pro-caspase-3 and the resulting increase of caspase-3 activity (which in turn cleaves pro-caspase-6 and activates the downstream executioner caspase-6) is also triggered by the initiator caspase-8 acting in the LCA-driven extrinsic pathway of apoptosis. In addition, activated in LCA-exposed NB cells caspase-8 causes MOMP and triggers the intrinsic (mitochondrial) pathway of apoptosis by cleaving and activating the BH-3 only protein BH3-interacting domain death agonist (BID). In my model, the LCA-driven inhibition of the inflammatory caspase-1 contributes to the anti-tumor effect of LCA in cultured NB cells by attenuating the processing and unconventional secretion of the cytokines interleukin-1β and interleukin-18 - thereby preventing growth and proliferation of neighbouring NB cells in culture.

Most of the findings described in Chapter 2 have been published in *The Biochemical Society Transactions* [Goldberg, A.A., Bourque, S.D., Kyryakov, P., Boukh-

Viner, T., Gregg, C., Beach, A., Burstein, M.T., Machkalyan, G., Richard, V., Rampersad, S. and Titorenko, V.I. (2009). A novel function of lipid droplets in regulating longevity. *Biochem. Soc. Trans.* 37:1050-1055] and *Experimental Gerontology* [Goldberg, A.A., Bourque, S.D., Kyryakov, P., Gregg, C., Boukh-Viner, T., Beach, A., Burstein, M.T., Machkalyan, G., Richard, V., Rampersad, S., Cyr, D., Milijevic, S. and Titorenko, V.I. (2009). Effect of calorie restriction on the metabolic history of chronologically aging yeast. *Exp. Gerontol*. 44:555-571]. I carried out and supervised more than 30% of all of the work described in each of these publications and prepared the first draft of sections relevant to my work. I am an equally contributed first co-author on both these publications. Dr. V. Titorenko provided intellectual leadership of these projects and edited both manuscripts. Moreover, some of the findings described in Chapter 2 are presented in the manuscript of a paper [Kyryakov, P., Goldberg, A.A., Beach, A., Burstein, M.T., Richard, V.R. and Titorenko, V.I. Caloric restriction extends longevity of chronologically aging yeast in part by remodeling trehalose and glycogen metabolism] that is currently in preparation for submission to *Aging*. I expect this manuscript to be submitted for publication in late July or early August 2011.

Most of the findings described in Chapter 3 have been published in *Aging* [Goldberg, A.A., Richard, V.R., Kyryakov, P., Bourque, S.D., Beach, A., Burstein, M.T., Glebov, A., Koupaki, O., Boukh-Viner, T., Gregg, C., Juneau, M., English, A.M., Thomas, D.Y. and Titorenko, V.I. (2010). Chemical genetic screen identifies lithocholic acid as an anti-aging compound that extends yeast chronological life span in a TOR-independent manner, by modulating housekeeping longevity assurance processes. *Aging* 2:393-414]. I carried out and supervised more than 30% of the work described in this

publication and prepared the first draft of sections relevant to my work. I am an equally contributed first co-author on this publication. Dr. V. Titorenko provided intellectual leadership of this project and edited the manuscript. Moreover, some of the findings described in Chapter 3 are presented in the manuscript of a paper [Kyryakov, P., Goldberg, A.A., Beach, A., Burstein, M.T., Richard, V.R. and Titorenko, V.I. Identification of novel gerontogenes reveals a complex signaling network regulating longevity in the chronologically aging yeast *Saccharomyces cerevisiae*.] that is currently in preparation for submission to *PLoS Genetics*. I expect this manuscript to be submitted for publication in November or December 2011.

Most of the findings described in Chapter 4 have been published in *Aging* [Goldberg, A.A., Kyryakov, P., Bourque, S.D. and Titorenko, V.I. (2010). Xenohormetic, hormetic and cytostatic selective forces driving longevity at the ecosystemic level. *Aging* 2:361-370]. I carried out and supervised more than 30% of the work described in this publication and prepared the first draft of sections relevant to my work. I am an equally contributed first co-author on this publication. Dr. V. Titorenko provided intellectual leadership of this project and edited the manuscript. Moreover, some of the findings described in Chapter 4 are presented in the manuscript of a paper [Kyryakov, P., Goldberg, A.A., Koupaki, o., Beach, A., Burstein, M.T., Richard, V.R. and Titorenko, V.I. Laboratory evolution of longevity regulation mechanisms by a lasting exposure of the yeast *Saccharomyces cerevisiae* to a bile acid] that is currently in preparation for submission to *Current Biology*. I expect this manuscript to be submitted for publication in the late spring or early summer of 2012.

Most of the findings described in Chapter 5 are presented in the manuscript of a paper [Goldberg, A.A., Beach, A., Davies, G.F., Harkness, T.A.A., LeBlanc, A. and Titorenko, V.I. Lithocholic acid exhibits a potent and selective anti-tumor effect in human neuroblastoma cells by activating both intrinsic and extrinsic apoptotic death pathways and sensitizing these cells to hydrogen peroxide-induced death] that is currently in preparation for submission to *Oncotarget*. I expect this manuscript to be submitted for publication in June of 2012.

All abbreviations, citations, and the numbering of figures and tables that have been used in the published paper and in the manuscripts in preparation have been changed to the format of this thesis.

# 2 Aging is the final step of a developmental program: The longevity of chronologically aging yeast is programmed by the level of metabolic capacity and organelle organization they developed, in a diet-specific fashion, prior to entry into a non-proliferative state

## 2.1 Abstract

Aging of multicellular and unicellular eukaryotic organisms is a multifactorial biological phenomenon that has various causes and affects a plethora of cellular activities [1 - 16]. I employ the yeast *Saccharomyces cerevisiae* as a model to study the basic biology and molecular mechanisms of cellular aging in multicellular eukaryotes [24, 246 - 248]. The use of this budding yeast as an advantageous model organism in aging research greatly contributed to the current understanding of the molecular and cellular mechanisms underlying longevity regulation in evolutionarily distant eukaryotic organisms, thereby convincingly demonstrating that longevity signaling pathways and mechanisms of their modulation by dietary and pharmacological interventions are conserved across phyla [6, 7, 31, 79, 134, 151 - 153].

To address the inherent complexity of aging from a systems perspective and to build an integrative spatiotemporal model of aging process, I investigated the effect of caloric restriction (CR), a low-calorie dietary regimen, on the metabolic history of chronologically aging yeast. CR has been shown not only to exhibit a robust longevity-extending effect in evolutionarily distant organisms ranging from yeast to rhesus monkeys, but also to improve health by attenuating age-related pathologies and delaying the onset of age-related diseases across phyla [76 - 83]. I examined how CR influences

the age-related dynamics of changes in the intracellular levels of numerous proteins and metabolites, carbohydrate metabolism, interorganellar metabolic flow, concentration of reactive oxygen species (ROS), mitochondrial morphology, essential oxidation-reduction processes in mitochondria, mitochondrial proteome, frequency of mitochondrial DNA mutations, dynamics of mitochondrial nucleoid, susceptibility to mitochondria-controlled apoptosis, and stress resistance.

Based on my comparison of the metabolic histories of long-lived CR yeast and short-lived non-CR yeast reported here, I concluded that yeast define their long-term viability by designing a diet-specific pattern of metabolism and organelle dynamics prior to reproductive maturation. My data imply that longevity in chronologically aging yeast is programmed by the level of metabolic capacity and organelle organization they developed, in a diet-specific fashion, prior to entry into a non-proliferative state. Therefore, my conclusion is that chronological aging in yeast is the final step of a developmental program progressing through a series of checkpoints.

## 2.2 Introduction

Aging is a highly complex biological phenomenon, which affects numerous processes within cells [1 - 16]. These cellular processes include cell cycle, cell growth, stress response, protein folding, apoptosis, autophagy, proteasomal protein degradation, actin organization, signal transduction, nuclear DNA replication, chromatin assembly and maintenance, ribosome biogenesis and translation, lipid and carbohydrate metabolism, oxidative metabolism in mitochondria, $NAD^+$ homeostasis, amino acid biosynthesis and degradation, and ammonium and amino acid uptake [5, 10, 13, 100, 31 - 34]. Some of

these processes damage cellular macromolecules and organelles, while the others prevent the collapse of cellular homeostasis by repairing the damage [1 - 3, 10, 13]. A lifelong accumulation of unrepaired cellular damage increases a risk of disease and death [1, 2, 11, 13]. A challenge is to understand how the spatiotemporal organization of damage-producing and damage-repairing processes influences longevity and how cells integrate and control these processes. The most important unanswered question is whether aging is the final step of a developmental program governed by a certain signaling network [19 - 24] or merely a result of the lifelong accumulation of unrepaired cellular and molecular damage [1, 3, 12 - 18]. To identify the cellular processes that play a critical role in longevity regulation and to rank their relative contributions to aging, the concepts and methodologies of so-called metabolic control analysis (MCA) can be useful [1, 8]. It has been envisioned that the application of these concepts and methodologies to the analysis of empirical data on the cell metabolic histories of model organisms will enable to 1) infer the relative contributions of various cellular processes to aging; and 2) define how interventions such as dietary restriction delay aging by modulating these processes [1, 8].

The budding yeast *Saccharomyces cerevisiae* is a valuable model for studying the basic biology of aging and revealing longevity regulation mechanisms in multicellular eukaryotes [6, 34, 152]. There are two different paradigms of aging of this unicellular eukaryote amenable to comprehensive biochemical, genetic, cell biological, chemical biological and system biological analyses. In the replicative aging paradigm, yeast aging is defined by the maximum number of daughter cells that a mother cell can produce before becoming senescent (Figure 1.2) [6, 31]. Replicative aging in yeast mimics aging of dividing ("mitotic") cells in a multicellular eukaryotic organism [6, 31]. In the

chronological aging paradigm, yeast aging is defined by the length of time during which a cell remains viable following entry into a non-proliferative state (Figure 1.2) [6, 63, 152]. Chronological aging in yeast is an advantageous model for studying aging of non-dividing ("post-mitotic") cells in a multicellular eukaryotic organism [6, 63, 152]. Yeast chronological aging is assessed using a simple clonogenic assay, which measures the percentage of yeast cells that remain viable at different time points following the entry of a cell population into the non-proliferative stationary phase [63]. A CR diet, which in yeast can be imposed by reducing the initial glucose concentration in a growth medium from 2% to 0.5% or lower, decelerates both replicative and chronological aging of yeast [6, 35, 63, 151].

In studies described in this chapter, I made a first step towards the use of MCA for defining the molecular causes of cellular aging by elucidating the effect of CR on the metabolic history of chronologically aging yeast. My comparison of the metabolic histories of long-lived CR yeast and short-lived non-CR yeast led me to the conclusion that longevity in chronologically aging yeast is programmed by the level of metabolic capacity and organelle organization they developed, in a diet-specific fashion, prior to reproductive maturation. I therefore propose here that chronological aging in yeast is the final step of a developmental program. By unveiling the different scenarios for a stepwise establishment of patterns of metabolism, inter-organellar communications and mitochondrial morphology in chronologically aging CR and non-CR yeast, my study enabled to define a distinct group of cellular metabolites and processes that play an essential role in longevity regulation.

## 2.3 Materials and Methods

### Strains and media

The wild-type strain *Saccharomyces cerevisiae* BY4742 (*MATα his3Δ1 leu2Δ0 lys2Δ0 ura3Δ0*) and mutant strains *tps1Δ* (*MATα his3Δ1 leu2Δ0 lys2Δ0 ura3Δ0 tps1Δ::kanMX4*), *tps2Δ* (*MATα his3Δ1 leu2Δ0 lys2Δ0 ura3Δ0 pex5Δ::kanMX4*), *pex6Δ* (*MATα his3Δ1 leu2Δ0 lys2Δ0 ura3Δ0 tps2Δ::kanMX4*), *tps3Δ* (*MATα his3Δ1 leu2Δ0 lys2Δ0 ura3Δ0 tps3Δ::kanMX4*), *tsl1Δ* (*MATα his3Δ1 leu2Δ0 lys2Δ0 ura3Δ0 tsl1Δ::kanMX4*), *ath1Δ* (*MATα his3Δ1 leu2Δ0 lys2Δ0 ura3Δ0 ath1Δ::kanMX4*), *nth1Δ* (*MATα his3Δ1 leu2Δ0 lys2Δ0 ura3Δ0 nth1Δ::kanMX4*), *nth2Δ* (*MATα his3Δ1 leu2Δ0 lys2Δ0 ura3Δ0 nth2Δ::kanMX4*), *tpk1Δ* (*MATα his3Δ1 leu2Δ0 lys2Δ0 ura3Δ0 tpk1Δ::kanMX4*), *glg2Δ* (*MATα his3Δ1 leu2Δ0 lys2Δ0 ura3Δ0 glg2Δ::kanMX4*), *glc3Δ* (*MATα his3Δ1 leu2Δ0 lys2Δ0 ura3Δ0 glc3Δ::kanMX4*), *gsy2Δ* (*MATα his3Δ1 leu2Δ0 lys2Δ0 ura3Δ0 gsy2Δ::kanMX4*), *pig1*Δ (*MATα his3Δ1 leu2Δ0 lys2Δ0 ura3Δ0 pig1Δ::kanMX4*), *pcl8Δ* (*MATα his3Δ1 leu2Δ0 lys2Δ0 ura3Δ0 pcl8Δ::kanMX4*), *gph1Δ* (*MATα his3Δ1 leu2Δ0 lys2Δ0 ura3Δ0 gph1Δ::kanMX4*), *gdb1Δ* (*MATα his3Δ1 leu2Δ0 lys2Δ0 ura3Δ0 gdb1Δ::kanMX4*), *snf1Δ* (*MATα his3Δ1 leu2Δ0 lys2Δ0 ura3Δ0 snf1Δ::kanMX4*) and *tpk1Δ* (*MATα his3Δ1 leu2Δ0 lys2Δ0 ura3Δ0 tpk1Δ::kanMX4*) were used in this study. Media components were as follows: 1) YEPD (0.2% Glucose), 1% yeast extract, 2% peptone, 0.2% glucose; and 2) YEPD (2% Glucose), 1% yeast extract, 2% peptone, 2% glucose.

### A plating assay for the analysis of chronological life span

Cells were grown in YEPD (0.2% Glucose) medium at 30°C with rotational shaking at 200 rpm in Erlenmeyer flasks at a flask volume/medium volume ratio of 5:1. A sample of cells was removed from each culture at various time points. A fraction of the cell sample was diluted in order to determine the total number of cells per ml of culture using a hemacytometer. 10 µl of serial dilutions (1:10 to $1:10^3$) of cells were applied to the hemacytometer, where each large square is calibrated to hold 0.1 µl. The number of cells in 4 large squares was then counted and an average was taken in order to ensure greater accuracy. The concentration of cells was calculated as follows: number of cells per large square x dilution factor × 10 × 1,000 = total number of cells per ml of culture. A second fraction of the cell sample was diluted and serial dilutions ($1:10^2$ to $1:10^5$) of cells were plated onto YEPD (2% Glucose) plates in triplicate in order to count the number of viable cells per ml of each culture. 100 µl of diluted culture was plated onto each plate. After a 48-h incubation at 30°C, the number of colonies per plate was counted. The number of colony forming units (CFU) equals to the number of viable cells in a sample. Therefore, the number of viable cells was calculated as follows: number of colonies × dilution factor × 10 = number of viable cells per ml. For each culture assayed, % viability of the cells was calculated as follows: number of viable cells per ml / total number of cells per ml × 100%. The % viability of cells in mid-logarithmic phase was set at 100% viability for that particular culture.

**Plating assays for the analysis of resistance to various stresses**

For the analysis of hydrogen peroxide resistance, serial dilutions ($1:10^0$ to $1:10^5$) of wild-type and mutant cells removed from mid-logarithmic phase (day 1) and from diauxic

phase (days 2 and 3) in YEPD (0.2% Glucose) were spotted onto two sets of plates. One set of plates contained YEPD (2% Glucose) medium alone, whereas the other set contained YEPD (2% Glucose) medium supplemented with 5 mM hydrogen peroxide. Pictures were taken after a 3-day incubation at 30$^{o}$C.

For the analysis of oxidative stress resistance, serial dilutions (1:$10^{0}$ to 1:$10^{5}$) of wild-type and mutant cells removed from mid-logarithmic phase (day 1) and from diauxic phase (days 2 and 3) in YEPD (0.2% Glucose) were spotted onto two sets of plates. One set of plates contained YEPD (2% Glucose) medium alone, whereas the other set contained YEPD (2% Glucose) medium supplemented with 2.5 mM of the superoxide/hydrogen peroxide-generating agent paraquat. Pictures were taken after a 3-day incubation at 30$^{o}$C.

For the analysis of heat-shock resistance, serial dilutions (1:$10^{0}$ to 1:$10^{5}$) of wild-type and mutant cells removed from mid-logarithmic phase (day 1) and from diauxic phase (days 2 and 3) in YEPD (0.2% Glucose) were spotted onto two sets of YEPD (2% Glucose) plates. One set of plates was incubated at 30$^{o}$C. The other set of plates was initially incubated at 55$^{o}$C for 30 min, and was then transferred to 30$^{o}$C. Pictures were taken after a 3-day incubation at 30$^{o}$C.

For the analysis of salt stress resistance, serial dilutions (1:$10^{0}$ to 1:$10^{5}$) of wild-type and mutant cells removed from mid-logarithmic phase (day 1) and from diauxic phase (days 2 and 3) in YEPD (0.2% Glucose) were spotted onto two sets of plates. One set of plates contained YEPD (2% Glucose) medium alone, whereas the other set contained YEPD (2% Glucose) medium supplemented with 0.5 M NaCl. Pictures were taken after a 3-day incubation at 30$^{o}$C.

For the analysis of osmotic stress resistance, serial dilutions ($1:10^0$ to $1:10^5$) of wild-type and mutant cells removed from mid-logarithmic phase (day 1) and from diauxic phase (days 2 and 3) in YEPD (0.2% Glucose) were spotted onto two sets of plates. One set of plates contained YEPD (2% Glucose) medium alone, whereas the other set contained YEPD (2% Glucose) medium supplemented with 1 M sorbitol. Pictures were taken after a 3-day incubation at 30°C.

**Monitoring the formation of ROS**

Wild-type and mutant cells grown in YEPD (0.2% Glucose) were tested microscopically for the production of ROS by incubation with dihydrorhodamine 123 (DHR). In the cell, this nonfluorescent compound can be oxidized to the fluorescent chromophore rhodamine 123 by ROS. Cells were also probed with a fluorescent counterstain Calcofluor White M2R (CW), which stains the yeast cell walls fluorescent blue. CW was added to each sample in order to label all cells for their proper visualization. DHR was stored in the dark at –20°C as 50 µl aliquots of a 1 mg/ml solution in ethanol. CW was stored in the dark at –20°C as the 5 mM stock solution in anhydrous DMSO (dimethylsulfoxide).

The concurrent staining of cells with DHR and CW was carried out as follows. The required amounts of the 50 µl DHR aliquots (1 mg/ml) and of the 5 mM stock solution of CW were taken out of the freezer and warmed to room temperature. The solutions of DHR and CW were then centrifuged at 21,000 × g for 5 min in order to clear them of any aggregates of fluorophores. For cell cultures with a titre of ~ $10^7$ cells/ml, 100 µl was taken out of the culture to be treated. If the cell titre was lower, proportionally larger volumes were used. 6 µl of the 1 mg/ml DHR and 1 µl of the 5 mM CW solutions were

added to each 100 µl aliquot of culture. After a 2-h incubation in the dark at room temperature, the samples were centrifuged at 21,000 × g for 5 min. Pellets were resuspended in 10 µl of PBS buffer (20 mM $KH_2PO_4$/KOH, pH 7.5, and 150 mM NaCl). Each sample was then supplemented with 5 µl of mounting medium, added to a microscope slide, covered with a coverslip, and sealed using nail polish. Once the slides were prepared, they were visualized under the Zeiss Axioplan fluorescence microscope mounted with a SPOT Insight 2 megapixel color mosaic digital camera. Several pictures of the cells on each slide were taken, with two pictures taken of each frame. One of the two pictures was of the cells seen through a rhodamine filter in order to detect cells dyed with DHR. The second picture was of the cells seen through a DAPI filter in order to visualize CW, and therefore all the cells present in the frame.

For evaluating the percentage of DHR-positive cells, the UTHSCSA Image Tool (Version 3.0) software was used to calculate both the total number of cells and the number of stained cells. Fluorescence of individual DHR-positive cells in arbitrary units was determined by using the UTHSCSA Image Tool software (Version 3.0). In each of 3-5 independent experiments, the value of median fluorescence was calculated by analyzing at least 800-1000 cells that were collected at each time point. The median fluorescence values were plotted as a function of the number of days cells were cultured.

**Immunofluorescence microscopy**

Cell cultures were fixed in 3.7% formaldehyde for 45 min at room temperature. The cells were washed in solution B (100 mM $KH_2PO4$/KOH pH 7.5, 1.2 M sorbitol), treated with Zymolyase 100T (MP Biomedicals, 1 µg Zymolyase 100T/1 mg cells) for 30 min at 30$^{o}$C

and then processed as previously described [249]. Monoclonal antibody raised against porin (Invitrogen, 0.25 μg/μl in TBSB buffer [20 mM Tris/HCl pH 7.5, 150 mM NaCl, 1 mg/ml BSA]) was used as a primary antibody. Alexa Fluor 568 goat anti-mouse IgG (Invitrogen, 2 μg/μl in TBSB buffer) was used as a secondary antibody. The labeled samples were mounted in mounting solution (16.7 mM Tris/HCl pH 9.0, 1.7 mg/ml *p*-phenylenediamine, 83% glycerol). Images were collected with a Zeiss Axioplan fluorescence microscope (Zeiss) mounted with a SPOT Insight 2 megapixel color mosaic digital camera (Spot Diagnostic Instruments).

**Oxygen consumption assay**

The rate of oxygen consumption by yeast cells recovered at various time points was measured continuously in a 2-ml stirred chamber using a custom-designed biological oxygen monitor (Science Technical Center of Concordia University) equipped with a Clark-type oxygen electrode. 1 ml of YEPD medium supplemented with 0.2% glucose was added to the electrode for approximately 5 minutes to obtain a baseline. Cultured cells of a known titre were spun down at 3,000 × g for 5 minutes. The resulting pellet was resuspended in YEPD medium supplemented with 0.2% glucose and then added to the electrode with the medium that was used to obtain a baseline. The resulting slope was used to calculate the rate of oxygen consumption in $O_2$% x $min^{-1}$ × $10^9$ cells.

**Measurement of mitochondrial mutations and nuclear mutations affecting mitochondrial components**

The frequency of spontaneous single-gene (*mit*$^-$ and *syn*$^-$) and deletion (*rho*$^-$ and *rho*$^o$) mutations in mitochondrial DNA (mtDNA) and spontaneous single-gene nuclear mutations (*pet*$^-$) affecting essential mitochondrial components was evaluated by measuring the fraction of respiratory-competent (*rho*$^+$) yeast cells remaining in their aging population. *rho*$^+$ cells maintained intact their mtDNA and their nuclear genes encoding essential mitochondrial components. Therefore, *rho*$^+$ cells were able to grow on glycerol, a non-fermentable carbon source. In contrast, mutant cells deficient in mitochondrial respiration were unable to grow on glycerol. Most of these mutant cells carried mutations in mtDNA (including single-gene *mit*$^-$ and *syn*$^-$ mutations or large deletions *rho*$^-$) or completely lacked this DNA (*rho*$^o$ mutants), whereas some of them carried so-called *pet*$^-$ mutations in nuclear genes that code for essential mitochondrial components [250]. Serial dilutions of cell samples removed from different phases of growth were plated in duplicate onto YP plates containing either 2% glucose or 3% glycerol as carbon source. Plates were incubated at 30$^o$C. The number of CFU on YP plates containing 2% glucose was counted after 2 d of incubation, whereas the number of CFU on YP plates containing 3% glycerol was counted after 6 d of incubation. For each culture, the percentage of respiratory-deficient (*mit*$^-$, *syn*$^-$, *rho*$^-$, *rho*$^o$ and *pet*$^-$) cells was calculated as follows: 100 - [(number of CFU per ml on YP plates containing 3% glycerol/number of CFU per ml on YP plates containing 2% glucose) × 100]. The frequency of spontaneous point mutations in the *rib2* and *rib3* loci of mtDNA was evaluated by measuring the frequency of mtDNA mutations that caused resistance to the antibiotic erythromycin [251]. These mutations impair only mtDNA [252, 253]. In each of the seven independent experiments performed, ten individual yeast cultures were

grown in YP medium containing 0.2%, 0.5%, 1% or 2% glucose as carbon source. A sample of cells was removed from each culture at various time-points. Cells were plated in duplicate onto YP plates containing 3% glycerol and erythromycin (1 mg/ml). In addition, serial dilutions of each sample were plated in duplicate onto YP plates containing 3% glycerol as carbon source for measuring the number of respiratory-competent (*rho*$^{+}$) cells. The number of CFU was counted after 6 d of incubation at 30$^{o}$C. For each culture, the frequency of mutations that caused resistance to erythromycin was calculated as follows: number of CFU per ml on YP plates containing 3% glycerol and erythromycin/number of CFU per ml on YP plates containing 3% glycerol.

**Preparation of total cell lysates**

An aliquot containing 1 × $10^{9}$ cells was centrifuged for 7 min at 3,000 rpm at room temperature. Pelleted cells were washed twice with distilled water and further centrifuged for 3 min at 16,000 × g at room temperature. The recovered cell pellet was then resuspended in 500 µl of 4% CHAPS in 25 mM Tris/HCl buffer (pH 8.5) and centrifuged for 15 sec at 16,000 × g at room temperature. The cells were then washed again, first by resuspending them in 500 µl of 4% CHAPS in 25 mM Tris/HCl buffer (pH 8.5) and then by centrifuging for 15 sec at 16,000 × g at room temperature. The pellet of washed cells was then resuspended in 1 ml of ice-cold 4% CHAPS in 25 mM Tris/HCl buffer (pH 8.5), divided into 5 equal aliquots of 200 µl each and placed in Eppendorf tubes kept on ice. Each 200 µl aliquot was supplemented with ~100 µl of glass beads and vortexed three times for 1 minute. Apart from the vortexing steps, the samples were kept on ice at all times. Glass beads and cell debris were then pelleted by 5 min centrifugation at 16,000 ×

g at 4°C. The resulting supernatant of the glass bead lysate was immediately transferred into a pre-chilled Eppendorf tube and stored at -20°C for further analysis.

**Isolation of the crude mitochondrial fraction**

Yeast cells were pelleted at 3,000 × g for 5 min at room temperature, washed twice with distilled water, resuspended in DTT buffer (100 mM Tris-$H_2SO_4$, pH 9.4, 10 mM dithiothreitol [DTT]), and incubated for 20 min at 30°C to weaken the cell wall. The cells were then washed with Zymolyase buffer (1.2 M sorbitol, 20 mM potassium phosphate, pH 7.4), centrifuged at 3,000 × g for 5 min at room temperature, and incubated with 3 mg/g (wet wt) of Zymolyase-100T in 7 ml/g (wet wt) Zymolyase buffer for 45 min at 30°C. Following an 8-min centrifugation at 2,200 × g at 4°C, the isolated spheroplasts were washed in ice-cold homogenization buffer (5 ml/g) (0.6 M sorbitol, 10 mM Tris-HCl, pH7.4, 1 mM EDTA, 0.2% (w/v) BSA) and then centrifuged at 2,200 × g for 8 min at 4°C. Washed spheroplasts were homogenized in ice-cold homogenization buffer using 15 strokes. The cell debris was removed by centrifuging the resulting homogenates at 1,500 × g for 5 min at 4°C. The supernatant was further centrifuged at 3,000 × g for 5 min at 4°C to remove residual cell debris. The resulting supernatant was then centrifuged at 12,000 × g for 15 min at 4°C to pellet mitochondria. The remnant cell debris was removed by centrifuging the mitochondrial fraction at 3,000 × g for 5 min at 4°C. The resulting supernatant was then centrifuged at 12,000 × g for 15 min at 4°C to obtain the crude mitochondrial pellet, which was then resuspended in 3 ml of SEM Buffer (250 mM sucrose, 1 mM EDTA, 10 mM MOPS, pH 7.2) and used for the purification of mitochondria as described below.

**Purification of mitochondria devoid of microsomal and cytosolic contaminations**

A sucrose gradient was made by carefully overlaying 1.5 ml of 60% sucrose with 4 ml of 32% sucrose, 1.5 ml of 23% sucrose, and then 1.5 ml of 15% sucrose (all in EM buffer; 1 mM EDTA, 10 mM MOPS, pH 7.2). Finally, a 3-ml aliquot of the crude mitochondrial fraction in SEM buffer was applied to the gradient and centrifuged at 134,000 × g (33,000 rpm) overnight at 2°C in vacuum (Rotor SW50Ti, Beckman). The purified mitochondria found at the 60%/32% sucrose interface were carefully removed and stored at - 80°C.

**Protein precipitation, SDS-PAGE and silver staining of gels**

Protein concentration was determined using the RC DC protein assay kit (Bio-Rad) according to the manufacturer's instructions. Proteins were precipitated by adding trichloroacetic acid (TCA) to the final concentration of 10%, incubated on ice for 30 min, pelleted by centrifugation, and then washed with ice-cold 80% acetone. Dried protein pellets were then resuspended in the SDS-PAGE sample buffer and the pH was adjusted to neutral using 2 M Tris/HCl (pH 8.8). The samples were boiled for 5 min at 63°C, centrifuged for 30 sec at 16,000 x g, loaded onto a 7.5%, 10%, 12.5% or 16% gel and resolved by SDS-PAGE. Following an overnight incubation of the gels in 50% methanol, proteins were visualized by silver staining using the mass spectrometry-compatible silver staining kit (Bio-Rad Silver Staining Plus) according to the manufacturer's instructions. The Bio-Rad unstained molecular marker and a 0.1 mg/ml solution of BSA in the SDS-

PAGE sample buffer were also subjected to SDS-PAGE. The proteins were then visualized by silver staining.

**Analysis of proteins by mass spectrometry**

Proteins were resolved by SDS-PAGE and visualized by silver staining [254]. Protein bands were excised from the gel, reduced, alkylated and in-gel digested with trypsin [254]. The proteins were identified by matrix-assisted laser desorption/ionization mass spectrometric (MALDI MS) peptide mapping [255], using a Micromass M@LDI time-of-flight (TOF) mass spectrometer (Waters). Database searching using peptide masses was performed with the Mascot web-based search engine. For evaluating relative levels of individual proteins recovered in total cell lysates or purified mitochondria, a selected protein band was excised from the silver-stained gel and placed into an Eppendorf tube. A band of BSA containing 2 μg of this protein, which was also excised from the silver-stained gel, was added to each of the protein bands to be analyzed. Protein bands were reduced, alkylated and in-gel digested with trypsin [254]. The desalted peptide mixture was added to the surface of a MALDI target plate and allowed to air dry. The sample spot was then overlaid with MALDI matrix solution containing the Angiotensin I peptide standard (1:1 ratio). The presence of Angiotensin I in the sample carrying the analyzed mixture of peptides provided an additional estimate of the mass measurement accuracy after calibration, giving an opportunity to calculate the value of peptide mass tolerance for each individual mass spectrum. After the desalted peptide mixture was analyzed by MALDI-TOF, the monoisotopic masses of recovered BSA peptides and the intensities of their monoisotopic peaks were grouped separately from the masses and intensities of

peptides originated from the protein of interest. These data provided an additional estimate of the mass measurement accuracy and were used for the quantitation of relative levels of the same protein recovered in different samples. For evaluating relative levels of the protein of interest found in the samples to be compared, a ratio "the intensity of the monoisotopic peak of a peptide originated from the protein of interest/the intensity of the monoisotopic peak of a BSA peptide with the monoisotopic mass closest to the mass of the peptide of interest" was calculated for each peptide originated from the protein of interest. Based on these data, the average value for relative levels of the protein of interest found in the two compared samples was calculated. The method for evaluating relative levels of the protein of interest recovered in different samples was validated by calculating relative levels of several standard proteins in the samples supplemented with different quantities of each of these proteins.

**Miscellaneous procedures**

SDS-PAGE and immunoblotting using a Trans-Blot SD semi-dry electrophoretic transfer system (Bio-Rad) were performed as previously described [256]. Blots were decorated with monoclonal antibodies raised against actin (Abcam) or porin (Invitrogen) or polyclonal antisera raised against Aco1p (kind gift of Dr. Ronald A. Butow, University of Texas Southwestern Medical Center) or cytochrome c (kind gift of Dr. Roland Lill, Philipps Universität Marburg). Antigen-antibody complexes were detected by enhanced chemiluminescence using an Amersham ECL Western blotting detection reagents (GE Healthcare). Purification of *in organello* formaldehyde-fixed proteins that bind to mitochondrial DNA was performed as previously described [257]. Enzymatic activities

of cytochrome c oxidase [258], succinate dehydrogenase [259] and aconitase [260] were determined by established methods. Preparation of cellular extracts and microanalytic biochemical assays for measuring ATP, glucose, trehalose and glycogen concentrations was performed as previously described [261].

## 2.4 Results

### 2.4.1 My rationale for choosing a nutrient-rich growth medium for studying yeast chronological aging

To study the effect of CR on the chronological life span of yeast, I cultured the wild-type strain BY4742 in the nutrient-rich YP (1% yeast extract, 2% peptone) medium initially containing 0.2%, 0.5%, 1% or 2% glucose. I chose YP medium for chronological aging studies because, in contrast to a synthetic medium, it is rich in amino acids, nucleotides, vitamins and other nutrients. I therefore thought that the reduction of glucose concentration in YP medium would lower the number of available calories without compromising the supply of essential nutrients, thereby modeling a traditional CR dietary regimen established in experiments with laboratory rodents [65, 55, 135, 262]. An equally important reason for choosing YP medium for chronological aging studies was that the recent isolation of quiescent and nonquiescent cells from yeast stationary (ST)-phase cultures grown in this medium provided a novel, valuable system for elucidating the mechanisms linking chronological aging to quiescence, the mitotic cell cycle and apoptosis [263, 264]. Furthermore, the shape of mortality curves for yeast grown in the nutrient-rich YP medium to ST phase was similar to mortality patterns observed in

multicellular eukaryotes; their mortality rates increased with age and then reached a plateau at advanced age [265]. This is in contrast to yeast grown in the nutrient-limited SC (synthetic complete) medium. Although this medium has been chosen for studies of chronologically aging yeast to mimic their survival in the wild [266], age-specific death rates of yeast that have reached ST phase in SC medium exhibited a complicated pattern that was not reminiscent of the shape of mortality curves seen in multicellular organisms [265]. I therefore thought that yeast cultured in the nutrient-rich YP medium would be a better model system for elucidating the mechanisms underlying chronological aging of multicellular eukaryotes, as compared to yeast incubated in the nutrient-limited SC medium.

Moreover, it is well known that homeostatic mechanisms maintain the pH values of body fluids (such as blood, semen, cerebrospinal fluid, pancreatic juice and bile) between 7.1 and 8.6 [267]. These pH values are much closer to those observed in yeast cultures grown in YP medium [24] than to the considerably more acidic pH of yeast cultures cultivated in SC medium [268]. This fact was another reason for which I chose YP medium for studying mechanisms of chronological aging.

My choice of the strain BY4742 was based on its relatively short chronological life span [269], thereby offering considerable time savings for chronological aging studies of yeast cultivated in YP medium. Importantly, this yeast strain serves as one of the two haploid genetic backgrounds of the widely used Open Biosystems' Yeast Knock-Out Collection.

### 2.4.2 CR extends the chronological life span of yeast

The full growth cycle of yeast cultured in YP medium initially containing 0.2%, 0.5%, 1% or 2% glucose began with logarithmic (L) phase and progressed through diauxic (D) and post-diauxic (PD) phases to stationary (ST) phase (Figure 2.1A). The rates of growth (Figure 2.1A) and glucose consumption (Figure 2.1B) in L phase were similar for cells cultured in any of the four media, whereas the maximum cell density in ST-phase cultures varied within a 28-% range and correlated with the initial glucose concentration (Figure 2.1A). CR cells grown on 0.2% or 0.5% glucose lived significantly longer than cells grown under non-CR conditions on 1% or 2% glucose (Figure 2.1C). In fact, the mean chronological life span of cells grown on 0.2% glucose was extended by more than 60% and that of cells grown on 0.5% glucose was extended by almost 2-fold, as compared to the mean chronological life span of cells grown on 2% glucose (Figure 2.1D).

Noteworthy, unlike yeast cells grown in the nutrient-limited SC medium [270, 271], cells cultured in the nutrient-rich YP medium with 0.5% glucose lived longer than cells cultured in YP medium containing 0.05% glucose (Figure 2.2). Thus, the largest increase in the chronological life span of yeast grown under CR conditions in YP medium occurs at 0.5% glucose. The observed difference in the lowest concentration of glucose that is optimal for life-span extension under CR conditions between yeast grown in SC or YP medium could be due to at least two factors. First, YP medium is enriched, as compared to SC medium, in amino acids, nucleotides, vitamins and other essential nutrients. It is conceivable that at least some of these nutrients could modulate the effect of different glucose concentrations on chronological life span by influencing certain metabolic and/or nutrient-sensing signaling pathways operating in CR yeast. Second, the

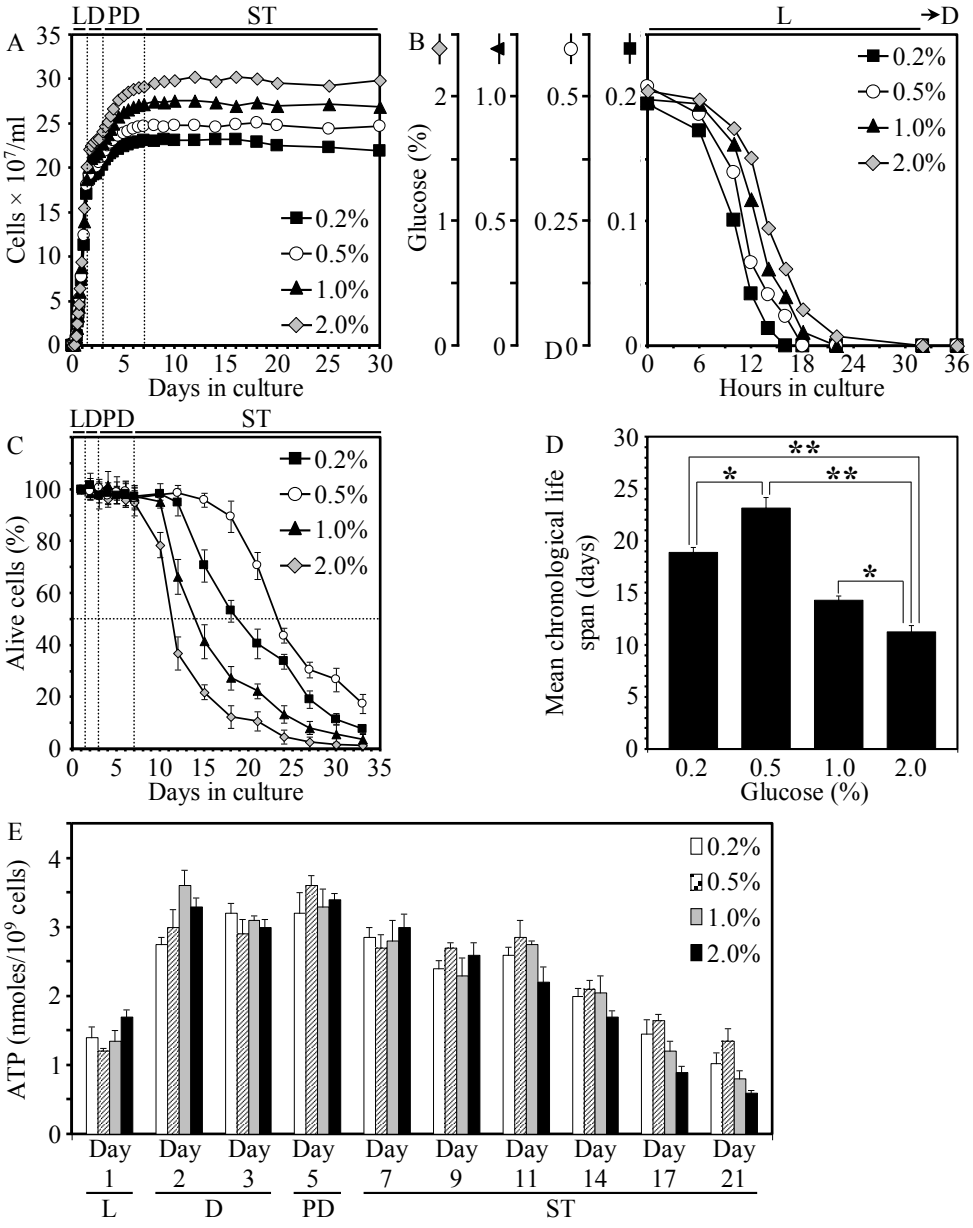


**Figure 2.1.** CR extends the chronological life span of yeast. (A and B) Kinetics of growth (A) and glucose consumption (B) for the WT strain BY4742. Each plot shows a representative experiment repeated 4-6 times in triplicate with similar results. (C) Survival of chronologically aging WT cells. Data are presented as mean ± SEM (n = 16-28). $p < 0.001$ at days 10 to 33 for cells grown on 0.2% or 0.5% glucose vs. cells grown on 2% glucose. (D) The mean chronological life spans of WT cells. Data are presented as mean ± SEM (n = 16-28); *$p < 0.01$, **$p < 0.001$. (E) ATP levels in chronologically aging WT cells. Data are presented as mean ± SEM (n = 3-5). (A-E) Cells were cultured in YP medium containing 0.2%, 0.5%, 1% or 2% glucose. Abbreviations: Diauxic (D), logarithmic (L), post-diauxic (PD) or stationary (ST) phase.

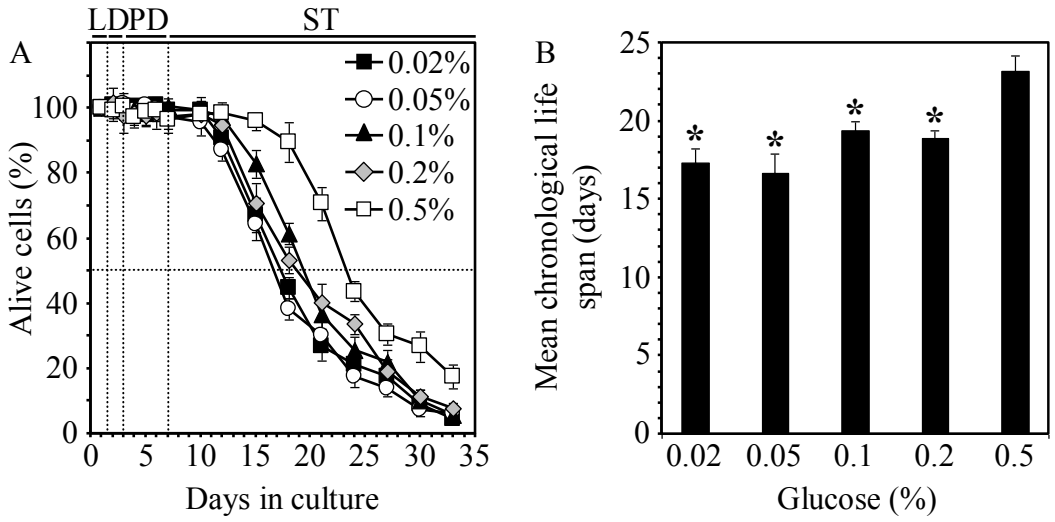


**Figure 2.2.** Survival of the chronologically aging wild-type strain BY4742 (A) and the mean chronological life spans of different cultures of BY4742 (B) grown in YP medium initially containing 0.02%, 0.05%, 0.1%, 0.2% or 0.5% glucose. Data are presented as mean ± SEM (n = 3 for cells grown on 0.02%, 0.05% or 0.1% glucose; n = 35 for cells grown on 0.2% glucose; n = 24 for cells grown on 0.5% glucose). *$p < 0.01$ (for cells grown on 0.02%, 0.05%, 0.1% or 0.2% glucose vs. cells grown on 0.5% glucose). Abbreviations: Diauxic (D), logarithmic (L), post-diauxic (PD) or stationary (ST) phase.

initial pH in yeast cultures grown in SC medium was 3.9-4.0 [268], whereas in yeast cultures grown in YP medium it was 6.9 [24]. Furthermore, both the dynamics of age-related changes in the pH of culture medium and the final medium pH reached after several days of growth in SC with 0.5% or 0.05% glucose [268] differ from those observed for yeast that aged chronologically in YP medium containing either of these two glucose concentrations [24]. It is feasible that such differences between SC and YP in the initial pH and/or its age-related homeostasis could contribute to the observed difference between these two media in the lowest concentration of glucose at which the highest beneficial effect of CR on chronological life span can be achieved.

Importantly, ATP levels and the dynamics of their change during chronological aging were very similar for CR and non-CR yeast (Figure 2.1E). Thus, CR yeast are not

starving. Based on this important conclusion, I hypothesized that: 1) CR yeast remodel their metabolism in order to match the level of ATP produced in non-CR yeast; and 2) such specific remodeling of metabolism in CR yeast prolongs their life span.

### 2.4.3 CR remodels the metabolism of trehalose and glycogen

To examine how exactly CR yeast remodel their metabolism in order to match the level of ATP generated in non-CR yeast, I first monitored the intracellular levels of trehalose and glycogen, the two major glucose stores of yeast [272].

Yeast began to accumulate trehalose when they entered PD phase (Figure 2.3B). Trehalose levels increased during PD and ST phases. The rise of trehalose was considerably greater in slowly aging CR yeast than in rapidly aging non-CR yeast (Figure 2.3B). Thus, CR promotes the age-dependent accumulation of this non-reducing disaccharide. Noteworthy, trehalose in CR yeast grown on 0.5% glucose, a diet that provides the maximal benefit of CR for longevity, increased mainly in PD phase and reached a plateau soon after cells have entered ST phase (Figure 2.3B). Conversely, trehalose in CR yeast grown on 0.2% glucose, a diet providing only a modest CR-dependent life-span extension, increased predominantly throughout ST phase and eventually reached the steady-state level exceeding that in CR yeast grown on 0.5% glucose (Figure 2.3B).

The intracellular levels of glycogen, the major reserve carbohydrate in yeast [272], increased sharply in L phase, regardless of initial glucose concentration in the medium (Figure 2.3C). During the subsequent D and PD phases, CR yeast continued to accumulate glycogen, whereas non-CR yeast rapidly consumed it (Figure 2.3D). In

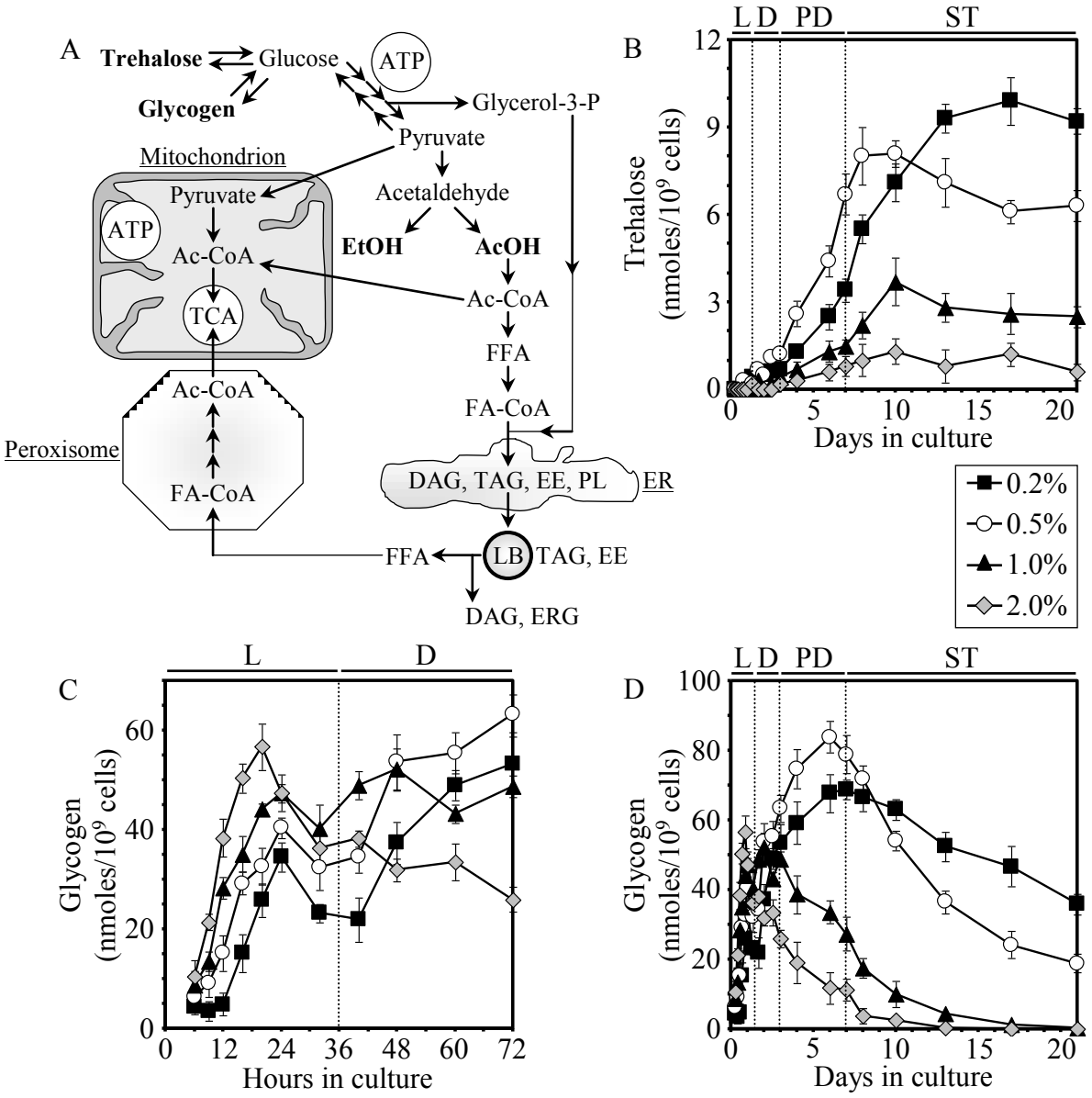


**Figure 2.3.** CR remodels trehalose and glycogen metabolism. (A) Outline of metabolic pathways and interorganellar communications operating in chronologically aging yeast. (B-D) The dynamics of age-dependent changes in the intracellular levels of trehalose (B) and glycogen (C and D) during chronological aging of yeast. Cells were cultured in YP medium initially containing 0.2%, 0.5%, 1% or 2% glucose. Data are presented as mean ± SEM (n = 4-6). For trehalose and glycogen levels, $p < 0.001$ at days 3 to 21 for cells grown on 0.2% or 0.5% glucose versus cells grown on 2% glucose. Abbreviations: Ac-CoA, acetyl-CoA; AcOH, acetic acid; DAG, diacylglycerols; EE, ethyl esters; ER, endoplasmic reticulum; ERG, ergosterol; EtOH, ethanol; FA-CoA, CoA esters of fatty acids; FFA, free fatty acids; LB, lipid bodies; PL, phospholipids; TAG, triacylglycerols; TCA, the tricarboxylic acid cycle in mitochondria.

contrast to non-CR yeast, yeast under CR began to degrade their reserved glycogen only when they entered ST phase (Figure 2.3D). Of note, the degree of CR influenced both glycogen storage and its consumption. In fact, CR yeast grown on 0.5% glucose reserved more glycogen by the end of PD phase and then consumed it in ST phase somewhat faster, as compared to CR yeast grown on 0.2% glucose (Figure 2.3D).

### 2.4.4 Life-span extension by CR relies in part on the ability of yeast to maintain trehalose concentration at optimal level

To evaluate the importance of maintaining trehalose homeostasis through consecutive growth phases on the observed longevity-extending effect of CR, I cultured a WT strain and several mutant strains, each carrying a single-gene-deletion mutation that affected trehalose biosynthesis or degradation [272], in YP medium initially containing 0.2% glucose. I monitored the chronological life spans of all these strains and assessed the dynamics of changes in trehalose concentration during their aging. I found that lack of trehalose or a substantial decrease in its concentration seen in CR cells of the *tps1Δ* and *tps2Δ* mutants, each missing a catalytic subunit of the trehalose synthase complex (Figure 2.4A), shortened their life spans (Figures 2.4B and 2.4D). A considerable, exceeding the level seen in WT, rise of trehalose during early and late stages of chronological aging, as it was observed in mutant cells lacking the Nth1p isozyme of neutral trehalase, also shortened life span (Figures 2.4C and 2.4E). Moreover, as I found, even if trehalose concentration exceeded the level seen in WT only after yeast have entered ST phase, as it occurred in mutant cells lacking the Nth2p isozyme of neutral trehalase, cells had shortened life span (Figure 2.4C and 2.4E). Importantly, I found that

some genetic manipulations changing trehalose concentration during early and/or late stages of chronological aging extended the life span of CR yeast. In fact, in long-lived mutants lacking the Tsl1p or Tps3p regulatory subunit of the trehalose synthase complex, trehalose concentration increased until the end of PD phase with the rate similar to that in WT, but then reached a plateau at the level that was 60-70% of that in WT (Figures 2.4B and 2.4D). Furthermore, in long-lived mutants lacking acid trehalase Ath1p or the catalytic subunit Tpk1p of cAMP-dependent protein kinase, trehalose concentration increased until the end of PD phase with the rate exceeding that in WT, but then reached a plateau at the level that was 50-60% of that in WT (Figures 2.4C and 2.4E).

Altogether, my findings imply that the chronological life span of CR yeast can be further expended by genetic manipulations that 1) do not decrease trehalose concentration until the end of PD phase; and 2) reduce trehalose concentration by 30-50% during ST phase. Noteworthy, trehalose stabilizes cytosolic proteins in their native conformation and prevents aggregation of proteins that have been denatured due to their exposure to elevated temperature or ROS [273, 274]. However, because of the ability of trehalose to interfere with the chaperone-assisted refolding of denatured cytosolic proteins, it must be rapidly degraded in order for molecular chaperones to restore the native conformation of these proteins [275]. Thus, it is conceivable that the high level of trehalose in CR yeast during an early stage of aging protects from aggregation those proteins that have been denatured due to their exposure to ROS (As I discuss further in this chapter, CR yeast accumulated substantial quantities of ROS at this stage). I hypothesize that some of the mutations that decrease trehalose concentration later in life can prolong chronological life span by promoting the refolding of proteins that have been oxidatively damaged earlier.

Recent unpublished data of Pavlo Kyryakov (a graduate student in Dr. Titorenko's laboratory) on protein unfolding/aggregation in response to elevated temperature or oxidative stress and on protein refolding following temperature or oxidative status restoration in various mutants impaired in different steps of the trehalose biosynthesis or degradation pathways (see Figure 2.4A) confirm the validity of my hypothesis.

### 2.4.5 Proper balance between the biosynthesis and degradation of glycogen is obligatory for life-span extension by CR

I next used a collection of mutants, each lacking a single protein that functions in glycogen biosynthesis or degradation (Figure 2.4G) [272], for functional analysis of the role for age-dependent glycogen dynamics in life-span extension by CR. I found that any genetic manipulation that substantially reduced glycogen concentration in CR cells entering ST phase of growth on 0.2% glucose shortened their chronological life span. This pattern was seen in mutants that lacked 1) the Glg2p isoform of self-glucosylating glycogenin glucosyltransferase; 2) the Gsy2p isoform of glycogen synthase; 3) Gac1p, Pig1p or Snf1p, all of which promote the dephosphorylation and activation of Gsy2p; or 4) the glycogen branching enzyme Glc3p (Figures 2.4F - 2.4I). My findings revealed that the chronological life span of CR yeast could be prolonged only by a genetic manipulation that simultaneously accelerates 1) glycogen biosynthesis during growth phases preceding ST phase; and 2) glycogen degradation during ST phase. In fact, lack of some proteins, although accelerated glycogen biosynthesis during growth phases preceding ST phase, impaired glycogen degradation during ST phase and resulted in a shortened life span. I observed this pattern in mutants that lacked 1) the Pcl8p or Pho85p,

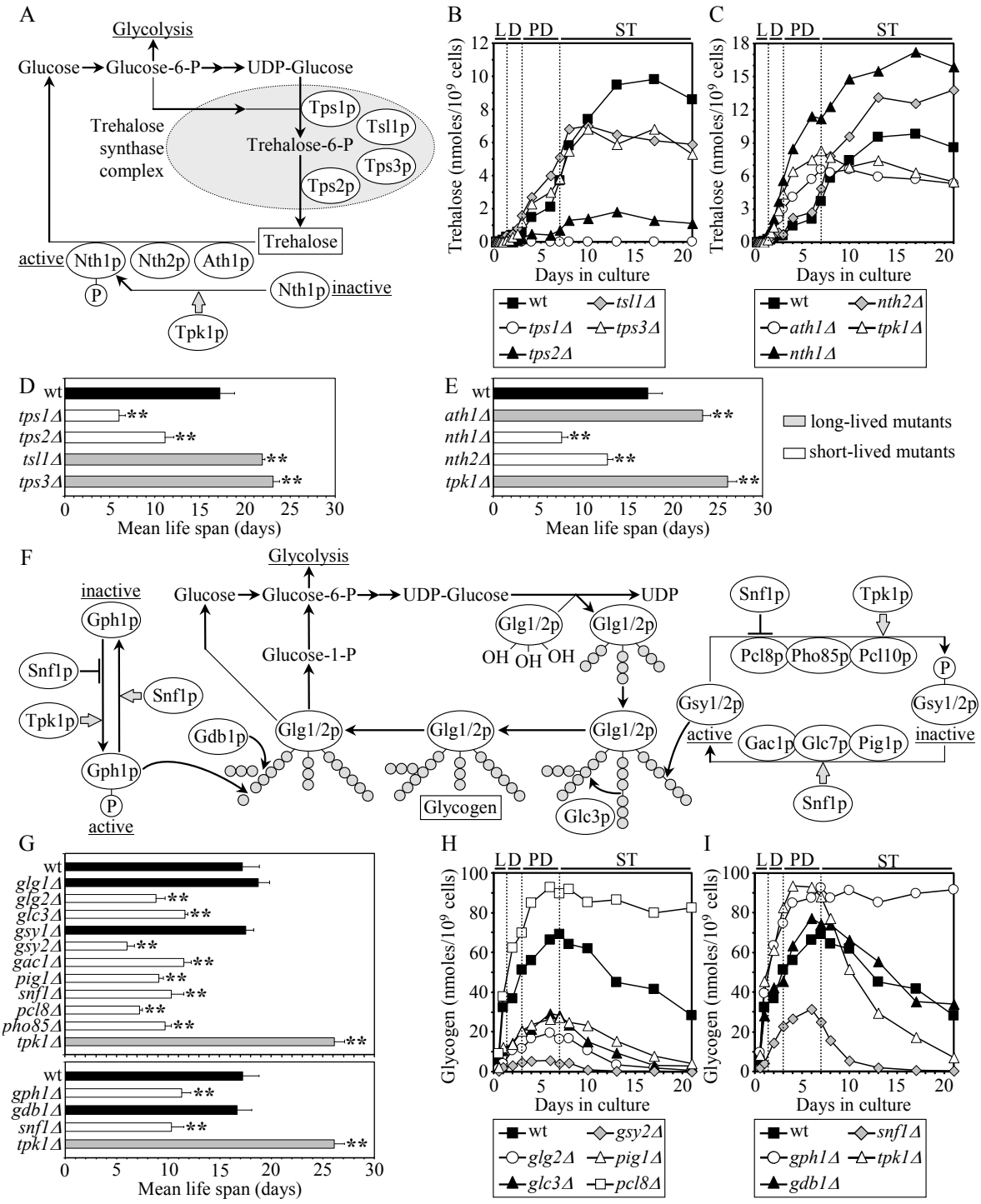


**Figure 2.4.** CR extends life span in part by maintaining a proper balance between the biosynthesis and degradation of trehalose and glycogen. (A) Outline of metabolic pathways of trehalose biosynthesis and degradation. (B and C) Trehalose concentrations in cells of WT and mutant strains. Each mutant carried a single-gene-deletion mutation that affects trehalose biosynthesis or degradation. Each plot shows a

representative experiment repeated 2-3 times with similar results. (D and E) The mean life spans of WT and mutant strains. Each mutant lacked a single enzyme that functions in trehalose biosynthesis or degradation. Each plot represents the average of 2-3 experiments; error bars show SEM. (F) Outline of metabolic pathways of glycogen biosynthesis and degradation. (G) The mean life spans of WT and mutant strains. Each mutant lacked a single enzyme that functions in glycogen biosynthesis or degradation. Each plot represents the average of 2-3 experiments; error bars show SEM. (H and I) Glycogen concentrations in cells of a WT strain and mutant strains. Each mutant carried a single-gene-deletion mutation that affects glycogen biosynthesis or degradation. Each plot shows a representative experiment repeated 2-3 times with similar results. (B-E and G-I) Cells were cultured in YP medium initially containing 0.2% glucose.

each promoting the phosphorylation and inactivation of Gsy2p; or 2) the Gph1p isoform of glycogen phosphorylase (Figures 2.4F - 2.4I). Only in the *tpk1Δ* mutant, which lacked the catalytic subunit Tpk1p of cAMP-dependent protein kinase, the acceleration of both glycogen biosynthesis prior to ST phase and glycogen degradation during ST phase led to a substantially extended life span (Figures 2.4G and 2.45I). Of note, I found that life span was not affected by any of the single-gene-deletion mutations that, by eliminating a low-abundance redundant component functioning in glycogen biosynthesis or degradation, did not have an effect on concentration of this major reserve carbohydrate. This pattern was seen in mutants that lacked 1) the Glg1p isoform of self-glucosylating glycogenin glucosyltransferase; 2) the Gsy1p isoform of glycogen synthase; or 3) the Gdb1p glycogen debranching enzyme (Figures 2.4G and 2.4I). In sum, my findings imply that life-span extension by CR relies in part on the establishment of a proper balance between the biosynthesis and degradation of glycogen. Current studies in Dr. Titorenko's laboratory are aimed at establishing molecular mechanisms underlying the longevity-defining role of such balance in chronologically aging yeast.

### 2.4.6 CR alters the abundance of many mitochondrial proteins, modulates oxidation-reduction processes in mitochondria and changes the age-related dynamics of mitochondrially produced ROS

To examine how CR influences mitochondria-confined processes that define longevity, I conducted the mass spectrometry-based identification and quantitation of proteins recovered from purified mitochondria of chronologically aging CR and non-CR cells. My comparative analysis of cellular and mitochondrial proteomes of CR and non-CR yeast revealed that CR altered the levels of numerous proteins that function in essential processes confined to mitochondria (Figure 2.5; Tables 2.1 and 2.2). I therefore sought to define the spectrum of mitochondrial processes affected by CR.

I found that, through D, PD and ST phases, mitochondria of CR yeast maintained the amplified rate of oxygen consumption, elevated the mitochondrial membrane potential ($\Delta\Psi$), and increased enzymatic activities of cytochrome c oxidase (CCO), succinate dehydrogenase (SDH) and aconitase (ACO), as compared to mitochondria of non-CR yeast (Figure 2.6). The observed amplification of these essential mitochondrial processes in CR yeast can be adequately explained by the CR-promoted rise in the levels of mitochondrial proteins that serve the formation of acetyl-CoA from pyruvate and its subsequent oxidation via the tricarboxylic acid (TCA) cycle, electron transport, and ATP-producing oxidative phosphorylation (Figure 2.5; Tables 2.1 and 2.2). Despite the elevated levels of cytosolic and mitochondrial ROS scavenging proteins in CR yeast (Figure 2.5; Tables 2.1 and 2.2), CR elevated the level of intracellular ROS (Figure 2.6E). ROS are mostly generated as by-products of mitochondrial respiration [276 - 278]. Thus, it is conceivable that, by promoting electron flow through the mitochondrial electron

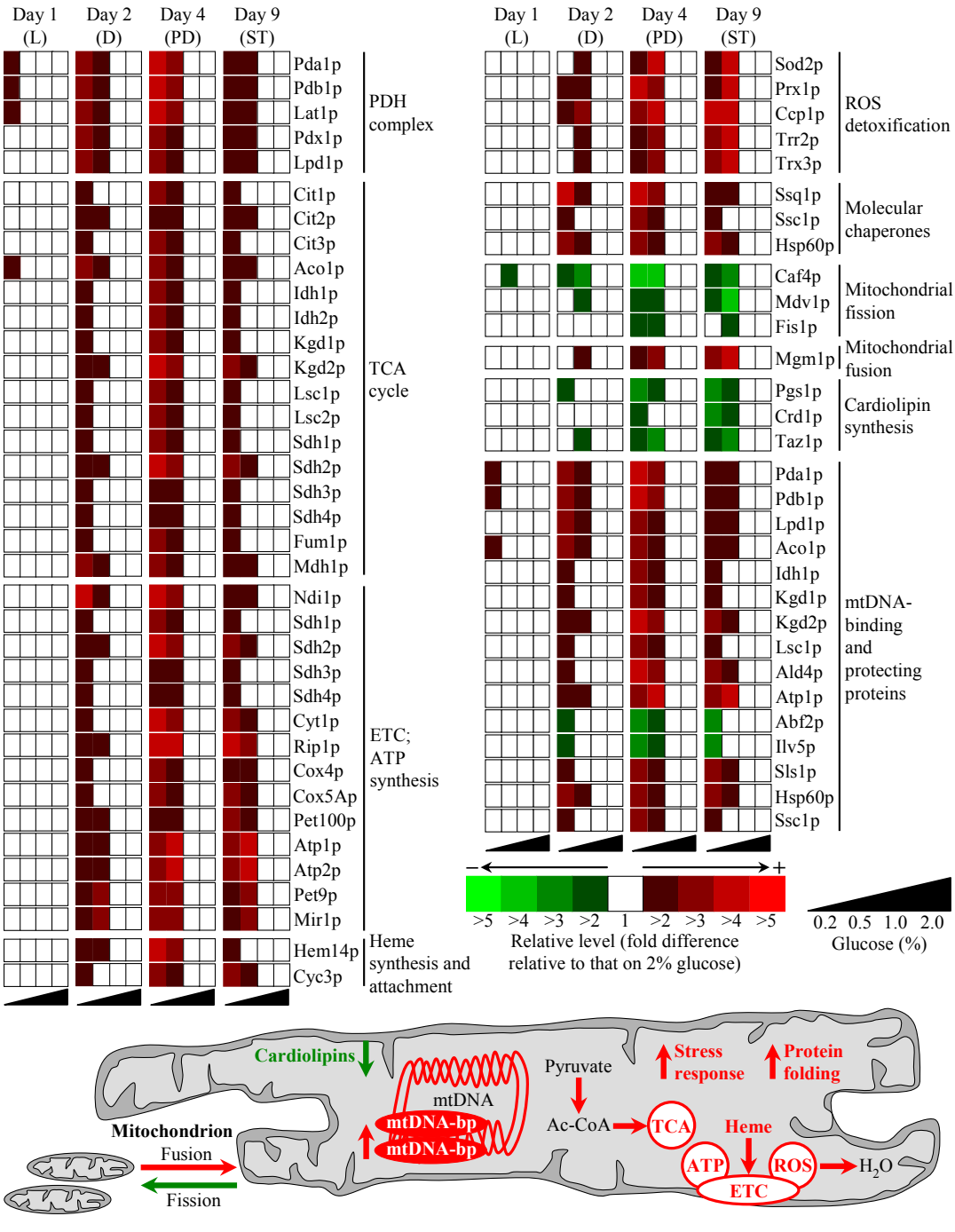


**Figure 2.5.** CR alters the abundance of a distinct set of proteins in mitochondria of chronologically aging yeast. Relative levels (fold difference relative to that on 2% glucose) of proteins recovered in purified yeast mitochondria. Proteins were identified and quantitated using mass spectrometry. The complete list of proteins and their relative levels are provided in Tables 2.1 and 2.2, respectively. From the data of proteomic analysis, I inferred an outline of mitochondria-confined processes that were activated (red arrows) or inhibited (green arrows) by CR prior to entry of yeast into the non-proliferative ST phase.

Abbreviations: Ac-CoA, acetyl-CoA; ETC, the mitochondrial electron transport chain; mtDNA, mitochondrial DNA; mtDNA-bp, mitochondrial DNA-binding proteins; PDH, the mutienzyme pyruvate dehydrogenase complex; ROS, reactive oxygen species; TCA, the tricarboxylic acid cycle in mitochondria.

transport chain (ETC), CR enhanced the ROS-generating transfer of a single electron to oxygen in mitochondria.

Importantly, I found that the degree of CR influenced essential mitochondrial processes and activities such as oxygen consumption and ROS production, the establishment and maintenance of $\Delta\Psi$, and enzymatic activities of CCO, SDH and ACO. In fact, in CR yeast grown on 0.2% glucose, a glucose concentration providing only a moderate CR-dependent life-span extension, the efficiencies of all these processes and enzymatic activities were 1) greatly amplified when yeast entered D phase; and 2) sharply declined through the following PD and ST phases (Figure 2.6). Of note, the sharply declined activity of ACO recovered from CR yeast grown on 0.2% glucose could be substantially increased *in vitro* by incubation of cell lysate with $Fe^{3+}$ and $S^{2-}$ (Figure 2.6F), which are able to restore the oxidation-dependent loss of one iron from the [4Fe-4S] cluster of ACO [279]. As I found, in CR yeast grown on 0.5% glucose, a glucose concentration that provides the maximal benefit of CR for longevity, the efficiencies of all these mitochondrial processes and enzymatic activities were 1) amplified to a much lesser extent during D phase than they were amplified in yeast grown on 0.2% glucose; and 2) reached a plateau in PD phase and remained mainly unchanged during the following ST phase (Figure 2.6). During the non-proliferative ST phase, the efficiencies and activities of all monitored mitochondrial processes and enzymes in CR yeast grown on 0.5% glucose exceeded those seen in CR yeast grown on 0.2% glucose. Altogether, these findings suggest that the observed early spike in oxygen consumption by

**Table 2.1.** List of proteins recovered in mitochondria purified from wild-type cells grown in YP media initially containing 0.2%, 0.5%, 1% or 2% glucose. Mitochondria were purified from wild-type cells collected at day 1 (L phase), day 2 (D phase), day 4 (PD phase) and day 9 (ST phase). Proteins were identified using matrix-assisted laser desorption/ionization mass spectrometric (MALDI MS) peptide mapping.

[1]The probability based Mowse score for comparing the calculated peptide masses for each entry in the sequence database with the set of experimental mass spectrometry data; Mowse scores greater than 54 are significant ($p < 0.05$).

[2]The expectation value for the matching peptides, which provides the number of matches with equal or better Mowse scores that are expected to occur by chance alone.

| Protein | NCBI accession no. | Function | Number of identified peptides | Sequence coverage (%) | Mowse score[1] | Expectation value[2] |
|---|---|---|---|---|---|---|
| **YP + 0.2% glucose; Day 1 (L phase)** | | | | | | |
| Pda1p | NP_011105 | Mitochondrial PDH complex; binds to mtDNA | 4 | 11 | 66 | 0.004 |
| Pdb1p | NP_009780 | Mitochondrial PDH complex; binds to mtDNA | 6 | 25 | 111 | 1.2e-07 |
| Lat1p | NP_014328 | Mitochondrial PDH complex | 11 | 27 | 161 | 1.2e-12 |
| Pdx1p | NP_011709 | Mitochondrial PDH complex | 10 | 33 | 174 | 6e-14 |
| Lpd1p | NP_116635 | Mitochondrial PDH complex; binds to mtDNA | 5 | 15 | 85 | 4.7e-05 |
| Cit1p | NP_014398 | Mitochondrial TCA cycle | 11 | 28 | 185 | 4.8e-15 |
| Cit2p | NP_009931 | Mitochondrial TCA cycle | 10 | 30 | 173 | 7.6e-14 |
| Cit3p | NP_015325 | Mitochondrial TCA cycle | 10 | 23 | 166 | 3.8e-13 |
| Aco1p | NP_013407 | Mitochondrial TCA cycle; binds to mtDNA | 6 | 11 | 90 | 1.3e-05 |
| Idh1p | NP_014361 | Mitochondrial TCA cycle; binds to mtDNA | 4 | 16 | 73 | 0.00083 |
| Idh2p | NP_014779 | Mitochondrial TCA cycle | 9 | 34 | 164 | 6e-13 |
| Kgd1p | NP_012141 | Mitochondrial TCA cycle; binds to mtDNA | 5 | 6 | 63 | 0.0079 |
| Kgd2p | NP_010432 | Mitochondrial TCA cycle; binds to mtDNA | 4 | 11 | 66 | 0.004 |
| Lsc1p | NP_014785 | Mitochondrial TCA cycle; binds to mtDNA | 8 | 37 | 152 | 9.5e-12 |
| Lsc2p | NP_011760 | Mitochondrial TCA cycle | 10 | 27 | 164 | 6e-13 |
| Sdh1p | NP_012774 | Mitochondrial TCA cycle and ETC | 11 | 23 | 174 | 6e-14 |
| Sdh2p | NP_013059 | Mitochondrial TCA cycle and ETC | 5 | 21 | 89 | 1.9e-05 |
| Sdh3p | NP_012781 | Mitochondrial TCA cycle and ETC | 7 | 50 | 146 | 3.8e-11 |
| Sdh4p | NP_010463 | Mitochondrial TCA cycle and ETC | 5 | 33 | 103 | 7.6e-07 |

| | | | | | | |
|---|---|---|---|---|---|---|
| Fum1p | NP_015061 | Mitochondrial TCA cycle | 9 | 21 | 151 | 1.2e-11 |
| Mdh1p | NP_012838 | Mitochondrial TCA cycle | 9 | 39 | 168 | 2.4e-13 |
| Ndi1p | NP_013586 | Mitochondrial ETC | 8 | 18 | 128 | 2.4e-09 |
| Cyt1p | NP_014708 | Mitochondrial ETC | 6 | 26 | 113 | 7.6e-08 |
| Rip1p | NP_010890 | Mitochondrial ETC | 6 | 51 | 80 | 0.00019 |
| Cox4p | NP_011328 | Mitochondrial ETC | 5 | 49 | 74 | 0.00081 |
| Cox5Ap | NP_014346 | Mitochondrial ETC | 6 | 58 | 86 | 5e-05 |
| Pet100p | NP_010364 | Mitochondrial ETC | 5 | 46 | 66 | 0.0054 |
| Atp1p | NP_009453 | Mitochondrial ATP synthase; binds to mtDNA | 6 | 17 | 102 | 9.5e-07 |
| Atp2p | NP_012655 | Mitochondrial ATP synthase | 7 | 17 | 116 | 3.8e-08 |
| Pet9p | NP_009523 | Mitochondrial ADP/ATP carrier | 6 | 20 | 102 | 9.5e-07 |
| Mir1p | NP_012611 | Mitochondrial phosphate carrier | 5 | 20 | 93 | 7.2e-06 |
| Hem14p | NP_010930 | Heme synthesis in mitochondria | 9 | 20 | 140 | 1.5e-10 |
| Cyc3p | NP_009361 | Heme attachment to apo-cytochrome c | 6 | 22 | 113 | 7.6e-08 |
| Sod2p | NP_011872 | Detoxification of ROS in mitochondria | 6 | 30 | 119 | 1.9e-08 |
| Prx1p | NP_009489 | Detoxification of ROS in mitochondria | 5 | 21 | 93 | 6.9e-06 |
| Ccp1p | NP_012992 | Detoxification of ROS in mitochondria | 12 | 50 | 135 | 6.7e-10 |
| Trr2p | NP_011974 | Detoxification of ROS in mitochondria | 7 | 39 | 78 | 0.00037 |
| Trx3p | NP_010006 | Detoxification of ROS in mitochondria | 5 | 37 | 59 | 0.026 |
| Ssq1p | NP_013473 | Assembly of Fe/S clusters into proteins | 7 | 12 | 102 | 9.5e-07 |
| Ssc1p | NP_012579 | Mitochondrial chaperone; binds to mtDNA | 7 | 16 | 113 | 7.6e-08 |
| Hsp60p | NP_013360 | Mitochondrial chaperone; binds to mtDNA | 7 | 18 | 113 | 7.6e-08 |
| Caf4p | NP_012962 | Mitochondrial fission | 11 | 25 | 83 | 0.00011 |
| Mdv1p | NP_012423 | Mitochondrial fission | 13 | 28 | 111 | 1.7e-07 |
| Fis1p | NP_012199 | Mitochondrial fission | 5 | 45 | 66 | 0.0048 |
| Mgm1p | NP_014854 | Mitochondrial fusion | 14 | 23 | 64 | 0.0083 |
| Pgs1p | NP_009923 | Cardiolipin synthesis in mitochondria | 8 | 21 | 57 | 0.041 |
| Crd1p | NP_010139 | Cardiolipin synthesis in mitochondria | 7 | 30 | 89 | 2.9e-05 |
| Taz1p | NP_015466 | Cardiolipin synthesis in mitochondria | 9 | 32 | 71 | 0.0018 |
| Ald4p | NP_015019 | Mitochondrial aldehyde dehydrogenase; binds to mtDNA | 5 | 13 | 84 | 6.1e-05 |
| Abf2p | NP_013788 | Mitochondrial genome maintenance; binds to mtDNA | 5 | 31 | 96 | 3.7e-06 |
| Ilv5p | NP_013459 | Branched-chain amino acid biosynthesis in | 5 | 18 | 89 | 1.9e-05 |

| | | | | | | |
|---|---|---|---|---|---|---|
| | | mitochondria; binds to mtDNA | | | | |
| Sls1p | NP_013240 | Mitochondrial chaperone; binds to mtDNA | 6 | 14 | 97 | 3.2e-06 |
| **YP + 0.5% glucose; Day 1 (L phase)** | | | | | | |
| Pda1p | NP_011105 | Mitochondrial PDH complex; binds to mtDNA | 5 | 13 | 81 | 0.00013 |
| Pdb1p | NP_009780 | Mitochondrial PDH complex; binds to mtDNA | 7 | 27 | 128 | 2.4e-09 |
| Lat1p | NP_014328 | Mitochondrial PDH complex | 9 | 25 | 147 | 3e-11 |
| Pdx1p | NP_011709 | Mitochondrial PDH complex | 8 | 28 | 142 | 9.5e-11 |
| Lpd1p | NP_116635 | Mitochondrial PDH complex; binds to mtDNA | 6 | 16 | 102 | 9.5e-07 |
| Cit1p | NP_014398 | Mitochondrial TCA cycle | 9 | 24 | 152 | 9.5e-12 |
| Cit2p | NP_009931 | Mitochondrial TCA cycle | 8 | 25 | 139 | 1.9e-10 |
| Cit3p | NP_015325 | Mitochondrial TCA cycle | 8 | 20 | 134 | 6e-10 |
| Aco1p | NP_013407 | Mitochondrial TCA cycle; binds to mtDNA | 7 | 12 | 104 | 6e-07 |
| Idh1p | NP_014361 | Mitochondrial TCA cycle; binds to mtDNA | 5 | 18 | 87 | 2.9e-05 |
| Idh2p | NP_014779 | Mitochondrial TCA cycle | 7 | 29 | 129 | 1.9e-09 |
| Kgd1p | NP_012141 | Mitochondrial TCA cycle; binds to mtDNA | 6 | 7 | 75 | 0.00048 |
| Kgd2p | NP_010432 | Mitochondrial TCA cycle; binds to mtDNA | 5 | 13 | 80 | 0.00016 |
| Lsc1p | NP_014785 | Mitochondrial TCA cycle | 6 | 30 | 116 | 3.8e-08 |
| Lsc2p | NP_011760 | Mitochondrial TCA cycle | 8 | 23 | 132 | 9.5e-10 |
| Sdh1p | NP_012774 | Mitochondrial TCA cycle and ETC | 9 | 20 | 144 | 6e-11 |
| Sdh2p | NP_013059 | Mitochondrial TCA cycle and ETC | 4 | 18 | 72 | 0.001 |
| Sdh3p | NP_012781 | Mitochondrial TCA cycle and ETC | 5 | 40 | 106 | 3.8e-07 |
| Sdh4p | NP_010463 | Mitochondrial TCA cycle and ETC | 4 | 29 | 83 | 8.1e-05 |
| Fum1p | NP_015061 | Mitochondrial TCA cycle | 7 | 18 | 119 | 1.9e-08 |
| Mdh1p | NP_012838 | Mitochondrial TCA cycle | 7 | 31 | 131 | 1.2e-09 |
| Ndi1p | NP_013586 | Mitochondrial ETC | 6 | 15 | 98 | 2.7e-06 |
| Cyt1p | NP_014708 | Mitochondrial ETC | 5 | 28 | 99 | 1.8e-06 |
| Rip1p | NP_010890 | Mitochondrial ETC | 6 | 51 | 80 | 0.00019 |
| Cox4p | NP_011328 | Mitochondrial ETC | 5 | 49 | 74 | 0.00081 |
| Cox5Ap | NP_014346 | Mitochondrial ETC | 6 | 58 | 86 | 5e-05 |
| Pet100p | NP_010364 | Mitochondrial ETC | 5 | 46 | 66 | 0.0054 |
| Atp1p | NP_009453 | Mitochondrial ATP synthase; binds to mtDNA | 7 | 19 | 118 | 2.4e-08 |
| Atp2p | NP_012655 | Mitochondrial ATP synthase | 6 | 15 | 100 | 1.6e-06 |
| Pet9p | NP_009523 | Mitochondrial ADP/ATP carrier | 5 | 17 | 85 | 5.2e-05 |
| Mir1p | NP_012611 | Mitochondrial phosphate carrier | 7 | 26 | 129 | 1.9e-09 |
| Hem14p | NP_010930 | Heme synthesis in | 8 | 18 | 125 | 4.8e-09 |

| | | | | | | |
|---|---|---|---|---|---|---|
| | | mitochondria | | | | |
| Cyc3p | NP_009361 | Heme attachment to apo-cytochrome c | 5 | 19 | 95 | 5.2e-06 |
| Sod2p | NP_011872 | Detoxification of ROS in mitochondria | 5 | 26 | 100 | 1.7e-06 |
| Prx1p | NP_009489 | Detoxification of ROS in mitochondria | 4 | 18 | 75 | 0.00046 |
| Ccp1p | NP_012992 | Detoxification of ROS in mitochondria | 12 | 50 | 135 | 6.7e-10 |
| Trr2p | NP_011974 | Detoxification of ROS in mitochondria | 7 | 39 | 78 | 0.00037 |
| Trx3p | NP_010006 | Detoxification of ROS in mitochondria | 5 | 37 | 59 | 0.026 |
| Ssq1p | NP_013473 | Assembly of Fe/S clusters into proteins | 9 | 14 | 128 | 2.4e-09 |
| Ssc1p | NP_012579 | Mitochondrial chaperone; binds to mtDNA | 8 | 18 | 128 | 2.4e-09 |
| Hsp60p | NP_013360 | Mitochondrial chaperone; binds to mtDNA | 8 | 19 | 127 | 3e-09 |
| Caf4p | NP_012962 | Mitochondrial fission | 11 | 25 | 83 | 0.00011 |
| Mdv1p | NP_012423 | Mitochondrial fission | 13 | 28 | 111 | 1.7e-07 |
| Fis1p | NP_012199 | Mitochondrial fission | 5 | 45 | 66 | 0.0048 |
| Mgm1p | NP_014854 | Mitochondrial fusion | 14 | 23 | 64 | 0.0083 |
| Pgs1p | NP_009923 | Cardiolipin synthesis in mitochondria | 8 | 21 | 57 | 0.041 |
| Crd1p | NP_010139 | Cardiolipin synthesis in mitochondria | 7 | 30 | 89 | 2.9e-05 |
| Taz1p | NP_015466 | Cardiolipin synthesis in mitochondria | 9 | 32 | 71 | 0.0018 |
| Ald4p | NP_015019 | Mitochondrial aldehyde dehydrogenase; binds to mtDNA | 6 | 15 | 100 | 1.7e-06 |
| Abf2p | NP_013788 | Mitochondrial genome maintenance; binds to mtDNA | 6 | 34 | 113 | 7.6e-08 |
| Ilv5p | NP_013459 | Branched-chain amino acid biosynthesis in mitochondria; binds to mtDNA | 6 | 20 | 104 | 6e-07 |
| Sls1p | NP_013240 | Mitochondrial chaperone; binds to mtDNA | 7 | 15 | 112 | 9.5e-08 |
| **YP + 1% glucose; Day 1 (L phase)** | | | | | | |
| Pda1p | NP_011105 | Mitochondrial PDH complex; binds to mtDNA | 6 | 14 | 96 | 4.2e-06 |
| Pdb1p | NP_009780 | Mitochondrial PDH complex; binds to mtDNA | 8 | 31 | 146 | 3.8e-11 |
| Lat1p | NP_014328 | Mitochondrial PDH complex | 7 | 19 | 102 | 9.5e-07 |
| Pdx1p | NP_011709 | Mitochondrial PDH complex | 6 | 23 | 108 | 2.4e-07 |
| Lpd1p | NP_116635 | Mitochondrial PDH complex; binds to mtDNA | 7 | 19 | 119 | 1.9e-08 |
| Cit1p | NP_014398 | Mitochondrial TCA cycle | 7 | 20 | 119 | 1.9e-08 |
| Cit2p | NP_009931 | Mitochondrial TCA cycle | 6 | 20 | 106 | 3.8e-07 |
| Cit3p | NP_015325 | Mitochondrial TCA cycle | 6 | 16 | 102 | 9.5e-07 |

| | | | | | | |
|---|---|---|---|---|---|---|
| Aco1p | NP_013407 | Mitochondrial TCA cycle; binds to mtDNA | 8 | 13 | 118 | 2.4e-08 |
| Idh1p | NP_014361 | Mitochondrial TCA cycle; binds to mtDNA | 6 | 21 | 103 | 7.6e-07 |
| Idh2p | NP_014779 | Mitochondrial TCA cycle | 5 | 23 | 94 | 6.4e-06 |
| Kgd1p | NP_012141 | Mitochondrial TCA cycle; binds to mtDNA | 6 | 7 | 82 | 1e-04 |
| Kgd2p | NP_010432 | Mitochondrial TCA cycle; binds to mtDNA | 6 | 16 | 96 | 3.7e-06 |
| Lsc1p | NP_014785 | Mitochondrial TCA cycle; binds to mtDNA | 5 | 23 | 95 | 4.8e-06 |
| Lsc2p | NP_011760 | Mitochondrial TCA cycle | 6 | 19 | 101 | 1.2e-06 |
| Sdh1p | NP_012774 | Mitochondrial TCA cycle and ETC | 7 | 17 | 113 | 7.6e-08 |
| Sdh2p | NP_013059 | Mitochondrial TCA cycle and ETC | 6 | 20 | 104 | 6e-07 |
| Sdh3p | NP_012781 | Mitochondrial TCA cycle and ETC | 4 | 35 | 86 | 3.5e-05 |
| Sdh4p | NP_010463 | Mitochondrial TCA cycle and ETC | 6 | 31 | 123 | 7.6e-09 |
| Fum1p | NP_015061 | Mitochondrial TCA cycle | 5 | 15 | 86 | 3.7e-05 |
| Mdh1p | NP_012838 | Mitochondrial TCA cycle | 5 | 24 | 95 | 4.6e-06 |
| Ndi1p | NP_013586 | Mitochondrial ETC | 6 | 14 | 97 | 3.2e-06 |
| Cyt1p | NP_014708 | Mitochondrial ETC | 5 | 23 | 95 | 4.8e-06 |
| Rip1p | NP_010890 | Mitochondrial ETC | 6 | 51 | 80 | 0.00019 |
| Cox4p | NP_011328 | Mitochondrial ETC | 5 | 49 | 74 | 0.00081 |
| Cox5Ap | NP_014346 | Mitochondrial ETC | 6 | 58 | 86 | 5e-05 |
| Pet100p | NP_010364 | Mitochondrial ETC | 5 | 46 | 66 | 0.0054 |
| Atp1p | NP_009453 | Mitochondrial ATP synthase; binds to mtDNA | 8 | 20 | 134 | 6e-10 |
| Atp2p | NP_012655 | Mitochondrial ATP synthase | 9 | 20 | 148 | 2.4e-11 |
| Pet9p | NP_009523 | Mitochondrial ADP/ATP carrier | 5 | 17 | 85 | 5.2e-05 |
| Mir1p | NP_012611 | Mitochondrial phosphate carrier | 7 | 27 | 130 | 1.5e-09 |
| Hem14p | NP_010930 | Heme synthesis in mitochondria | 11 | 23 | 169 | 1.9e-13 |
| Cyc3p | NP_009361 | Heme attachment to apo-cytochrome c | 5 | 18 | 94 | 5.6e-06 |
| Sod2p | NP_011872 | Detoxification of ROS in mitochondria | 5 | 26 | 99 | 1.7e-06 |
| Prx1p | NP_009489 | Detoxification of ROS in mitochondria | 8 | 31 | 148 | 2.4e-11 |
| Ccp1p | NP_012992 | Detoxification of ROS in mitochondria | 12 | 50 | 135 | 6.7e-10 |
| Trr2p | NP_011974 | Detoxification of ROS in mitochondria | 7 | 39 | 78 | 0.00037 |
| Trx3p | NP_010006 | Detoxification of ROS in mitochondria | 5 | 37 | 59 | 0.026 |
| Ssq1p | NP_013473 | Assembly of Fe/S clusters into proteins | 9 | 15 | 129 | 1.9e-09 |
| Ssc1p | NP_012579 | Mitochondrial chaperone; binds to mtDNA | 9 | 19 | 142 | 9.5e-11 |

| | | | | | | |
|---|---|---|---|---|---|---|
| Hsp60p | NP_013360 | Mitochondrial chaperone; binds to mtDNA | 9 | 21 | 142 | 9.5e-11 |
| Caf4p | NP_012962 | Mitochondrial fission | 11 | 25 | 83 | 0.00011 |
| Mdv1p | NP_012423 | Mitochondrial fission | 13 | 28 | 111 | 1.7e-07 |
| Fis1p | NP_012199 | Mitochondrial fission | 5 | 45 | 66 | 0.0048 |
| Mgm1p | NP_014854 | Mitochondrial fusion | 14 | 23 | 64 | 0.0083 |
| Pgs1p | NP_009923 | Cardiolipin synthesis in mitochondria | 8 | 21 | 57 | 0.041 |
| Crd1p | NP_010139 | Cardiolipin synthesis in mitochondria | 7 | 30 | 89 | 2.9e-05 |
| Taz1p | NP_015466 | Cardiolipin synthesis in mitochondria | 9 | 32 | 71 | 0.0018 |
| Ald4p | NP_015019 | Mitochondrial aldehyde dehydrogenase; binds to mtDNA | 7 | 17 | 116 | 3.8e-08 |
| Abf2p | NP_013788 | Mitochondrial genome maintenance; binds to mtDNA | 7 | 39 | 131 | 1.2e-09 |
| Ilv5p | NP_013459 | Branched-chain amino acid biosynthesis in mitochondria; binds to mtDNA | 7 | 22 | 121 | 1.2e-08 |
| Sls1p | NP_013240 | Mitochondrial chaperone; binds to mtDNA | 8 | 16 | 112 | 9.5e-08 |
| **YP + 2% glucose; Day 1 (L phase)** | | | | | | |
| Pda1p | NP_011105 | Mitochondrial PDH complex; binds to mtDNA | 7 | 17 | 109 | 1.9e-07 |
| Pdb1p | NP_009780 | Mitochondrial PDH complex; binds to mtDNA | 9 | 34 | 164 | 6e-13 |
| Lat1p | NP_014328 | Mitochondrial PDH complex | 5 | 16 | 85 | |
| Pdx1p | NP_011709 | Mitochondrial PDH complex | 5 | 19 | 90 | |
| Lpd1p | NP_116635 | Mitochondrial PDH complex; binds to mtDNA | 8 | 21 | 136 | 3.8e-10 |
| Cit1p | NP_014398 | Mitochondrial TCA cycle | 5 | 15 | 86 | 3.8e-05 |
| Cit2p | NP_009931 | Mitochondrial TCA cycle | 5 | 16 | 88 | 2.5e-05 |
| Cit3p | NP_015325 | Mitochondrial TCA cycle | 5 | 14 | 85 | 4.3e-05 |
| Aco1p | NP_013407 | Mitochondrial TCA cycle; binds to mtDNA | 9 | 14 | 132 | 9.5e-10 |
| Idh1p | NP_014361 | Mitochondrial TCA cycle; binds to mtDNA | 7 | 21 | 105 | 4.8e-07 |
| Idh2p | NP_014779 | Mitochondrial TCA cycle | 5 | 15 | 88 | 2.2e-05 |
| Kgd1p | NP_012141 | Mitochondrial TCA cycle; binds to mtDNA | 7 | 8 | 93 | 6.9e-06 |
| Kgd2p | NP_010432 | Mitochondrial TCA cycle; binds to mtDNA | 7 | 18 | 111 | 1.2e-07 |
| Lsc1p | NP_014785 | Mitochondrial TCA cycle | 5 | 14 | 90 | 1.7e-05 |
| Lsc2p | NP_011760 | Mitochondrial TCA cycle | 5 | 16 | 84 | 5.5e-05 |
| Sdh1p | NP_012774 | Mitochondrial TCA cycle and ETC | 6 | 14 | 97 | 2.7e-06 |
| Sdh2p | NP_013059 | Mitochondrial TCA cycle and ETC | 5 | 18 | 88 | 2.5e-05 |
| Sdh3p | NP_012781 | Mitochondrial TCA cycle | 5 | 22 | 100 | 1.6e-06 |

| | | | | | | |
|---|---|---|---|---|---|---|
| | | and ETC | | | | |
| Sdh4p | NP_010463 | Mitochondrial TCA cycle and ETC | 4 | 19 | 81 | 0.00011 |
| Fum1p | NP_015061 | Mitochondrial TCA cycle | 6 | 13 | 99 | 1.9e-06 |
| Mdh1p | NP_012838 | Mitochondrial TCA cycle | 5 | 20 | 93 | 7.6e-06 |
| Ndi1p | NP_013586 | Mitochondrial ETC | 7 | 16 | 113 | 7.6e-08 |
| Cyt1p | NP_014708 | Mitochondrial ETC | 5 | 22 | 94 | 5.5e-06 |
| Rip1p | NP_010890 | Mitochondrial ETC | 6 | 51 | 80 | 0.00019 |
| Cox4p | NP_011328 | Mitochondrial ETC | 5 | 49 | 74 | 0.00081 |
| Cox5Ap | NP_014346 | Mitochondrial ETC | 6 | 58 | 86 | 5e-05 |
| Pet100p | NP_010364 | Mitochondrial ETC | 5 | 46 | 66 | 0.0054 |
| Atp1p | NP_009453 | Mitochondrial ATP synthase; binds to mtDNA | 9 | 21 | 148 | 2.4e-11 |
| Atp2p | NP_012655 | Mitochondrial ATP synthase | 6 | 15 | 100 | 1.6e-06 |
| Pet9p | NP_009523 | Mitochondrial ADP/ATP carrier | 8 | 27 | 136 | 8.1e-08 |
| Mir1p | NP_012611 | Mitochondrial phosphate carrier | 7 | 26 | 129 | 1.9e-09 |
| Hem14p | NP_010930 | Heme synthesis in mitochondria | 8 | 18 | 124 | 6e-09 |
| Cyc3p | NP_009361 | Heme attachment to apo-cytochrome c | 5 | 19 | 95 | 5.2e-06 |
| Sod2p | NP_011872 | Detoxification of ROS in mitochondria | 5 | 29 | 102 | 9.5e-07 |
| Prx1p | NP_009489 | Detoxification of ROS in mitochondria | 8 | 30 | 147 | 3e-11 |
| Ccp1p | NP_012992 | Detoxification of ROS in mitochondria | 12 | 50 | 135 | 6.7e-10 |
| Trr2p | NP_011974 | Detoxification of ROS in mitochondria | 7 | 39 | 78 | 0.00037 |
| Trx3p | NP_010006 | Detoxification of ROS in mitochondria | 5 | 37 | 59 | 0.026 |
| Ssq1p | NP_013473 | Assembly of Fe/S clusters into proteins | 10 | 16 | 145 | 4.8e-11 |
| Ssc1p | NP_012579 | Mitochondrial chaperone; binds to mtDNA | 10 | 21 | 156 | 3.8e-12 |
| Hsp60p | NP_013360 | Mitochondrial chaperone; binds to mtDNA | 11 | 20 | 157 | 3e-12 |
| Caf4p | NP_012962 | Mitochondrial fission | 11 | 25 | 83 | 0.00011 |
| Mdv1p | NP_012423 | Mitochondrial fission | 13 | 28 | 111 | 1.7e-07 |
| Fis1p | NP_012199 | Mitochondrial fission | 5 | 45 | 66 | 0.0048 |
| Mgm1p | NP_014854 | Mitochondrial fusion | 14 | 23 | 64 | 0.0083 |
| Pgs1p | NP_009923 | Cardiolipin synthesis in mitochondria | 8 | 21 | 57 | 0.041 |
| Crd1p | NP_010139 | Cardiolipin synthesis in mitochondria | 7 | 30 | 89 | 2.9e-05 |
| Taz1p | NP_015466 | Cardiolipin synthesis in mitochondria | 9 | 32 | 71 | 0.0018 |
| Ald4p | NP_015019 | Mitochondrial aldehyde dehydrogenase; binds to mtDNA | 8 | 19 | 132 | 9.5e-10 |
| Abf2p | NP_013788 | Mitochondrial genome maintenance; binds to | 8 | 44 | 149 | 1.9e-11 |

| | | | | | | |
|---|---|---|---|---|---|---|
| | | mtDNA | | | | |
| Ilv5p | NP_013459 | Branched-chain amino acid biosynthesis in mitochondria; binds to mtDNA | 8 | 25 | 138 | 2.4e-10 |
| Sls1p | NP_013240 | Mitochondrial chaperone; binds to mtDNA | 9 | 19 | 143 | 7.6e-11 |
| **YP + 0.2% glucose; Day 2 (D phase)** | | | | | | |
| Pda1p | NP_011105 | Mitochondrial PDH complex; binds to mtDNA | 4 | 11 | 66 | 0.004 |
| Pdb1p | NP_009780 | Mitochondrial PDH complex; binds to mtDNA | 6 | 25 | 111 | 1.2e-07 |
| Lat1p | NP_014328 | Mitochondrial PDH complex | 11 | 27 | 161 | 1.2e-12 |
| Pdx1p | NP_011709 | Mitochondrial PDH complex | 10 | 33 | 174 | 6e-14 |
| Lpd1p | NP_116635 | Mitochondrial PDH complex; binds to mtDNA | 5 | 15 | 85 | 4.7e-05 |
| Cit1p | NP_014398 | Mitochondrial TCA cycle | 11 | 28 | 185 | 4.8e-15 |
| Cit2p | NP_009931 | Mitochondrial TCA cycle | 10 | 30 | 173 | 7.6e-14 |
| Cit3p | NP_015325 | Mitochondrial TCA cycle | 10 | 23 | 166 | 3.8e-13 |
| Aco1p | NP_013407 | Mitochondrial TCA cycle; binds to mtDNA | 6 | 11 | 90 | 1.3e-05 |
| Idh1p | NP_014361 | Mitochondrial TCA cycle; binds to mtDNA | 4 | 16 | 73 | 0.00083 |
| Idh2p | NP_014779 | Mitochondrial TCA cycle | 9 | 34 | 164 | 6e-13 |
| Kgd1p | NP_012141 | Mitochondrial TCA cycle; binds to mtDNA | 5 | 6 | 63 | 0.0079 |
| Kgd2p | NP_010432 | Mitochondrial TCA cycle; binds to mtDNA | 4 | 11 | 66 | 0.004 |
| Lsc1p | NP_014785 | Mitochondrial TCA cycle; binds to mtDNA | 8 | 37 | 152 | 9.5e-12 |
| Lsc2p | NP_011760 | Mitochondrial TCA cycle | 10 | 27 | 164 | 6e-13 |
| Sdh1p | NP_012774 | Mitochondrial TCA cycle and ETC | 11 | 23 | 174 | 6e-14 |
| Sdh2p | NP_013059 | Mitochondrial TCA cycle and ETC | 5 | 21 | 89 | 1.9e-05 |
| Sdh3p | NP_012781 | Mitochondrial TCA cycle and ETC | 7 | 50 | 146 | 3.8e-11 |
| Sdh4p | NP_010463 | Mitochondrial TCA cycle and ETC | 5 | 33 | 103 | 7.6e-07 |
| Fum1p | NP_015061 | Mitochondrial TCA cycle | 9 | 21 | 151 | 1.2e-11 |
| Mdh1p | NP_012838 | Mitochondrial TCA cycle | 9 | 39 | 168 | 2.4e-13 |
| Ndi1p | NP_013586 | Mitochondrial ETC | 8 | 18 | 128 | 2.4e-09 |
| Cyt1p | NP_014708 | Mitochondrial ETC | 6 | 26 | 113 | 7.6e-08 |
| Rip1p | NP_010890 | Mitochondrial ETC | 6 | 51 | 80 | 0.00019 |
| Cox4p | NP_011328 | Mitochondrial ETC | 5 | 49 | 74 | 0.00081 |
| Cox5Ap | NP_014346 | Mitochondrial ETC | 6 | 58 | 86 | 5e-05 |
| Pet100p | NP_010364 | Mitochondrial ETC | 5 | 46 | 66 | 0.0054 |
| Atp1p | NP_009453 | Mitochondrial ATP synthase; binds to mtDNA | 6 | 17 | 102 | 9.5e-07 |
| Atp2p | NP_012655 | Mitochondrial ATP synthase | 7 | 17 | 116 | 3.8e-08 |
| Pet9p | NP_009523 | Mitochondrial ADP/ATP | 6 | 20 | 102 | 9.5e-07 |

| | | carrier | | | | |
|---|---|---|---|---|---|---|
| Mir1p | NP_012611 | Mitochondrial phosphate carrier | 5 | 20 | 93 | 7.2e-06 |
| Hem14p | NP_010930 | Heme synthesis in mitochondria | 9 | 20 | 140 | 1.5e-10 |
| Cyc3p | NP_009361 | Heme attachment to apo-cytochrome c | 6 | 22 | 113 | 7.6e-08 |
| Sod2p | NP_011872 | Detoxification of ROS in mitochondria | 6 | 30 | 119 | 1.9e-08 |
| Prx1p | NP_009489 | Detoxification of ROS in mitochondria | 5 | 21 | 93 | 6.9e-06 |
| Ccp1p | NP_012992 | Detoxification of ROS in mitochondria | 12 | 50 | 135 | 6.7e-10 |
| Trr2p | NP_011974 | Detoxification of ROS in mitochondria | 7 | 39 | 78 | 0.00037 |
| Trx3p | NP_010006 | Detoxification of ROS in mitochondria | 5 | 37 | 59 | 0.026 |
| Ssq1p | NP_013473 | Assembly of Fe/S clusters into proteins | 7 | 12 | 102 | 9.5e-07 |
| Ssc1p | NP_012579 | Mitochondrial chaperone; binds to mtDNA | 7 | 16 | 113 | 7.6e-08 |
| Hsp60p | NP_013360 | Mitochondrial chaperone; binds to mtDNA | 7 | 18 | 113 | 7.6e-08 |
| Caf4p | NP_012962 | Mitochondrial fission | 11 | 25 | 83 | 0.00011 |
| Mdv1p | NP_012423 | Mitochondrial fission | 13 | 28 | 111 | 1.7e-07 |
| Fis1p | NP_012199 | Mitochondrial fission | 5 | 45 | 66 | 0.0048 |
| Mgm1p | NP_014854 | Mitochondrial fusion | 14 | 23 | 64 | 0.0083 |
| Pgs1p | NP_009923 | Cardiolipin synthesis in mitochondria | 8 | 21 | 57 | 0.041 |
| Crd1p | NP_010139 | Cardiolipin synthesis in mitochondria | 7 | 30 | 89 | 2.9e-05 |
| Taz1p | NP_015466 | Cardiolipin synthesis in mitochondria | 9 | 32 | 71 | 0.0018 |
| Ald4p | NP_015019 | Mitochondrial aldehyde dehydrogenase; binds to mtDNA | 5 | 13 | 84 | 6.1e-05 |
| Abf2p | NP_013788 | Mitochondrial genome maintenance; binds to mtDNA | 5 | 31 | 96 | 3.7e-06 |
| Ilv5p | NP_013459 | Branched-chain amino acid biosynthesis in mitochondria; binds to mtDNA | 5 | 18 | 89 | 1.9e-05 |
| Sls1p | NP_013240 | Mitochondrial chaperone; binds to mtDNA | 6 | 14 | 97 | 3.2e-06 |
| **YP + 0.5% glucose; Day 2 (D phase)** | | | | | | |
| Pda1p | NP_011105 | Mitochondrial PDH complex; binds to mtDNA | 5 | 13 | 81 | 0.00013 |
| Pdb1p | NP_009780 | Mitochondrial PDH complex; binds to mtDNA | 7 | 27 | 128 | 2.4e-09 |
| Lat1p | NP_014328 | Mitochondrial PDH complex | 9 | 25 | 147 | 3e-11 |
| Pdx1p | NP_011709 | Mitochondrial PDH complex | 8 | 28 | 142 | 9.5e-11 |
| Lpd1p | NP_116635 | Mitochondrial PDH | 6 | 16 | 102 | 9.5e-07 |

| | | | | | | |
|---|---|---|---|---|---|---|
| | | complex; binds to mtDNA | | | | |
| Cit1p | NP_014398 | Mitochondrial TCA cycle | 9 | 24 | 152 | 9.5e-12 |
| Cit2p | NP_009931 | Mitochondrial TCA cycle | 8 | 25 | 139 | 1.9e-10 |
| Cit3p | NP_015325 | Mitochondrial TCA cycle | 8 | 20 | 134 | 6e-10 |
| Aco1p | NP_013407 | Mitochondrial TCA cycle; binds to mtDNA | 7 | 12 | 104 | 6e-07 |
| Idh1p | NP_014361 | Mitochondrial TCA cycle; binds to mtDNA | 5 | 18 | 87 | 2.9e-05 |
| Idh2p | NP_014779 | Mitochondrial TCA cycle | 7 | 29 | 129 | 1.9e-09 |
| Kgd1p | NP_012141 | Mitochondrial TCA cycle; binds to mtDNA | 6 | 7 | 75 | 0.00048 |
| Kgd2p | NP_010432 | Mitochondrial TCA cycle; binds to mtDNA | 5 | 13 | 80 | 0.00016 |
| Lsc1p | NP_014785 | Mitochondrial TCA cycle | 6 | 30 | 116 | 3.8e-08 |
| Lsc2p | NP_011760 | Mitochondrial TCA cycle | 8 | 23 | 132 | 9.5e-10 |
| Sdh1p | NP_012774 | Mitochondrial TCA cycle and ETC | 9 | 20 | 144 | 6e-11 |
| Sdh2p | NP_013059 | Mitochondrial TCA cycle and ETC | 4 | 18 | 72 | 0.001 |
| Sdh3p | NP_012781 | Mitochondrial TCA cycle and ETC | 5 | 40 | 106 | 3.8e-07 |
| Sdh4p | NP_010463 | Mitochondrial TCA cycle and ETC | 4 | 29 | 83 | 8.1e-05 |
| Fum1p | NP_015061 | Mitochondrial TCA cycle | 7 | 18 | 119 | 1.9e-08 |
| Mdh1p | NP_012838 | Mitochondrial TCA cycle | 7 | 31 | 131 | 1.2e-09 |
| Ndi1p | NP_013586 | Mitochondrial ETC | 6 | 15 | 98 | 2.7e-06 |
| Cyt1p | NP_014708 | Mitochondrial ETC | 5 | 28 | 99 | 1.8e-06 |
| Rip1p | NP_010890 | Mitochondrial ETC | 6 | 51 | 80 | 0.00019 |
| Cox4p | NP_011328 | Mitochondrial ETC | 5 | 49 | 74 | 0.00081 |
| Cox5Ap | NP_014346 | Mitochondrial ETC | 6 | 58 | 86 | 5e-05 |
| Pet100p | NP_010364 | Mitochondrial ETC | 5 | 46 | 66 | 0.0054 |
| Atp1p | NP_009453 | Mitochondrial ATP synthase; binds to mtDNA | 7 | 19 | 118 | 2.4e-08 |
| Atp2p | NP_012655 | Mitochondrial ATP synthase | 6 | 15 | 100 | 1.6e-06 |
| Pet9p | NP_009523 | Mitochondrial ADP/ATP carrier | 5 | 17 | 85 | 5.2e-05 |
| Mir1p | NP_012611 | Mitochondrial phosphate carrier | 7 | 26 | 129 | 1.9e-09 |
| Hem14p | NP_010930 | Heme synthesis in mitochondria | 8 | 18 | 125 | 4.8e-09 |
| Cyc3p | NP_009361 | Heme attachment to apo-cytochrome c | 5 | 19 | 95 | 5.2e-06 |
| Sod2p | NP_011872 | Detoxification of ROS in mitochondria | 5 | 26 | 100 | 1.7e-06 |
| Prx1p | NP_009489 | Detoxification of ROS in mitochondria | 4 | 18 | 75 | 0.00046 |
| Ccp1p | NP_012992 | Detoxification of ROS in mitochondria | 12 | 50 | 135 | 6.7e-10 |
| Trr2p | NP_011974 | Detoxification of ROS in mitochondria | 7 | 39 | 78 | 0.00037 |
| Trx3p | NP_010006 | Detoxification of ROS in mitochondria | 5 | 37 | 59 | 0.026 |
| Ssq1p | NP_013473 | Assembly of Fe/S clusters | 9 | 14 | 128 | 2.4e-09 |

| | | into proteins | | | | |
|---|---|---|---|---|---|---|
| Ssc1p | NP_012579 | Mitochondrial chaperone; binds to mtDNA | 8 | 18 | 128 | 2.4e-09 |
| Hsp60p | NP_013360 | Mitochondrial chaperone; binds to mtDNA | 8 | 19 | 127 | 3e-09 |
| Caf4p | NP_012962 | Mitochondrial fission | 11 | 25 | 83 | 0.00011 |
| Mdv1p | NP_012423 | Mitochondrial fission | 13 | 28 | 111 | 1.7e-07 |
| Fis1p | NP_012199 | Mitochondrial fission | 5 | 45 | 66 | 0.0048 |
| Mgm1p | NP_014854 | Mitochondrial fusion | 14 | 23 | 64 | 0.0083 |
| Pgs1p | NP_009923 | Cardiolipin synthesis in mitochondria | 8 | 21 | 57 | 0.041 |
| Crd1p | NP_010139 | Cardiolipin synthesis in mitochondria | 7 | 30 | 89 | 2.9e-05 |
| Taz1p | NP_015466 | Cardiolipin synthesis in mitochondria | 9 | 32 | 71 | 0.0018 |
| Ald4p | NP_015019 | Mitochondrial aldehyde dehydrogenase; binds to mtDNA | 6 | 15 | 100 | 1.7e-06 |
| Abf2p | NP_013788 | Mitochondrial genome maintenance; binds to mtDNA | 6 | 34 | 113 | 7.6e-08 |
| Ilv5p | NP_013459 | Branched-chain amino acid biosynthesis in mitochondria; binds to mtDNA | 6 | 20 | 104 | 6e-07 |
| Sls1p | NP_013240 | Mitochondrial chaperone; binds to mtDNA | 7 | 15 | 112 | 9.5e-08 |
| **YP + 1% glucose; Day 2 (D phase)** | | | | | | |
| Pda1p | NP_011105 | Mitochondrial PDH complex; binds to mtDNA | 6 | 14 | 96 | 4.2e-06 |
| Pdb1p | NP_009780 | Mitochondrial PDH complex; binds to mtDNA | 8 | 31 | 146 | 3.8e-11 |
| Lat1p | NP_014328 | Mitochondrial PDH complex | 7 | 19 | 102 | 9.5e-07 |
| Pdx1p | NP_011709 | Mitochondrial PDH complex | 6 | 23 | 108 | 2.4e-07 |
| Lpd1p | NP_116635 | Mitochondrial PDH complex; binds to mtDNA | 7 | 19 | 119 | 1.9e-08 |
| Cit1p | NP_014398 | Mitochondrial TCA cycle | 7 | 20 | 119 | 1.9e-08 |
| Cit2p | NP_009931 | Mitochondrial TCA cycle | 6 | 20 | 106 | 3.8e-07 |
| Cit3p | NP_015325 | Mitochondrial TCA cycle | 6 | 16 | 102 | 9.5e-07 |
| Aco1p | NP_013407 | Mitochondrial TCA cycle; binds to mtDNA | 8 | 13 | 118 | 2.4e-08 |
| Idh1p | NP_014361 | Mitochondrial TCA cycle; binds to mtDNA | 6 | 21 | 103 | 7.6e-07 |
| Idh2p | NP_014779 | Mitochondrial TCA cycle | 5 | 23 | 94 | 6.4e-06 |
| Kgd1p | NP_012141 | Mitochondrial TCA cycle; binds to mtDNA | 6 | 7 | 82 | 1e-04 |
| Kgd2p | NP_010432 | Mitochondrial TCA cycle; binds to mtDNA | 6 | 16 | 96 | 3.7e-06 |
| Lsc1p | NP_014785 | Mitochondrial TCA cycle; binds to mtDNA | 5 | 23 | 95 | 4.8e-06 |
| Lsc2p | NP_011760 | Mitochondrial TCA cycle | 6 | 19 | 101 | 1.2e-06 |
| Sdh1p | NP_012774 | Mitochondrial TCA cycle | 7 | 17 | 113 | 7.6e-08 |

| | | | | | | |
|---|---|---|---|---|---|---|
| | | and ETC | | | | |
| Sdh2p | NP_013059 | Mitochondrial TCA cycle and ETC | 6 | 20 | 104 | 6e-07 |
| Sdh3p | NP_012781 | Mitochondrial TCA cycle and ETC | 4 | 35 | 86 | 3.5e-05 |
| Sdh4p | NP_010463 | Mitochondrial TCA cycle and ETC | 6 | 31 | 123 | 7.6e-09 |
| Fum1p | NP_015061 | Mitochondrial TCA cycle | 5 | 15 | 86 | 3.7e-05 |
| Mdh1p | NP_012838 | Mitochondrial TCA cycle | 5 | 24 | 95 | 4.6e-06 |
| Ndi1p | NP_013586 | Mitochondrial ETC | 6 | 14 | 97 | 3.2e-06 |
| Cyt1p | NP_014708 | Mitochondrial ETC | 5 | 23 | 95 | 4.8e-06 |
| Rip1p | NP_010890 | Mitochondrial ETC | 6 | 51 | 80 | 0.00019 |
| Cox4p | NP_011328 | Mitochondrial ETC | 5 | 49 | 74 | 0.00081 |
| Cox5Ap | NP_014346 | Mitochondrial ETC | 6 | 58 | 86 | 5e-05 |
| Pet100p | NP_010364 | Mitochondrial ETC | 5 | 46 | 66 | 0.0054 |
| Atp1p | NP_009453 | Mitochondrial ATP synthase; binds to mtDNA | 8 | 20 | 134 | 6e-10 |
| Atp2p | NP_012655 | Mitochondrial ATP synthase | 9 | 20 | 148 | 2.4e-11 |
| Pet9p | NP_009523 | Mitochondrial ADP/ATP carrier | 5 | 17 | 85 | 5.2e-05 |
| Mir1p | NP_012611 | Mitochondrial phosphate carrier | 7 | 27 | 130 | 1.5e-09 |
| Hem14p | NP_010930 | Heme synthesis in mitochondria | 11 | 23 | 169 | 1.9e-13 |
| Cyc3p | NP_009361 | Heme attachment to apo-cytochrome c | 5 | 18 | 94 | 5.6e-06 |
| Sod2p | NP_011872 | Detoxification of ROS in mitochondria | 5 | 26 | 99 | 1.7e-06 |
| Prx1p | NP_009489 | Detoxification of ROS in mitochondria | 8 | 31 | 148 | 2.4e-11 |
| Ccp1p | NP_012992 | Detoxification of ROS in mitochondria | 12 | 50 | 135 | 6.7e-10 |
| Trr2p | NP_011974 | Detoxification of ROS in mitochondria | 7 | 39 | 78 | 0.00037 |
| Trx3p | NP_010006 | Detoxification of ROS in mitochondria | 5 | 37 | 59 | 0.026 |
| Ssq1p | NP_013473 | Assembly of Fe/S clusters into proteins | 9 | 15 | 129 | 1.9e-09 |
| Ssc1p | NP_012579 | Mitochondrial chaperone; binds to mtDNA | 9 | 19 | 142 | 9.5e-11 |
| Hsp60p | NP_013360 | Mitochondrial chaperone; binds to mtDNA | 9 | 21 | 142 | 9.5e-11 |
| Caf4p | NP_012962 | Mitochondrial fission | 11 | 25 | 83 | 0.00011 |
| Mdv1p | NP_012423 | Mitochondrial fission | 13 | 28 | 111 | 1.7e-07 |
| Fis1p | NP_012199 | Mitochondrial fission | 5 | 45 | 66 | 0.0048 |
| Mgm1p | NP_014854 | Mitochondrial fusion | 14 | 23 | 64 | 0.0083 |
| Pgs1p | NP_009923 | Cardiolipin synthesis in mitochondria | 8 | 21 | 57 | 0.041 |
| Crd1p | NP_010139 | Cardiolipin synthesis in mitochondria | 7 | 30 | 89 | 2.9e-05 |
| Taz1p | NP_015466 | Cardiolipin synthesis in mitochondria | 9 | 32 | 71 | 0.0018 |
| Ald4p | NP_015019 | Mitochondrial aldehyde | 7 | 17 | 116 | 3.8e-08 |

| | | | | | | |
|---|---|---|---|---|---|---|
| | | dehydrogenase; binds to mtDNA | | | | |
| Abf2p | NP_013788 | Mitochondrial genome maintenance; binds to mtDNA | 7 | 39 | 131 | 1.2e-09 |
| Ilv5p | NP_013459 | Branched-chain amino acid biosynthesis in mitochondria; binds to mtDNA | 7 | 22 | 121 | 1.2e-08 |
| Sls1p | NP_013240 | Mitochondrial chaperone; binds to mtDNA | 8 | 16 | 112 | 9.5e-08 |
| **YP + 2% glucose; Day 2 (D phase)** | | | | | | |
| Pda1p | NP_011105 | Mitochondrial PDH complex; binds to mtDNA | 7 | 17 | 109 | 1.9e-07 |
| Pdb1p | NP_009780 | Mitochondrial PDH complex; binds to mtDNA | 9 | 34 | 164 | 6e-13 |
| Lat1p | NP_014328 | Mitochondrial PDH complex | 5 | 16 | 85 | |
| Pdx1p | NP_011709 | Mitochondrial PDH complex | 5 | 19 | 90 | |
| Lpd1p | NP_116635 | Mitochondrial PDH complex; binds to mtDNA | 8 | 21 | 136 | 3.8e-10 |
| Cit1p | NP_014398 | Mitochondrial TCA cycle | 5 | 15 | 86 | 3.8e-05 |
| Cit2p | NP_009931 | Mitochondrial TCA cycle | 5 | 16 | 88 | 2.5e-05 |
| Cit3p | NP_015325 | Mitochondrial TCA cycle | 5 | 14 | 85 | 4.3e-05 |
| Aco1p | NP_013407 | Mitochondrial TCA cycle; binds to mtDNA | 9 | 14 | 132 | 9.5e-10 |
| Idh1p | NP_014361 | Mitochondrial TCA cycle; binds to mtDNA | 7 | 21 | 105 | 4.8e-07 |
| Idh2p | NP_014779 | Mitochondrial TCA cycle | 5 | 15 | 88 | 2.2e-05 |
| Kgd1p | NP_012141 | Mitochondrial TCA cycle; binds to mtDNA | 7 | 8 | 93 | 6.9e-06 |
| Kgd2p | NP_010432 | Mitochondrial TCA cycle; binds to mtDNA | 7 | 18 | 111 | 1.2e-07 |
| Lsc1p | NP_014785 | Mitochondrial TCA cycle | 5 | 14 | 90 | 1.7e-05 |
| Lsc2p | NP_011760 | Mitochondrial TCA cycle | 5 | 16 | 84 | 5.5e-05 |
| Sdh1p | NP_012774 | Mitochondrial TCA cycle and ETC | 6 | 14 | 97 | 2.7e-06 |
| Sdh2p | NP_013059 | Mitochondrial TCA cycle and ETC | 5 | 18 | 88 | 2.5e-05 |
| Sdh3p | NP_012781 | Mitochondrial TCA cycle and ETC | 5 | 22 | 100 | 1.6e-06 |
| Sdh4p | NP_010463 | Mitochondrial TCA cycle and ETC | 4 | 19 | 81 | 0.00011 |
| Fum1p | NP_015061 | Mitochondrial TCA cycle | 6 | 13 | 99 | 1.9e-06 |
| Mdh1p | NP_012838 | Mitochondrial TCA cycle | 5 | 20 | 93 | 7.6e-06 |
| Ndi1p | NP_013586 | Mitochondrial ETC | 7 | 16 | 113 | 7.6e-08 |
| Cyt1p | NP_014708 | Mitochondrial ETC | 5 | 22 | 94 | 5.5e-06 |
| Rip1p | NP_010890 | Mitochondrial ETC | 6 | 51 | 80 | 0.00019 |
| Cox4p | NP_011328 | Mitochondrial ETC | 5 | 49 | 74 | 0.00081 |
| Cox5Ap | NP_014346 | Mitochondrial ETC | 6 | 58 | 86 | 5e-05 |
| Pet100p | NP_010364 | Mitochondrial ETC | 5 | 46 | 66 | 0.0054 |
| Atp1p | NP_009453 | Mitochondrial ATP synthase; binds to mtDNA | 9 | 21 | 148 | 2.4e-11 |

| | | | | | | |
|---|---|---|---|---|---|---|
| Atp2p | NP_012655 | Mitochondrial ATP synthase | 6 | 15 | 100 | 1.6e-06 |
| Pet9p | NP_009523 | Mitochondrial ADP/ATP carrier | 8 | 27 | 136 | 8.1e-08 |
| Mir1p | NP_012611 | Mitochondrial phosphate carrier | 7 | 26 | 129 | 1.9e-09 |
| Hem14p | NP_010930 | Heme synthesis in mitochondria | 8 | 18 | 124 | 6e-09 |
| Cyc3p | NP_009361 | Heme attachment to apo-cytochrome c | 5 | 19 | 95 | 5.2e-06 |
| Sod2p | NP_011872 | Detoxification of ROS in mitochondria | 5 | 29 | 102 | 9.5e-07 |
| Prx1p | NP_009489 | Detoxification of ROS in mitochondria | 8 | 30 | 147 | 3e-11 |
| Ccp1p | NP_012992 | Detoxification of ROS in mitochondria | 12 | 50 | 135 | 6.7e-10 |
| Trr2p | NP_011974 | Detoxification of ROS in mitochondria | 7 | 39 | 78 | 0.00037 |
| Trx3p | NP_010006 | Detoxification of ROS in mitochondria | 5 | 37 | 59 | 0.026 |
| Ssq1p | NP_013473 | Assembly of Fe/S clusters into proteins | 10 | 16 | 145 | 4.8e-11 |
| Ssc1p | NP_012579 | Mitochondrial chaperone; binds to mtDNA | 10 | 21 | 156 | 3.8e-12 |
| Hsp60p | NP_013360 | Mitochondrial chaperone; binds to mtDNA | 11 | 20 | 157 | 3e-12 |
| Caf4p | NP_012962 | Mitochondrial fission | 11 | 25 | 83 | 0.00011 |
| Mdv1p | NP_012423 | Mitochondrial fission | 13 | 28 | 111 | 1.7e-07 |
| Fis1p | NP_012199 | Mitochondrial fission | 5 | 45 | 66 | 0.0048 |
| Mgm1p | NP_014854 | Mitochondrial fusion | 14 | 23 | 64 | 0.0083 |
| Pgs1p | NP_009923 | Cardiolipin synthesis in mitochondria | 8 | 21 | 57 | 0.041 |
| Crd1p | NP_010139 | Cardiolipin synthesis in mitochondria | 7 | 30 | 89 | 2.9e-05 |
| Taz1p | NP_015466 | Cardiolipin synthesis in mitochondria | 9 | 32 | 71 | 0.0018 |
| Ald4p | NP_015019 | Mitochondrial aldehyde dehydrogenase; binds to mtDNA | 8 | 19 | 132 | 9.5e-10 |
| Abf2p | NP_013788 | Mitochondrial genome maintenance; binds to mtDNA | 8 | 44 | 149 | 1.9e-11 |
| Ilv5p | NP_013459 | Branched-chain amino acid biosynthesis in mitochondria; binds to mtDNA | 8 | 25 | 138 | 2.4e-10 |
| Sls1p | NP_013240 | Mitochondrial chaperone; binds to mtDNA | 9 | 19 | 143 | 7.6e-11 |
| **YP + 0.2% glucose; Day 4 (PD phase)** | | | | | | |
| Pda1p | NP_011105 | Mitochondrial PDH complex; binds to mtDNA | 7 | 17 | 109 | 1.9e-07 |
| Pdb1p | NP_009780 | Mitochondrial PDH complex; binds to mtDNA | 9 | 34 | 164 | 6e-13 |
| Lat1p | NP_014328 | Mitochondrial PDH complex | 5 | 16 | 85 | |

| | | | | | | |
|---|---|---|---|---|---|---|
| Pdx1p | NP_011709 | Mitochondrial PDH complex | 5 | 19 | 90 | |
| Lpd1p | NP_116635 | Mitochondrial PDH complex; binds to mtDNA | 8 | 21 | 136 | 3.8e-10 |
| Cit1p | NP_014398 | Mitochondrial TCA cycle | 5 | 15 | 86 | 3.8e-05 |
| Cit2p | NP_009931 | Mitochondrial TCA cycle | 5 | 16 | 88 | 2.5e-05 |
| Cit3p | NP_015325 | Mitochondrial TCA cycle | 5 | 14 | 85 | 4.3e-05 |
| Aco1p | NP_013407 | Mitochondrial TCA cycle; binds to mtDNA | 9 | 14 | 132 | 9.5e-10 |
| Idh1p | NP_014361 | Mitochondrial TCA cycle; binds to mtDNA | 7 | 21 | 105 | 4.8e-07 |
| Idh2p | NP_014779 | Mitochondrial TCA cycle | 5 | 15 | 88 | 2.2e-05 |
| Kgd1p | NP_012141 | Mitochondrial TCA cycle; binds to mtDNA | 7 | 8 | 93 | 6.9e-06 |
| Kgd2p | NP_010432 | Mitochondrial TCA cycle; binds to mtDNA | 7 | 18 | 111 | 1.2e-07 |
| Lsc1p | NP_014785 | Mitochondrial TCA cycle | 5 | 14 | 90 | 1.7e-05 |
| Lsc2p | NP_011760 | Mitochondrial TCA cycle | 5 | 16 | 84 | 5.5e-05 |
| Sdh1p | NP_012774 | Mitochondrial TCA cycle and ETC | 6 | 14 | 97 | 2.7e-06 |
| Sdh2p | NP_013059 | Mitochondrial TCA cycle and ETC | 5 | 18 | 88 | 2.5e-05 |
| Sdh3p | NP_012781 | Mitochondrial TCA cycle and ETC | 5 | 22 | 100 | 1.6e-06 |
| Sdh4p | NP_010463 | Mitochondrial TCA cycle and ETC | 4 | 19 | 81 | 0.00011 |
| Fum1p | NP_015061 | Mitochondrial TCA cycle | 6 | 13 | 99 | 1.9e-06 |
| Mdh1p | NP_012838 | Mitochondrial TCA cycle | 5 | 20 | 93 | 7.6e-06 |
| Ndi1p | NP_013586 | Mitochondrial ETC | 7 | 16 | 113 | 7.6e-08 |
| Cyt1p | NP_014708 | Mitochondrial ETC | 5 | 22 | 94 | 5.5e-06 |
| Rip1p | NP_010890 | Mitochondrial ETC | 6 | 51 | 80 | 0.00019 |
| Cox4p | NP_011328 | Mitochondrial ETC | 5 | 49 | 74 | 0.00081 |
| Cox5Ap | NP_014346 | Mitochondrial ETC | 6 | 58 | 86 | 5e-05 |
| Pet100p | NP_010364 | Mitochondrial ETC | 5 | 46 | 66 | 0.0054 |
| Atp1p | NP_009453 | Mitochondrial ATP synthase; binds to mtDNA | 9 | 21 | 148 | 2.4e-11 |
| Atp2p | NP_012655 | Mitochondrial ATP synthase | 6 | 15 | 100 | 1.6e-06 |
| Pet9p | NP_009523 | Mitochondrial ADP/ATP carrier | 8 | 27 | 136 | 8.1e-08 |
| Mir1p | NP_012611 | Mitochondrial phosphate carrier | 7 | 26 | 129 | 1.9e-09 |
| Hem14p | NP_010930 | Heme synthesis in mitochondria | 8 | 18 | 124 | 6e-09 |
| Cyc3p | NP_009361 | Heme attachment to apo-cytochrome c | 5 | 19 | 95 | 5.2e-06 |
| Sod2p | NP_011872 | Detoxification of ROS in mitochondria | 5 | 29 | 102 | 9.5e-07 |
| Prx1p | NP_009489 | Detoxification of ROS in mitochondria | 8 | 30 | 147 | 3e-11 |
| Ccp1p | NP_012992 | Detoxification of ROS in mitochondria | 12 | 50 | 135 | 6.7e-10 |
| Trr2p | NP_011974 | Detoxification of ROS in mitochondria | 7 | 39 | 78 | 0.00037 |

| | | | | | | |
|---|---|---|---|---|---|---|
| Trx3p | NP_010006 | Detoxification of ROS in mitochondria | 5 | 37 | 59 | 0.026 |
| Ssq1p | NP_013473 | Assembly of Fe/S clusters into proteins | 10 | 16 | 145 | 4.8e-11 |
| Ssc1p | NP_012579 | Mitochondrial chaperone; binds to mtDNA | 10 | 21 | 156 | 3.8e-12 |
| Hsp60p | NP_013360 | Mitochondrial chaperone; binds to mtDNA | 11 | 20 | 157 | 3e-12 |
| Caf4p | NP_012962 | Mitochondrial fission | 11 | 25 | 83 | 0.00011 |
| Mdv1p | NP_012423 | Mitochondrial fission | 13 | 28 | 111 | 1.7e-07 |
| Fis1p | NP_012199 | Mitochondrial fission | 5 | 45 | 66 | 0.0048 |
| Mgm1p | NP_014854 | Mitochondrial fusion | 14 | 23 | 64 | 0.0083 |
| Pgs1p | NP_009923 | Cardiolipin synthesis in mitochondria | 8 | 21 | 57 | 0.041 |
| Crd1p | NP_010139 | Cardiolipin synthesis in mitochondria | 7 | 30 | 89 | 2.9e-05 |
| Taz1p | NP_015466 | Cardiolipin synthesis in mitochondria | 9 | 32 | 71 | 0.0018 |
| Ald4p | NP_015019 | Mitochondrial aldehyde dehydrogenase; binds to mtDNA | 8 | 19 | 132 | 9.5e-10 |
| Abf2p | NP_013788 | Mitochondrial genome maintenance; binds to mtDNA | 8 | 44 | 149 | 1.9e-11 |
| Ilv5p | NP_013459 | Branched-chain amino acid biosynthesis in mitochondria; binds to mtDNA | 8 | 25 | 138 | 2.4e-10 |
| Sls1p | NP_013240 | Mitochondrial chaperone; binds to mtDNA | 9 | 19 | 143 | 7.6e-11 |
| **YP + 0.5% glucose; Day 4 (PD phase)** | | | | | | |
| Pda1p | NP_011105 | Mitochondrial PDH complex; binds to mtDNA | 5 | 13 | 81 | 0.00013 |
| Pdb1p | NP_009780 | Mitochondrial PDH complex; binds to mtDNA | 7 | 27 | 128 | 2.4e-09 |
| Lat1p | NP_014328 | Mitochondrial PDH complex | 9 | 25 | 147 | 3e-11 |
| Pdx1p | NP_011709 | Mitochondrial PDH complex | 8 | 28 | 142 | 9.5e-11 |
| Lpd1p | NP_116635 | Mitochondrial PDH complex; binds to mtDNA | 6 | 16 | 102 | 9.5e-07 |
| Cit1p | NP_014398 | Mitochondrial TCA cycle | 9 | 24 | 152 | 9.5e-12 |
| Cit2p | NP_009931 | Mitochondrial TCA cycle | 8 | 25 | 139 | 1.9e-10 |
| Cit3p | NP_015325 | Mitochondrial TCA cycle | 8 | 20 | 134 | 6e-10 |
| Aco1p | NP_013407 | Mitochondrial TCA cycle; binds to mtDNA | 7 | 12 | 104 | 6e-07 |
| Idh1p | NP_014361 | Mitochondrial TCA cycle; binds to mtDNA | 5 | 18 | 87 | 2.9e-05 |
| Idh2p | NP_014779 | Mitochondrial TCA cycle | 7 | 29 | 129 | 1.9e-09 |
| Kgd1p | NP_012141 | Mitochondrial TCA cycle; binds to mtDNA | 6 | 7 | 75 | 0.00048 |
| Kgd2p | NP_010432 | Mitochondrial TCA cycle; binds to mtDNA | 5 | 13 | 80 | 0.00016 |
| Lsc1p | NP_014785 | Mitochondrial TCA cycle | 6 | 30 | 116 | 3.8e-08 |

| | | | | | | |
|---|---|---|---|---|---|---|
| Lsc2p | NP_011760 | Mitochondrial TCA cycle | 8 | 23 | 132 | 9.5e-10 |
| Sdh1p | NP_012774 | Mitochondrial TCA cycle and ETC | 9 | 20 | 144 | 6e-11 |
| Sdh2p | NP_013059 | Mitochondrial TCA cycle and ETC | 4 | 18 | 72 | 0.001 |
| Sdh3p | NP_012781 | Mitochondrial TCA cycle and ETC | 5 | 40 | 106 | 3.8e-07 |
| Sdh4p | NP_010463 | Mitochondrial TCA cycle and ETC | 4 | 29 | 83 | 8.1e-05 |
| Fum1p | NP_015061 | Mitochondrial TCA cycle | 7 | 18 | 119 | 1.9e-08 |
| Mdh1p | NP_012838 | Mitochondrial TCA cycle | 7 | 31 | 131 | 1.2e-09 |
| Ndi1p | NP_013586 | Mitochondrial ETC | 6 | 15 | 98 | 2.7e-06 |
| Cyt1p | NP_014708 | Mitochondrial ETC | 5 | 28 | 99 | 1.8e-06 |
| Rip1p | NP_010890 | Mitochondrial ETC | 6 | 51 | 80 | 0.00019 |
| Cox4p | NP_011328 | Mitochondrial ETC | 5 | 49 | 74 | 0.00081 |
| Cox5Ap | NP_014346 | Mitochondrial ETC | 6 | 58 | 86 | 5e-05 |
| Pet100p | NP_010364 | Mitochondrial ETC | 5 | 46 | 66 | 0.0054 |
| Atp1p | NP_009453 | Mitochondrial ATP synthase; binds to mtDNA | 7 | 19 | 118 | 2.4e-08 |
| Atp2p | NP_012655 | Mitochondrial ATP synthase | 6 | 15 | 100 | 1.6e-06 |
| Pet9p | NP_009523 | Mitochondrial ADP/ATP carrier | 5 | 17 | 85 | 5.2e-05 |
| Mir1p | NP_012611 | Mitochondrial phosphate carrier | 7 | 26 | 129 | 1.9e-09 |
| Hem14p | NP_010930 | Heme synthesis in mitochondria | 8 | 18 | 125 | 4.8e-09 |
| Cyc3p | NP_009361 | Heme attachment to apo-cytochrome c | 5 | 19 | 95 | 5.2e-06 |
| Sod2p | NP_011872 | Detoxification of ROS in mitochondria | 5 | 26 | 100 | 1.7e-06 |
| Prx1p | NP_009489 | Detoxification of ROS in mitochondria | 4 | 18 | 75 | 0.00046 |
| Ccp1p | NP_012992 | Detoxification of ROS in mitochondria | 12 | 50 | 135 | 6.7e-10 |
| Trr2p | NP_011974 | Detoxification of ROS in mitochondria | 7 | 39 | 78 | 0.00037 |
| Trx3p | NP_010006 | Detoxification of ROS in mitochondria | 5 | 37 | 59 | 0.026 |
| Ssq1p | NP_013473 | Assembly of Fe/S clusters into proteins | 9 | 14 | 128 | 2.4e-09 |
| Ssc1p | NP_012579 | Mitochondrial chaperone; binds to mtDNA | 8 | 18 | 128 | 2.4e-09 |
| Hsp60p | NP_013360 | Mitochondrial chaperone; binds to mtDNA | 8 | 19 | 127 | 3e-09 |
| Caf4p | NP_012962 | Mitochondrial fission | 11 | 25 | 83 | 0.00011 |
| Mdv1p | NP_012423 | Mitochondrial fission | 13 | 28 | 111 | 1.7e-07 |
| Fis1p | NP_012199 | Mitochondrial fission | 5 | 45 | 66 | 0.0048 |
| Mgm1p | NP_014854 | Mitochondrial fusion | 14 | 23 | 64 | 0.0083 |
| Pgs1p | NP_009923 | Cardiolipin synthesis in mitochondria | 8 | 21 | 57 | 0.041 |
| Crd1p | NP_010139 | Cardiolipin synthesis in mitochondria | 7 | 30 | 89 | 2.9e-05 |
| Taz1p | NP_015466 | Cardiolipin synthesis in | 9 | 32 | 71 | 0.0018 |

| | | | | | | |
|---|---|---|---|---|---|---|
| | | mitochondria | | | | |
| Ald4p | NP_015019 | Mitochondrial aldehyde dehydrogenase; binds to mtDNA | 6 | 15 | 100 | 1.7e-06 |
| Abf2p | NP_013788 | Mitochondrial genome maintenance; binds to mtDNA | 6 | 34 | 113 | 7.6e-08 |
| Ilv5p | NP_013459 | Branched-chain amino acid biosynthesis in mitochondria; binds to mtDNA | 6 | 20 | 104 | 6e-07 |
| Sls1p | NP_013240 | Mitochondrial chaperone; binds to mtDNA | 7 | 15 | 112 | 9.5e-08 |
| **YP + 1% glucose; Day 4 (PD phase)** | | | | | | |
| Pda1p | NP_011105 | Mitochondrial PDH complex; binds to mtDNA | 6 | 14 | 96 | 4.2e-06 |
| Pdb1p | NP_009780 | Mitochondrial PDH complex; binds to mtDNA | 8 | 31 | 146 | 3.8e-11 |
| Lat1p | NP_014328 | Mitochondrial PDH complex | 7 | 19 | 102 | 9.5e-07 |
| Pdx1p | NP_011709 | Mitochondrial PDH complex | 6 | 23 | 108 | 2.4e-07 |
| Lpd1p | NP_116635 | Mitochondrial PDH complex; binds to mtDNA | 7 | 19 | 119 | 1.9e-08 |
| Cit1p | NP_014398 | Mitochondrial TCA cycle | 7 | 20 | 119 | 1.9e-08 |
| Cit2p | NP_009931 | Mitochondrial TCA cycle | 6 | 20 | 106 | 3.8e-07 |
| Cit3p | NP_015325 | Mitochondrial TCA cycle | 6 | 16 | 102 | 9.5e-07 |
| Aco1p | NP_013407 | Mitochondrial TCA cycle; binds to mtDNA | 8 | 13 | 118 | 2.4e-08 |
| Idh1p | NP_014361 | Mitochondrial TCA cycle; binds to mtDNA | 6 | 21 | 103 | 7.6e-07 |
| Idh2p | NP_014779 | Mitochondrial TCA cycle | 5 | 23 | 94 | 6.4e-06 |
| Kgd1p | NP_012141 | Mitochondrial TCA cycle; binds to mtDNA | 6 | 7 | 82 | 1e-04 |
| Kgd2p | NP_010432 | Mitochondrial TCA cycle; binds to mtDNA | 6 | 16 | 96 | 3.7e-06 |
| Lsc1p | NP_014785 | Mitochondrial TCA cycle; binds to mtDNA | 5 | 23 | 95 | 4.8e-06 |
| Lsc2p | NP_011760 | Mitochondrial TCA cycle | 6 | 19 | 101 | 1.2e-06 |
| Sdh1p | NP_012774 | Mitochondrial TCA cycle and ETC | 7 | 17 | 113 | 7.6e-08 |
| Sdh2p | NP_013059 | Mitochondrial TCA cycle and ETC | 6 | 20 | 104 | 6e-07 |
| Sdh3p | NP_012781 | Mitochondrial TCA cycle and ETC | 4 | 35 | 86 | 3.5e-05 |
| Sdh4p | NP_010463 | Mitochondrial TCA cycle and ETC | 6 | 31 | 123 | 7.6e-09 |
| Fum1p | NP_015061 | Mitochondrial TCA cycle | 5 | 15 | 86 | 3.7e-05 |
| Mdh1p | NP_012838 | Mitochondrial TCA cycle | 5 | 24 | 95 | 4.6e-06 |
| Ndi1p | NP_013586 | Mitochondrial ETC | 6 | 14 | 97 | 3.2e-06 |
| Cyt1p | NP_014708 | Mitochondrial ETC | 5 | 23 | 95 | 4.8e-06 |
| Rip1p | NP_010890 | Mitochondrial ETC | 6 | 51 | 80 | 0.00019 |
| Cox4p | NP_011328 | Mitochondrial ETC | 5 | 49 | 74 | 0.00081 |
| Cox5Ap | NP_014346 | Mitochondrial ETC | 6 | 58 | 86 | 5e-05 |

| | | | | | | |
|---|---|---|---|---|---|---|
| Pet100p | NP_010364 | Mitochondrial ETC | 5 | 46 | 66 | 0.0054 |
| Atp1p | NP_009453 | Mitochondrial ATP synthase; binds to mtDNA | 8 | 20 | 134 | 6e-10 |
| Atp2p | NP_012655 | Mitochondrial ATP synthase | 9 | 20 | 148 | 2.4e-11 |
| Pet9p | NP_009523 | Mitochondrial ADP/ATP carrier | 5 | 17 | 85 | 5.2e-05 |
| Mir1p | NP_012611 | Mitochondrial phosphate carrier | 7 | 27 | 130 | 1.5e-09 |
| Hem14p | NP_010930 | Heme synthesis in mitochondria | 11 | 23 | 169 | 1.9e-13 |
| Cyc3p | NP_009361 | Heme attachment to apo-cytochrome c | 5 | 18 | 94 | 5.6e-06 |
| Sod2p | NP_011872 | Detoxification of ROS in mitochondria | 5 | 26 | 99 | 1.7e-06 |
| Prx1p | NP_009489 | Detoxification of ROS in mitochondria | 8 | 31 | 148 | 2.4e-11 |
| Ccp1p | NP_012992 | Detoxification of ROS in mitochondria | 12 | 50 | 135 | 6.7e-10 |
| Trr2p | NP_011974 | Detoxification of ROS in mitochondria | 7 | 39 | 78 | 0.00037 |
| Trx3p | NP_010006 | Detoxification of ROS in mitochondria | 5 | 37 | 59 | 0.026 |
| Ssq1p | NP_013473 | Assembly of Fe/S clusters into proteins | 9 | 15 | 129 | 1.9e-09 |
| Ssc1p | NP_012579 | Mitochondrial chaperone; binds to mtDNA | 9 | 19 | 142 | 9.5e-11 |
| Hsp60p | NP_013360 | Mitochondrial chaperone; binds to mtDNA | 9 | 21 | 142 | 9.5e-11 |
| Caf4p | NP_012962 | Mitochondrial fission | 11 | 25 | 83 | 0.00011 |
| Mdv1p | NP_012423 | Mitochondrial fission | 13 | 28 | 111 | 1.7e-07 |
| Fis1p | NP_012199 | Mitochondrial fission | 5 | 45 | 66 | 0.0048 |
| Mgm1p | NP_014854 | Mitochondrial fusion | 14 | 23 | 64 | 0.0083 |
| Pgs1p | NP_009923 | Cardiolipin synthesis in mitochondria | 8 | 21 | 57 | 0.041 |
| Crd1p | NP_010139 | Cardiolipin synthesis in mitochondria | 7 | 30 | 89 | 2.9e-05 |
| Taz1p | NP_015466 | Cardiolipin synthesis in mitochondria | 9 | 32 | 71 | 0.0018 |
| Ald4p | NP_015019 | Mitochondrial aldehyde dehydrogenase; binds to mtDNA | 7 | 17 | 116 | 3.8e-08 |
| Abf2p | NP_013788 | Mitochondrial genome maintenance; binds to mtDNA | 7 | 39 | 131 | 1.2e-09 |
| Ilv5p | NP_013459 | Branched-chain amino acid biosynthesis in mitochondria; binds to mtDNA | 7 | 22 | 121 | 1.2e-08 |
| Sls1p | NP_013240 | Mitochondrial chaperone; binds to mtDNA | 8 | 16 | 112 | 9.5e-08 |
| **YP + 2% glucose; Day 4 (PD phase)** | | | | | | |
| Pda1p | NP_011105 | Mitochondrial PDH complex; binds to mtDNA | 4 | 11 | 66 | 0.004 |
| Pdb1p | NP_009780 | Mitochondrial PDH | 6 | 25 | 111 | 1.2e-07 |

| | | | | | | |
|---|---|---|---|---|---|---|
| | | complex; binds to mtDNA | | | | |
| Lat1p | NP_014328 | Mitochondrial PDH complex | 11 | 27 | 161 | 1.2e-12 |
| Pdx1p | NP_011709 | Mitochondrial PDH complex | 10 | 33 | 174 | 6e-14 |
| Lpd1p | NP_116635 | Mitochondrial PDH complex; binds to mtDNA | 5 | 15 | 85 | 4.7e-05 |
| Cit1p | NP_014398 | Mitochondrial TCA cycle | 11 | 28 | 185 | 4.8e-15 |
| Cit2p | NP_009931 | Mitochondrial TCA cycle | 10 | 30 | 173 | 7.6e-14 |
| Cit3p | NP_015325 | Mitochondrial TCA cycle | 10 | 23 | 166 | 3.8e-13 |
| Aco1p | NP_013407 | Mitochondrial TCA cycle; binds to mtDNA | 6 | 11 | 90 | 1.3e-05 |
| Idh1p | NP_014361 | Mitochondrial TCA cycle; binds to mtDNA | 4 | 16 | 73 | 0.00083 |
| Idh2p | NP_014779 | Mitochondrial TCA cycle | 9 | 34 | 164 | 6e-13 |
| Kgd1p | NP_012141 | Mitochondrial TCA cycle; binds to mtDNA | 5 | 6 | 63 | 0.0079 |
| Kgd2p | NP_010432 | Mitochondrial TCA cycle; binds to mtDNA | 4 | 11 | 66 | 0.004 |
| Lsc1p | NP_014785 | Mitochondrial TCA cycle; binds to mtDNA | 8 | 37 | 152 | 9.5e-12 |
| Lsc2p | NP_011760 | Mitochondrial TCA cycle | 10 | 27 | 164 | 6e-13 |
| Sdh1p | NP_012774 | Mitochondrial TCA cycle and ETC | 11 | 23 | 174 | 6e-14 |
| Sdh2p | NP_013059 | Mitochondrial TCA cycle and ETC | 5 | 21 | 89 | 1.9e-05 |
| Sdh3p | NP_012781 | Mitochondrial TCA cycle and ETC | 7 | 50 | 146 | 3.8e-11 |
| Sdh4p | NP_010463 | Mitochondrial TCA cycle and ETC | 5 | 33 | 103 | 7.6e-07 |
| Fum1p | NP_015061 | Mitochondrial TCA cycle | 9 | 21 | 151 | 1.2e-11 |
| Mdh1p | NP_012838 | Mitochondrial TCA cycle | 9 | 39 | 168 | 2.4e-13 |
| Ndi1p | NP_013586 | Mitochondrial ETC | 8 | 18 | 128 | 2.4e-09 |
| Cyt1p | NP_014708 | Mitochondrial ETC | 6 | 26 | 113 | 7.6e-08 |
| Rip1p | NP_010890 | Mitochondrial ETC | 6 | 51 | 80 | 0.00019 |
| Cox4p | NP_011328 | Mitochondrial ETC | 5 | 49 | 74 | 0.00081 |
| Cox5Ap | NP_014346 | Mitochondrial ETC | 6 | 58 | 86 | 5e-05 |
| Pet100p | NP_010364 | Mitochondrial ETC | 5 | 46 | 66 | 0.0054 |
| Atp1p | NP_009453 | Mitochondrial ATP synthase; binds to mtDNA | 6 | 17 | 102 | 9.5e-07 |
| Atp2p | NP_012655 | Mitochondrial ATP synthase | 7 | 17 | 116 | 3.8e-08 |
| Pet9p | NP_009523 | Mitochondrial ADP/ATP carrier | 6 | 20 | 102 | 9.5e-07 |
| Mir1p | NP_012611 | Mitochondrial phosphate carrier | 5 | 20 | 93 | 7.2e-06 |
| Hem14p | NP_010930 | Heme synthesis in mitochondria | 9 | 20 | 140 | 1.5e-10 |
| Cyc3p | NP_009361 | Heme attachment to apo-cytochrome c | 6 | 22 | 113 | 7.6e-08 |
| Sod2p | NP_011872 | Detoxification of ROS in mitochondria | 6 | 30 | 119 | 1.9e-08 |
| Prx1p | NP_009489 | Detoxification of ROS in mitochondria | 5 | 21 | 93 | 6.9e-06 |

| | | | | | | |
|---|---|---|---|---|---|---|
| Ccp1p | NP_012992 | Detoxification of ROS in mitochondria | 12 | 50 | 135 | 6.7e-10 |
| Trr2p | NP_011974 | Detoxification of ROS in mitochondria | 7 | 39 | 78 | 0.00037 |
| Trx3p | NP_010006 | Detoxification of ROS in mitochondria | 5 | 37 | 59 | 0.026 |
| Ssq1p | NP_013473 | Assembly of Fe/S clusters into proteins | 7 | 12 | 102 | 9.5e-07 |
| Ssc1p | NP_012579 | Mitochondrial chaperone; binds to mtDNA | 7 | 16 | 113 | 7.6e-08 |
| Hsp60p | NP_013360 | Mitochondrial chaperone; binds to mtDNA | 7 | 18 | 113 | 7.6e-08 |
| Caf4p | NP_012962 | Mitochondrial fission | 11 | 25 | 83 | 0.00011 |
| Mdv1p | NP_012423 | Mitochondrial fission | 13 | 28 | 111 | 1.7e-07 |
| Fis1p | NP_012199 | Mitochondrial fission | 5 | 45 | 66 | 0.0048 |
| Mgm1p | NP_014854 | Mitochondrial fusion | 14 | 23 | 64 | 0.0083 |
| Pgs1p | NP_009923 | Cardiolipin synthesis in mitochondria | 8 | 21 | 57 | 0.041 |
| Crd1p | NP_010139 | Cardiolipin synthesis in mitochondria | 7 | 30 | 89 | 2.9e-05 |
| Taz1p | NP_015466 | Cardiolipin synthesis in mitochondria | 9 | 32 | 71 | 0.0018 |
| Ald4p | NP_015019 | Mitochondrial aldehyde dehydrogenase; binds to mtDNA | 5 | 13 | 84 | 6.1e-05 |
| Abf2p | NP_013788 | Mitochondrial genome maintenance; binds to mtDNA | 5 | 31 | 96 | 3.7e-06 |
| Ilv5p | NP_013459 | Branched-chain amino acid biosynthesis in mitochondria; binds to mtDNA | 5 | 18 | 89 | 1.9e-05 |
| Sls1p | NP_013240 | Mitochondrial chaperone; binds to mtDNA | 6 | 14 | 97 | 3.2e-06 |
| **YP + 0.2% glucose; Day 9 (ST phase)** | | | | | | |
| Pda1p | NP_011105 | Mitochondrial PDH complex; binds to mtDNA | 6 | 14 | 96 | 4.2e-06 |
| Pdb1p | NP_009780 | Mitochondrial PDH complex; binds to mtDNA | 8 | 31 | 146 | 3.8e-11 |
| Lat1p | NP_014328 | Mitochondrial PDH complex | 7 | 19 | 102 | 9.5e-07 |
| Pdx1p | NP_011709 | Mitochondrial PDH complex | 6 | 23 | 108 | 2.4e-07 |
| Lpd1p | NP_116635 | Mitochondrial PDH complex; binds to mtDNA | 7 | 19 | 119 | 1.9e-08 |
| Cit1p | NP_014398 | Mitochondrial TCA cycle | 7 | 20 | 119 | 1.9e-08 |
| Cit2p | NP_009931 | Mitochondrial TCA cycle | 6 | 20 | 106 | 3.8e-07 |
| Cit3p | NP_015325 | Mitochondrial TCA cycle | 6 | 16 | 102 | 9.5e-07 |
| Aco1p | NP_013407 | Mitochondrial TCA cycle; binds to mtDNA | 8 | 13 | 118 | 2.4e-08 |
| Idh1p | NP_014361 | Mitochondrial TCA cycle; binds to mtDNA | 6 | 21 | 103 | 7.6e-07 |
| Idh2p | NP_014779 | Mitochondrial TCA cycle | 5 | 23 | 94 | 6.4e-06 |
| Kgd1p | NP_012141 | Mitochondrial TCA cycle; binds to mtDNA | 6 | 7 | 82 | 1e-04 |

| | | | | | | |
|---|---|---|---|---|---|---|
| Kgd2p | NP_010432 | Mitochondrial TCA cycle; binds to mtDNA | 6 | 16 | 96 | 3.7e-06 |
| Lsc1p | NP_014785 | Mitochondrial TCA cycle; binds to mtDNA | 5 | 23 | 95 | 4.8e-06 |
| Lsc2p | NP_011760 | Mitochondrial TCA cycle | 6 | 19 | 101 | 1.2e-06 |
| Sdh1p | NP_012774 | Mitochondrial TCA cycle and ETC | 7 | 17 | 113 | 7.6e-08 |
| Sdh2p | NP_013059 | Mitochondrial TCA cycle and ETC | 6 | 20 | 104 | 6e-07 |
| Sdh3p | NP_012781 | Mitochondrial TCA cycle and ETC | 4 | 35 | 86 | 3.5e-05 |
| Sdh4p | NP_010463 | Mitochondrial TCA cycle and ETC | 6 | 31 | 123 | 7.6e-09 |
| Fum1p | NP_015061 | Mitochondrial TCA cycle | 5 | 15 | 86 | 3.7e-05 |
| Mdh1p | NP_012838 | Mitochondrial TCA cycle | 5 | 24 | 95 | 4.6e-06 |
| Ndi1p | NP_013586 | Mitochondrial ETC | 6 | 14 | 97 | 3.2e-06 |
| Cyt1p | NP_014708 | Mitochondrial ETC | 5 | 23 | 95 | 4.8e-06 |
| Rip1p | NP_010890 | Mitochondrial ETC | 6 | 51 | 80 | 0.00019 |
| Cox4p | NP_011328 | Mitochondrial ETC | 5 | 49 | 74 | 0.00081 |
| Cox5Ap | NP_014346 | Mitochondrial ETC | 6 | 58 | 86 | 5e-05 |
| Pet100p | NP_010364 | Mitochondrial ETC | 5 | 46 | 66 | 0.0054 |
| Atp1p | NP_009453 | Mitochondrial ATP synthase; binds to mtDNA | 8 | 20 | 134 | 6e-10 |
| Atp2p | NP_012655 | Mitochondrial ATP synthase | 9 | 20 | 148 | 2.4e-11 |
| Pet9p | NP_009523 | Mitochondrial ADP/ATP carrier | 5 | 17 | 85 | 5.2e-05 |
| Mir1p | NP_012611 | Mitochondrial phosphate carrier | 7 | 27 | 130 | 1.5e-09 |
| Hem14p | NP_010930 | Heme synthesis in mitochondria | 11 | 23 | 169 | 1.9e-13 |
| Cyc3p | NP_009361 | Heme attachment to apo-cytochrome c | 5 | 18 | 94 | 5.6e-06 |
| Sod2p | NP_011872 | Detoxification of ROS in mitochondria | 5 | 26 | 99 | 1.7e-06 |
| Prx1p | NP_009489 | Detoxification of ROS in mitochondria | 8 | 31 | 148 | 2.4e-11 |
| Ccp1p | NP_012992 | Detoxification of ROS in mitochondria | 12 | 50 | 135 | 6.7e-10 |
| Trr2p | NP_011974 | Detoxification of ROS in mitochondria | 7 | 39 | 78 | 0.00037 |
| Trx3p | NP_010006 | Detoxification of ROS in mitochondria | 5 | 37 | 59 | 0.026 |
| Ssq1p | NP_013473 | Assembly of Fe/S clusters into proteins | 9 | 15 | 129 | 1.9e-09 |
| Ssc1p | NP_012579 | Mitochondrial chaperone; binds to mtDNA | 9 | 19 | 142 | 9.5e-11 |
| Hsp60p | NP_013360 | Mitochondrial chaperone; binds to mtDNA | 9 | 21 | 142 | 9.5e-11 |
| Caf4p | NP_012962 | Mitochondrial fission | 11 | 25 | 83 | 0.00011 |
| Mdv1p | NP_012423 | Mitochondrial fission | 13 | 28 | 111 | 1.7e-07 |
| Fis1p | NP_012199 | Mitochondrial fission | 5 | 45 | 66 | 0.0048 |
| Mgm1p | NP_014854 | Mitochondrial fusion | 14 | 23 | 64 | 0.0083 |
| Pgs1p | NP_009923 | Cardiolipin synthesis in | 8 | 21 | 57 | 0.041 |

| | | | | | | |
|---|---|---|---|---|---|---|
| | | mitochondria | | | | |
| Crd1p | NP_010139 | Cardiolipin synthesis in mitochondria | 7 | 30 | 89 | 2.9e-05 |
| Taz1p | NP_015466 | Cardiolipin synthesis in mitochondria | 9 | 32 | 71 | 0.0018 |
| Ald4p | NP_015019 | Mitochondrial aldehyde dehydrogenase; binds to mtDNA | 7 | 17 | 116 | 3.8e-08 |
| Abf2p | NP_013788 | Mitochondrial genome maintenance; binds to mtDNA | 7 | 39 | 131 | 1.2e-09 |
| Ilv5p | NP_013459 | Branched-chain amino acid biosynthesis in mitochondria; binds to mtDNA | 7 | 22 | 121 | 1.2e-08 |
| Sls1p | NP_013240 | Mitochondrial chaperone; binds to mtDNA | 8 | 16 | 112 | 9.5e-08 |
| **YP + 0.5% glucose; Day 9 (ST phase)** | | | | | | |
| Pda1p | NP_011105 | Mitochondrial PDH complex; binds to mtDNA | 7 | 17 | 109 | 1.9e-07 |
| Pdb1p | NP_009780 | Mitochondrial PDH complex; binds to mtDNA | 9 | 34 | 164 | 6e-13 |
| Lat1p | NP_014328 | Mitochondrial PDH complex | 5 | 16 | 85 | |
| Pdx1p | NP_011709 | Mitochondrial PDH complex | 5 | 19 | 90 | |
| Lpd1p | NP_116635 | Mitochondrial PDH complex; binds to mtDNA | 8 | 21 | 136 | 3.8e-10 |
| Cit1p | NP_014398 | Mitochondrial TCA cycle | 5 | 15 | 86 | 3.8e-05 |
| Cit2p | NP_009931 | Mitochondrial TCA cycle | 5 | 16 | 88 | 2.5e-05 |
| Cit3p | NP_015325 | Mitochondrial TCA cycle | 5 | 14 | 85 | 4.3e-05 |
| Aco1p | NP_013407 | Mitochondrial TCA cycle; binds to mtDNA | 9 | 14 | 132 | 9.5e-10 |
| Idh1p | NP_014361 | Mitochondrial TCA cycle; binds to mtDNA | 7 | 21 | 105 | 4.8e-07 |
| Idh2p | NP_014779 | Mitochondrial TCA cycle | 5 | 15 | 88 | 2.2e-05 |
| Kgd1p | NP_012141 | Mitochondrial TCA cycle; binds to mtDNA | 7 | 8 | 93 | 6.9e-06 |
| Kgd2p | NP_010432 | Mitochondrial TCA cycle; binds to mtDNA | 7 | 18 | 111 | 1.2e-07 |
| Lsc1p | NP_014785 | Mitochondrial TCA cycle | 5 | 14 | 90 | 1.7e-05 |
| Lsc2p | NP_011760 | Mitochondrial TCA cycle | 5 | 16 | 84 | 5.5e-05 |
| Sdh1p | NP_012774 | Mitochondrial TCA cycle and ETC | 6 | 14 | 97 | 2.7e-06 |
| Sdh2p | NP_013059 | Mitochondrial TCA cycle and ETC | 5 | 18 | 88 | 2.5e-05 |
| Sdh3p | NP_012781 | Mitochondrial TCA cycle and ETC | 5 | 22 | 100 | 1.6e-06 |
| Sdh4p | NP_010463 | Mitochondrial TCA cycle and ETC | 4 | 19 | 81 | 0.00011 |
| Fum1p | NP_015061 | Mitochondrial TCA cycle | 6 | 13 | 99 | 1.9e-06 |
| Mdh1p | NP_012838 | Mitochondrial TCA cycle | 5 | 20 | 93 | 7.6e-06 |
| Ndi1p | NP_013586 | Mitochondrial ETC | 7 | 16 | 113 | 7.6e-08 |
| Cyt1p | NP_014708 | Mitochondrial ETC | 5 | 22 | 94 | 5.5e-06 |

| | | | | | | |
|---|---|---|---|---|---|---|
| Rip1p | NP_010890 | Mitochondrial ETC | 6 | 51 | 80 | 0.00019 |
| Cox4p | NP_011328 | Mitochondrial ETC | 5 | 49 | 74 | 0.00081 |
| Cox5Ap | NP_014346 | Mitochondrial ETC | 6 | 58 | 86 | 5e-05 |
| Pet100p | NP_010364 | Mitochondrial ETC | 5 | 46 | 66 | 0.0054 |
| Atp1p | NP_009453 | Mitochondrial ATP synthase; binds to mtDNA | 9 | 21 | 148 | 2.4e-11 |
| Atp2p | NP_012655 | Mitochondrial ATP synthase | 6 | 15 | 100 | 1.6e-06 |
| Pet9p | NP_009523 | Mitochondrial ADP/ATP carrier | 8 | 27 | 136 | 8.1e-08 |
| Mir1p | NP_012611 | Mitochondrial phosphate carrier | 7 | 26 | 129 | 1.9e-09 |
| Hem14p | NP_010930 | Heme synthesis in mitochondria | 8 | 18 | 124 | 6e-09 |
| Cyc3p | NP_009361 | Heme attachment to apo-cytochrome c | 5 | 19 | 95 | 5.2e-06 |
| Sod2p | NP_011872 | Detoxification of ROS in mitochondria | 5 | 29 | 102 | 9.5e-07 |
| Prx1p | NP_009489 | Detoxification of ROS in mitochondria | 8 | 30 | 147 | 3e-11 |
| Ccp1p | NP_012992 | Detoxification of ROS in mitochondria | 12 | 50 | 135 | 6.7e-10 |
| Trr2p | NP_011974 | Detoxification of ROS in mitochondria | 7 | 39 | 78 | 0.00037 |
| Trx3p | NP_010006 | Detoxification of ROS in mitochondria | 5 | 37 | 59 | |
| Ssq1p | NP_013473 | Assembly of Fe/S clusters into proteins | 10 | 16 | 145 | 4.8e-11 |
| Ssc1p | NP_012579 | Mitochondrial chaperone; binds to mtDNA | 10 | 21 | 156 | 3.8e-12 |
| Hsp60p | NP_013360 | Mitochondrial chaperone; binds to mtDNA | 11 | 20 | 157 | 3e-12 |
| Caf4p | NP_012962 | Mitochondrial fission | 11 | 25 | 83 | 0.00011 |
| Mdv1p | NP_012423 | Mitochondrial fission | 13 | 28 | 111 | 1.7e-07 |
| Fis1p | NP_012199 | Mitochondrial fission | 5 | 45 | 66 | 0.0048 |
| Mgm1p | NP_014854 | Mitochondrial fusion | 14 | 23 | 64 | 0.0083 |
| Pgs1p | NP_009923 | Cardiolipin synthesis in mitochondria | 8 | 21 | 57 | 0.041 |
| Crd1p | NP_010139 | Cardiolipin synthesis in mitochondria | 7 | 30 | 89 | 2.9e-05 |
| Taz1p | NP_015466 | Cardiolipin synthesis in mitochondria | 9 | 32 | 71 | 0.0018 |
| Ald4p | NP_015019 | Mitochondrial aldehyde dehydrogenase; binds to mtDNA | 8 | 19 | 132 | 9.5e-10 |
| Abf2p | NP_013788 | Mitochondrial genome maintenance; binds to mtDNA | 8 | 44 | 149 | 1.9e-11 |
| Ilv5p | NP_013459 | Branched-chain amino acid biosynthesis in mitochondria; binds to mtDNA | 8 | 25 | 138 | 2.4e-10 |
| Sls1p | NP_013240 | Mitochondrial chaperone; binds to mtDNA | 9 | 19 | 143 | 7.6e-11 |
| **YP + 1% glucose; Day 9 (ST phase)** | | | | | | |

| | | | | | | |
|---|---|---|---|---|---|---|
| Pda1p | NP_011105 | Mitochondrial PDH complex; binds to mtDNA | 5 | 13 | 81 | 0.00013 |
| Pdb1p | NP_009780 | Mitochondrial PDH complex; binds to mtDNA | 7 | 27 | 128 | 2.4e-09 |
| Lat1p | NP_014328 | Mitochondrial PDH complex | 9 | 25 | 147 | 3e-11 |
| Pdx1p | NP_011709 | Mitochondrial PDH complex | 8 | 28 | 142 | 9.5e-11 |
| Lpd1p | NP_116635 | Mitochondrial PDH complex; binds to mtDNA | 6 | 16 | 102 | 9.5e-07 |
| Cit1p | NP_014398 | Mitochondrial TCA cycle | 9 | 24 | 152 | 9.5e-12 |
| Cit2p | NP_009931 | Mitochondrial TCA cycle | 8 | 25 | 139 | 1.9e-10 |
| Cit3p | NP_015325 | Mitochondrial TCA cycle | 8 | 20 | 134 | 6e-10 |
| Aco1p | NP_013407 | Mitochondrial TCA cycle; binds to mtDNA | 7 | 12 | 104 | 6e-07 |
| Idh1p | NP_014361 | Mitochondrial TCA cycle; binds to mtDNA | 5 | 18 | 87 | 2.9e-05 |
| Idh2p | NP_014779 | Mitochondrial TCA cycle | 7 | 29 | 129 | 1.9e-09 |
| Kgd1p | NP_012141 | Mitochondrial TCA cycle; binds to mtDNA | 6 | 7 | 75 | 0.00048 |
| Kgd2p | NP_010432 | Mitochondrial TCA cycle; binds to mtDNA | 5 | 13 | 80 | 0.00016 |
| Lsc1p | NP_014785 | Mitochondrial TCA cycle | 6 | 30 | 116 | 3.8e-08 |
| Lsc2p | NP_011760 | Mitochondrial TCA cycle | 8 | 23 | 132 | 9.5e-10 |
| Sdh1p | NP_012774 | Mitochondrial TCA cycle and ETC | 9 | 20 | 144 | 6e-11 |
| Sdh2p | NP_013059 | Mitochondrial TCA cycle and ETC | 4 | 18 | 72 | 0.001 |
| Sdh3p | NP_012781 | Mitochondrial TCA cycle and ETC | 5 | 40 | 106 | 3.8e-07 |
| Sdh4p | NP_010463 | Mitochondrial TCA cycle and ETC | 4 | 29 | 83 | 8.1e-05 |
| Fum1p | NP_015061 | Mitochondrial TCA cycle | 7 | 18 | 119 | 1.9e-08 |
| Mdh1p | NP_012838 | Mitochondrial TCA cycle | 7 | 31 | 131 | 1.2e-09 |
| Ndi1p | NP_013586 | Mitochondrial ETC | 6 | 15 | 98 | 2.7e-06 |
| Cyt1p | NP_014708 | Mitochondrial ETC | 5 | 28 | 99 | 1.8e-06 |
| Rip1p | NP_010890 | Mitochondrial ETC | 6 | 51 | 80 | 0.00019 |
| Cox4p | NP_011328 | Mitochondrial ETC | 5 | 49 | 74 | 0.00081 |
| Cox5Ap | NP_014346 | Mitochondrial ETC | 6 | 58 | 86 | 5e-05 |
| Pet100p | NP_010364 | Mitochondrial ETC | 5 | 46 | 66 | 0.0054 |
| Atp1p | NP_009453 | Mitochondrial ATP synthase; binds to mtDNA | 7 | 19 | 118 | 2.4e-08 |
| Atp2p | NP_012655 | Mitochondrial ATP synthase | 6 | 15 | 100 | 1.6e-06 |
| Pet9p | NP_009523 | Mitochondrial ADP/ATP carrier | 5 | 17 | 85 | 5.2e-05 |
| Mir1p | NP_012611 | Mitochondrial phosphate carrier | 7 | 26 | 129 | 1.9e-09 |
| Hem14p | NP_010930 | Heme synthesis in mitochondria | 8 | 18 | 125 | 4.8e-09 |
| Cyc3p | NP_009361 | Heme attachment to apo-cytochrome c | 5 | 19 | 95 | 5.2e-06 |
| Sod2p | NP_011872 | Detoxification of ROS in mitochondria | 5 | 26 | 100 | 1.7e-06 |

| | | | | | | |
|---|---|---|---|---|---|---|
| Prx1p | NP_009489 | Detoxification of ROS in mitochondria | 4 | 18 | 75 | 0.00046 |
| Ccp1p | NP_012992 | Detoxification of ROS in mitochondria | 12 | 50 | 135 | 6.7e-10 |
| Trr2p | NP_011974 | Detoxification of ROS in mitochondria | 7 | 39 | 78 | 0.00037 |
| Trx3p | NP_010006 | Detoxification of ROS in mitochondria | 5 | 37 | 59 | 0.026 |
| Ssq1p | NP_013473 | Assembly of Fe/S clusters into proteins | 9 | 14 | 128 | 2.4e-09 |
| Ssc1p | NP_012579 | Mitochondrial chaperone; binds to mtDNA | 8 | 18 | 128 | 2.4e-09 |
| Hsp60p | NP_013360 | Mitochondrial chaperone; binds to mtDNA | 8 | 19 | 127 | 3e-09 |
| Caf4p | NP_012962 | Mitochondrial fission | 11 | 25 | 83 | 0.00011 |
| Mdv1p | NP_012423 | Mitochondrial fission | 13 | 28 | 111 | 1.7e-07 |
| Fis1p | NP_012199 | Mitochondrial fission | 5 | 45 | 66 | 0.0048 |
| Mgm1p | NP_014854 | Mitochondrial fusion | 14 | 23 | 64 | 0.0083 |
| Pgs1p | NP_009923 | Cardiolipin synthesis in mitochondria | 8 | 21 | 57 | 0.041 |
| Crd1p | NP_010139 | Cardiolipin synthesis in mitochondria | 7 | 30 | 89 | 2.9e-05 |
| Taz1p | NP_015466 | Cardiolipin synthesis in mitochondria | 9 | 32 | 71 | 0.0018 |
| Ald4p | NP_015019 | Mitochondrial aldehyde dehydrogenase; binds to mtDNA | 6 | 15 | 100 | 1.7e-06 |
| Abf2p | NP_013788 | Mitochondrial genome maintenance; binds to mtDNA | 6 | 34 | 113 | 7.6e-08 |
| Ilv5p | NP_013459 | Branched-chain amino acid biosynthesis in mitochondria; binds to mtDNA | 6 | 20 | 104 | 6e-07 |
| Sls1p | NP_013240 | Mitochondrial chaperone; binds to mtDNA | 7 | 15 | 112 | 9.5e-08 |
| **YP + 2% glucose; Day 9 (ST phase)** | | | | | | |
| Pda1p | NP_011105 | Mitochondrial PDH complex; binds to mtDNA | 7 | 17 | 109 | 1.9e-07 |
| Pdb1p | NP_009780 | Mitochondrial PDH complex; binds to mtDNA | 9 | 34 | 164 | 6e-13 |
| Lat1p | NP_014328 | Mitochondrial PDH complex | 5 | 16 | 85 | |
| Pdx1p | NP_011709 | Mitochondrial PDH complex | 5 | 19 | 90 | |
| Lpd1p | NP_116635 | Mitochondrial PDH complex; binds to mtDNA | 8 | 21 | 136 | 3.8e-10 |
| Cit1p | NP_014398 | Mitochondrial TCA cycle | 5 | 15 | 86 | 3.8e-05 |
| Cit2p | NP_009931 | Mitochondrial TCA cycle | 5 | 16 | 88 | 2.5e-05 |
| Cit3p | NP_015325 | Mitochondrial TCA cycle | 5 | 14 | 85 | 4.3e-05 |
| Aco1p | NP_013407 | Mitochondrial TCA cycle; binds to mtDNA | 9 | 14 | 132 | 9.5e-10 |
| Idh1p | NP_014361 | Mitochondrial TCA cycle; binds to mtDNA | 7 | 21 | 105 | 4.8e-07 |
| Idh2p | NP_014779 | Mitochondrial TCA cycle | 5 | 15 | 88 | 2.2e-05 |

| | | | | | | |
|---|---|---|---|---|---|---|
| Kgd1p | NP_012141 | Mitochondrial TCA cycle; binds to mtDNA | 7 | 8 | 93 | 6.9e-06 |
| Kgd2p | NP_010432 | Mitochondrial TCA cycle; binds to mtDNA | 7 | 18 | 111 | 1.2e-07 |
| Lsc1p | NP_014785 | Mitochondrial TCA cycle | 5 | 14 | 90 | 1.7e-05 |
| Lsc2p | NP_011760 | Mitochondrial TCA cycle | 5 | 16 | 84 | 5.5e-05 |
| Sdh1p | NP_012774 | Mitochondrial TCA cycle and ETC | 6 | 14 | 97 | 2.7e-06 |
| Sdh2p | NP_013059 | Mitochondrial TCA cycle and ETC | 5 | 18 | 88 | 2.5e-05 |
| Sdh3p | NP_012781 | Mitochondrial TCA cycle and ETC | 5 | 22 | 100 | 1.6e-06 |
| Sdh4p | NP_010463 | Mitochondrial TCA cycle and ETC | 4 | 19 | 81 | 0.00011 |
| Fum1p | NP_015061 | Mitochondrial TCA cycle | 6 | 13 | 99 | 1.9e-06 |
| Mdh1p | NP_012838 | Mitochondrial TCA cycle | 5 | 20 | 93 | 7.6e-06 |
| Ndi1p | NP_013586 | Mitochondrial ETC | 7 | 16 | 113 | 7.6e-08 |
| Cyt1p | NP_014708 | Mitochondrial ETC | 5 | 22 | 94 | 5.5e-06 |
| Rip1p | NP_010890 | Mitochondrial ETC | 6 | 51 | 80 | 0.00019 |
| Cox4p | NP_011328 | Mitochondrial ETC | 5 | 49 | 74 | 0.00081 |
| Cox5Ap | NP_014346 | Mitochondrial ETC | 6 | 58 | 86 | 5e-05 |
| Pet100p | NP_010364 | Mitochondrial ETC | 5 | 46 | 66 | 0.0054 |
| Atp1p | NP_009453 | Mitochondrial ATP synthase; binds to mtDNA | 9 | 21 | 148 | 2.4e-11 |
| Atp2p | NP_012655 | Mitochondrial ATP synthase | 6 | 15 | 100 | 1.6e-06 |
| Pet9p | NP_009523 | Mitochondrial ADP/ATP carrier | 8 | 27 | 136 | 8.1e-08 |
| Mir1p | NP_012611 | Mitochondrial phosphate carrier | 7 | 26 | 129 | 1.9e-09 |
| Hem14p | NP_010930 | Heme synthesis in mitochondria | 8 | 18 | 124 | 6e-09 |
| Cyc3p | NP_009361 | Heme attachment to apo-cytochrome c | 5 | 19 | 95 | 5.2e-06 |
| Sod2p | NP_011872 | Detoxification of ROS in mitochondria | 5 | 29 | 102 | 9.5e-07 |
| Prx1p | NP_009489 | Detoxification of ROS in mitochondria | 8 | 30 | 147 | 3e-11 |
| Ccp1p | NP_012992 | Detoxification of ROS in mitochondria | 12 | 50 | 135 | 6.7e-10 |
| Trr2p | NP_011974 | Detoxification of ROS in mitochondria | 7 | 39 | 78 | 0.00037 |
| Trx3p | NP_010006 | Detoxification of ROS in mitochondria | 5 | 37 | 59 | 0.026 |
| Ssq1p | NP_013473 | Assembly of Fe/S clusters into proteins | 10 | 16 | 145 | 4.8e-11 |
| Ssc1p | NP_012579 | Mitochondrial chaperone; binds to mtDNA | 10 | 21 | 156 | 3.8e-12 |
| Hsp60p | NP_013360 | Mitochondrial chaperone; binds to mtDNA | 11 | 20 | 157 | 3e-12 |
| Caf4p | NP_012962 | Mitochondrial fission | 11 | 25 | 83 | 0.00011 |
| Mdv1p | NP_012423 | Mitochondrial fission | 13 | 28 | 111 | 1.7e-07 |
| Fis1p | NP_012199 | Mitochondrial fission | 5 | 45 | 66 | 0.0048 |
| Mgm1p | NP_014854 | Mitochondrial fusion | 14 | 23 | 64 | 0.0083 |

| | | | | | | |
|---|---|---|---|---|---|---|
| Pgs1p | NP_009923 | Cardiolipin synthesis in mitochondria | 8 | 21 | 57 | 0.041 |
| Crd1p | NP_010139 | Cardiolipin synthesis in mitochondria | 7 | 30 | 89 | 2.9e-05 |
| Taz1p | NP_015466 | Cardiolipin synthesis in mitochondria | 9 | 32 | 71 | 0.0018 |
| Ald4p | NP_015019 | Mitochondrial aldehyde dehydrogenase; binds to mtDNA | 8 | 19 | 132 | 9.5e-10 |
| Abf2p | NP_013788 | Mitochondrial genome maintenance; binds to mtDNA | 8 | 44 | 149 | 1.9e-11 |
| Ilv5p | NP_013459 | Branched-chain amino acid biosynthesis in mitochondria; binds to mtDNA | 8 | 25 | 138 | 2.4e-10 |
| Sls1p | NP_013240 | Mitochondrial chaperone; binds to mtDNA | 9 | 19 | 143 | 7.6e-11 |

**Table 2.2.** Relative levels of proteins recovered in mitochondria purified from wild-type cells grown in YP media initially containing 0.2%, 0.5%, 1% or 2% glucose. Mitochondria were purified from wild-type cells collected at day 1 (L phase), day 2 (D phase), day 4 (PD phase) and day 9 (ST phase). Proteins were identified and quantified using MALDI MS peptide mapping. Relative protein levels are presented as fold difference relative to that on 2% glucose.

| Protein | NCBI accession no. | Function | Protein level | | | |
|---|---|---|---|---|---|---|
| | | | Glucose concentration (%) | | | |
| | | | 0.2 | 0.5 | 1 | 2 |
| **Day 1 (L phase)** | | | | | | |
| Pda1p | NP_011105 | Mitochondrial PDH complex; binds to mtDNA | 2.49 ± 0.34 | 1.76 ± 0.23 | 1.24 ± 0.16 | 1 |
| Pdb1p | NP_009780 | Mitochondrial PDH complex; binds to mtDNA | 2.79 ± 0.42 | 1.53 ± 0.34 | 0.87 ± 0.29 | 1 |
| Lat1p | NP_014328 | Mitochondrial PDH complex | 2.67 ± 0.42 | 1.49 ± 0.33 | 0.83 ± 0.18 | 1 |
| Pdx1p | NP_011709 | Mitochondrial PDH complex | 1.79 ± 0.30 | 1.62 ± 0.27 | 1.19 ± 0.12 | 1 |
| Lpd1p | NP_116635 | Mitochondrial PDH complex; binds to mtDNA | 1.63 ± 0.31 | 1.24 ± 0.22 | 0.96 ± 0.13 | 1 |
| Cit1p | NP_014398 | Mitochondrial TCA cycle | 1.54 ± 0.25 | 1.28 ± 0.14 | 0.77 ± 0.09 | 1 |
| Cit2p | NP_009931 | Mitochondrial TCA cycle | 1.88 ± 0.34 | 1.34 ± 0.30 | 1.29 ± 0.16 | 1 |
| Cit3p | NP_015325 | Mitochondrial TCA cycle | 1.47 ± 0.19 | 1.23 ± 0.22 | 1.38 ± 0.35 | 1 |
| Aco1p | NP_013407 | Mitochondrial TCA cycle; binds to mtDNA | 2.82 ± 0.55 | 1.38 ± 0.16 | 0.81 ± 0.11 | 1 |
| Idh1p | NP_014361 | Mitochondrial TCA cycle; binds to mtDNA | 1.35 ± 0.24 | 0.88 ± 0.29 | 0.73 ± 0.08 | 1 |
| Idh2p | NP_014779 | Mitochondrial TCA cycle | 1.84 ± 0.21 | 1.35 ± 0.14 | 0.91 ± 0.27 | |
| Kgd1p | NP_012141 | Mitochondrial TCA cycle; binds to mtDNA | 1.67 ± 0.19 | 1.23 ± 0.32 | 1.17 ± 0.15 | 1 |
| Kgd2p | NP_010432 | Mitochondrial TCA cycle; binds to mtDNA | 1.39 ± 0.23 | 1.68 ± 0.19 | 0.83 ± 0.21 | 1 |
| Lsc1p | NP_014785 | Mitochondrial TCA cycle; binds to mtDNA | 1.66 ± 0.13 | 1.27 ± 0.28 | 1.19 ± 0.19 | 1 |

| | | | | | | |
|---|---|---|---|---|---|---|
| Lsc2p | NP_011760 | Mitochondrial TCA cycle | 1.71 ± 0.35 | 1.53 ± 0.21 | 0.89 ± 0.07 | 1 |
| Sdh1p | NP_012774 | Mitochondrial TCA cycle and ETC | 1.32 ± 0.11 | 0.87 ± 0.06 | 1.18 ± 0.21 | 1 |
| Sdh2p | NP_013059 | Mitochondrial TCA cycle and ETC | 1.86 ± 0.23 | 1.52 ± 0.18 | 0.76 ± 0.08 | 1 |
| Sdh3p | NP_012781 | Mitochondrial TCA cycle and ETC | 1.39 ± 0.32 | 1.28 ± 0.24 | 0.93 ± 0.15 | 1 |
| Sdh4p | NP_010463 | Mitochondrial TCA cycle and ETC | 1.56 ± 0.14 | 1.19 ± 0.23 | 0.75 ± 0.09 | 1 |
| Fum1p | NP_015061 | Mitochondrial TCA cycle | 1.33 ± 0.22 | 1.47 ± 0.15 | 0.84 ± 0.17 | 1 |
| Mdh1p | NP_012838 | Mitochondrial TCA cycle | 1.45 ± 0.13 | 1.26 ± 0.17 | 1.05 ± 0.23 | 1 |
| Ndi1p | NP_013586 | Mitochondrial ETC | 1.69 ± 0.20 | 1.31 ± 0.08 | 1.09 ± 0.15 | 1 |
| Cyt1p | NP_014708 | Mitochondrial ETC | 1.39 ± 0.11 | 1.12 ± 0.17 | 0.87 ± 0.13 | 1 |
| Rip1p | NP_010890 | Mitochondrial ETC | 1.26 ± 0.19 | 1.48 ± 0.16 | 0.95 ± 0.11 | 1 |
| Cox4p | NP_011328 | Mitochondrial ETC | 1.43 ± 0.17 | 1.11 ± 0.13 | 1.04 ± 0.25 | 1 |
| Cox5Ap | NP_014346 | Mitochondrial ETC | 1.67 ± 0.29 | 1.32 ± 0.25 | 0.84 ± 0.18 | 1 |
| Pet100p | NP_010364 | Mitochondrial ETC | 1.51 ± 0.13 | 1.59 ± 0.31 | 1.09 ± 0.15 | 1 |
| Atp1p | NP_009453 | Mitochondrial ATP synthase; binds to mtDNA | 1.29 ± 0.18 | 1.43 ± 0.24 | 1.18 ± 0.07 | 1 |
| Atp2p | NP_012655 | Mitochondrial ATP synthase | 1.49± 0.09 | 1.31 ± 0.14 | 1.06 ± 0.21 | 1 |
| Pet9p | NP_009523 | Mitochondrial ADP/ATP carrier | 1.17 ± 0.21 | 1.28 ± 0.26 | 0.95 ± 0.17 | 1 |
| Mir1p | NP_012611 | Mitochondrial phosphate carrier | 1.29 ± 0.14 | 1.46 ± 0.09 | 1.11 ± 0.33 | 1 |
| Hem14p | NP_010930 | Heme synthesis in mitochondria | 1.56 ± 0.27 | 1.67 ± 0.16 | 0.87 ± 0.06 | 1 |
| Cyc3p | NP_009361 | Heme attachment to apo-cytochrome c | 1.72 ± 0.32 | 1.23 ± 0.08 | 1.09 ± 0.16 | 1 |
| Sod2p | NP_011872 | Detoxification of ROS in mitochondria | 1.24 ± 0.15 | 1.48 ± 0.19 | 0.94 ± 0.12 | 1 |
| Prx1p | NP_009489 | Detoxification of ROS in mitochondria | 1.57 ± 0.33 | 1.69 ± 0.21 | 1.18 ± 0.19 | 1 |
| Ccp1p | NP_012992 | Detoxification of ROS in mitochondria | 1.45 ± 0.23 | 1.78 ± 0.34 | 1.07 ± 0.08 | 1 |
| Trr2p | NP_011974 | Detoxification of ROS in mitochondria | 1.28 ± 0.12 | 1.53 ± 0.27 | 0.88 ± 0.14 | 1 |
| Trx3p | NP_010006 | Detoxification of ROS in mitochondria | 1.52 ± 0.17 | 1.27 ± 0.13 | 1.12 ± 0.18 | 1 |
| Ssq1p | NP_013473 | Assembly of Fe/S clusters into proteins | 1.74 ± 0.41 | 1.58 ± 0.23 | 1.04 ± 0.13 | 1 |
| Ssc1p | NP_012579 | Mitochondrial chaperone; binds to mtDNA | 1.34 ± 0.18 | 1.15 ± 0.09 | 0.79 ± 0.06 | 1 |
| Hsp60p | NP_013360 | Mitochondrial chaperone; binds to mtDNA | 1.76 ± 0.21 | 1.52 ± 0.18 | 0.83 ± 0.13 | 1 |
| Caf4p | NP_012962 | Mitochondrial fission | 0.69 ± 0.11 | 0.43 ± 0.09 | 1.13 ± 0.18 | 1 |
| Mdv1p | NP_012423 | Mitochondrial fission | 0.87 ± 0.23 | 0.73 ± 0.12 | 0.92 ± 0.15 | 1 |
| Fis1p | NP_012199 | Mitochondrial fission | 0.93 ± 0.15 | 1.07 ± 0.24 | 1.20 ± 0.32 | 1 |
| Mgm1p | NP_014854 | Mitochondrial fusion | 1.32 ± 0.21 | 1.49 ± 0.15 | 0.89 ± 0.13 | 1 |
| Pgs1p | NP_009923 | Cardiolipin synthesis in mitochondria | 0.81 ± 0.19 | 0.97 ± 0.12 | 0.93 ± 0.19 | 1 |
| Crd1p | NP_010139 | Cardiolipin synthesis in mitochondria | 0.96 ± 0.23 | 1.05 ± 0.14 | 0.87 ± 0.27 | 1 |
| Taz1p | NP_015466 | Cardiolipin synthesis in mitochondria | 0.88 ± 0.17 | 0.67 ± 0.11 | 1.06 ± 0.13 | 1 |
| Ald4p | NP_015019 | Mitochondrial aldehyde dehydrogenase; binds to mtDNA | 1.43 ± 0.23 | 1.22 ± 0.11 | 0.83 ± 0.09 | 1 |
| Abf2p | NP_013788 | Mitochondrial genome maintenance; binds to mtDNA | 0.71 ± 0.21 | 0.92 ± 0.08 | 1.14 ± 0.29 | 1 |
| Ilv5p | NP_013459 | Branched-chain amino acid biosynthesis in mitochondria; binds to mtDNA | 0.63 ± 0.13 | 0.88 ± 0.26 | 0.92 ± 0.14 | 1 |
| Sls1p | NP_013240 | Mitochondrial chaperone; binds to mtDNA | 1.57 ± 0.13 | 0.93 ± 0.11 | 1.34 ± 0.29 | 1 |
| **Day 2 (D phase)** | | | | | | |
| Pda1p | NP_011105 | Mitochondrial PDH complex; binds to mtDNA | 3.67 ± 0.42 | 2.53 ± 0.34 | 1.34 ± 0.23 | 1 |
| Pdb1p | NP_009780 | Mitochondrial PDH complex; binds to mtDNA | 3.89 ± 0.27 | 2.76 ± 0.39 | 1.17 ± 0.18 | 1 |
| Lat1p | NP_014328 | Mitochondrial PDH complex | 3.87 ± 0.45 | 2.56 ± 0.32 | 1.34 ± 0.19 | 1 |
| Pdx1p | NP_011709 | Mitochondrial PDH complex | 3.79 ± 0.31 | 2.67 ± 0.24 | 1.46 ± 0.15 | 1 |
| Lpd1p | NP_116635 | Mitochondrial PDH complex; binds to | 3.36 ± 0.32 | 2.29 ± 0.21 | 0.88 ± 0.09 | 1 |

| | | mtDNA | | | | |
|---|---|---|---|---|---|---|
| Cit1p | NP_014398 | Mitochondrial TCA cycle | 2.65 ± 0.23 | 1.83 ± 0.17 | 0.84 ± 0.23 | 1 |
| Cit2p | NP_009931 | Mitochondrial TCA cycle | 2.48 ± 0.15 | 2.39 ± 0.28 | 1.32 ± 0.19 | 1 |
| Cit3p | NP_015325 | Mitochondrial TCA cycle | 2.79 ± 0.34 | 1.38 ± 0.14 | 0.76 ± 0.08 | 1 |
| Aco1p | NP_013407 | Mitochondrial TCA cycle; binds to mtDNA | 3.44 ± 0.43 | 2.78 ± 0.35 | 1.34 ± 0.17 | 1 |
| Idh1p | NP_014361 | Mitochondrial TCA cycle; binds to mtDNA | 2.67 ± 0.18 | 1.29 ± 0.24 | 0.83 ± 0.21 | 1 |
| Idh2p | NP_014779 | Mitochondrial TCA cycle | 2.56 ± 0.22 | 1.83 ± 0.33 | 1.19 ± 0.17 | 1 |
| Kgd1p | NP_012141 | Mitochondrial TCA cycle; binds to mtDNA | 2.75 ± 0.42 | 1.45 ± 0.25 | 1.29 ± 0.09 | 1 |
| Kgd2p | NP_010432 | Mitochondrial TCA cycle; binds to mtDNA | 2.53 ± 0.30 | 2.69 ± 0.17 | 1.17 ± 0.23 | 1 |
| Lsc1p | NP_014785 | Mitochondrial TCA cycle; binds to mtDNA | 2.89 ± 0.21 | 1.67 ± 0.06 | 0.85 ± 0.12 | 1 |
| Lsc2p | NP_011760 | Mitochondrial TCA cycle | 2.73 ± 0.43 | 1.69 ± 0.15 | 1.24 ± 0.37 | 1 |
| Sdh1p | NP_012774 | Mitochondrial TCA cycle and ETC | 2.69 ± 0.28 | 1.44 ± 0.22 | 0.86 ± 0.12 | 1 |
| Sdh2p | NP_013059 | Mitochondrial TCA cycle and ETC | 2.92 ± 0.41 | 2.57 ± 0.34 | 1.37 ± 0.28 | 1 |
| Sdh3p | NP_012781 | Mitochondrial TCA cycle and ETC | 2.85 ± 0.33 | 1.69 ± 0.19 | 1.24 ± 0.07 | 1 |
| Sdh4p | NP_010463 | Mitochondrial TCA cycle and ETC | 2.42 ± 0.27 | 1.73 ± 0.14 | 0.78 ± 0.19 | 1 |
| Fum1p | NP_015061 | Mitochondrial TCA cycle | 2.65 ± 0.08 | 1.48 ± 0.22 | 1.17 ± 0.28 | 1 |
| Mdh1p | NP_012838 | Mitochondrial TCA cycle | 3.54 ± 0.43 | 2.76 ± 0.31 | 1.49 ± 0.17 | 1 |
| Ndi1p | NP_013586 | Mitochondrial ETC | 3.87 ± 0.12 | 2.54 ± 0.17 | 1.24 ± 0.15 | 1 |
| Cyt1p | NP_014708 | Mitochondrial ETC | 2.41 ± 0.24 | 1.69 ± 0.18 | 1.06 ± 0.13 | 1 |
| Rip1p | NP_010890 | Mitochondrial ETC | 2.77 ± 0.14 | 2.89 ± 0.32 | 1.19 ± 0.18 | 1 |
| Cox4p | NP_011328 | Mitochondrial ETC | 2.58 ± 0.21 | 1.78 ± 0.14 | 0.93 ± 0.21 | 1 |
| Cox5Ap | NP_014346 | Mitochondrial ETC | 2.69 ± 0.33 | 1.85 ± 0.26 | 1.21 ± 0.42 | 1 |
| Pet100p | NP_010364 | Mitochondrial ETC | 2.44 ± 0.21 | 2.58 ± 0.17 | 0.92 ± 0.19 | 1 |
| Atp1p | NP_009453 | Mitochondrial ATP synthase; binds to mtDNA | 2.76 ± 0.51 | 2.87 ± 0.32 | 1.34 ± 0.05 | 1 |
| Atp2p | NP_012655 | Mitochondrial ATP synthase | 2.54 ± 0.23 | 2.75 ± 0.15 | 1.16 ± 0.19 | 1 |
| Pet9p | NP_009523 | Mitochondrial ADP/ATP carrier | 2.79 ± 0.14 | 3.49 ± 0.23 | 1.07 ± 0.28 | 1 |
| Mir1p | NP_012611 | Mitochondrial phosphate carrier | 2.83 ± 0.31 | 3.57 ± 0.35 | 0.91 ± 0.18 | 1 |
| Hem14p | NP_010930 | Heme synthesis in mitochondria | 2.92 ± 0.27 | 2.43 ± 0.14 | 1.19 ± 0.22 | 1 |
| Cyc3p | NP_009361 | Heme attachment to apo-cytochrome c | 2.64 ± 0.18 | 1.65 ± 0.23 | 1.07 ± 0.14 | 1 |
| Sod2p | NP_011872 | Detoxification of ROS in mitochondria | 1.65 ± 0.15 | 2.49 ± 0.27 | 0.93 ± 0.19 | 1 |
| Prx1p | NP_009489 | Detoxification of ROS in mitochondria | 2.77 ± 0.26 | 2.58 ± 0.32 | 1.16 ± 0.09 | 1 |
| Ccp1p | NP_012992 | Detoxification of ROS in mitochondria | 2.39 ± 0.13 | 3.67 ± 0.25 | 1.25 ± 0.34 | 1 |
| Trr2p | NP_011974 | Detoxification of ROS in mitochondria | 1.78 ± 0.15 | 2.63 ± 0.19 | 0.87 ± 0.26 | 1 |
| Trx3p | NP_010006 | Detoxification of ROS in mitochondria | 1.84 ± 0.22 | 2.74 ± 0.31 | 1.11 ± 0.09 | 1 |
| Ssq1p | NP_013473 | Assembly of Fe/S clusters into proteins | 4.19 ± 0.14 | 2.58 ± 0.16 | 0.92 ± 0.11 | 1 |
| Ssc1p | NP_012579 | Mitochondrial chaperone; binds to mtDNA | 2.78 ± 0.23 | 1.51 ± 0.14 | 1.18 ± 0.28 | 1 |
| Hsp60p | NP_013360 | Mitochondrial chaperone; binds to mtDNA | 3.34 ± 0.30 | 2.56 ± 0.42 | 1.39 ± 0.24 | 1 |
| Caf4p | NP_012962 | Mitochondrial fission | 0.81 ± 0.13 | 0.41 ± 0.07 | 0.92 ± 0.32 | 1 |
| Mdv1p | NP_012423 | Mitochondrial fission | 1.11 ± 0.24 | 0.76 ± 0.11 | 1.08 ± 0.23 | 1 |
| Fis1p | NP_012199 | Mitochondrial fission | 0.93 ± 0.19 | 1.12 ± 0.30 | 0.86 ± 0.18 | 1 |
| Mgm1p | NP_014854 | Mitochondrial fusion | 1.23 ± 0.15 | 1.49 ± 0.24 | 1.16 ± 0.13 | 1 |
| Pgs1p | NP_009923 | Cardiolipin synthesis in mitochondria | 0.63 ± 0.17 | 0.85 ± 0.11 | 1.03 ± 0.24 | 1 |
| Crd1p | NP_010139 | Cardiolipin synthesis in mitochondria | 1.15 ± 0.22 | 0.92 ± 0.31 | 0.95 ± 0.25 | 1 |
| Taz1p | NP_015466 | Cardiolipin synthesis in mitochondria | 0.88 ± 0.11 | 0.65 ± 0.18 | 1.14 ± 0.13 | 1 |
| Ald4p | NP_015019 | Mitochondrial aldehyde dehydrogenase; binds to mtDNA | 2.38 ± 0.17 | 1.34 ± 0.21 | 1.18 ± 0.27 | 1 |

| | | | | | | |
|---|---|---|---|---|---|---|
| Abf2p | NP_013788 | Mitochondrial genome maintenance; binds to mtDNA | 0.35 ± 0.09 | 0.74 ± 0.17 | 1.25 ± 0.21 | 1 |
| Ilv5p | NP_013459 | Branched-chain amino acid biosynthesis in mitochondria; binds to mtDNA | 0.39 ± 0.15 | 0.68 ± 0.19 | 0.87 ± 0.12 | 1 |
| Sls1p | NP_013240 | Mitochondrial chaperone; binds to mtDNA | 2.72 ± 0.43 | 1.65 ± 0.21 | 1.16 ± 0.07 | 1 |
| **Day 4 (PD phase)** | | | | | | |
| Pda1p | NP_011105 | Mitochondrial PDH complex; binds to mtDNA | 4.65 ± 0.54 | 3.87 ± 0.42 | 1.43 ± 0.21 | 1 |
| Pdb1p | NP_009780 | Mitochondrial PDH complex; binds to mtDNA | 4.78 ± 0.41 | 3.54 ± 0.27 | 1.21 ± 0.13 | 1 |
| Lat1p | NP_014328 | Mitochondrial PDH complex | 4.57 ± 0.18 | 3.49 ± 0.28 | 1.56 ± 0.27 | 1 |
| Pdx1p | NP_011709 | Mitochondrial PDH complex | 3.69 ± 0.45 | 2.66 ± 0.21 | 1.27 ± 0.34 | 1 |
| Lpd1p | NP_116635 | Mitochondrial PDH complex; binds to mtDNA | 3.56 ± 0.32 | 2.74 ± 0.35 | 1.18 ± 0.19 | 1 |
| Cit1p | NP_014398 | Mitochondrial TCA cycle | 3.84 ± 0.32 | 2.76 ± 0.16 | 1.49 ± 0.13 | 1 |
| Cit2p | NP_009931 | Mitochondrial TCA cycle | 2.68 ± 0.14 | 2.89 ± 0.28 | 1.33 ± 0.22 | 1 |
| Cit3p | NP_015325 | Mitochondrial TCA cycle | 3.85 ± 0.29 | 2.63 ± 0.35 | 1.26 ± 0.41 | 1 |
| Aco1p | NP_013407 | Mitochondrial TCA cycle; binds to mtDNA | 3.72 ± 0.49 | 2.37 ± 0.18 | 0.84 ± 0.23 | 1 |
| Idh1p | NP_014361 | Mitochondrial TCA cycle; binds to mtDNA | 3.59 ± 0.52 | 2.62 ± 0.36 | 1.24 ± 0.28 | 1 |
| Idh2p | NP_014779 | Mitochondrial TCA cycle | 3.43 ± 0.30 | 2.72 ± 0.17 | 1.67 ± 0.25 | 1 |
| Kgd1p | NP_012141 | Mitochondrial TCA cycle; binds to mtDNA | 3.75 ± 0.41 | 2.88 ± 0.28 | 1.18 ± 0.17 | 1 |
| Kgd2p | NP_010432 | Mitochondrial TCA cycle; binds to mtDNA | 4.39 ± 0.25 | 3.65 ± 0.42 | 1.56 ± 0.12 | 1 |
| Lsc1p | NP_014785 | Mitochondrial TCA cycle; binds to mtDNA | 3.64 ± 0.19 | 2.72 ± 0.36 | 1.33 ± 0.23 | 1 |
| Lsc2p | NP_011760 | Mitochondrial TCA cycle | 3.87 ± 0.45 | 2.56 ± 0.33 | 0.86 ± 0.17 | 1 |
| Sdh1p | NP_012774 | Mitochondrial TCA cycle and ETC | 3.49 ± 0.36 | 2.85 ± 0.27 | 1.28 ± 0.19 | 1 |
| Sdh2p | NP_013059 | Mitochondrial TCA cycle and ETC | 4.53 ± 0.28 | 3.77 ± 0.16 | 1.61 ± 0.22 | 1 |
| Sdh3p | NP_012781 | Mitochondrial TCA cycle and ETC | 2.56 ± 0.17 | 2.83 ± 0.25 | 1.24 ± 0.33 | 1 |
| Sdh4p | NP_010463 | Mitochondrial TCA cycle and ETC | 2.77 ± 0.08 | 2.69 ± 0.13 | 1.13 ± 0.05 | 1 |
| Fum1p | NP_015061 | Mitochondrial TCA cycle | 3.84 ± 0.14 | 2.76 ± 0.25 | 1.29 ± 0.14 | 1 |
| Mdh1p | NP_012838 | Mitochondrial TCA cycle | 3.72 ± 0.28 | 2.88 ± 0.17 | 1.18 ± 0.25 | 1 |
| Ndi1p | NP_013586 | Mitochondrial ETC | 4.65 ± 0.19 | 3.59 ± 0.28 | 1.45 ± 0.18 | 1 |
| Cyt1p | NP_014708 | Mitochondrial ETC | 4.53 ± 0.31 | 3.78 ± 0.15 | 1.28 ± 0.11 | 1 |
| Rip1p | NP_010890 | Mitochondrial ETC | 4.32 ± 0.24 | 4.49 ± 0.35 | 1.13 ± 0.22 | 1 |
| Cox4p | NP_011328 | Mitochondrial ETC | 3.65 ± 0.19 | 2.73 ± 0.26 | 1.18 ± 0.25 | 1 |
| Cox5Ap | NP_014346 | Mitochondrial ETC | 3.78 ± 0.24 | 2.85 ± 0.17 | 1.27 ± 0.19 | 1 |
| Pet100p | NP_010364 | Mitochondrial ETC | 2.66 ± 0.13 | 2.79 ± 0.23 | 1.06 ± 0.31 | 1 |
| Atp1p | NP_009453 | Mitochondrial ATP synthase; binds to mtDNA | 3.76 ± 0.44 | 4.48 ± 0.31 | 1.75 ± 0.32 | 1 |
| Atp2p | NP_012655 | Mitochondrial ATP synthase | 3.49 ± 0.19 | 4.53 ± 0.38 | 0.95 ± 0.11 | 1 |
| Pet9p | NP_009523 | Mitochondrial ADP/ATP carrier | 3.61 ± 0.25 | 3.78 ± 0.16 | 1.08 ± 0.17 | 1 |
| Mir1p | NP_012611 | Mitochondrial phosphate carrier | 3.34 ± 0.13 | 3.63 ± 0.27 | 1.24 ± 0.33 | 1 |
| Hem14p | NP_010930 | Heme synthesis in mitochondria | 4.87 ± 0.36 | 3.58 ± 0.18 | 1.16 ± 0.21 | 1 |
| Cyc3p | NP_009361 | Heme attachment to apo-cytochrome c | 3.59 ± 0.28 | 2.66 ± 0.14 | 1.13 ± 0.17 | 1 |
| Sod2p | NP_011872 | Detoxification of ROS in mitochondria | 2.73 ± 0.17 | 4.20 ± 0.36 | 1.31 ± 0.28 | 1 |
| Prx1p | NP_009489 | Detoxification of ROS in mitochondria | 4.65 ± 0.26 | 3.39 ± 0.18 | 0.94 ± 0.36 | 1 |
| Ccp1p | NP_012992 | Detoxification of ROS in mitochondria | 3.49 ± 0.32 | 4.72 ± 0.21 | 1.26 ± 0.24 | 1 |
| Trr2p | NP_011974 | Detoxification of ROS in mitochondria | 2.72 ± 0.21 | 3.83 ± 0.35 | 1.09 ± 0.17 | 1 |

| | | | | | | |
|---|---|---|---|---|---|---|
| Trx3p | NP_010006 | Detoxification of ROS in mitochondria | 2.54 ± 0.15 | 3.39 ± 0.11 | 1.28 ± 0.33 | 1 |
| Ssq1p | NP_013473 | Assembly of Fe/S clusters into proteins | 4.81 ± 0.37 | 3.56 ± 0.28 | 1.41 ± 0.42 | 1 |
| Ssc1p | NP_012579 | Mitochondrial matrix ATPase; binds to mtDNA | 3.65 ± 0.44 | 2.71 ± 0.36 | 1.34 ± 0.15 | 1 |
| Hsp60p | NP_013360 | Mitochondrial chaperone; binds to mtDNA | 3.84 ± 0.26 | 2.56 ± 0.39 | 1.45 ± 0.23 | 1 |
| Caf4p | NP_012962 | Mitochondrial fission | 0.23 ± 0.04 | 0.24 ± 0.08 | 0.88 ± 0.15 | 1 |
| Mdv1p | NP_012423 | Mitochondrial fission | 0.44 ± 0.13 | 0.39 ± 0.11 | 0.97 ± 0.24 | 1 |
| Fis1p | NP_012199 | Mitochondrial fission | 0.36 ± 0.08 | 0.41 ± 0.15 | 0.84 ± 0.31 | 1 |
| Mgm1p | NP_014854 | Mitochondrial fusion | 2.42 ± 0.17 | 3.57 ± 0.28 | 1.17 ± 0.13 | 1 |
| Pgs1p | NP_009923 | Cardiolipin synthesis in mitochondria | 0.30 ± 0.11 | 0.44 ± 0.09 | 0.92 ± 0.21 | 1 |
| Crd1p | NP_010139 | Cardiolipin synthesis in mitochondria | 0.44 ± 0.17 | 0.76 ± 0.22 | 1.23 ± 0.34 | 1 |
| Taz1p | NP_015466 | Cardiolipin synthesis in mitochondria | 0.38 ± 0.06 | 0.27 ± 0.05 | 0.92 ± 0.17 | 1 |
| Ald4p | NP_015019 | Mitochondrial aldehyde dehydrogenase; binds to mtDNA | 4.67 ± 0.53 | 3.56 ± 0.24 | 1.22 ± 0.19 | 1 |
| Abf2p | NP_013788 | Mitochondrial genome maintenance; binds to mtDNA | 0.27 ± 0.06 | 0.41 ± 0.14 | 0.89 ± 0.13 | 1 |
| Ilv5p | NP_013459 | Branched-chain amino acid biosynthesis in mitochondria; binds to mtDNA | 0.31 ± 0.09 | 0.36 ± 0.11 | 0.91 ± 0.27 | 1 |
| Sls1p | NP_013240 | Mitochondrial chaperone; binds to mtDNA | 3.59 ± 0.41 | 2.74 ± 0.26 | 1.66 ± 0.34 | 1 |
| **Day 9 (ST phase)** | | | | | | |
| Pda1p | NP_011105 | Mitochondrial PDH complex; binds to mtDNA | 2.88 ± 0.31 | 2.45 ± 0.28 | 1.32 ± 0.19 | 1 |
| Pdb1p | NP_009780 | Mitochondrial PDH complex; binds to mtDNA | 2.87 ± 0.51 | 2.54 ± 0.39 | 1.46 ± 0.17 | 1 |
| Lat1p | NP_014328 | Mitochondrial PDH complex | 2.76 ± 0.21 | 2.32 ± 0.32 | 1.45 ± 0.27 | 1 |
| Pdx1p | NP_011709 | Mitochondrial PDH complex | 2.93 ± 0.42 | 2.67 ± 0.17 | 1.32 ± 0.34 | 1 |
| Lpd1p | NP_116635 | Mitochondrial PDH complex; binds to mtDNA | 2.65 ± 0.32 | 2.37 ± 0.44 | 1.34 ± 0.38 | 1 |
| Cit1p | NP_014398 | Mitochondrial TCA cycle | 2.59 ± 0.33 | 1.56 ± 0.27 | 0.84 ± 0.13 | 1 |
| Cit2p | NP_009931 | Mitochondrial TCA cycle | 2.88 ± 0.46 | 2.91 ± 0.39 | 1.39 ± 0.26 | 1 |
| Cit3p | NP_015325 | Mitochondrial TCA cycle | 2.61 ± 0.41 | 1.82 ± 0.21 | 0.78 ± 0.09 | 1 |
| Aco1p | NP_013407 | Mitochondrial TCA cycle; binds to mtDNA | 2.84 ± 0.48 | 2.52 ± 0.25 | 1.14 ± 0.17 | 1 |
| Idh1p | NP_014361 | Mitochondrial TCA cycle; binds to mtDNA | 2.77 ± 0.31 | 1.85 ± 0.38 | 0.84 ± 0.12 | 1 |
| Idh2p | NP_014779 | Mitochondrial TCA cycle | 2.73 ± 0.24 | 1.45 ± 0.16 | 0.97 ± 0.14 | 1 |
| Kgd1p | NP_012141 | Mitochondrial TCA cycle; binds to mtDNA | 2.56 ± 0.23 | 1.63 ± 0.46 | 0.76 ± 0.09 | 1 |
| Kgd2p | NP_010432 | Mitochondrial TCA cycle; binds to mtDNA | 3.75 ± 0.45 | 2.87 ± 0.29 | 1.34 ± 0.31 | 1 |
| Lsc1p | NP_014785 | Mitochondrial TCA cycle; binds to mtDNA | 2.79 ± 0.39 | 1.73 ± 0.32 | 1.15 ± 0.11 | 1 |
| Lsc2p | NP_011760 | Mitochondrial TCA cycle | 2.87 ± 0.17 | 1.29 ± 0.06 | 0.73 ± 0.25 | 1 |
| Sdh1p | NP_012774 | Mitochondrial TCA cycle and ETC | 2.66 ± 0.28 | 1.78 ± 0.14 | 1.12 ± 0.33 | 1 |
| Sdh2p | NP_013059 | Mitochondrial TCA cycle and ETC | 3.78 ± 0.41 | 2.69 ± 0.28 | 1.45 ± 0.16 | 1 |
| Sdh3p | NP_012781 | Mitochondrial TCA cycle and ETC | 2.85 ± 0.18 | 1.81 ± 0.09 | 1.18 ± 0.23 | 1 |
| Sdh4p | NP_010463 | Mitochondrial TCA cycle and ETC | 2.69 ± 0.26 | 1.74 ± 0.18 | 1.26 ± 0.14 | 1 |
| Fum1p | NP_015061 | Mitochondrial TCA cycle | 2.96 ± 0.32 | 1.68 ± 0.29 | 1.09 ± 0.27 | 1 |
| Mdh1p | NP_012838 | Mitochondrial TCA cycle | 2.77 ± 0.13 | 2.53 ± 0.30 | 0.87 ± 0.19 | 1 |
| Ndi1p | NP_013586 | Mitochondrial ETC | 2.89 ± 0.21 | 2.37 ± 0.14 | 1.12 ± 0.25 | 1 |
| Cyt1p | NP_014708 | Mitochondrial ETC | 3.65 ± 0.37 | 2.54 ± 0.19 | 0.95 ± 0.14 | 1 |

| | | | | | | |
|---|---|---|---|---|---|---|
| Rip1p | NP_010890 | Mitochondrial ETC | 4.88 ± 0.41 | 3.67 ± 0.31 | 1.27 ± 0.22 | 1 |
| Cox4p | NP_011328 | Mitochondrial ETC | 2.64 ± 0.21 | 2.42 ± 0.27 | 1.13 ± 0.18 | 1 |
| Cox5Ap | NP_014346 | Mitochondrial ETC | 3.58 ± 0.37 | 2.83 ± 0.19 | 1.34 ± 0.36 | 1 |
| Pet100p | NP_010364 | Mitochondrial ETC | 3.77 ± 0.24 | 2.61 ± 0.40 | 1.19 ± 0.24 | 1 |
| Atp1p | NP_009453 | Mitochondrial ATP synthase; binds to mtDNA | 3.65 ± 0.38 | 4.72 ± 0.44 | 1.12 ± 0.33 | 1 |
| Atp2p | NP_012655 | Mitochondrial ATP synthase | 3.43 ± 0.21 | 4.56 ± 0.33 | 1.32 ± 0.46 | 1 |
| Pet9p | NP_009523 | Mitochondrial ADP/ATP carrier | 2.58 ± 0.16 | 3.38 ± 0.25 | 1.14 ± 0.21 | 1 |
| Mir1p | NP_012611 | Mitochondrial phosphate carrier | 2.75 ± 0.32 | 3.59 ± 0.17 | 0.94 ± 0.36 | 1 |
| Hem14p | NP_010930 | Heme synthesis in mitochondria | 2.49 ± 0.18 | 1.76 ± 0.21 | 1.17 ± 0.25 | 1 |
| Cyc3p | NP_009361 | Heme attachment to apo-cytochrome c | 3.58 ± 0.26 | 2.77 ± 0.34 | 1.26 ± 0.37 | 1 |
| Sod2p | NP_011872 | Detoxification of ROS in mitochondria | 2.71 ± 0.31 | 4.69 ± 0.42 | 1.15 ± 0.19 | 1 |
| Prx1p | NP_009489 | Detoxification of ROS in mitochondria | 2.48 ± 0.23 | 4.55 ± 0.36 | 1.34 ± 0.42 | 1 |
| Ccp1p | NP_012992 | Detoxification of ROS in mitochondria | 4.53 ± 0.39 | 4.71 ± 0.42 | 1.21 ± 0.16 | 1 |
| Trr2p | NP_011974 | Detoxification of ROS in mitochondria | 3.67 ± 0.25 | 4.29 ± 0.21 | 1.09 ± 0.25 | 1 |
| Trx3p | NP_010006 | Detoxification of ROS in mitochondria | 3.88 ± 0.32 | 4.64 ± 0.25 | 1.35 ± 0.38 | 1 |
| Ssq1p | NP_013473 | Assembly of Fe/S clusters into proteins | 2.75 ± 0.24 | 2.29 ± 0.11 | 0.88 ± 0.14 | 1 |
| Ssc1p | NP_012579 | Mitochondrial chaperone; binds to mtDNA | 2.56 ± 0.12 | 1.45 ± 0.28 | 0.87 ± 0.28 | 1 |
| Hsp60p | NP_013360 | Mitochondrial chaperone; binds to mtDNA | 3.78 ± 0.28 | 2.81 ± 0.37 | 1.27 ± 0.13 | 1 |
| Caf4p | NP_012962 | Mitochondrial fission | 0.41 ± 0.12 | 0.32 ± 0.09 | 0.92 ± 0.15 | 1 |
| Mdv1p | NP_012423 | Mitochondrial fission | 0.37 ± 0.08 | 0.23 ± 0.04 | 1.17 ± 0.22 | 1 |
| Fis1p | NP_012199 | Mitochondrial fission | 0.72 ± 0.21 | 0.37 ± 0.12 | 0.89 ± 0.36 | 1 |
| Mgm1p | NP_014854 | Mitochondrial fusion | 3.69 ± 0.35 | 4.72 ± 0.26 | 1.15 ± 0.25 | 1 |
| Pgs1p | NP_009923 | Cardiolipin synthesis in mitochondria | 0.28 ± 0.11 | 0.39 ± 0.08 | 0.95 ± 0.17 | 1 |
| Crd1p | NP_010139 | Cardiolipin synthesis in mitochondria | 0.31 ± 0.07 | 0.42 ± 0.14 | 1.23 ± 0.26 | 1 |
| Taz1p | NP_015466 | Cardiolipin synthesis in mitochondria | 0.42 ± 0.13 | 0.36 ± 0.11 | 1.19 ± 0.34 | 1 |
| Ald4p | NP_015019 | Mitochondrial aldehyde dehydrogenase; binds to mtDNA | 3.84 ± 0.27 | 2.68 ± 0.21 | 0.87 ± 0.18 | 1 |
| Abf2p | NP_013788 | Mitochondrial genome maintenance; binds to mtDNA | 0.27 ± 0.08 | 0.61 ± 0.17 | 0.87 ± 0.21 | 1 |
| Ilv5p | NP_013459 | Branched-chain amino acid biosynthesis in mitochondria; binds to mtDNA | 0.31 ± 0.11 | 0.73 ± 0.09 | 1.27 ± 0.32 | 1 |
| Sls1p | NP_013240 | Mitochondrial chaperone; binds to mtDNA | 3.85 ± 0.34 | 2.76 ± 0.31 | 1.63 ± 0.15 | 1 |

mitochondria of yeast grown on 0.2% glucose, which exceeded the modest increase seen in yeast grown on 0.5% glucose, resulted in a greatly elevated level of mitochondrial ROS. This, in turn, led to the oxidative damage and inactivation of CCO, SDH, ACO and, perhaps, some other components of the mitochondrial ETC and TCA cycle. Late in ST phase, the resulting decline in the rate of electron flow through the mitochondrial

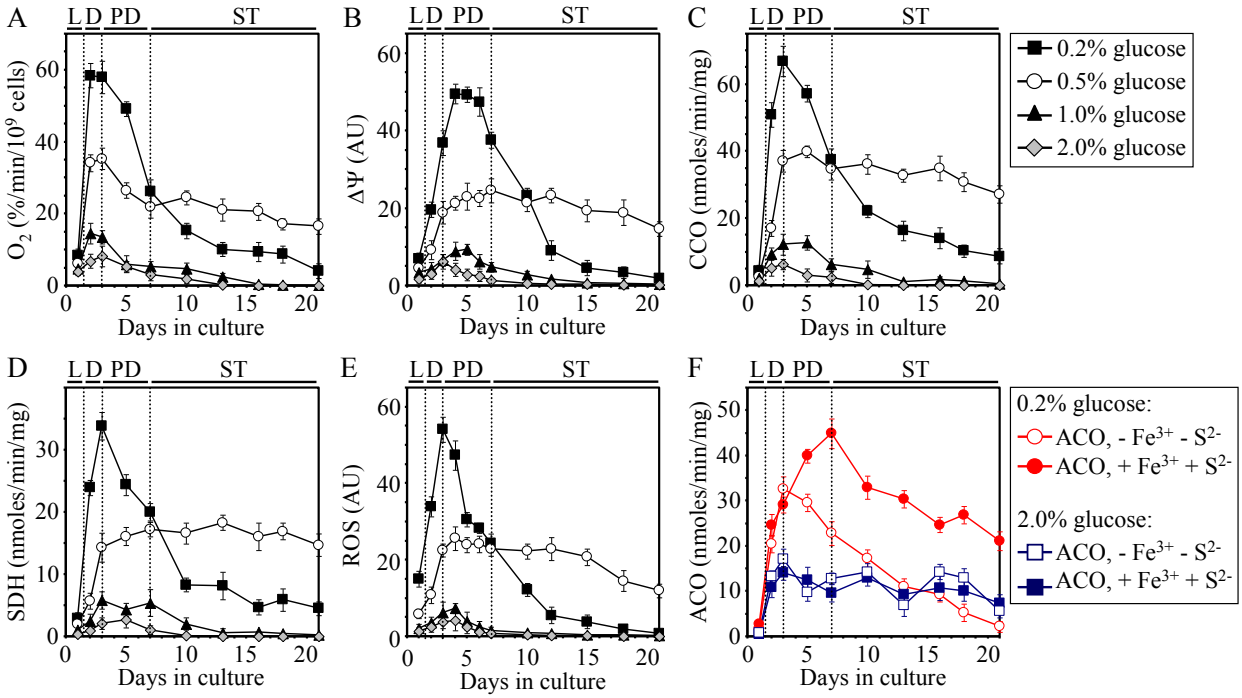


**Figure 2.6.** CR influences oxidation-reduction processes in mitochondria and modulates the level of mitochondrially produced ROS. (A) The dynamics of age-dependent changes in the rate of oxygen consumption by cells. Data are presented as mean ± SEM (n = 15-19). (B) The dynamics of age-dependent changes in the mitochondrial membrane potential (ΔΨ) during chronological aging of yeast. ΔΨ was visualized using R123. At least 800 cells were used for quantitation of R123 staining for each of 3 independent experiments. Data are presented as mean ± SEM (n = 15-19). (C and D) Enzymatic activities of CCO (C) and SDH (D) in purified mitochondria. Data are presented as mean ± SEM (n = 6-10). (E) The dynamics of age-dependent changes in the intracellular levels of ROS during chronological aging of yeast. ROS were visualized using DHR. At least 800 cells were used for quantitation of DHR staining for each of 5 independent experiments. Data are presented as mean ± SEM (n = 8-13). (F) Enzymatic activities of ACO in total cell lysates. The ACO activity was measured with or without the reactivation agents $Fe^{3+}$ and $Na_2S$. Data are presented as mean ± SEM (n = 5). (A-E) Cells were cultured in YP media initially containing four different concentrations of glucose. (F) Cells were cultured in YP medium initially containing 0.2% or 2% glucose.

ETC of yeast grown on 0.2% glucose substantially decreased mitochondrial ROS below the level observed in mitochondria of yeast grown on 0.5% glucose (Figure 2.6).

### 2.4.7 CR influences the frequency of mitochondrial DNA (mtDNA) mutations and modulates the abundance and mtDNA-binding activity of mitochondrial nucleoid-associated proteins

My data imply that the observed during D and PD phases spike in ROS production by mitochondria of CR yeast grown on 0.2% glucose can oxidatively damage their mitochondrial DNA (mtDNA), eventually (*i.e.*, during ST phase) introducing deletions and point mutations into it. In fact, during ST phase, the population of these CR cells accumulated an increasing fraction of respiratory-deficient mutants (Figure 2.7A). Most of these mutants are known to carry mutations in mtDNA (including single-gene *mit*$^-$ and *syn*$^-$ mutations or large deletions *rho*$^-$) or completely lack mtDNA (*rho*$^o$ mutants), whereas some of them carry so-called *pet*$^-$ mutations in nuclear genes that code for essential mitochondrial components [250, 280]. Furthermore, I found that only cells under CR at 0.2% glucose exhibited an increased frequency of mtDNA mutations that caused resistance to erythromycin (Figure 2.7B). Resistance to this antibiotic can be acquired only through a distinct set of point mutations in the mitochondrial *rib2* and *rib3* genes that encode two different rRNAs confined to mitochondria [251 - 253]. Importantly, the highest amplitude of the early spike in ROS production by yeast under CR at 0.2% glucose (Figure 2.6E) correlated with their elevated frequencies of mtDNA mutations (Figures 2.7A and 2.7B) and shortened life span (Figures 2.1C and 2.1D), as compared to yeast under CR at 0.5% glucose. Thus, it is conceivable that the frequency of ROS-induced deletions and point mutations in mtDNA influence yeast longevity under CR conditions. This hypothesis could satisfactorily explain my observation that yeast under CR at 0.5% glucose live longer than yeast under CR at 0.2% glucose. Conversely,

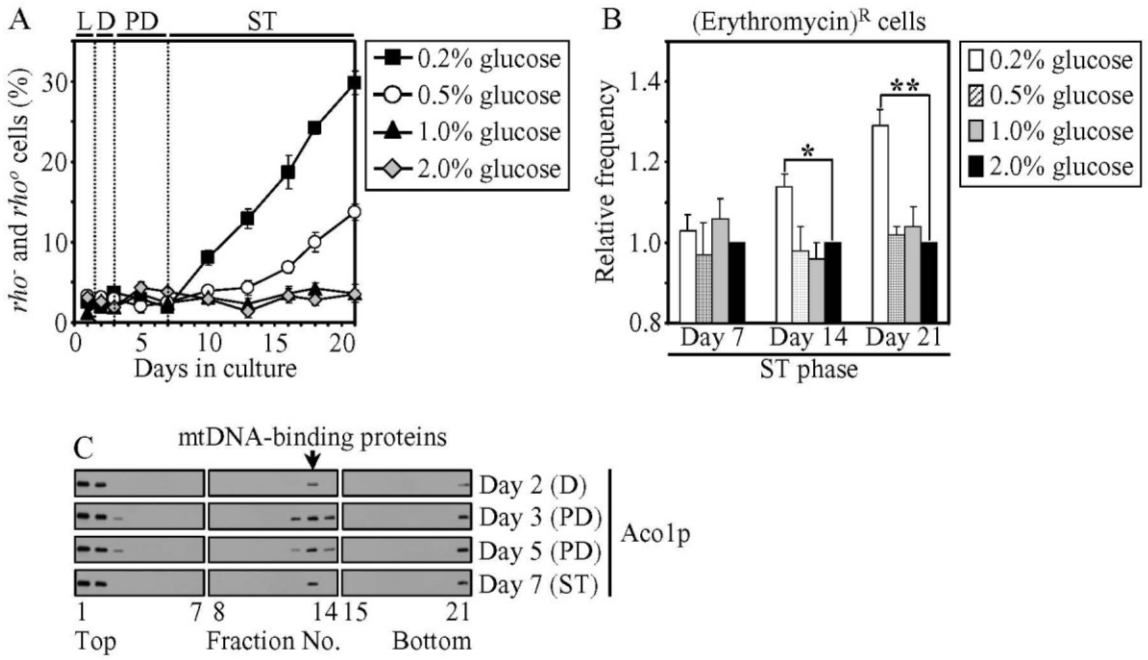


**Figure 2.7.** CR modulates the frequency of mtDNA mutations and influences the efficiency of aconitase binding to mtDNA. (A) The percentage of respiratory-deficient cells that were unable to grow in medium containing 3% glycerol because they carried large mtDNA deletions (*rho*$^-$) or lacked mtDNA (*rho*$^o$). Data are presented as mean ± SEM (n = 7). (B) Relative frequencies (fold difference relative to that on 2% glucose) of mtDNA point mutations that caused resistance to erythromycin. Data are presented as mean ± SEM (n = 70); *$p < 0.01$, **$p < 0.001$. (C) Western blot analysis of aconitase (Aco1p) recovery in fractions of a CsCl gradient that was used for the purification of mitochondrial nucleoids. The peak fraction for the mitochondrial Aco1p-DNA complex (arrow) is indicated. (A and B) Cells were cultured in YP media initially containing four different concentrations of glucose. (C) Cells were cultured in YP medium initially containing 0.2% glucose.

it seems that the frequency of mtDNA deletions and point mutations does not affect the longevity of chronologically aging yeast grown on 1% or 2% glucose, *i.e.* under non-CR conditions. In fact, I found that, despite these yeast had much lower frequencies of mtDNA mutations than CR yeast grown on 0.2% glucose (Figures 2.7A and 2.7B), they lived a shorter life (Figures 2.1C and 2.1D).

Of note, I found that the observed elevated frequencies of mtDNA deletions and point mutations in CR yeast grown on 0.2% glucose occurred despite an effort that these yeast have made to protect the stability of mtDNA by remodeling mitochondrial nucleoids early in their life. In fact, during D and PD phases, these CR yeast induced the synthesis of a distinct set of mtDNA-binding proteins (Figure 2.5; Tables 2.1 and 2.2) known for their essential role in maintaining mtDNA and protecting it from oxidative damage [280]. One of these proteins, the TCA-cycle enzyme aconitase (Aco1p) known for its ability to interact with mtDNA and to maintain its integrity when cells are shifted to respiratory conditions [281], associated with mtDNA of aging CR yeast grown on 0.2% glucose (Figure 2.7C). Importantly, I found that the efficiency of such Aco1p binding to mtDNA at different stages of the aging process (Figure 2.7C) correlated with the concentration of ROS generated by mitochondria of these CR yeast (Figure 2.6E). Noteworthy, CR decreased the levels of mitochondrial Abf2p and Ilv5p (Figure 2.5), the two mtDNA-binding proteins that associate with mitochondrial nucleoids under conditions of low respiration or amino-acid starvation, respectively [280]. Therefore, I suggest the following scenario for metabolic remodeling of mitochondrial nucleoids in chronologically aging CR yeast. In response to the early spike in oxygen consumption and ROS generation by their mitochondria, CR yeast induce the synthesis of Aco1p and other bifunctional mitochondrial proteins that, in addition to their essential role in respiratory metabolism, are able to interact specifically with mtDNA. Concomitantly, CR yeast repress the synthesis of both Abf2p and Ilv5p. Because of their increased concentrations and due to their partial oxidation by mitochondrial ROS, Aco1p and other mtDNA-binding proteins bind to mtDNA in order to protect it from oxidative damage.

Such binding of Aco1p and other respiratory-metabolism sensing proteins to mtDNA may substitute for Abf2p and Ilv5p, thereby remodeling mitochondrial nucleoids by converting them into the conformation that is more resistant to oxidative damage. Noteworthy, the level of Aco1p in yeast cells is known to be modulated by the mitochondrial retrograde (RTG) signaling pathway. This pathway activates transcription of the *ACO1* gene in response to a decline in mitochondrial respiratory function caused by mtDNA damage [282, 283]. It is conceivable therefore that chronologically aging CR yeast respond to the partial oxidative damage of their mtDNA by turning on the RTG pathway. By activating transcription of *ACO1* and, perhaps, other genes encoding bifunctional mtDNA-binding proteins known to maintain the integrity of mtDNA in yeast shifted to respiratory conditions [280, 281], this signaling pathway may govern the resulting conversion of mitochondrial nucleoids into the conformation that is more resistant to oxidative damage.

### 2.4.8 CR alters mitochondrial morphology and delays mitochondria-controlled apoptosis

My findings imply that CR yeast influenced the aforementioned oxidation-reduction processes in mitochondria and modulated the levels of a distinct set of mitochondrial proteins not by altering the abundance of mitochondria. In fact, I found that the intracellular levels of porin, one of the most abundant mitochondrial proteins, were very similar in chronologically aging CR and non-CR yeast (Figure 2.8A). Rather, the CR diet provided mitochondria of aging yeast with an ability to maintain the shape of a tubular network (Figures 2.8B and 2.8C). In contrast, this tubular network in non-CR

yeast entering ST phase was fragmented into individual mitochondria (Figures 2.8B and 2.8C), consistent with the increased levels of some protein components of the mitochondrial fission machine and decreased level of the Mgm1p component of the mitochondrial fusion machine in their cells (Figure 2.5; Tables 2.1 and 2.2). In fact, it is known that the morphology of mitochondria depends on a balance between the processes of mitochondrial fission and fusion [284 - 286].

Furthermore, my fluorescence microscopy analysis revealed that chronologically aging non-CR yeast died exhibiting characteristic markers of apoptosis such as nuclear fragmentation, phosphatidylserine (PS) translocation from the inner to the outer leaflet of the plasma membrane, and cleavage of chromosomal DNA (Figures 2.8D - 2.8F). A CR diet - which prevented the fragmentation of the mitochondrial tubular network early in ST phase (Figures 2.8B and 2.8C) - delayed such age-related apoptosis (Figures 2.8D - 2.8F). Moreover, I found that the ability of CR to delay mitochondrial fragmentation in early ST phase and attenuate the age-related form of apoptotic cell death coincided with its ability to slow down the release of cytochrome c from mitochondria into the cytosol (Figure 2.8G). Of note, although some data suggest that - akin to its essential role in triggering the apoptotic caspase cascade in mammalian cells [287] - cytochrome c in the cytosol of yeast cells promotes mitochondria-controlled apoptosis by activating the metacaspase Yca1p [288 - 292], the involvement of cytosolic cytochrome c in Yca1p activation and apoptotic death in yeast remains a controversial issue [293, 294].

Altogether, these findings imply that the premature chronological aging of non-CR yeast grown in the nutrient-rich YP medium is linked to an apoptosis-like cell death. This age-related cell death could be controlled by mitochondria, perhaps through the

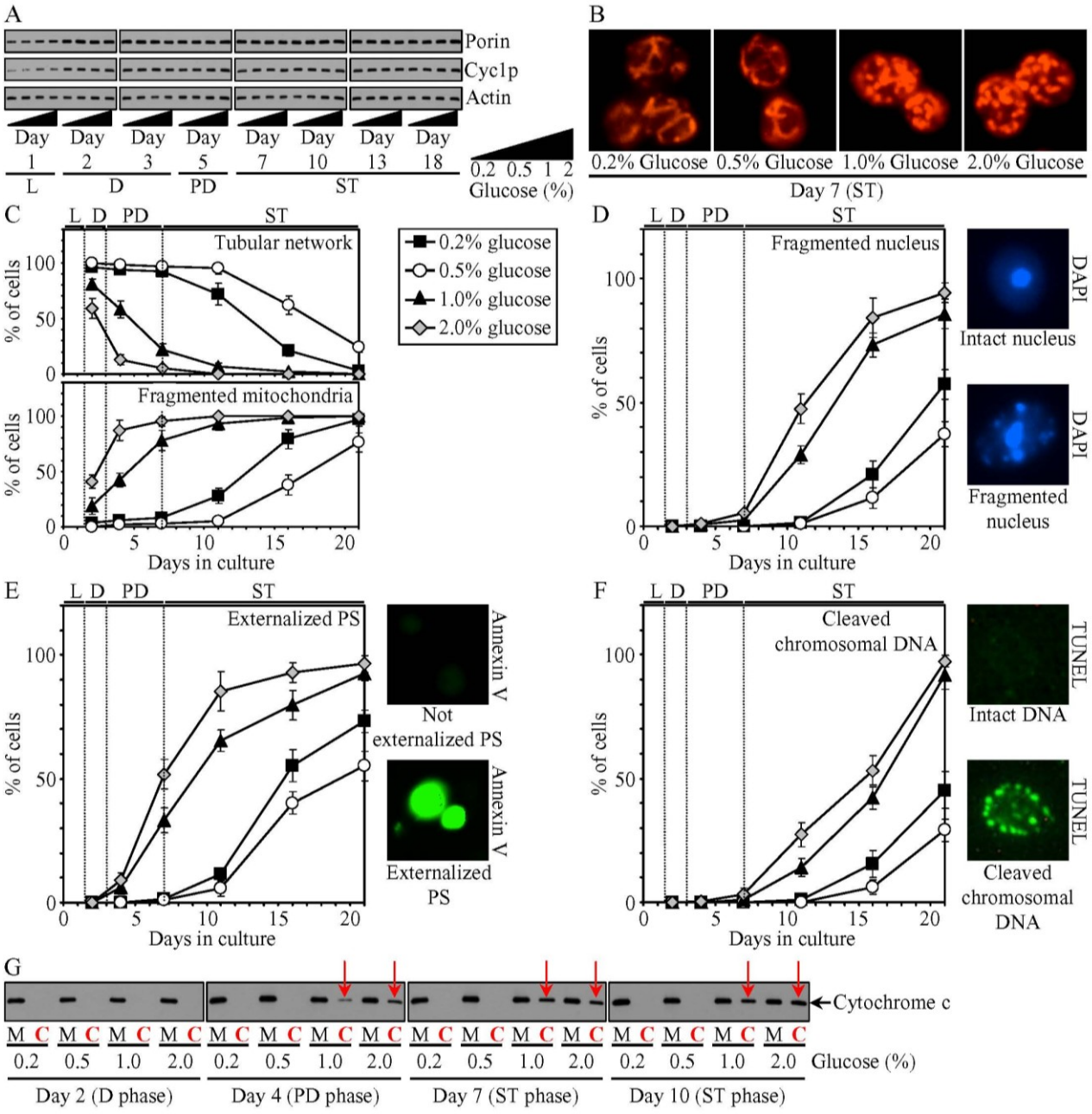


**Figure 2.8.** CR influences mitochondrial morphology and delays age-related apoptosis. (A) Western blot analysis of porin, the Cyc1p isoform of cytochrome c and actin in cells taken at the indicated time-points. Proteins recovered in total cell lysates were resolved by SDS-PAGE and detected by immunoblotting. (B) Morphology of mitochondria in yeast cells recovered from ST phase. Mitochondria were visualized by indirect immunofluorescence microscopy using monoclonal anti-porin primary antibodies and Alexa Fluor 568-conjugated goat anti-mouse IgG secondary antibodies. Representative images are shown. (C) The percentage of cells exhibiting a tubular mitochondrial network or fragmented mitochondria was calculated. At least 800 cells were used for quantitation at each time point. Data are presented as mean ± SEM (n = 3). (D and E) Fluorescence microscopy of cells stained with DAPI (D) or Annexin V (E) was used for analysis

of nuclear morphology or the presence of phosphatidylserine (PS) in the outer leaflet of the plasma membrane, respectively. The percentage of cells exhibiting fragmented nuclei (D) or externalized PS (E) was calculated. At least 800 cells were used for quantitation at each time point. Data are presented as mean ± SEM (n = 3). (F) DNA fragmentation was monitored using a TUNEL (terminal deoxynucleotidyl transferase dUTP nick-end labelling) assay. The percentage of cells exhibiting cleaved chromosomal DNA was calculated. At least 800 cells were used for quantitation at each time point. Data are presented as mean ± SEM (n = 2). (G) Western blot analysis of cytochrome c in purified mitochondria (M) and in the cytosolic fraction (C) recovered from cells taken at the indicated time-points. Equal portions of mitochondrial and cytosolic fractions were analyzed by immunoblotting to cytochrome c. Cells were cultured in YP media initially containing four different concentrations of glucose.

efflux of cytochrome c (and, maybe, several other pro-apoptotic proteins) from the intermembrane space of mitochondria undergoing massive fragmentation in non-CR yeast that have reached ST phase.

### 2.4.9 CR increases the resistance of aging yeast to chronic thermal and oxidative stresses

As I found, consistent with the elevated levels of cytosolic and mitochondrial stress-protecting and ROS scavenging proteins in CR yeast entering the non-proliferative ST phase (Figure 2.5; Tables 2.1 and 2.2), the CR diet enhanced the resistance of aging yeast to chronic thermal and oxidative stresses (Figure 2.9).

## 2.5 Discussion

Along with published data from Dr. Titorenko's laboratory on the molecular mechanism underlying the ability of CR to extend longevity of chronologically aging yeast by specifically remodelling lipid metabolism in the endoplasmic reticulum, lipid bodies and peroxisomes [24, 246, 247, 278], the analysis of the metabolic history of

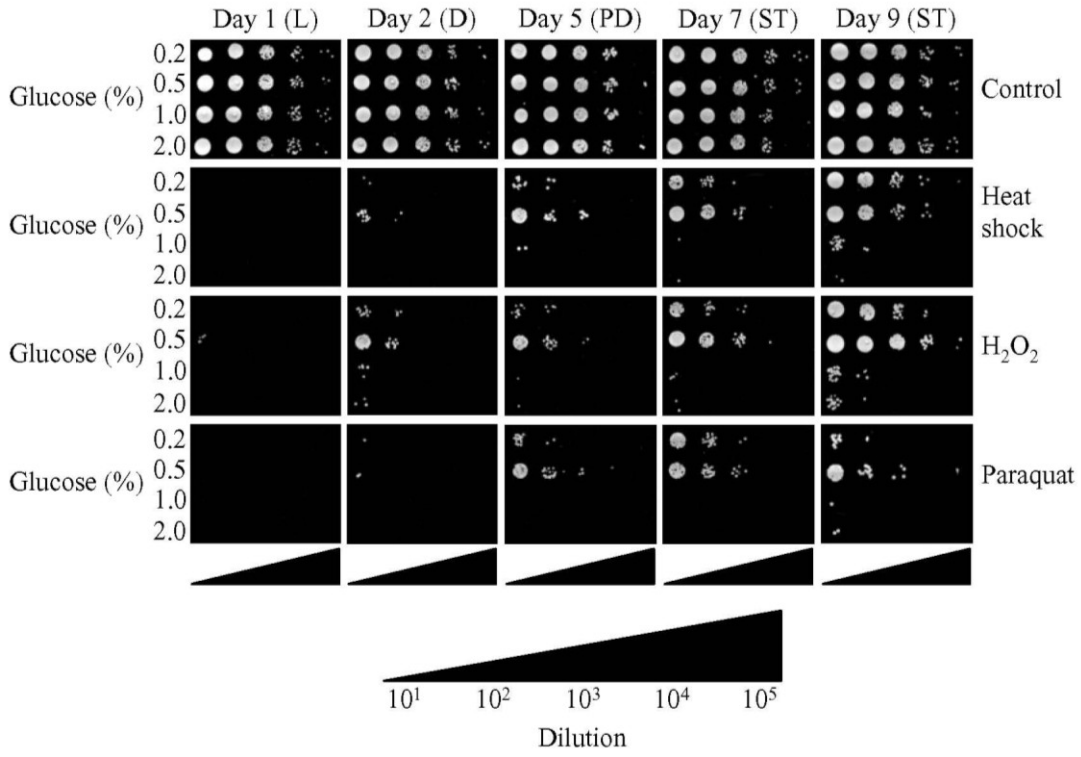


**Figure 2.9.** CR enhances the resistance of aging yeast to chronic thermal and oxidative stress. Heat-shock and oxidative stress resistance of yeast cells taken for a stress-resistance spot assay at the indicated time-points. Serial dilutions of cells were spotted onto four sets of YP plates containing 2% glucose as carbon source. The first set of plates (control) was placed at 30°C immediately after spotting. The second set of plates (heat-shocked) was initially incubated at 55°C for 30 min, and was then transferred to 30°C. The third set of plates, which contained 5 mM hydrogen peroxide, was placed at 30°C immediately after spotting. The fourth set of plates, which contained 2.5 mM paraquat, was placed at 30°C immediately after spotting. All pictures were taken after 3 d of incubation at 30°C. Cell were cultured in YP media initially containing four different concentrations of glucose.

chronologically aging yeast outlined in this chapter of my thesis provides evidence that, before yeast enter the non-proliferative ST phase, they establish a diet-specific pattern of metabolism and organelle dynamics during D and PD phases. Both CR and non-CR yeast develop such a pattern after they entirely consume glucose during L phase. Due to their different metabolic histories prior to entry into a non-proliferative state, CR and non-CR

yeast that reach ST phase have different patterns of metabolism, inter-organellar communications and mitochondrial morphology (Figure 2.10). Combined, my findings and other data from Dr. Titorenko's laboratory [24, 246, 247, 278] suggest the following scenario for a stepwise establishment of such patterns prior to reproductive maturation (Figure 2.10).

Chronologically aging CR yeast shift carbohydrate metabolism toward glucose formation via gluconeogenesis by elevating the levels of the key enzymes involved in this reverse to glycolysis process. By activating the synthesis of enzymes catalyzing the biosynthesis of trehalose and glycogen and by suppressing the synthesis of enzymes required for their degradation, CR promotes the accumulation of these two major glucose stores (Figure 2.10) [24, 278]. CR yeast avoid ethanol accumulation by differentially modulating the levels of Adh1p or Adh2p, which are required for ethanol synthesis or degradation, respectively [24, 246, 278]. While CR yeast amass glucose stores, they rapidly hydrolyze their two major lipid stores, the neutral lipids triacylglycerols and ergosteryl esters, prior to entry into ST phase. Such lipolysis of lipid bodies-deposited neutral lipids in CR yeast produces substantial amounts of free fatty acids (Figure 2.10) [24, 246, 247, 278]. Free fatty acids are then rapidly oxidized to acetyl-CoA via a peroxisome-confined pathway greatly activated by CR. The subsequent oxidation of the peroxisome-derived acetyl-CoA in mitochondria generates the bulk of ATP in CR yeast (Figure 2.10). This process also generates considerable quantities of mitochondrial ROS. Within the mitochondrion, ROS are decomposed in antioxidant scavenger reactions catalyzed by a distinct set of enzymes, all of which are induced by CR (Figure 2.5; Tables 2.1 and 2.2). ROS homeostasis in chronologically aging CR yeast is also maintained by a

group of ROS scavenging enzymes that detoxify ROS released from mitochondria into the cytosol [24, 278]. CR increases levels of all these cytosolic antioxidant enzymes. The observed elevated levels of numerous mitochondrial and cytosolic anti-stress chaperones in chronologically aging CR yeast (Figure 2.5; Tables 2.1 and 2.2; [24]) are likely to be responsible for the observed increase in their resistance to chronic thermal and oxidative stresses (Figure 2.9). Consistent with the altered levels of several protein components of the mitochondrial fission and fusion machines in their cells (Figure 2.5; Tables 2.1 and 2.2), CR yeast that enter ST phase avoid fragmentation of their mitochondrial tubular network into individual mitochondria (Figures 2.8B and 2.8C).

Unlike CR yeast, chronologically aging non-CR yeast that enter ST phase generate the bulk of ATP via glycolytic oxidation of glycogen- and trehalose-derived glucose (Figure 2.10). The glycolytic oxidation of glucose to pyruvate in non-CR yeast is followed by its conversion to ethanol, which accumulates in non-CR yeast (Figure 2.10) [24, 246, 278]. In contrast to CR yeast, non-CR yeast entering ST phase amass substantial quantities of triacylglycerols and ergosteryl esters in their lipid bodies and endoplasmic reticulum (Figure 2.10) [24, 246, 247, 278]. Such accumulation of the two major lipid stores in non-CR yeast is due to the observed high levels of lipid bodies- and endoplasmic reticulum-associated enzymes involved in their biosynthesis and low levels of lipid bodies-bound enzymes that function in their degradation [24, 246, 278]. Furthermore, the low levels of enzymes functioning in the formation of FA-CoA and in their uptake and subsequent oxidation by peroxisomes seen in non-CR yeast that reached ST phase result in their diminished ability to oxidize FFA to acetyl-CoA via a

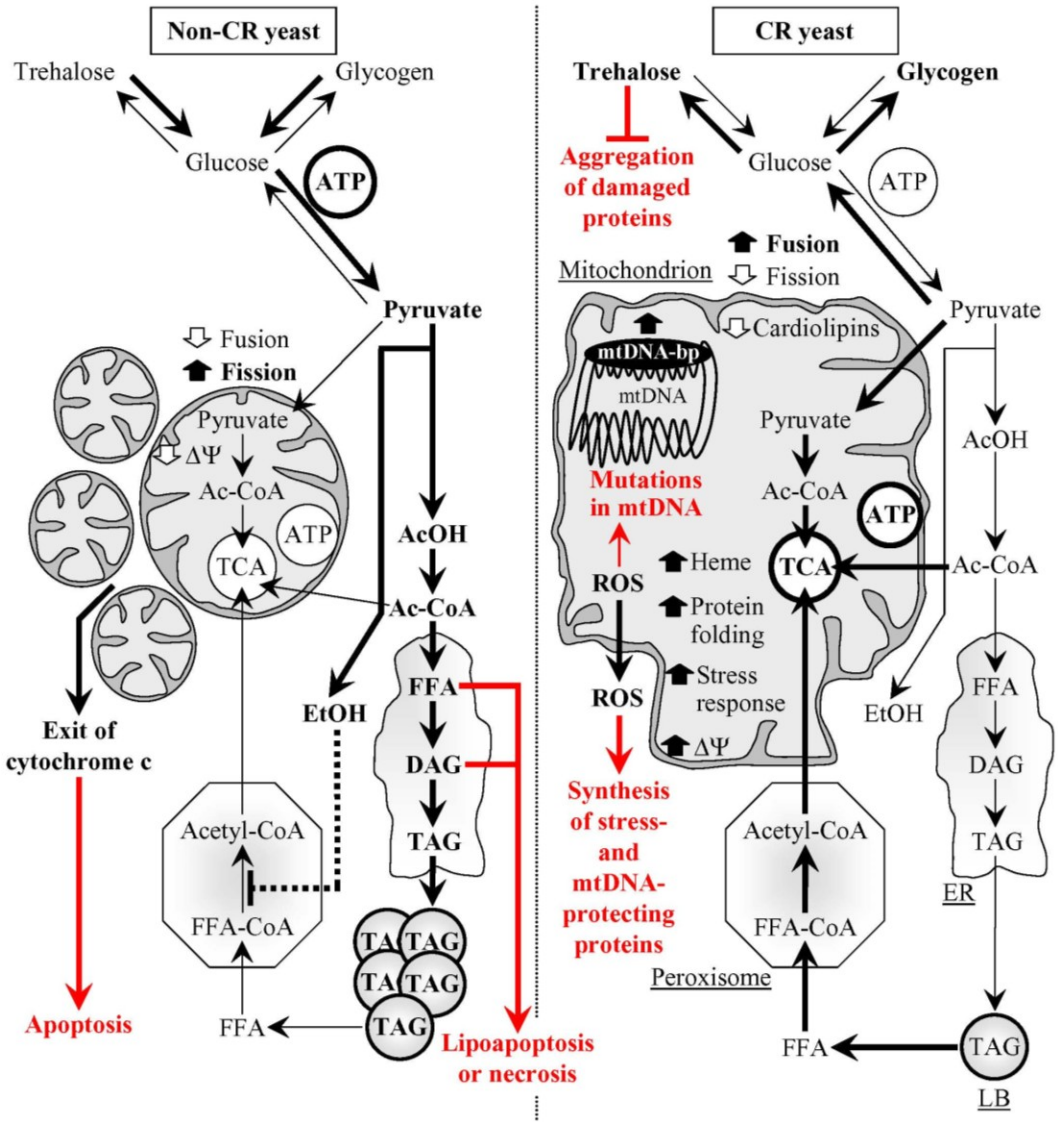


**Figure 2.10.** CR and non-CR yeast that enter ST phase have different patterns of metabolism, interorganellar communications and mitochondrial morphology. Before yeast enter the non-proliferative ST phase, they establish a diet-specific pattern of metabolism and organelle dynamics during D and PD phases. By designing such specific pattern prior to entry into a non-proliferative state, yeast could define their long-term viability. See text for details. The thickness of arrows correlates with the rates of the processes taking place in CR and non-CR yeast that have reached ST phase. The metabolites accumulated in bulk quantities are shown in bold. T bars denote inhibition of the process. The processes that may play an essential role in regulating the longevity of ST-phase yeast are displayed in red color. Dotted line denotes a proposed negative regulatory effect of ethanol on fatty acid oxidation in peroxisomes. Abbreviations: Ac-CoA, acetyl-CoA; AcOH, acetic acid; DAG, diacylglycerols; EE, ethyl esters; ER, endoplasmic reticulum; ERG, ergosterol; EtOH, ethanol; FA-CoA, CoA esters of fatty acids; FFA, free fatty acids; LB, lipid bodies;

mtDNA, mitochondrial DNA; mtDNA-bp, mtDNA-binding proteins; PL, phospholipids; ROS, reactive oxygen species; TAG, triacylglycerols; TCA, the tricarboxylic acid cycle in mitochondria.

peroxisome-confined pathway (Figure 2.10) [24, 246, 247, 278]. Because of the low efficiency of acetyl-CoA formation in peroxisomes of non-CR yeast they are unable to generate significant quantities of ATP by oxidizing peroxisome-derived acetyl-CoA in mitochondria. The resulting low efficiency of electron flow through the mitochondrial ETC of non-CR yeast reduces the transfer of a single electron to oxygen in mitochondria, thereby greatly decreasing mitochondrial ROS production (Figure 2.10) [24, 246, 247, 278]. The reduced (as compared to CR yeast) levels of cytosolic and mitochondrial stress-protecting proteins in non-CR yeast (Figure 2.5; Tables 2.1 and 2.2; [24, 246, 278]) can adequately explain why they are more sensitive to chronic thermal and oxidative stresses than CR yeast (Figure 2.9). The mitochondrial tubular network in non-CR yeast entering ST phase is fragmented into individual mitochondria (Figures 2.8B and 2.8C). Such fragmentation of mitochondria in non-CR yeast could be due to the increased levels of some protein components of the mitochondrial fission machine and decreased level of the Mgm1p component of the mitochondrial fusion machine in their cells (Figure 2.5; Tables 2.1 and 2.2).

Based on my comparison of the metabolic histories of long-lived CR yeast and short-lived non-CR yeast and on published data from Dr. Titorenko's laboratory [24, 246, 247, 278], I propose that, by designing a diet-specific pattern of metabolism and organelle dynamics prior to entry into a non-proliferative state, yeast define their long-term viability. I hypothesize that longevity in chronologically aging yeast is programmed by the level of metabolic capacity and organelle organization they developed, in a diet-

specific fashion, prior to reproductive maturation. In my hypothesis, the following metabolites and processes could play an essential role in regulating the chronological life span of yeast by defining their viability during ST phase (Figure 2.10).

**Trehalose.** Although trehalose has been long considered only as a reserve carbohydrate [272], it seems that the major function of this non-reducing disaccharide in yeast consists in enabling the survival of cells exposed to elevated temperature or ROS [273, 274]. In fact, trehalose in yeast cells prevents aggregation of proteins denatured during and immediately after their exposure to these stresses [274, 275]. I therefore propose that the elevated levels of trehalose seen in CR yeast during PD phase (Figure 2.3B) protect from aggregation those proteins that have been denatured due to their exposure to ROS accumulated during this growth phase (Figure 2.6E). Such protective effect of high trehalose concentrations could contribute to the enhanced (as compared to non-CR yeast) survival of CR yeast during the following ST phase. Moreover, because of the ability of trehalose to interfere with the chaperone-assisted refolding of denatured cytosolic proteins, it must be rapidly degraded in order for molecular chaperones to restore the native conformation of these proteins [273, 275]. Hence, one could expect that a diet providing yeast with the ability to maintain trehalose concentration at a certain "optimal" level (at which trehalose prevents aggregation of oxidatively damaged proteins and does not inhibit their refolding) would extend their longevity. It should be stressed, therefore, that 1) trehalose in CR yeast grown on 0.5% glucose, a diet that provides the maximal benefit of CR for longevity, increased mainly in PD phase and reached a plateau soon after cells have entered ST phase (Figure 2.3B); and 2) trehalose in CR yeast grown on 0.2% glucose, a diet providing only a modest CR-dependent life-span extension,

increased predominantly throughout ST phase and eventually reached the steady-state level exceeding that in CR yeast grown on 0.5% glucose (Figure 2.3B). Of note, recent unpublished data of Pavlo Kyryakov (a graduate student in Dr. Titorenko's laboratory) on protein unfolding/aggregation in response to elevated temperature or oxidative stress and on protein refolding following temperature or oxidative status restoration in various mutants impaired in different steps of the trehalose biosynthesis or degradation pathways (see Figure 2.4A) confirm the validity of my hypothesis on the essential role of trehalose in regulating the chronological life span of yeast and defining their viability during ST phase.

**Ethanol.** It is plausible that the observed stimulatory effect of CR on ethanol catabolism could play a role in longevity extension by CR (Figure 2.10). In fact, it has been shown that CR yeast completely consumed ethanol by day 2, at least 10 days before the beginning of their viability decline [24]. Conversely, it has been found that non-CR yeast are unable to consume substantial quantities of ethanol prior to the age-dependent decline of their viability [24]. Of note, ethanol in yeast cells suppresses the synthesis of certain proteins localized to peroxisomes [24, 246, 278, 296]. Furthermore, recent proteomic analysis revealed that CR elevated the levels of Fox1p, Fox2p and Fox3p [24], all of which are the core enzymes of peroxisomal β-oxidation of free fatty acids [297]. This finding can adequately explain the recently reported low levels of free fatty acids in CR yeast and their fast consumption throughout PD phase [24, 246], suggesting that the elevated levels of Fox1p, Fox2p and Fox3p in these yeast are due to the rapid depletion of ethanol in their cells (Figure 2.10). Therefore, it has been proposed that the accumulation of ethanol in non-CR yeast cultures suppresses peroxisomal oxidation of

free fatty acids by repressing the synthesis of Fox1p, Fox2p and Fox3p (Figure 2.10) [24, 246]. In this hypothesis, because of the low efficiency of free fatty acid oxidation in peroxisomes of aging non-CR yeast, they die during ST phase in part due to the induced by free fatty acids age-related form of necrotic cell death (Figure 2.10) [24, 246]. Of note, soon-to-be submitted for publication data of Simon Bourque (a graduate student in Dr. Titorenko's laboratory) on the molecular mechanism underlying the ability of CR to extend longevity of chronologically aging yeast by specifically remodelling lipid metabolism in the endoplasmic reticulum, lipid bodies and peroxisomes confirm the validity of the above hypothesis on the essential role of ethanol in regulating the chronological life span of yeast and defining their viability during ST phase.

**ROS.** Based on the findings presented in this chapter of my thesis, I hypothesize that ROS, which are mostly generated as by-products of mitochondrial respiration [276, 277], play a dual role in regulating the longevity of chronologically aging yeast (Figure 2.10). First, if yeast mitochondria are unable (due to a dietary regimen) to maintain ROS concentration below a toxic threshold, ROS promote aging by oxidatively damaging certain mitochondrial proteins (such as CCO, SDH and ACO) and mtDNA. In fact, I found that the highest amplitude of the early spike in ROS production in CR yeast entering D phase on 0.2% glucose (Figure 2.6E) correlated with their 1) shortened (as compared to CR yeast grown on 0.5% glucose) life span (Figures 2.1C and 2.1D); 2) sharply declined activities of CCO, SDH and ACO through the following PD and ST phases (Figures 2.6C, 2.6D and 2.6F); and 3) elevated frequencies of mtDNA deletions and point mutations, as compared to yeast under CR at 0.5% glucose (Figures 2.7A and 2.7B). Second, if yeast mitochondria can (due to a dietary regimen) maintain ROS

concentration at a certain "optimal" level, ROS delay chronological aging. I propose that this "optimal" level of ROS is insufficient to damage cellular macromolecules but can activate certain signaling networks [278, 277, 298] that extend life span by increasing the abundance or activity of stress-protecting and other anti-aging proteins (Figure 2.10); the term "mitohormesis" has been coined for such anti-aging role of mitochondrially produced ROS [299]. Indeed, I found that elevated (as compared to non-CR yeast) ROS concentrations in CR yeast (Figure 2.6E) correlated with their extended chronological longevity (Figures 2.1C and 2.1D), increased abundance of numerous mitochondrial and cytosolic anti-stress chaperones and mtDNA-binding proteins (Figure 2.5; Tables 2.1 and 2.2; [24]), and augmented resistance to chronic thermal and oxidative stresses (Figure 2.9). Moreover, although the low concentration of ROS seen in non-CR yeast could play a key role in protecting their mtDNA from "spontaneous" mutagenesis (Figures 2.7A and 2.7B), the inability of these yeast to generate ROS in sufficiently high, "optimal" quantities could contribute to their lowered (as compared to CR yeast) levels of cytosolic and mitochondrial stress-protecting proteins (Figure 2.5; Tables 2.1 and 2.2; [24]) and reduced resistance to chronic thermal and oxidative stresses (Figure 2.9). Noteworthy, the view that mitochondrially produced ROS in "optimal" concentrations contribute to extension of yeast life span by promoting "mitohormesis" is controversial [300, 301].

**Accumulation of mtDNA mutations.** My data imply that mtDNA mutations do not contribute to longevity regulation in non-CR yeast grown on 1% or 2% glucose. In fact, despite these yeast lived a shorter life than CR yeast grown on 0.2% glucose (Figures 2.1C and 2.1D), they had much lower frequencies of mtDNA deletions and point mutations, as compared to yeast under CR at 0.2% glucose (Figures 2.7A and 2.7B). In

contrast, it seems that the frequency of mtDNA mutations is an important contributing factor to yeast longevity under CR conditions (Figure 2.10). Indeed, the elevated frequencies of mtDNA mutations in yeast under CR at 0.2% glucose (Figures 2.7A and 2.7B) correlated with their shortened life span, as compared to yeast under CR at 0.5% glucose (Figures 2.1C and 2.1D).

**Mitochondria-controlled, age-related apoptosis.** The observed ability of CR to delay mitochondrial fragmentation in early ST phase (Figures 2.8B and 2.8C) could be responsible for the demonstrated capability of this diet to attenuate the age-related form of apoptotic cell death (Figures 2.8D, 2.8E and 2.8F), perhaps by preventing the efflux of cytochrome c (and, maybe, several other pro-apoptotic proteins) from the intermembrane space of mitochondria (Figure 2.8G). Moreover, the observed in non-CR yeast fragmentation of the mitochondrial tubular network could trigger age-related apoptosis by causing the age-related exit of cytochrome c (and, possibly, other pro-apoptotic proteins) from the intermembrane space of their fragmented mitochondria (Figure 2.8). Therefore, I propose that mitochondria-controlled, age-related apoptosis could play an essential role in regulating the chronological life span of yeast by defining their viability during ST phase (Figure 2.10).

## 2.6 Conclusions

As my comparison of the metabolic histories of long-lived CR yeast and short-lived non-CR yeast reported here revealed, yeast define their long-term viability by designing a diet-specific pattern of metabolism and organelle dynamics prior to reproductive maturation. My data imply that longevity in chronologically aging yeast is

programmed by the level of metabolic capacity and organelle organization they developed, in a diet-specific fashion, prior to entry into a non-proliferative state. Therefore, my conclusion is that chronological aging in yeast is the final step of a developmental program progressing through a series of checkpoints.

The major challenges now are 1) to validate my hypothesis that the longevity of chronologically aging yeast is programmed by the level of metabolic capacity and organelle organization they developed, in a diet-specific fashion, prior to reproductive maturation; and 2) to rank the relative contributions of different metabolites and processes (see Figure 2.10) to the chronological aging of yeast. To address these challenges, Dr. Titorenko' laboratory is currently evaluating how genetic manipulations that alter concentrations of these critical metabolites and affect these essential processes influence yeast longevity by modulating age-related protein aggregation, mitochondria-controlled apoptosis, free fatty acid- and diacylglycerol-induced necrosis, susceptibility to oxidative stress, and frequency of mtDNA mutations. A challenge for the future will be to elucidate how a longevity regulatory network centered on the Ras2p/cAMP/PKA/Rim15p/Msn2p/Msn4p and Tor1p/Sch9p/Rim15p/Gis1p nutrient-sensing pathways [278, 296, 301] governs the development of the diet-specific pattern of metabolism and organelle dynamics in chronologically aging yeast under CR conditions. Moreover, it would be interesting to examine whether the pattern established in yeast cells grown under CR conditions can be reversed upon their transfer to calorie-rich medium. Another challenge for the future will be to test the validity of my hypothesis that chronologically aging CR yeast protect their mitochondrial nucleoids from oxidative damage by turning on the RTG signaling pathway, which then activates transcription of

*ACO1* and other genes encoding bifunctional mtDNA-binding proteins known to maintain the integrity of mtDNA under respiratory conditions.

Finally, I expect that this knowledge will be instrumental for designing high-throughput screening of novel anti-aging drugs that can extend longevity by modulating the envisioned here developmental program of chronological aging operating in yeast.

# 3 Chemical genetic screen identifies lithocholic acid as an anti-aging compound that extends yeast chronological life span in a TOR-independent manner, by modulating housekeeping longevity assurance processes

## 3.1 Abstract

In chronologically aging yeast, longevity can be extended by administering a caloric restriction (CR) diet [6, 7, 10, 24, 35, 63] or some small molecules [101, 110, 114, 134]. These life-extending interventions target the adaptable target of rapamycin (TOR) and cAMP/protein kinase A (cAMP/PKA) signaling pathways that are under the stringent control of calorie availability [6, 7, 10, 35, 101, 110, 114, 134]. I designed a chemical genetic screen for small molecules that increase the chronological life span (CLS) of yeast under CR by targeting lipid metabolism and modulating housekeeping longevity pathways that regulate longevity irrespective of the number of available calories. My screen identifies lithocholic acid (LCA) as one of such molecules. My evaluation of the life-extending efficacy of LCA in WT strain on a high- or low-calorie diet revealed that this compound extends yeast CLS irrespective of the number of available calories. I found that the extent to which LCA extends longevity is highest under CR conditions, when the pro-aging processes modulated by the adaptable TOR and cAMP/PKA pathways are suppressed and the anti-aging processes are activated [6, 7, 10]. Furthermore, the life-extending efficacy of LCA in CR yeast significantly exceeded that in yeast on a high-calorie diet, in which the adaptable TOR and cAMP/PKA pathways greatly activate the pro-aging processes and suppress the anti-aging processes [4, 5, 7, 35, 279]. Altogether, my findings suggest that, consistent with its sought-after effect on a

longevity signaling network, LCA mostly targets certain housekeeping longevity assurance pathways that do not overlap (or only partially overlap) with the adaptable TOR and cAMP/PKA pathways modulated by calorie availability.

Consistent with my assumption that LCA extends longevity not by modulating the adaptable TOR pathway, I found that lack of Tor1p does not impair the life-extending efficacy of LCA under CR. I also revealed that, LCA extends longevity of the *tor1Δ* mutant strain to a very similar degree under CR and non-CR conditions. Thus, by eliminating a master regulator of this key adaptable pathway that shortens the CLS of yeast on a high-calorie diet, the *tor1Δ* mutation abolished the dependence of the anti-aging efficacy of LCA on the number of available calories.

My findings, along with some recently published data from Dr. Titorenko's laboratory, revealed two mechanisms underlying the life-extending effect of LCA in chronologically aging yeast. One mechanism operates in a calorie availability-independent fashion and involves the LCA-governed modulation of housekeeping longevity assurance pathways that do not overlap with the adaptable TOR and cAMP/PKA pathways. The other mechanism extends yeast longevity under non-CR conditions and consists in LCA-driven unmasking of the previously unknown anti-aging potential of PKA. I provide evidence that LCA modulates housekeeping longevity assurance pathways by 1) attenuating mitochondrial fragmentation, a hallmark event of age-related cell death; 2) altering oxidation-reduction processes in mitochondria, including oxygen consumption, the maintenance of membrane potential, and reactive oxygen species production; 3) enhancing resistance to oxidative and thermal stresses; 4)

suppressing mitochondria-controlled apoptosis; and 5) enhancing stability of nuclear and mitochondrial DNA.

## 3.2 Introduction

Aging of multicellular and unicellular eukaryotic organisms is a multifactorial biological phenomenon that has various causes and affects a plethora of cellular activities [1 - 3, 5, 8, 10, 24]. These numerous activities are modulated by only a few nutrient- and energy-sensing signaling pathways that are conserved across phyla and include the insulin/insulin-like growth factor 1 (IGF-1), AMP-activated protein kinase/target of rapamycin (AMPK/TOR) and cAMP/protein kinase A (cAMP/PKA) pathways [4, 10, 36]. By sharing a compendium of protein kinases and adaptor proteins, the insulin/IGF-1, AMPK/TOR and cAMP/PKA pathways in yeast, worms, fruit flies and mammals converge into a network regulating longevity [4, 10, 36 - 38, 301]. This network may also include several proteins that currently are not viewed as being in any of these three pathways [4, 10, 36, 73, 74]. Moreover, this network responds to the age-related partial mitochondrial dysfunction and is modulated by mitochondrially produced reactive oxygen species (ROS) [36, 73, 75, 147]. By sensing the nutritional status of the whole organism as well as the intracellular nutrient and energy status, functional state of mitochondria, and concentration of ROS produced in mitochondria, the longevity network regulates life span across species by coordinating information flow along its convergent, divergent and multiply branched signaling pathways.

By defining the organismal and intracellular nutrient and energy status, nutrient intake plays an important role in modulating life span and influences age-related

pathologies [7, 208]. Two dietary regimens are known to have the most profound life-extending effects across species and to improve overall health by delaying the onset of age-related diseases. They include: 1) caloric restriction (CR), a diet in which only calorie intake is reduced but the supply of amino acids, vitamins and other nutrients is not compromised [13, 76, 77, 80, 208]; and 2) dietary restriction (DR), in which the intake of nutrients (but not necessarily of calories) is reduced by limiting food supply without causing malnutrition [66, 76, 77, 91]. In a "TOR-centric" view of longevity regulation, TOR alone governs the life-extending and health-improving effects of CR/DR by: 1) integrating the flow of information on the organismal and intracellular nutrient and energy status from the protein kinases AMPK, PKA, PKB/AKT (the insulin/IGF-1 pathway) and ERK1/2 (the PKA-inhibited Raf/MEK/ERK protein kinase cascade) as well as from the mitochondrial redox protein $P66^{Shc}$; 2) sensing the intracellular levels of amino acids in an AMPK-independent manner; and 3) operating as a control center which, based on the information it has gathered and processed, modulates many longevity-related processes in a sirtuin-independent fashion [84 - 86]. The inability of CR to increase the replicative life span (RLS) of yeast mutants lacking components of the TOR pathway [87] and the lack of the beneficial effect of DR on life span in worms with reduced TOR signaling [88, 89] support the proposed central role for TOR in orchestrating the life-extending effect of CR/DR in these two longevity paradigms. Moreover, while the postulated by the TOR-centric model dispensability of sirtuins for the longevity benefit associated with DR has been confirmed in worms [89], the importance of the sirtuin Sir2p in mediating the life-extending effect of CR in replicatively aging yeast is debated [56, 87, 145, 151]. Noteworthy, while TOR is a

central regulator of the life-extending effect of CR in replicatively aging yeast, the longevity benefit associated with CR in chronologically aging yeast is mediated by a signaling network that includes: 1) the TOR and cAMP/PKA pathways converged on Rim15p, which therefore acts as a nutritional integrator; and 2) some other, currently unknown pathways that are not centered on Rim15p [301]. Considering the likely convergence of the insulin/IGF-1, AMPK/TOR and cAMP/PKA signaling pathways into a network regulating longevity in worms, fruit flies and mammals (see above), it is conceivable that - akin to TOR - the insulin/IGF-1 and cAMP/PKA pathways may contribute to the beneficial effect of CR/DR on their longevity. Although some findings in worms, fruit flies and mammals support the involvement of the insulin/IGF-1 pathway in the longevity benefit associated with CR/DR, other data imply that such benefit is independent of insulin/IGF-1 (reviewed by Narasimhan *et al*. [36]). The role of cAMP/PKA signaling in the life-extending effect of CR/DR in these multicellular eukaryotes remains to be tested. Importantly, the recently reported in worms involvement of both independent and overlapping pathways in life span extension by different DR regimens [100] supports the notion that the longevity benefit associated with nutrient limitation is mediated by a signaling network that integrates several pathways.

Akin to CR and DR regimens, certain pharmacological interventions can extend longevity across phyla and improve health by beneficially influencing age-related pathologies. Noteworthy, all of the currently known anti-aging compounds increase life span under non-CR or non-DR conditions (see chapter 1 of my thesis for a detailed discussion of this topic). Under such conditions, these compounds have been shown to: 1) provide the longevity and health benefits associated with CR and DR, but without

restricting caloric and nutrient intake; and 2) mimic numerous life-extending effects of CR and DR on gene expression pattern, metabolic and physiological processes, and stress response pathways. Therefore, the names "CR mimetics" and "DR mimetics" have been coined for them [149, 150]. Importantly, most CR mimetics and DR mimetics target signaling pathways that modulate longevity in response to the organismal and intracellular nutrient and energy status, including the insulin/IGF-1 and AMPK/TOR pathways as well as the sirtuin-governed protein deacetylation module of the longevity signaling network integrating these pathways (see chapter 1 of my thesis for a detailed discussion of this topic). Furthermore, such compounds as resveratrol, metformin and mianserin increase life span only under non-CR or non-DR conditions, but are unable to do so if the supply of calories or nutrients is limited [107, 112, 119 - 121]. Hence, one could envision that most, if not all, longevity pathways are "adaptable" by nature, *i.e.*, that they modulate longevity only in response to certain changes in the extracellular and intracellular nutrient and energy status of an organism. However, $Li^+$ in worms and rapamycin in fruits flies extend life span even under DR conditions [103, 113]. It is likely therefore that some longevity pathways could be "constitutive" or "housekeeping" by nature, *i.e.*, that they: 1) modulate longevity irrespective of the organismal and intracellular nutrient and energy status; and 2) do not overlap (or only partially overlap) with the adaptable longevity pathways that are under the stringent control of calorie and/or nutrient availability. The challenge is to identify such housekeeping longevity pathways, perhaps by using a chemical screen for compounds that can extend longevity even under CR/DR conditions. Because under such conditions the adaptable pro-aging pathways are fully suppressed and the adaptable anti-aging pathways are fully activated,

a compound that can increase life span is expected to target the housekeeping longevity pathways.

Noteworthy, two anti-aging compounds alter lipid levels in mammals and fruit flies under non-DR conditions. In fact, resveratrol treatment reduces the levels of the neutral lipids triacylglycerols (TAG) and increases free fatty acid (FFA) levels in mouse adipocytes [127]. Furthermore, feeding rapamycin to fruit flies results in elevated TAG levels [113]. Although it remains to be seen if such effects of resveratrol and rapamycin on lipid levels play a casual role in their anti-aging action under non-DR conditions, it should be stressed that lipid metabolism has been shown to be involved in longevity regulation in yeast [24, 246], worms [50, 74, 302, 303], fruit flies [302, 304] and mice [127, 302, 305 - 308]. Recently, our laboratory proposed a mechanism linking yeast longevity and lipid dynamics in the endoplasmic reticulum (ER), lipid bodies and peroxisomes. In this mechanism, a CR diet extends yeast CLS by activating FFA oxidation in peroxisomes [24, 246]. It is conceivable that the identification of small molecules targeting this mechanism could yield novel anti-aging compounds. Such compounds can be used as research tools for defining the roles for different longevity pathways in modulating lipid metabolism and in integrating lipid dynamics with other longevity-related processes. Furthermore, the availability of such compounds would enable a quest for housekeeping longevity assurance pathways that do not overlap (or only partially overlap) with the adaptable TOR and cAMP/PKA pathways. Moreover, such compounds would have a potential to be used as pharmaceutical agents for increasing life span and promoting healthy aging by delaying the onset of age-related diseases, regardless of an organism's dietary regimen.

I sought to identify small molecules that increase the CLS of yeast under CR conditions by targeting lipid metabolism and modulating housekeeping longevity assurance pathways. My chemical genetic screen identified lithocholic acid (LCA) as one of such small molecules. My analysis of how LCA influences various longevity-related processes and how it affects the CLS of yeast mutants impaired in the adaptable longevity pathways provided important new insights into mechanisms of longevity regulation, as outlined below.

## 3.3 Materials and Methods

### Strains and media

The wild-type strain *Saccharomyces cerevisiae* BY4742 (*MATα his3Δ1 leu2Δ0 lys2Δ0 ura3Δ0*) and mutant strains *pex5Δ* (*MATα his3Δ1 leu2Δ0 lys2Δ0 ura3Δ0 pex5Δ::kanMX4*), *tor1Δ* (*MATα his3Δ1 leu2Δ0 lys2Δ0 ura3Δ0 tor1Δ::kanMX4*), *ras2Δ* (*MATα his3Δ1 leu2Δ0 lys2Δ0 ura3Δ0 ras2Δ::kanMX4*) and *rim15*Δ (*MATα his3Δ1 leu2Δ0 lys2Δ0 ura3Δ0 rim15Δ::kanMX4*) were used in this study. Media components were as follows: 1) YEPD (0.2% Glucose), 1% yeast extract, 2% peptone, 0.2% glucose; 2) YEPD (0.5% Glucose), 1% yeast extract, 2% peptone, 0.5% glucose; 3) YEPD (1% Glucose), 1% yeast extract, 2% peptone, 1% glucose; and 4) YEPD (2% Glucose), 1% yeast extract, 2% peptone, 2% glucose.

### A plating assay for the analysis of chronological life span

Cells were grown in YEPD medium initially containing 0.2%, 0.5%, 1% or 2% glucose as carbon source at 30$^{o}$C with rotational shaking at 200 rpm in Erlenmeyer flasks at a

flask volume/medium volume ratio of 5:1. A sample of cells was removed from each culture at various time points. A fraction of the cell sample was diluted in order to determine the total number of cells per ml of culture using a hemacytometer. 10 µl of serial dilutions (1:10 to $1:10^3$) of cells were applied to the hemacytometer, where each large square is calibrated to hold 0.1 µl. The number of cells in 4 large squares was then counted and an average was taken in order to ensure greater accuracy. The concentration of cells was calculated as follows: number of cells per large square x dilution factor × 10 × 1,000 = total number of cells per ml of culture. A second fraction of the cell sample was diluted and serial dilutions ($1:10^2$ to $1:10^5$) of cells were plated onto YEPD (2% Glucose) plates in triplicate in order to count the number of viable cells per ml of each culture. 100 µl of diluted culture was plated onto each plate. After a 48-h incubation at $30^oC$, the number of colonies per plate was counted. The number of colony forming units (CFU) equals to the number of viable cells in a sample. Therefore, the number of viable cells was calculated as follows: number of colonies × dilution factor × 10 = number of viable cells per ml. For each culture assayed, % viability of the cells was calculated as follows: number of viable cells per ml / total number of cells per ml × 100%. The % viability of cells in mid-logarithmic phase was set at 100% viability for that particular culture.

**Plating assays for the analysis of resistance to various stresses**

For the analysis of hydrogen peroxide resistance, serial dilutions ($1:10^0$ to $1:10^5$) of wild-type and mutant cells removed from mid-logarithmic phase (day 1) and from diauxic phase (days 2 and 3) in YEPD (0.2% Glucose) were spotted onto two sets of plates. One

set of plates contained YEPD (2% Glucose) medium alone, whereas the other set contained YEPD (2% Glucose) medium supplemented with 5 mM hydrogen peroxide. Pictures were taken after a 3-day incubation at 30$^{o}$C.

For the analysis of oxidative stress resistance, serial dilutions (1:$10^{0}$ to 1:$10^{5}$) of wild-type and mutant cells removed from mid-logarithmic phase (day 1) and from diauxic phase (days 2 and 3) in YEPD (0.2% Glucose) were spotted onto two sets of plates. One set of plates contained YEPD (2% Glucose) medium alone, whereas the other set contained YEPD (2% Glucose) medium supplemented with 2.5 mM of the superoxide/hydrogen peroxide-generating agent paraquat. Pictures were taken after a 3-day incubation at 30$^{o}$C.

For the analysis of heat-shock resistance, serial dilutions (1:$10^{0}$ to 1:$10^{5}$) of wild-type and mutant cells removed from mid-logarithmic phase (day 1) and from diauxic phase (days 2 and 3) in YEPD (0.2% Glucose) were spotted onto two sets of YEPD (2% Glucose) plates. One set of plates was incubated at 30$^{o}$C. The other set of plates was initially incubated at 55$^{o}$C for 30 min, and was then transferred to 30$^{o}$C. Pictures were taken after a 3-day incubation at 30$^{o}$C.

For the analysis of salt stress resistance, serial dilutions (1:$10^{0}$ to 1:$10^{5}$) of wild-type and mutant cells removed from mid-logarithmic phase (day 1) and from diauxic phase (days 2 and 3) in YEPD (0.2% Glucose) were spotted onto two sets of plates. One set of plates contained YEPD (2% Glucose) medium alone, whereas the other set contained YEPD (2% Glucose) medium supplemented with 0.5 M NaCl. Pictures were taken after a 3-day incubation at 30$^{o}$C.

For the analysis of osmotic stress resistance, serial dilutions ($1:10^0$ to $1:10^5$) of wild-type and mutant cells removed from mid-logarithmic phase (day 1) and from diauxic phase (days 2 and 3) in YEPD (0.2% Glucose) were spotted onto two sets of plates. One set of plates contained YEPD (2% Glucose) medium alone, whereas the other set contained YEPD (2% Glucose) medium supplemented with 1 M sorbitol. Pictures were taken after a 3-day incubation at 30°C.

**Chemical genetic screen for compounds that increase chronological life span (CLS)**

The screen was conducted at the High Throughput/Content Screening Facility at McGill University. The single-gene-deletion mutant strain *pex5Δ* (*MATα his3Δ1 leu2Δ0 lys2Δ0 ura3Δ0 pex5Δ::kanMX4*) from Open Biosystems was grown in YPA0.5D medium (1% yeast extract, 2% peptone, 50 µg/ml ampicillin, 0.5% glucose). 3-µl aliquots of the *pex5Δ* culture recovered from mid-logarithmic phase at a cell titre of $2 \times 10^7$ cells/ml were aliquoted into 96-well master microplates using a Beckman Coulter high density Biomek FXII replica pinning robot. Each well of a master microplate contained 96 µl of YPA0.5D medium. 1 µl of a compound stock solution from a commercially available library (each compound at 5 mM in dimethylsulfoxide (DMSO)) was added to each well using a Beckman Coulter high density Biomek FXII replica pinning robot. Wells of a master microplate supplemented with 1% DMSO (1 µl of DMSO per a well containing 3 µl of the *pex5Δ* culture and 96 µl of YPA0.5D medium) were used as negative controls. Each master plate was created in duplicate. The master microplates were sealed and incubated without shaking at 30°C in a moist chamber. At days 1, 7, 10 and 14 of the incubation of master microplates, a 3-µl aliquot of each culture was transferred into

individual wells of a new (replica) microplate containing 97 µl of YPA0.5D medium. Following incubation of sealed replica microplates in a moist chamber for 16 hours at 30$^{o}$C (to allow for growth of cells that were still viable), the optical density at 600 nm ($OD_{600}$) of the culture in each well of the replica microplate was measured using a Molecular Devices Analyst HT plate reader. To calculate survival at each time point, the $OD_{600}$ at a particular time point was divided by the $OD_{600}$ at day 1. "Cherry-picking" of the identified "lead" compounds for possible "hits" was carried out as described above, with each lead compound being used at a final concentration of 5, 10, 25 or 50 µM and assessed in triplicate for validation. Commercially available structural analogs of hit compounds were identified using the web-based eMolecules searching engine. In total, approximately 19,000 representative compounds from the BIOMOL, Chembridge, Maybridge, MicroSource Discovery, NIH Clinical Collection, Prestwick Chemical Inc. and Sigma-LOPAC commercial libraries were tested using the screen for chemical modulators of longevity.

**Pharmacological manipulation of CLS**

CLS analysis was performed as described above in this section. The chenodeoxycholic (C9377), cholic (C1129), dehydrocholic (D3750), deoxycholic (D2510), hyodeoxycholic (H3878), lithocholic (L6250) and ursodeoxycholic (U5127) bile acids were from Sigma. Their stock solutions in DMSO were made on the day of adding each of these compounds to cell cultures. Compounds were added to growth medium at the indicated concentration immediately following cell inoculation. The final concentration of DMSO in yeast

cultures supplemented with a bile acid (and in the corresponding control cultures supplemented with drug vehicle) was 1% (v/v).

**Monitoring the formation of ROS**

Wild-type and mutant cells grown in YEPD (0.2% Glucose) were tested microscopically for the production of ROS by incubation with dihydrorhodamine 123 (DHR). In the cell, this nonfluorescent compound can be oxidized to the fluorescent chromophore rhodamine 123 by ROS. Cells were also probed with a fluorescent counterstain Calcofluor White M2R (CW), which stains the yeast cell walls fluorescent blue. CW was added to each sample in order to label all cells for their proper visualization. DHR was stored in the dark at –20$^{o}$C as 50 µl aliquots of a 1 mg/ml solution in ethanol. CW was stored in the dark at –20$^{o}$C as the 5 mM stock solution in anhydrous DMSO (dimethylsulfoxide).

The concurrent staining of cells with DHR and CW was carried out as follows. The required amounts of the 50 µl DHR aliquots (1 mg/ml) and of the 5 mM stock solution of CW were taken out of the freezer and warmed to room temperature. The solutions of DHR and CW were then centrifuged at 21,000 × g for 5 min in order to clear them of any aggregates of fluorophores. For cell cultures with a titre of ~ $10^7$ cells/ml, 100 µl was taken out of the culture to be treated. If the cell titre was lower, proportionally larger volumes were used. 6 µl of the 1 mg/ml DHR and 1 µl of the 5 mM CW solutions were added to each 100 µl aliquot of culture. After a 2-h incubation in the dark at room temperature, the samples were centrifuged at 21,000 × g for 5 min. Pellets were resuspended in 10 µl of PBS buffer (20 mM $KH_2PO_4$/KOH, pH 7.5, and 150 mM NaCl). Each sample was then supplemented with 5 µl of mounting medium, added to a

microscope slide, covered with a coverslip, and sealed using nail polish. Once the slides were prepared, they were visualized under the Zeiss Axioplan fluorescence microscope mounted with a SPOT Insight 2 megapixel color mosaic digital camera. Several pictures of the cells on each slide were taken, with two pictures taken of each frame. One of the two pictures was of the cells seen through a rhodamine filter in order to detect cells dyed with DHR. The second picture was of the cells seen through a DAPI filter in order to visualize CW, and therefore all the cells present in the frame.

For evaluating the percentage of DHR-positive cells, the UTHSCSA Image Tool (Version 3.0) software was used to calculate both the total number of cells and the number of stained cells. Fluorescence of individual DHR-positive cells in arbitrary units was determined by using the UTHSCSA Image Tool software (Version 3.0). In each of 3-5 independent experiments, the value of median fluorescence was calculated by analyzing at least 800-1000 cells that were collected at each time point. The median fluorescence values were plotted as a function of the number of days cells were cultured.

**Immunofluorescence microscopy**

Cell cultures were fixed in 3.7% formaldehyde for 45 min at room temperature. The cells were washed in solution B (100 mM $KH_2PO4$/KOH pH 7.5, 1.2 M sorbitol), treated with Zymolyase 100T (MP Biomedicals, 1 µg Zymolyase 100T/1 mg cells) for 30 min at 30$^{o}$C and then processed as previously described [249]. Monoclonal antibody raised against porin (Invitrogen, 0.25 µg/µl in TBSB buffer [20 mM Tris/HCl pH 7.5, 150 mM NaCl, 1 mg/ml BSA]) was used as a primary antibody. Alexa Fluor 568 goat anti-mouse IgG (Invitrogen, 2 µg/µl in TBSB buffer) was used as a secondary antibody. The labeled

samples were mounted in mounting solution (16.7 mM Tris/HCl pH 9.0, 1.7 mg/ml *p*-phenylenediamine, 83% glycerol). Images were collected with a Zeiss Axioplan fluorescence microscope (Zeiss) mounted with a SPOT Insight 2 megapixel color mosaic digital camera (Spot Diagnostic Instruments).

**Oxygen consumption assay**

The rate of oxygen consumption by yeast cells recovered at various time points was measured continuously in a 2-ml stirred chamber using a custom-designed biological oxygen monitor (Science Technical Center of Concordia University) equipped with a Clark-type oxygen electrode. 1 ml of YEPD medium supplemented with 0.2% glucose was added to the electrode for approximately 5 minutes to obtain a baseline. Cultured cells of a known titre were spun down at 3,000 × g for 5 minutes. The resulting pellet was resuspended in YEPD medium supplemented with 0.2% glucose and then added to the electrode with the medium that was used to obtain a baseline. The resulting slope was used to calculate the rate of oxygen consumption in $O_2$% x $min^{-1}$ × $10^9$ cells.

**Measurement of mitochondrial mutations and nuclear mutations affecting mitochondrial components**

The frequency of spontaneous single-gene (*mit*$^-$ and *syn*$^-$) and deletion (*rho*$^-$ and *rho*$^o$) mutations in mitochondrial DNA (mtDNA) and spontaneous single-gene nuclear mutations (*pet*$^-$) affecting essential mitochondrial components was evaluated by measuring the fraction of respiratory-competent (*rho*$^+$) yeast cells remaining in their aging population. *rho*$^+$ cells maintained intact their mtDNA and their nuclear genes

encoding essential mitochondrial components. Therefore, *rho*$^{+}$ cells were able to grow on glycerol, a non-fermentable carbon source. In contrast, mutant cells deficient in mitochondrial respiration were unable to grow on glycerol. Most of these mutant cells carried mutations in mtDNA (including single-gene *mit*$^{-}$ and *syn*$^{-}$ mutations or large deletions *rho*$^{-}$) or completely lacked this DNA (*rho*$^{o}$ mutants), whereas some of them carried so-called *pet*$^{-}$ mutations in nuclear genes that code for essential mitochondrial components [250]. Serial dilutions of cell samples removed from different phases of growth were plated in duplicate onto YP plates containing either 2% glucose or 3% glycerol as carbon source. Plates were incubated at 30$^{o}$C. The number of CFU on YP plates containing 2% glucose was counted after 2 d of incubation, whereas the number of CFU on YP plates containing 3% glycerol was counted after 6 d of incubation. For each culture, the percentage of respiratory-deficient (*mit*$^{-}$, *syn*$^{-}$, *rho*$^{-}$, *rho*$^{o}$ and *pet*$^{-}$) cells was calculated as follows: 100 - [(number of CFU per ml on YP plates containing 3% glycerol/number of CFU per ml on YP plates containing 2% glucose) × 100]. The frequency of spontaneous point mutations in the *rib2* and *rib3* loci of mtDNA was evaluated by measuring the frequency of mtDNA mutations that caused resistance to the antibiotic erythromycin [251]. These mutations impair only mtDNA [252, 253]. In each of the seven independent experiments performed, ten individual yeast cultures were grown in YP medium containing 0.2%, 0.5%, 1% or 2% glucose as carbon source. A sample of cells was removed from each culture at various time-points. Cells were plated in duplicate onto YP plates containing 3% glycerol and erythromycin (1 mg/ml). In addition, serial dilutions of each sample were plated in duplicate onto YP plates containing 3% glycerol as carbon source for measuring the number of respiratory-

competent (*rho*$^+$) cells. The number of CFU was counted after 6 d of incubation at 30$^o$C. For each culture, the frequency of mutations that caused resistance to erythromycin was calculated as follows: number of CFU per ml on YP plates containing 3% glycerol and erythromycin/number of CFU per ml on YP plates containing 3% glycerol.

**Preparation of total cell lysates**

An aliquot containing 1 × $10^9$ cells was centrifuged for 7 min at 3,000 rpm at room temperature. Pelleted cells were washed twice with distilled water and further centrifuged for 3 min at 16,000 × g at room temperature. The recovered cell pellet was then resuspended in 500 µl of 4% CHAPS in 25 mM Tris/HCl buffer (pH 8.5) and centrifuged for 15 sec at 16,000 × g at room temperature. The cells were then washed again, first by resuspending them in 500 µl of 4% CHAPS in 25 mM Tris/HCl buffer (pH 8.5) and then by centrifuging for 15 sec at 16,000 × g at room temperature. The pellet of washed cells was then resuspended in 1 ml of ice-cold 4% CHAPS in 25 mM Tris/HCl buffer (pH 8.5), divided into 5 equal aliquots of 200 µl each and placed in Eppendorf tubes kept on ice. Each 200 µl aliquot was supplemented with ~100 µl of glass beads and vortexed three times for 1 minute. Apart from the vortexing steps, the samples were kept on ice at all times. Glass beads and cell debris were then pelleted by 5 min centrifugation at 16,000 × g at 4$^o$C. The resulting supernatant of the glass bead lysate was immediately transferred into a pre-chilled Eppendorf tube and stored at -20$^o$C for further analysis.

**Isolation of the crude mitochondrial fraction**

Yeast cells were pelleted at 3,000 × g for 5 min at room temperature, washed twice with distilled water, resuspended in DTT buffer (100 mM Tris-$H_2SO_4$, pH 9.4, 10 mM dithiothreitol [DTT]), and incubated for 20 min at 30°C to weaken the cell wall. The cells were then washed with Zymolyase buffer (1.2 M sorbitol, 20 mM potassium phosphate, pH 7.4), centrifuged at 3,000 × g for 5 min at room temperature, and incubated with 3 mg/g (wet wt) of Zymolyase-100T in 7 ml/g (wet wt) Zymolyase buffer for 45 min at 30°C. Following an 8-min centrifugation at 2,200 × g at 4°C, the isolated spheroplasts were washed in ice-cold homogenization buffer (5 ml/g) (0.6 M sorbitol, 10 mM Tris-HCl, pH7.4, 1 mM EDTA, 0.2% (w/v) BSA) and then centrifuged at 2,200 × g for 8 min at 4°C. Washed spheroplasts were homogenized in ice-cold homogenization buffer using 15 strokes. The cell debris was removed by centrifuging the resulting homogenates at 1,500 × g for 5 min at 4°C. The supernatant was further centrifuged at 3,000 × g for 5 min at 4°C to remove residual cell debris. The resulting supernatant was then centrifuged at 12,000 × g for 15 min at 4°C to pellet mitochondria. The remnant cell debris was removed by centrifuging the mitochondrial fraction at 3,000 × g for 5 min at 4°C. The resulting supernatant was then centrifuged at 12,000 × g for 15 min at 4°C to obtain the crude mitochondrial pellet, which was then resuspended in 3 ml of SEM Buffer (250 mM sucrose, 1 mM EDTA, 10 mM MOPS, pH 7.2) and used for the purification of mitochondria as described below.

**Purification of mitochondria devoid of microsomal and cytosolic contaminations**

A sucrose gradient was made by carefully overlaying 1.5 ml of 60% sucrose with 4 ml of 32% sucrose, 1.5 ml of 23% sucrose, and then 1.5 ml of 15% sucrose (all in EM buffer; 1

mM EDTA, 10 mM MOPS, pH 7.2). Finally, a 3-ml aliquot of the crude mitochondrial fraction in SEM buffer was applied to the gradient and centrifuged at 134,000 × g (33,000 rpm) overnight at 2°C in vacuum (Rotor SW50Ti, Beckman). The purified mitochondria found at the 60%/32% sucrose interface were carefully removed and stored at - 80°C.

**Purification of the ER**

**Reagents and solutions**

1. TSD reduction buffer: 0.1 M Tris/Sulfate (pH 9.4), 10 mM DTT

2. HEPES lysis buffer: 20 mM HEPES/KOH, pH 6.8, 50 mM KCl, 200 mM sorbitol, 2 mM EDTA, 1 mM DTT

3. Spheroplast medium A (pH 7.5): 0.67% yeast nitrogen base (w/o) amino acids, 2 % (w/v) glucose, 1 M sorbitol, 20 mM Tris/HCl (pH 7.5)

4. Spheroplast medium B: 0.67% yeast nitrogen base (w/o) amino acids, 2 % (w/v) glucose, 1 M sorbitol

5. 1.2 M sucrose/ HEPES, 36% (w/w): 7.2 g sucrose + 12.8 ml HEPES lysis buffer

6. 1.5 M sucrose/ HEPES, 43% (w/w): 8.6 g sucrose + 11.4 ml HEPES lysis buffer

7. MES buffer 1 (MES breaking buffer): 10 mM MES/Tris (pH 6.9), 12 % (w/w) Ficoll 400, 0.2 mM EDTA

8. MES buffer 2: 10 mM MES/Tris (pH 6.9), 8 % (w/w) Ficoll 400, 0.2 mM EDTA

9. MES buffer 3: 10 mM MES/Tris (pH 6.9), 0.6 M sorbitol, 8 % (w/w) Ficoll 400, 0.2 mM EDTA

10. MES buffer 4: 10 mM MES/Tris (pH 6.9), 0.25 M sorbitol, 0.2 mM EDTA

11. KPi buffer (pH 7.4): 20 mM $KH_2PO_4$/KOH (pH 7.4), 1.2 M sorbitol

**Procedure**

Wild-type and mutant cells were grown in YEPD medium initially containing 0.2%, 0.5%, 1% or 2% glucose as carbon source. Cultures were harvested at mid-exponential and diauxic phases, checked for contamination by bright-field microscopy and used to measure cell density at $OD_{600}$. The non-contaminated wild-type and mutant cells were pelleted at 4,000 × g for 5 min at room temperature. Cells were then resuspended at 10 $OD_{600}$ units/ml in TSD reduction buffer, incubated for 10 min at room temperature and centrifuged for 5 min at 4,000 × g at room temperature. Pelleted cells were then resuspended at 20 $OD_{600}$ units/ml in Spheroplast medium A and supplemented with Zymolyase 100T at a concentration of 7.5 µg per $OD_{600}$ units of cells. 10 µl of each cell suspension was then removed, diluted in 990 µl of $H_2O$ and used to measure the $OD_{600}$. The remaining cell suspensions were incubated at 30°C for 30 min and the efficiency of cell wall removal was monitored by measuring the $OD_{600}$. Cell wall digestion was allowed to proceed until the $OD_{600}$ measurement of the diluted cell suspension became 5% of the original value, with the total digestion time not exceeding 1 hour. Spheroplasts were then harvested by centrifugation at 1,500 × g for 5 min at room temperature, followed by resuspending at 1 to 5 $OD_{600}$ units/ml in Spheroplast medium B by gentle swirling of the tube or gentle stirring with a glass rod. Spheroplasts were then harvested by centrifugation at 1,500 × g for 5 min at 4°C and then resuspended at a concentration of 1,000 $OD_{600}$ units/ml of ice-cold HEPES lysis buffer with freshly-added DTT. Spheroplasts were then homogenized using 20 strokes and resulting lysates were

centrifuged at 1, 000 × g for 10 min at 4°C. The supernatants ($S_{1000}$) were subjected to another round of centrifugation at 1, 000 × g for 10 min at 4°C, and resulting supernatants were further centrifuged at 27,000 × g for 10 min at 4°C. The pelleted membranes ($P_{27,000}$) were resuspended in 1.0 ml of HEPES lysis buffer (5,000 $OD_{600}$ equivalents per ml) using a trimmed 1-ml pipette tip and carefully layered on top of a sucrose gradient prepared in advance (2.1 ml of 1.5 M sucrose/HEPES solution was deposited to the bottom of a Beckman Ultra-Clear centrifuge tube for the Beckman MLS-50 rotor, and then overlaid with 2.1 ml of 1.2 M sucrose/HEPES solution). The gradient tubes were then placed in the pre-chilled swinging bucket Beckman MLS-50 rotor and centrifuged at 100,000 × g (36,000 rpm) for 1 hr at 4°C using the slow acceleration and deceleration setting to minimize disruption of gradients. 18 gradient fractions of 227 µl each were then collected starting from the top of the sucrose gradient and stored at -20°C for further analyses.

**Protein precipitation, SDS-PAGE and silver staining of gels**

Protein concentration was determined using the RC DC protein assay kit (Bio-Rad) according to the manufacturer's instructions. Proteins were precipitated by adding trichloroacetic acid (TCA) to the final concentration of 10%, incubated on ice for 30 min, pelleted by centrifugation, and then washed with ice-cold 80% acetone. Dried protein pellets were then resuspended in the SDS-PAGE sample buffer and the pH was adjusted to neutral using 2 M Tris/HCl (pH 8.8). The samples were boiled for 5 min at 63°C, centrifuged for 30 sec at 16,000 x g, loaded onto a 7.5%, 10%, 12.5% or 16% gel and resolved by SDS-PAGE. Following an overnight incubation of the gels in 50% methanol,

proteins were visualized by silver staining using the mass spectrometry-compatible silver staining kit (Bio-Rad Silver Staining Plus) according to the manufacturer's instructions. The Bio-Rad unstained molecular marker and a 0.1 mg/ml solution of BSA in the SDS-PAGE sample buffer were also subjected to SDS-PAGE. The proteins were then visualized by silver staining.

**Analysis of proteins by mass spectrometry**

Proteins were resolved by SDS-PAGE and visualized by silver staining [254]. Protein bands were excised from the gel, reduced, alkylated and in-gel digested with trypsin [254]. The proteins were identified by matrix-assisted laser desorption/ionization mass spectrometric (MALDI MS) peptide mapping [255], using a Micromass M@LDI time-of-flight (TOF) mass spectrometer (Waters). Database searching using peptide masses was performed with the Mascot web-based search engine. For evaluating relative levels of individual proteins recovered in total cell lysates or purified mitochondria, a selected protein band was excised from the silver-stained gel and placed into an Eppendorf tube. A band of BSA containing 2 μg of this protein, which was also excised from the silver-stained gel, was added to each of the protein bands to be analyzed. Protein bands were reduced, alkylated and in-gel digested with trypsin [254]. The desalted peptide mixture was added to the surface of a MALDI target plate and allowed to air dry. The sample spot was then overlaid with MALDI matrix solution containing the Angiotensin I peptide standard (1:1 ratio). The presence of Angiotensin I in the sample carrying the analyzed mixture of peptides provided an additional estimate of the mass measurement accuracy after calibration, giving an opportunity to calculate the value of peptide mass tolerance

for each individual mass spectrum. After the desalted peptide mixture was analyzed by MALDI-TOF, the monoisotopic masses of recovered BSA peptides and the intensities of their monoisotopic peaks were grouped separately from the masses and intensities of peptides originated from the protein of interest. These data provided an additional estimate of the mass measurement accuracy and were used for the quantitation of relative levels of the same protein recovered in different samples. For evaluating relative levels of the protein of interest found in the samples to be compared, a ratio "the intensity of the monoisotopic peak of a peptide originated from the protein of interest/the intensity of the monoisotopic peak of a BSA peptide with the monoisotopic mass closest to the mass of the peptide of interest" was calculated for each peptide originated from the protein of interest. Based on these data, the average value for relative levels of the protein of interest found in the two compared samples was calculated. The method for evaluating relative levels of the protein of interest recovered in different samples was validated by calculating relative levels of several standard proteins in the samples supplemented with different quantities of each of these proteins.

## 3.4 Results

### 3.4.1 My rationale for choosing a mutant strain and growth conditions to screen compound libraries for anti-aging small molecules

To perform a chemical genetic screen for small molecules that increase the CLS of yeast by targeting lipid metabolism, I chose the single-gene-deletion mutant strain *pex5Δ*. Because *pex5Δ* lacks a cytosolic shuttling receptor for peroxisomal import of

Fox1p and Fox2p, these two enzymes of the β-oxidation of FFA reside in the cytosol of *pex5Δ* cells [309] (Figure 3.1A). In contrast, the Pex5p-independent peroxisomal import of Fox3p, the third enzyme of the FFA β-oxidation pathway, sorts it to the peroxisome in *pex5Δ* cells [309]. By spatially separating Fox1p and Fox2p from Fox3p within a cell, the *pex5Δ* mutation impairs FFA oxidation (Figure 3.1A). In chronologically aging yeast grown under CR conditions on 0.2% or 0.5% glucose, peroxisomal FFA oxidation regulates longevity by 1) efficiently generating acetyl-CoA to synthesize the bulk of ATP in mitochondria; and 2) acting as a rheostat that modulates the age-related dynamics of FFA and diacylglycerol (DAG), two regulatory lipids known to promote longevity-defining cell death [24, 246, 278, 310]. Unlike CR yeast, chronologically aging non-CR yeast grown on 1% or 2% glucose are unable to generate significant quantities of ATP by oxidizing peroxisome-derived acetyl-CoA in mitochondria and, instead, produce the bulk of ATP via glycolytic oxidation of glycogen- and trehalose-derived glucose [24, 246, 278]. Consistent with the essential role of peroxisomal FFA oxidation as a longevity assurance process only under CR, the *pex5Δ* mutation substantially shortened the CLS of CR yeast but caused a significantly lower reduction of longevity in non-CR yeast, especially in yeast grown on 2% glucose (Figures 3.1B - 3.1F).

In chronologically aging CR yeast, peroxisomal FFA oxidation modulates, perhaps via several negative feedback loops, the following three processes: 1) the ER-confined biosynthesis of TAG from FFA and DAG; 2) the subsequent deposition of TAG, the major neutral lipid reserves, in lipid bodies; and 3) the consequent lipolysis of deposited TAG and the resulting formation of FFA and DAG [24, 246, 278]. By impairing the ability of peroxisomal FFA oxidation to act as a rheostat that regulates

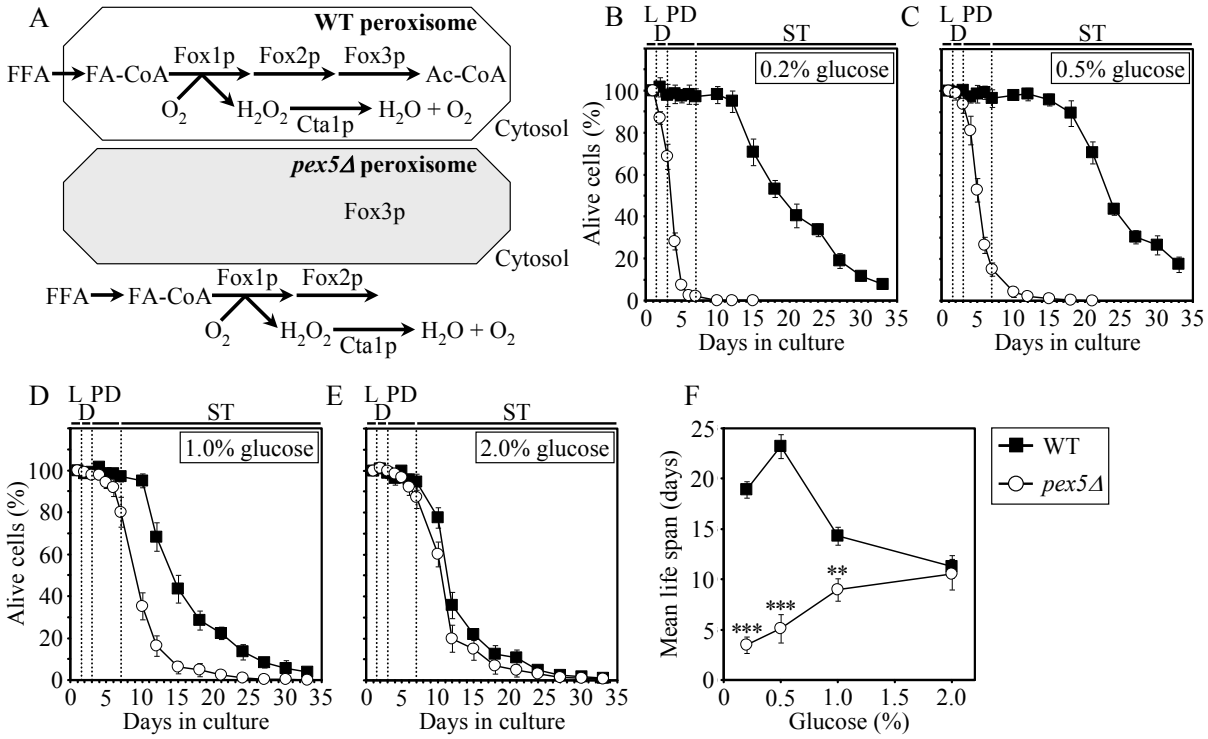


**Figure 3.1.** The *pex5Δ* mutation shortens chronological life span (CLS). (A) Outline of subcellular localization of the Fox1p, Fox2p and Fox3p enzymes of fatty acid ß-oxidation in WT and *pex5Δ* cells. (B - F) Survival and the mean life spans of chronologically aging WT and *pex5Δ* yeast cultured in medium initially containing 0.2%, 0.5%, 1% or 2% glucose. Data are presented as means ± SEM (n = 16-38; ***p < 0.001; **p < 0.01). Abbreviations: Cta1p, peroxisomal catalase; D, diauxic growth phase; FA-CoA, CoA esters of fatty acids; L, logarithmic growth phase; PD, post-diauxic growth phase; ST, stationary growth phase.

cellular aging by modulating the age-related dynamics of FFA, DAG and TAG in the ER and lipid bodies, the *pex5Δ* mutation has been found to cause the accumulation of the closely apposed ER membranes and ER-originated lipid bodies in CR yeast [24]. Noteworthy, these morphological features of *pex5Δ* yeast under CR were similar to those observed in a mouse model for the peroxisome biogenesis disorder Zellweger syndrome with hepatocyte-specific elimination of the *PEX5* gene [311]. Furthermore, it has been

demonstrated that the *pex5Δ* mutation 1) increases the concentrations of FFA, DAG and TAG in CR yeast, promoting their build-up in the ER and lipid bodies; and 2) causes the accumulation of the ER-derived and lipid bodies-deposited ergosteryl esters (EE), neutral lipid species [24]. Moreover, a brief exposure of WT cells grown under CR conditions to exogenous FFA or DAG has been shown to cause their necrotic, not apoptotic, death [24]. Importantly, it has been also demonstrated that the *pex5Δ* mutation enhances the susceptibility of CR yeast to necrotic death caused by a short-term exposure to exogenous FFA or DAG, perhaps due to the increased concentrations of endogenous FFA and DAG seen in *pex5Δ* cells under CR [24].

As I found, in addition to such profound effect of the *pex5Δ* mutation on lipid metabolism and lipid-induced necrotic cell death, this mutation also altered mitochondrial morphology and oxidation-reduction processes in mitochondria of CR yeast. In fact, this mutation caused the fragmentation of a tubular mitochondrial network into individual mitochondria under CR conditions (Figures 3.2A and 3.2B). Furthermore, in CR yeast the *pex5Δ* mutation 1) greatly reduced the rate of oxygen consumption by mitochondria (Figure 3.2C); 2) substantially decreased the mitochondrial membrane potential (Figure 3.2D); and 3) diminished the level of intracellular ROS (Figure 3.2E), known to be generated mostly as by-products of mitochondrial respiration [75, 276]. Interestingly, all these mitochondrial abnormalities in *pex5Δ* yeast under CR were reminiscent of changes in mitochondrial morphology and functions seen in mice with hepatocyte-specific elimination of the *PEX5* gene, a model for the peroxisome biogenesis disorder Zellweger syndrome [311].

Besides its profound effect on lipid metabolism, lipid-induced necrosis,

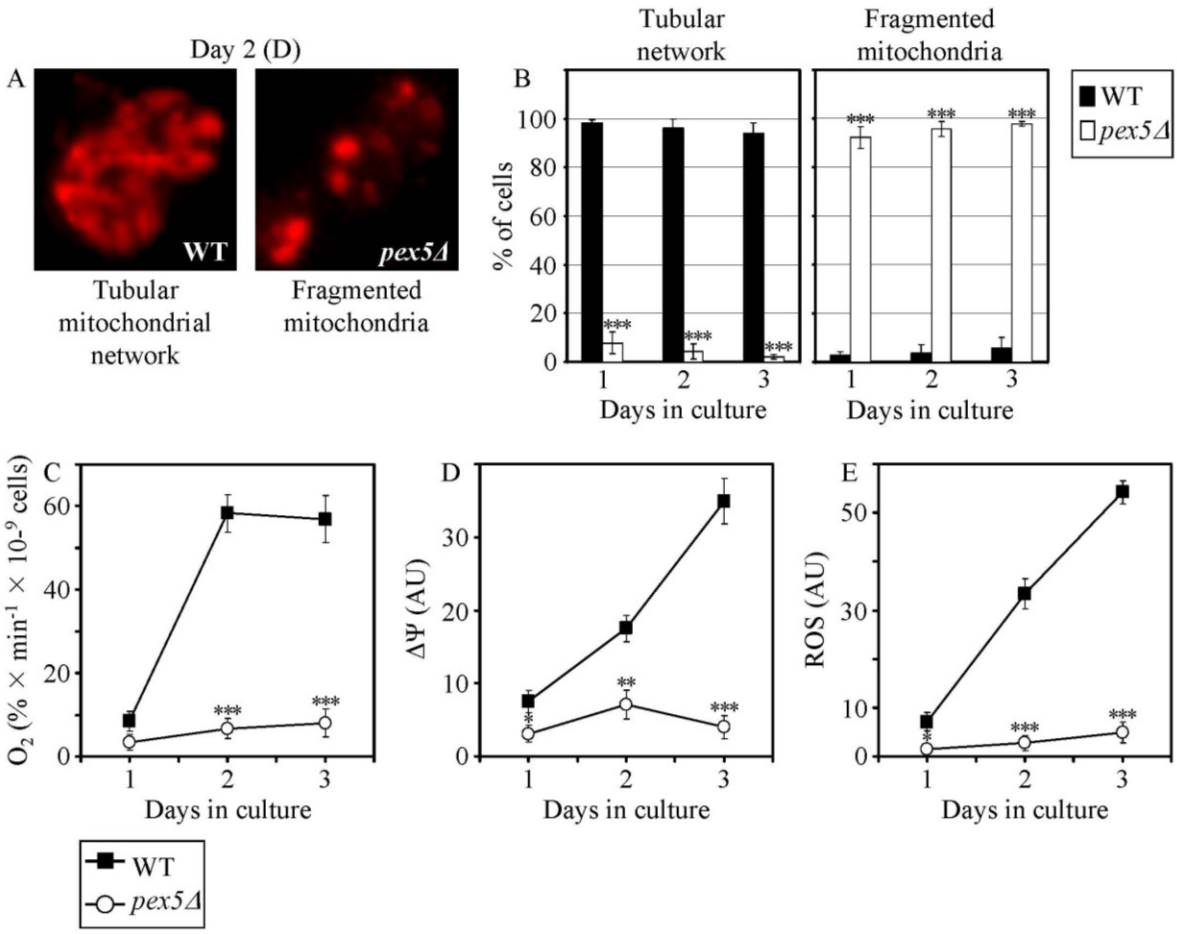


**Figure 3.2.** The *pex5Δ* mutation alters mitochondrial morphology and functions in CR yeast. (A) Morphology of mitochondria in WT and *pex5Δ* cells. Mitochondria were visualized by indirect immunofluorescence microscopy using monoclonal anti-porin primary antibodies and Alexa Fluor 568-conjugated goat anti-mouse IgG secondary antibodies. (B) Percent of WT and *pex5Δ* cells exhibiting a tubular mitochondrial network or fragmented mitochondria. (C - E) Oxygen consumption (C) by WT and *pex5Δ* cells, their mitochondrial membrane potential ΔΨ (D) and their ROS levels (E). ΔΨ and ROS were visualized in living cells by fluorescence microscopy using fluorescent dyes Rhodamine 123 or Dihydrorhodamine 123, respectively. CR yeast grown on 0.2% glucose were taken for analyses at the indicated time-points. Data in B - E are presented as means ± SEM (n = 4-15; ***p < 0.001; **p < 0.01; *p < 0.05). Abbreviation: D, diauxic growth phase.

mitochondrial morphology and functions, the *pex5Δ* mutation also 1) reduced the resistance of chronologically aging CR yeast to chronic oxidative, thermal and osmotic stresses (Figure 3.3A); 2) sensitized CR yeast to death that was initiated in response to a

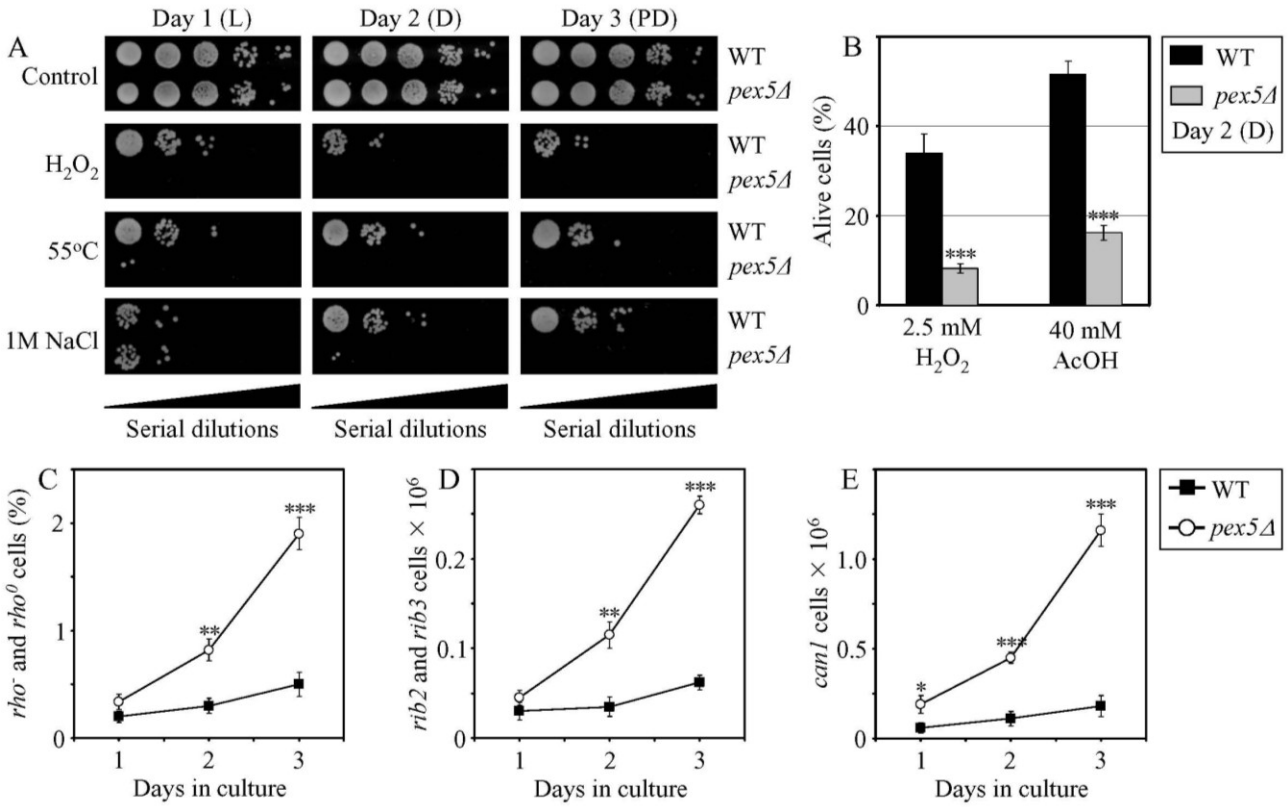


**Figure 3.3.** The *pex5Δ* mutation reduces the resistance of CR yeast to stresses, sensitizes them to exogenously induced apoptosis and elevates the frequencies of mutations in their mitochondrial and nuclear DNA. (A) The resistance of WT and *pex5Δ* to chronic oxidative, thermal and osmotic stresses. (B) Viability of WT and *pex5Δ* cells treated for 1 h with hydrogen peroxide or acetic acid (AcOH) to induce mitochondria-controlled apoptosis. (C - E) The frequencies of *rho-* and *rho0* deletion mutations in mitochondrial DNA (C), *rib2* and *rib3* point mutations in mitochondrial DNA (D), and of *can1* point mutations in nuclear DNA (E) of WT and *pex5Δ* cells. CR yeast grown on 0.2% glucose were taken for analyses at the indicated time-points. Data in B to E are presented as means ± SEM (n = 6-9; ***p < 0.001; **p < 0.01; *p < 0.05). Abbreviations: AcOH, acetic acid; D, diauxic growth phase; L, logarithmic growth phase; PD, post-diauxic growth phase.

short-term exposure to exogenous hydrogen peroxide or acetic acid (Figure 3.3B) and that is known to be caused by mitochondria-controlled apoptosis [312, 313]; and 3) elevated the frequencies of deletion and point mutations in mitochondrial and nuclear DNA of CR yeast (Figures 3.3C to 3.3E).

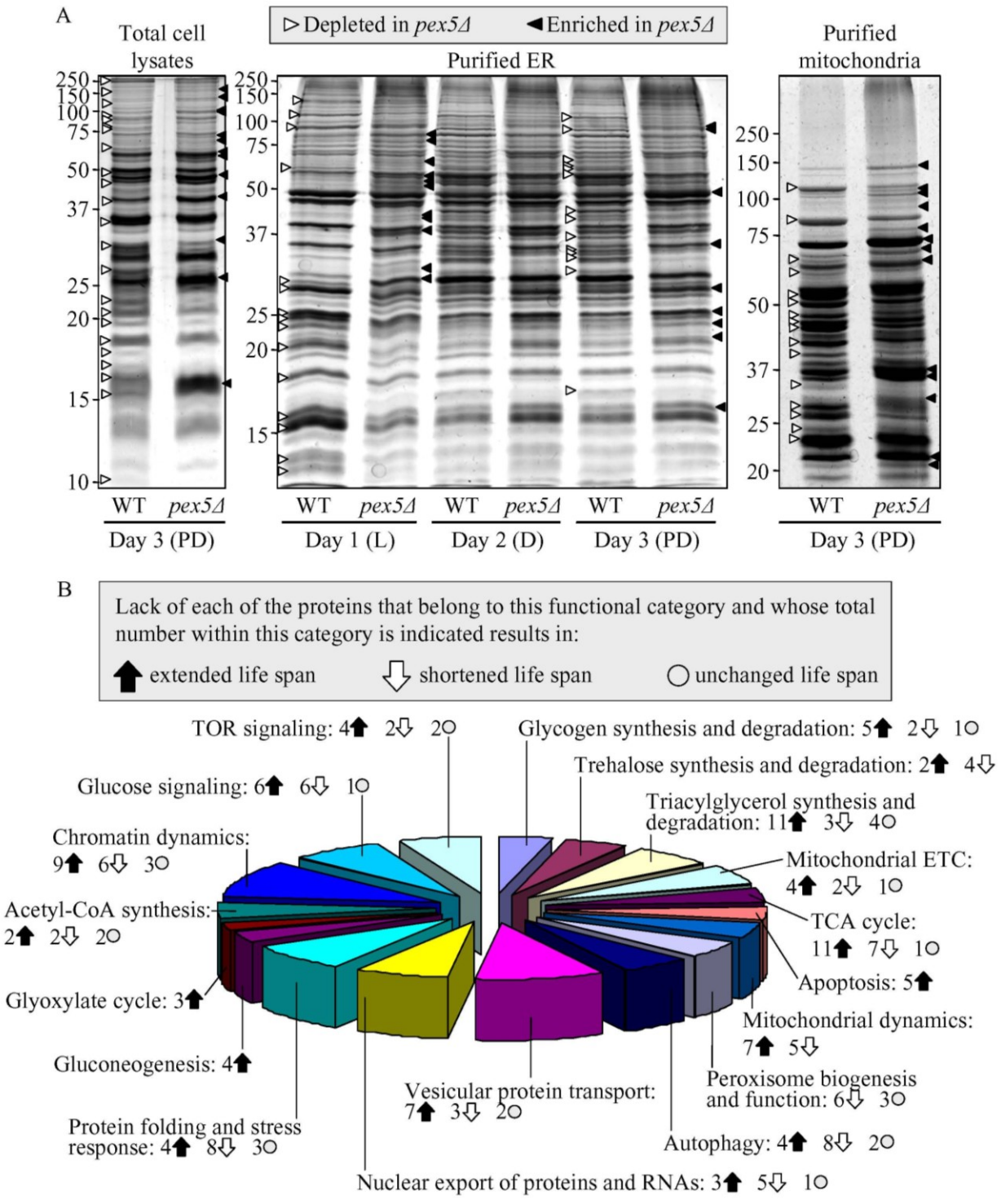


**Figure 3.4.** The *pex5Δ* mutation alters the abundance of many proteins recovered in total cell lysates, purified ER and mitochondria of CR yeast. (A) The spectra of proteins recovered in total cell lysates, purified ER and mitochondria of WT and *pex5Δ* cells that were grown under CR on 0.2% glucose and taken for analyses at the indicated time-points. (B) Functional categories of proteins that were enriched or

depleted in the total cell lysate, ER and mitochondria of *pex5Δ* cells (as compared to WT cells) under CR conditions. Lack of 91 of these proteins increased the CLS of yeast under CR, suggesting their essential pro-aging role in longevity regulation when calorie supply is limited.

As I found, the profound changes in cell morphology and physiology, stress resistance, susceptibility to lipid-induced necrosis and mitochondria-controlled apoptosis, and stability of nuclear and mitochondrial DNA seen in *pex5Δ* yeast under CR conditions (see above) coincided with considerable changes in their proteome. Indeed, my mass spectrometry-based quantitative proteomic analysis of proteins recovered in total cell lysates as well as in purified ER and mitochondria revealed that the *pex5Δ* mutation altered the abundance of many proteins (Figure 3.4A). Protein species that were depleted or enriched in the total cell lysate, ER and mitochondria of *pex5Δ* yeast grown under CR conditions included proteins involved in a number of cellular processes (Figure 3.4B). Importantly, my unpublished data and unpublished findings of Pavlo Kyryakov, Simon Bourque, Adam Beach, Michelle Tali Burstein and Vincent Richard (all are graduate students in Dr. Titorenko's laboratory) revealed that lack of 91 of these proteins increased the CLS of yeast under CR (Figure 3.4B), suggesting their essential pro-aging role in longevity regulation when calorie supply is limited. Noteworthy, the above graduate students and I together found that 58 of the genes encoding these proteins and termed gerontogenes (*i.e.*, the genes whose mutant alleles extend life span; [79]) have not been previously known as being critical for defining the CLS of yeast. The identities of protein species that were depleted or enriched in *pex5Δ* yeast grown under CR conditions, the extent to which their levels were altered and the names of gerontogenes identified in our functional analysis will be reported elsewhere (Kyryakov *et al.*, manuscript in

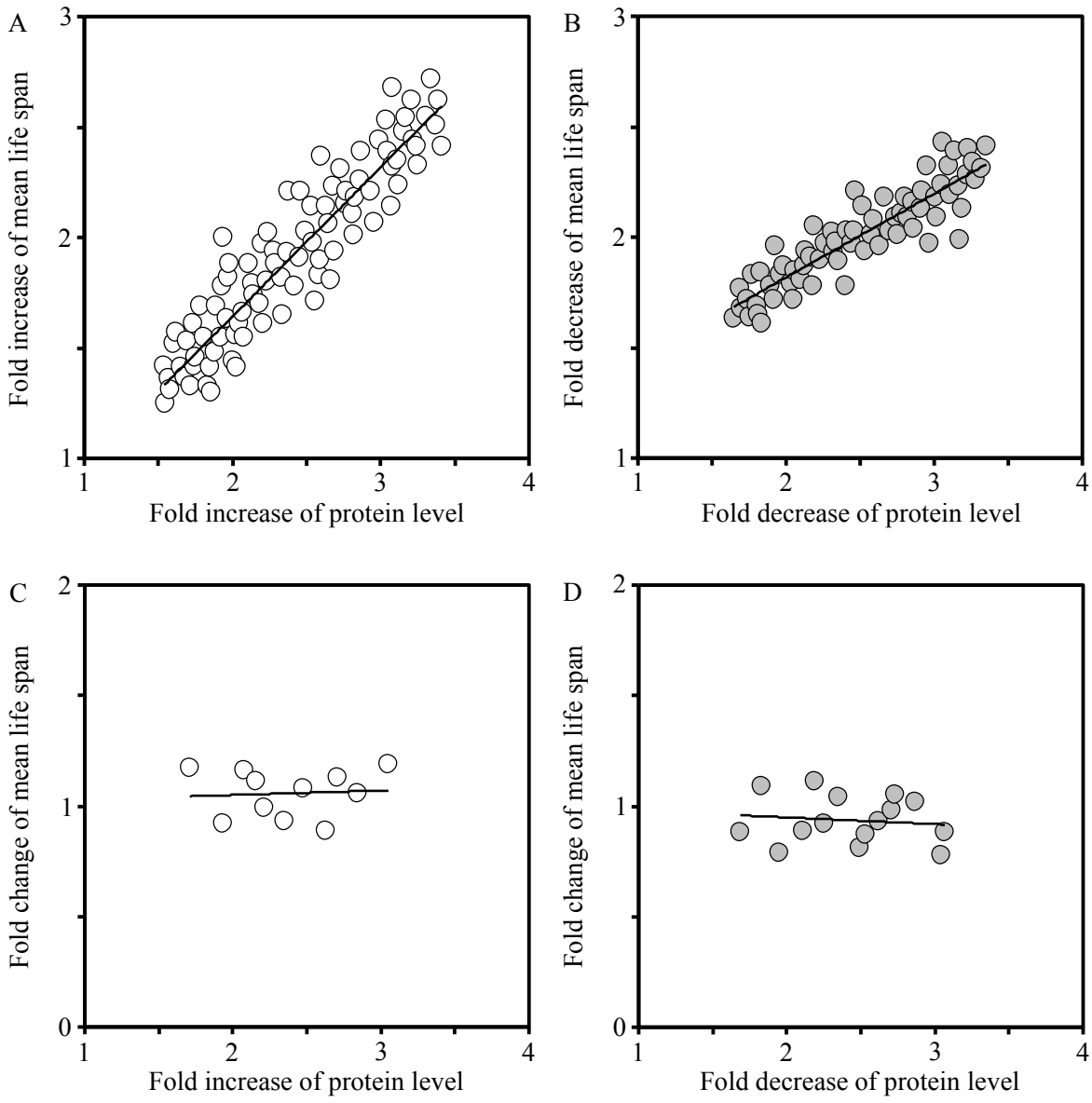


**Figure 3.5.** For many proteins, the fold increase or decrease in the level of a protein enriched or depleted in *pex5Δ* yeast under CR correlates with the fold increase or decrease (respectively) in the mean CLS of a mutant strain lacking it. Plots comparing the fold increase or decrease in the levels of proteins enriched or depleted in *pex5Δ* yeast when calorie supply is limited and the fold increase or decrease (respectively) in the mean CLS of the single-gene-deletion mutant strains that lack these proteins and grow under CR. Each point shows the data for a single protein and a mutant strain that lacks it. Data are presented only for proteins whose levels were increased or decreased by more than 50% in *pex5Δ* cells (as compared to WT cells) grown under CR on 0.2% glucose. Linear regression is shown.

preparation). Importantly, for most of these proteins (with some exceptions, see Figures 3.5C and 3.5D) the fold increase or decrease in the level of a protein enriched or depleted in *pex5Δ* was found to be in good correlation with the fold increase or decrease (respectively) in the mean CLS of a mutant strain lacking it (Figures 3.5A and 3.5B).

Altogether, these findings imply that, by impairing peroxisomal FFA oxidation and affecting lipid metabolism in the ER and lipid bodies, the *pex5Δ* mutation alters the levels of numerous pro- and anti-aging proteins and impacts many longevity-related processes, thereby shortening the CLS of yeast when calorie supply is limited. I therefore chose the short-lived *pex5Δ* strain to carry out a chemical genetic screen for anti-aging compounds that target lipid metabolism to extend CLS in yeast placed on a CR diet.

### 3.4.2 A chemical genetic screen for small molecules that extend the CLS of yeast under CR conditions

To facilitate a high-throughput screen of compound libraries for anti-aging small molecules, I adopted a previously described microplate assay [110] for measuring CLS by monitoring optical density at 600 nm ($OD_{600}$) (Figure 3.6A). In the microplate assay that I developed, a small aliquot of the *pex5Δ* culture grown in a nutrient-rich medium containing 0.5% glucose and recovered from mid-logarithmic phase was transferred into each well of a 96-well master microplate containing the same growth medium and a compound from a commercially available library. At days 1, 7, 10 and 14 of the incubation of master microplates, a small aliquot of each culture was transferred into individual wells of a new (replica) microplate containing growth medium only. Following incubation of replica microplates for 16 hours, the $OD_{600}$ of the culture in each well of the

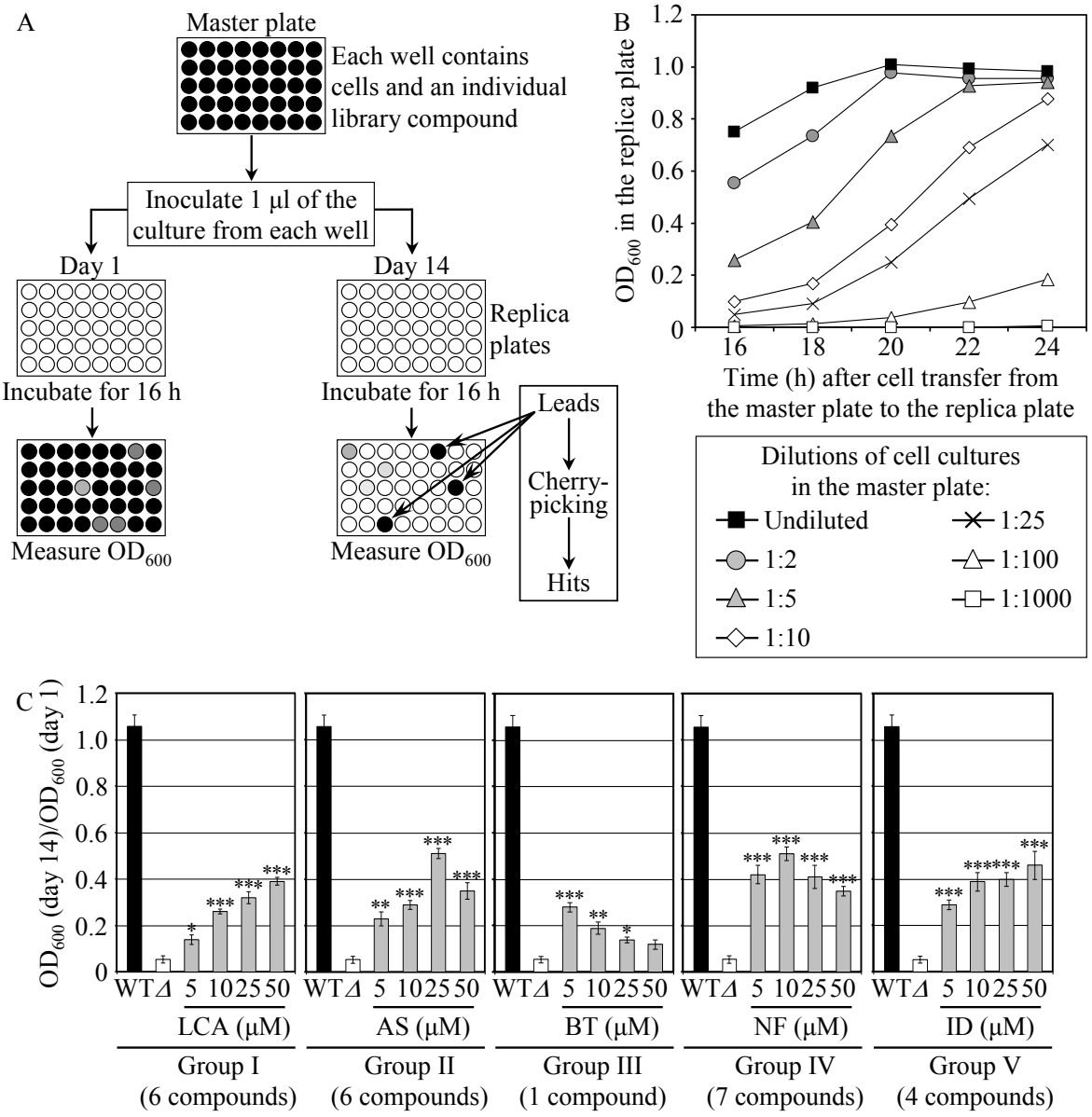


**Figure 3.6.** A high-throughput screen of compound libraries for small molecules that extend the CLS of yeast under CR conditions. (A) A microplate assay for measuring yeast CLS by monitoring optical density at 600 nm ($OD_{600}$) was used for screening representative compounds from several commercial libraries for small molecules that extend the CLS of *pex5Δ* cells grown under CR on 0.5% glucose. (B) The $OD_{600}$ of a cell culture in the replica microplate following incubation for 16 to 24 hours correlates with the number of viable cells present in this culture before it was taken from the master microplate for replica plating. (C) The effect of various concentrations of the identified anti-aging small molecules on the CLS of the *pex5*Δ (Δ) strain under CR conditions. The "$OD_{600}$ at day 14/$OD_{600}$ at day 1" ratio was used as a measure of CLS.

Data are presented as means ± SEM (n = 3-5; ***p < 0.001; **p < 0.01; *p < 0.05). The anti-aging small molecules LCA, AS, BT, NF and ID belong to five chemical groups.

replica microplate was measured. Importantly, I found that under such conditions the $OD_{600}$ of a cell culture in a well of the replica microplate correlates with the number of viable cells in the corresponding well of the master microplate (Figure 3.6B). To calculate survival at each time point, the $OD_{600}$ at a particular time point was divided by the $OD_{600}$ at day 1. By translating my microplate assay into high-throughput format and screening representative compounds from the NIH Clinical Collection, Prestwick Chemical Inc. and Sigma-LOPAC commercial libraries, I identified "lead" compounds. The subsequent "cherry-picking" analysis of these small molecules revealed "hit" compounds that in my microplate assay reproducibly extended the CLS of *pex5Δ*. Using the web-based eMolecules searching engine, I identified commercially available structural analogs of the hit compounds and then tested their life-extending efficacy in the microplate assay that I developed for measuring the CLS of *pex5Δ*. By screening the total of approximately 19,000 representative compounds from seven commercial libraries, I identified 24 small molecules that greatly extend the CLS of *pex5Δ* under CR and belong to 5 chemical groups (Figure 3.6C). Group I consisted of 6 bile acids, including lithocholic acid (LCA), deoxycholic acid (DCA), chenodeoxycholic acid (CDCA), cholic acid (CA), dehydrocholic acid (DHCA) and hyodeoxycholic acid (HDCA) (Figures 3.6C and 3.7). Noteworthy, I found that the anti-aging efficacy of these bile acids correlated with their hydrophobicity. In fact, LCA - the most hydrophobic bile acid species [314] - displayed the highest ability to delay chronological aging of *pex5Δ* under CR conditions in the microplate assay (Figure 3.7). The identities of small molecules that belong to

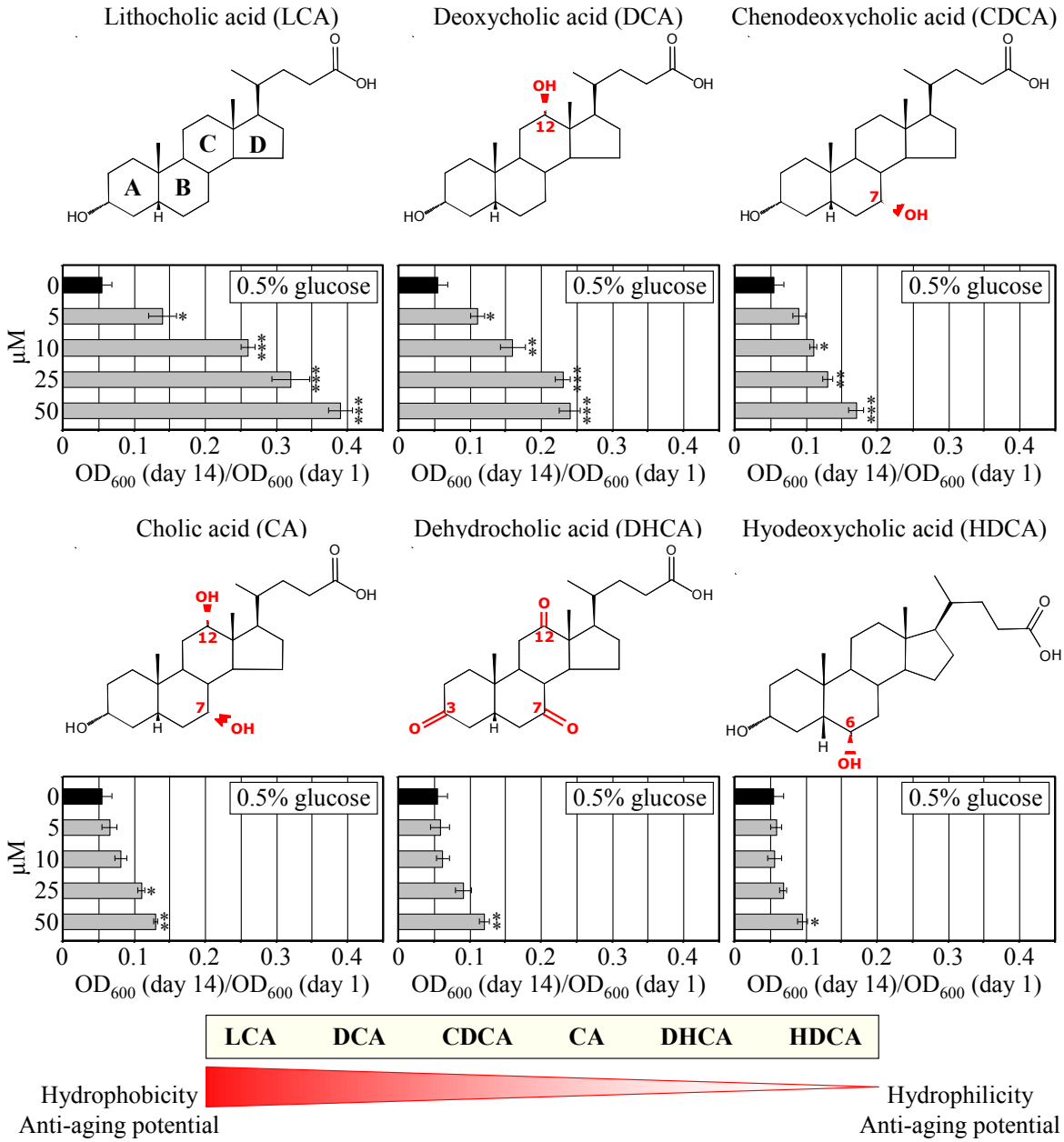


**Figure 3.7.** The life-extending potential of a bile acid correlates with its hydrophobicity. In the microplate assay, lithocholic acid (LCA) - the most hydrophobic bile acid species - displays the greatest ability to extend the CLS of the short-lived *pex5*Δ mutant strain under CR conditions. The effect of various concentrations of different bile acids on the CLS of the short-lived *pex5*Δ mutant strain grown under CR on 0.5% glucose is shown. The "OD600 at day 14/OD600 at day 1" ratio was used as a measure of CLS. Data are presented as means ± SEM (n = 3-5; ***p < 0.001; **p < 0.01; *p < 0.05).

groups II to V (Figure 3.6C) of the anti-aging compounds identified in the high-throughput screen and the structure-activity analysis of their life-extending potential will be reported elsewhere (Richard *et al*., manuscript in preparation).

Noteworthy, I found that none of the small molecules that has been previously shown to extend CLS (*i.e*., caffeine, methionine sulfoximine, rapamycin and spermidine; see chapter 1 of my thesis for a detailed discussion of this topic [101, 110, 134]) and/or RLS (*i.e*., rapamycin and resveratrol; see chapter 1 of my thesis for a detailed discussion of this topic; [56, 119]) in yeast has been identified in my screen for compounds capable of increasing the CLS of *pex5Δ* under CR. Furthermore, none of these currently known life-extending molecules is structurally related to the anti-aging compounds that I revealed. Thus, it is likely that LCA and all other novel anti-aging compounds identified in my screen target longevity-related cellular processes that are not modulated by the presently known anti-aging small molecules.

### 3.4.3 Pharmacophore modeling of the anti-aging potential of bile acids

Similar to their effect on *pex5Δ*, some of the group I anti-aging compounds extended the CLS of WT strain under CR conditions. Specifically, I found that LCA and two other bile acids - DCA and CDCA - increased both the mean and maximum CLS of WT yeast grown under CR on 0.2% glucose (Figures 3.8A to 3.8D). Moreover, DHCA increased only the mean CLS of WT yeast under CR at 0.2% glucose, whereas HDCA increased only their maximum CLS (Figures 3.8A to 3.8D). Akin to its highest life-extending efficacy in *pex5Δ* under CR, the most hydrophobic bile acid - LCA [314] - provided WT cells with the greatest longevity benefit when calorie supply was limited. In

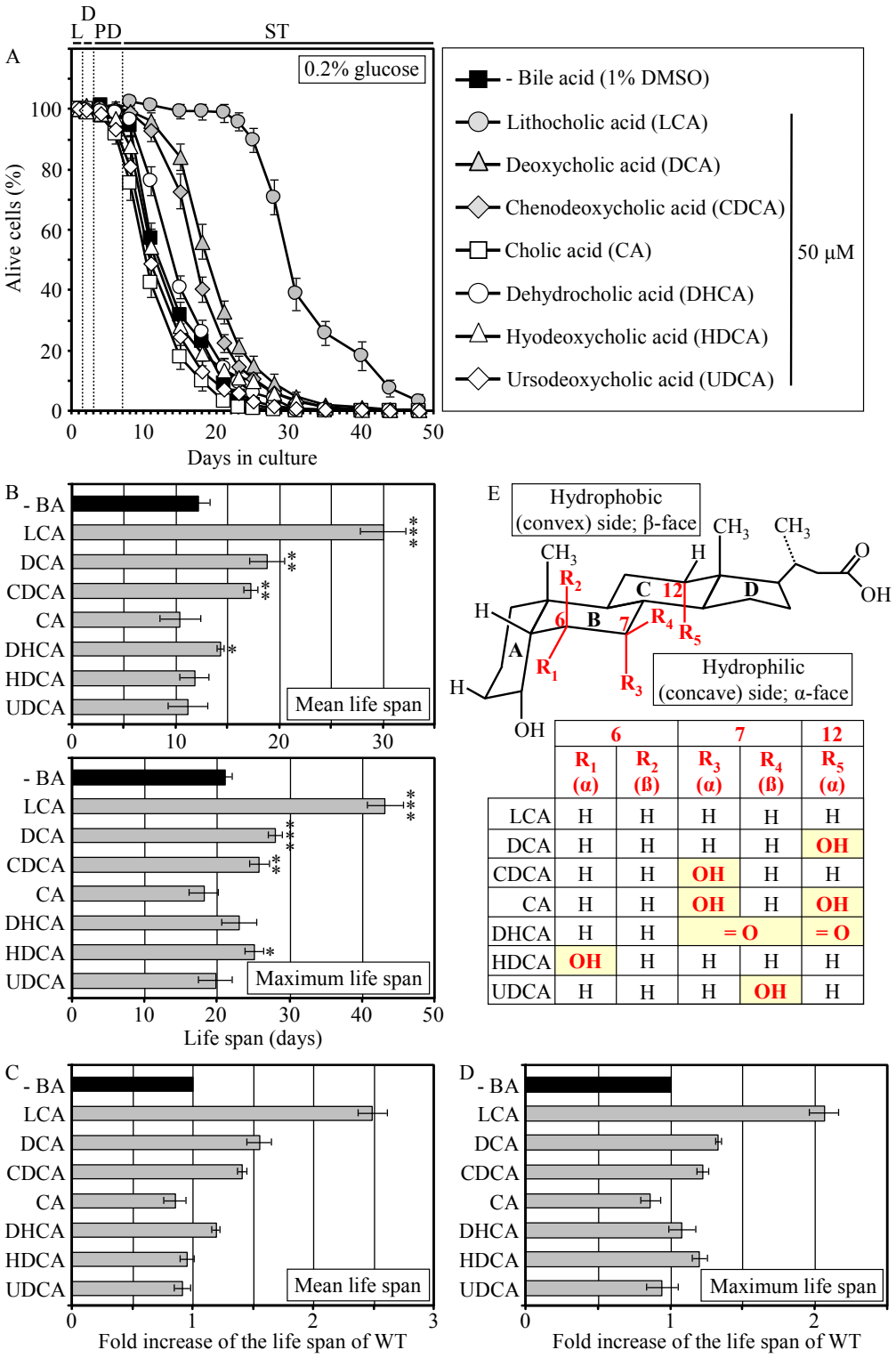


| | 6 | | 7 | | 12 |
|---|---|---|---|---|---|
| | $R_1$ (α) | $R_2$ (ß) | $R_3$ (α) | $R_4$ (ß) | $R_5$ (α) |
| LCA | H | H | H | H | H |
| DCA | H | H | H | H | OH |
| CDCA | H | H | OH | H | H |
| CA | H | H | OH | H | OH |
| DHCA | H | H | = O | | = O |
| HDCA | OH | H | H | H | H |
| UDCA | H | H | H | OH | H |

**Figure 3.8.** LCA and some other bile acids extend the CLS of WT strain under CR conditions. (A - D) Effect of various bile acids on survival (A) and on the mean and maximum life spans (B - D) of chronologically aging WT strain grown under CR conditions on 0.2% glucose. Data are presented as means

± SEM (n = 3-28; ***p < 0.001; **p < 0.01; *p < 0.05). (E) Structure and hydrophilic/hydrophobic properties of bile acids. The R1 (α), R3 (α) and R5 (α) hydroxyl groups at the positions 6, 7 and 12 in the six-member rings B and C of the steroid nucleus increase polarity of the hydrophilic (concave) side [α-face] of the nucleus by being located below the nucleus and axially to its plane. The R4 (β) hydroxyl group at the position 7 in the six-member ring B of the steroid nucleus confers polarity of the hydrophobic (convex) side [β-face] of the nucleus by being located above the nucleus and equatorially to its plane.

fact, I found that LCA increased the mean CLS of WT strain under CR at 0.2% glucose by almost 250% and its maximum CLS by more than 200% (Figures 3.8A - 3.8D). My comparative analysis of the structural differences between various bile acids and their relative life-extending efficacies revealed that the positions 6, 7 and 12 in the six-member rings B and C of the steroid nucleus are important for the anti-aging potential of a bile acid. Indeed, the ability of LCA to extend both the mean and maximum CLS of WT yeast under CR can be: 1) eliminated (with respect to the mean CLS) or greatly reduced (with respect to the maximum CLS) by attaching an α-oriented hydroxyl group at the position 6 (as in HDCA); 2) greatly reduced (with respect to both the mean and maximum CLS) by attaching an α-oriented hydroxyl group at the position 7 (as in CDCA); and 3) greatly reduced (with respect to both the mean and maximum CLS) by attaching an α-oriented hydroxyl group at the position 12 (as in DCA) (Figures 3.8B to 3.8E). All these modifications to the structure of LCA increase polarity of the hydrophilic (concave) side [α-face] of the steroid nucleus by positioning a hydroxyl group below the nucleus and axially to its plane (Figure 3.8E). Furthermore, the anti-aging potential of LCA can be abolished by attaching a β-oriented hydroxyl group at the position 7 (as in UDCA), thereby conferring polarity to the hydrophobic (convex) side [β-face] of the steroid nucleus by positioning a hydroxyl group above the nucleus and equatorially to its plane (Figures 3.8B to 3.8E). Moreover, the simultaneous attachments of two α-oriented

hydroxyl groups (as in CA) or two keto groups (as in DHCA) at the positions 7 and 12 eliminated the ability of LCA to extend both the mean and maximum CLS of WT yeast under CR (Figures 3.8B to 3.8E).

Altogether, the results of my pharmacophore modeling of the anti-aging potential of bile acids imply that the maintenance of the minimal polarity of both the hydrophilic (concave) and hydrophobic (convex) sides of the steroid nucleus - by avoiding the presence of polar substituents at the positions 6, 7 and 12 - is mandatory for the extreme life-extending efficacy of LCA under CR conditions. Such stringent structural requirements are consistent with a target specificity of LCA action as an anti-aging small molecule.

### 3.4.4 LCA extends the CLS of WT yeast under both CR and non-CR conditions, although to a different extent

I found that, if added to growth medium at the time of cell inoculation, LCA increased both the mean and maximum CLS of WT strain not only under CR at 0.2% or 0.5% glucose (Figures 3.9A, 3.9B and 3.9G – 3.9I) but also under non-CR conditions administered by culturing yeast in medium initially containing 1% or 2% glucose (Figures 3.9C, 3.9D and 3.9G - 3.9I). At any tested concentration of glucose in growth medium, LCA displayed the greatest beneficial effect on both the mean and maximum CLS of WT strain if used at a final concentration of 50 μM (Figures 3.9E and 3.9F). It should be stressed that the life-extending efficacy of 50 μM LCA under CR exceeded that under non-CR conditions, being inversely proportional to the concentration of glucose in growth medium and thus in correlation with the extent of calorie supply limitation

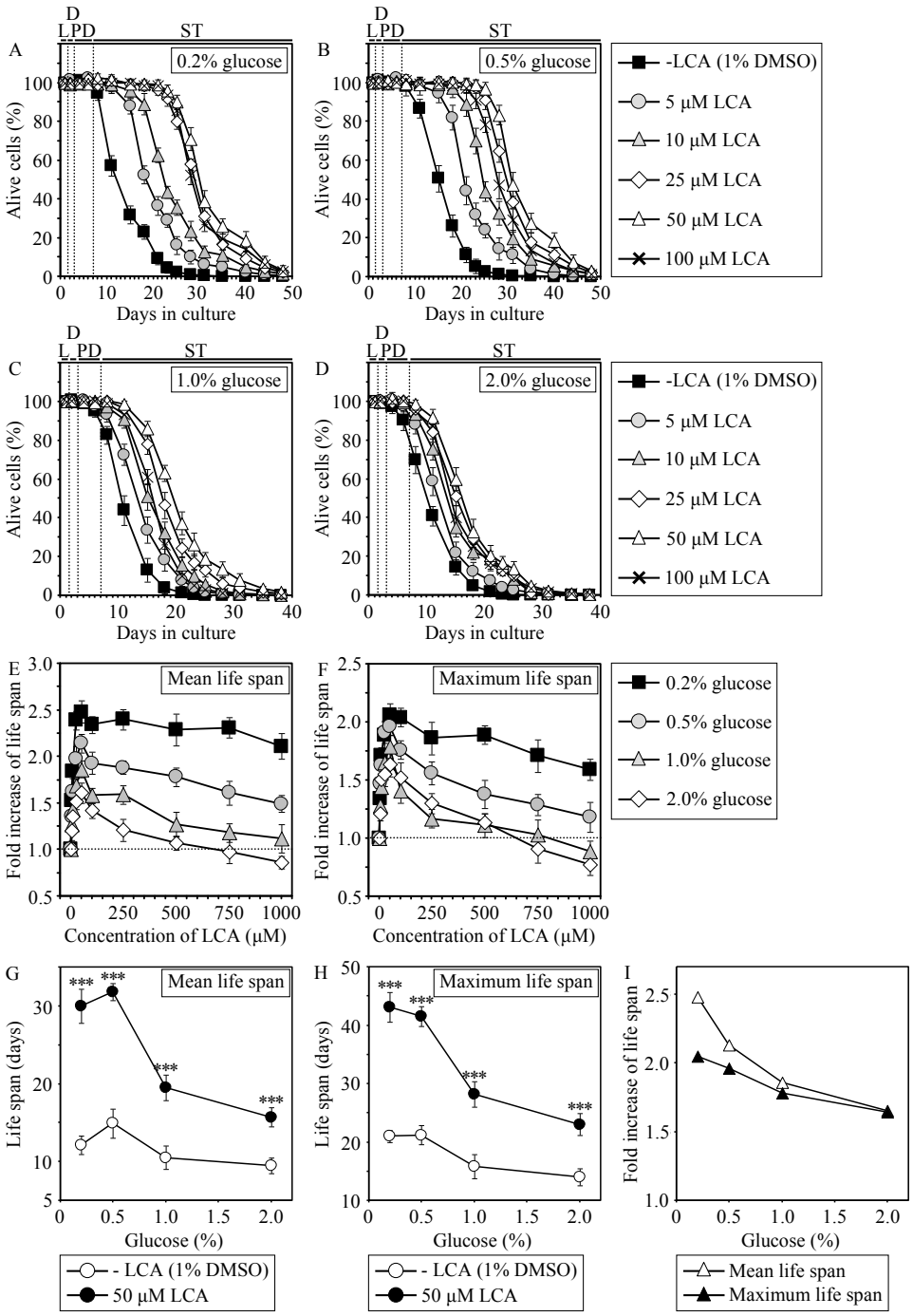


**Figure 3.9.** In chronologically aging WT yeast, the life-extending efficacy of LCA under CR exceeds that under non-CR conditions. (A - F) Effect of various concentrations of LCA on survival (A - D) and on the fold increase in the mean (E) or maximum (F) life span of chronologically aging WT strain cultured in medium initially containing 0.2%, 0.5%, 1% or 2% glucose. Data are presented as means ± SEM (n = 3-28). (G - I) Effect of 50 μM LCA on the mean or maximum CLS of WT yeast cultured in medium initially containing 0.2%, 0.5%, 1% or 2% glucose. Data are presented as means ± SEM (n = 12-28; ***$p < 0.001$).

(Figures 3.9G to 3.9I). Importantly, although 50 μM LCA displayed a profound effect on CLS, it did not cause significant changes in growth of WT strain at any tested concentration of glucose in medium. In fact, I found that both growth rate in logarithmic phase and time prior to entry into stationary (ST) phase were similar for WT cells cultured in medium with or without LCA (Figure 3.10).

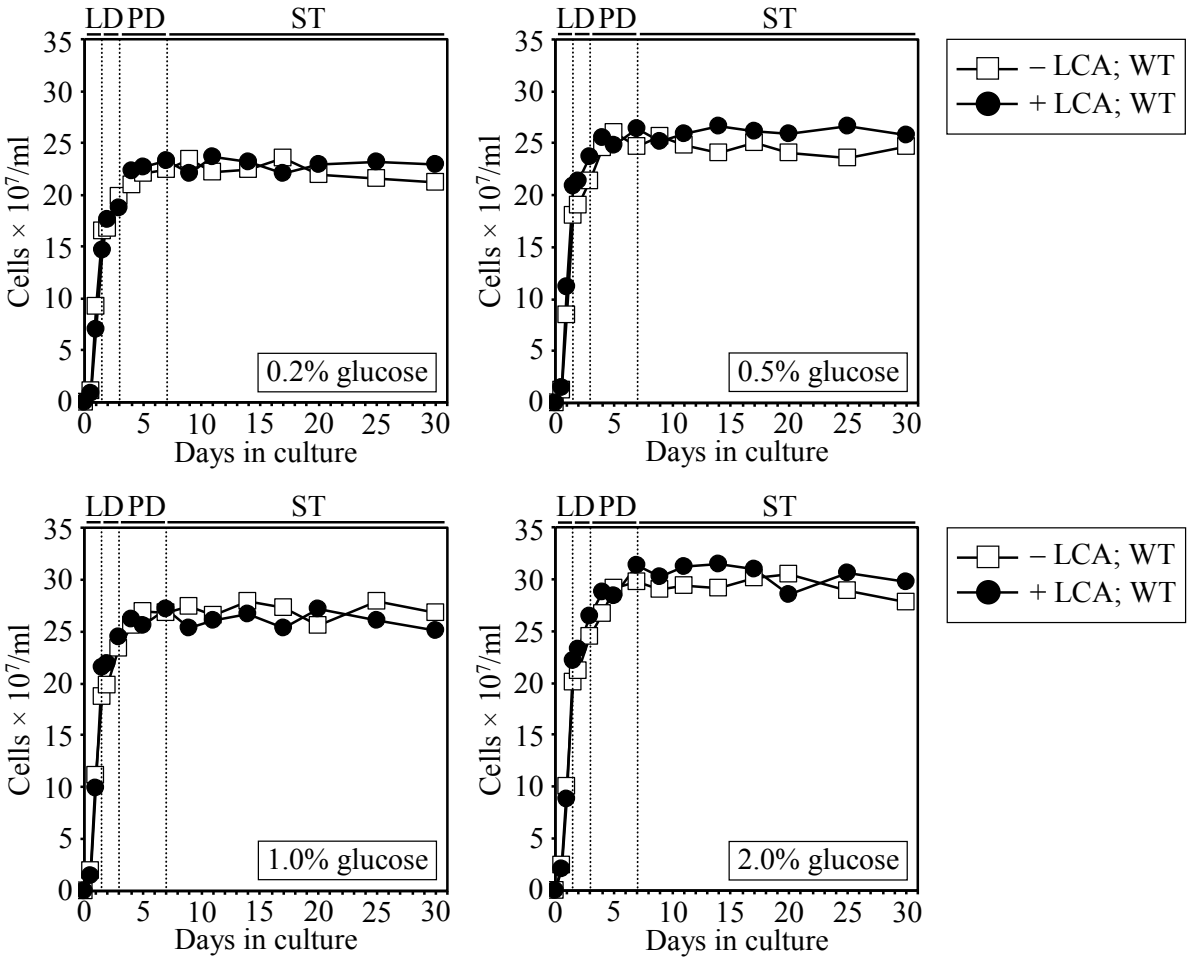


**Figure 3.10.** LCA does not cause significant changes in growth pattern of wild-type (WT) strain at any tested concentration of glucose in medium. Kinetics of growth for WT strain in medium initially containing 0.2%, 0.5%, 1.0% or 2.0% glucose in the presence of LCA (50 μM ) or in its presence. Each plot shows a representative experiment repeated 4-7 times in triplicate with similar results. Abbreviations: D, diauxic growth phase; L, logarithmic growth phase; PD, post-diauxic growth phase; ST, stationary growth phase.

### 3.4.5 LCA extends the CLS of WT yeast under CR by modulating several longevity-related processes

My chemical genetic screen identified LCA as a compound that under CR conditions extends the CLS of *pex5Δ*, a prematurely aging mutant strain displaying profound changes in lipid metabolism, lipid-induced necrotic cell death, mitochondrial morphology and functions, stress resistance, mitochondria-controlled apoptosis, and stability of nuclear and mitochondrial DNA (see sections 3.4.1 and 3.4.2 of my thesis). I found that LCA also greatly increases the mean and maximum CLS of WT yeast limited in calorie supply (see sections 3.4.3 and 3.4.4 of my thesis). This finding prompted me and other graduate students in Dr. Titorenko's laboratory to investigate how the exposure of WT cells to LCA under CR conditions influences a compendium of longevity-related processes impaired in *pex5Δ*.

As Simon Bourque (a graduate student in Dr. Titorenko's laboratory) has shown, in chronologically aging WT yeast that reached reproductive maturation by entering into ST phase under CR conditions on 0.2% glucose, LCA 1) elevated the concentration of TAG; 2) substantially reduced the intracellular levels of FFA and DAG; and 3) greatly reduced the susceptibility of these yeast cells to necrotic cell death that was caused by a short-term exposure to exogenous FFA or DAG [24, 246].

I found that the exposure of reproductively mature WT cells to LCA under CR conditions also influenced other longevity-related processes impaired in *pex5Δ*, including those confined to mitochondria. Indeed, in WT cells that entered the non-proliferative ST phase under CR at 0.2% glucose, LCA 1) attenuated the fragmentation of a tubular mitochondrial network into individual mitochondria (Figure 3.11A); 2) elevated the rate

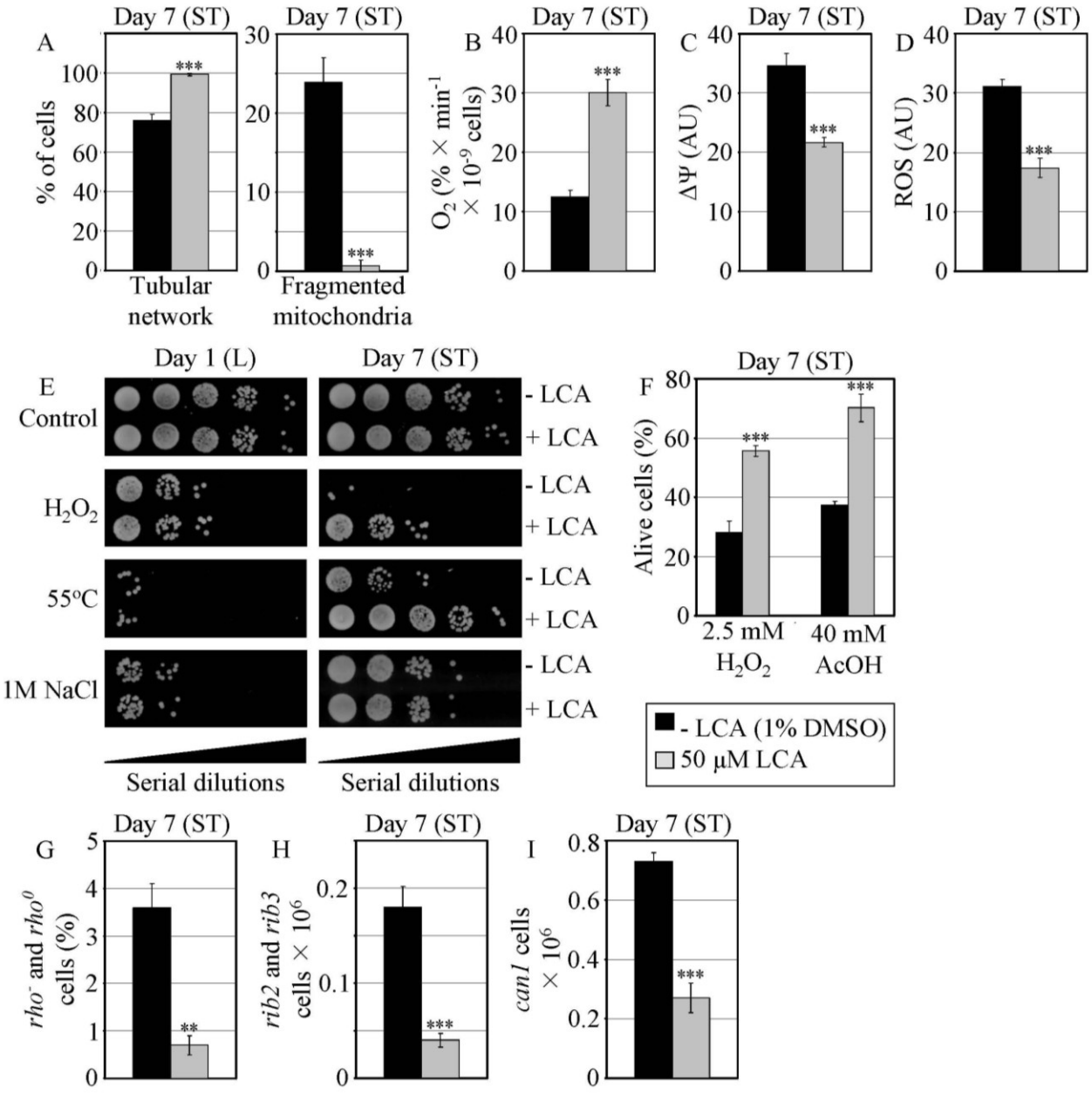


**Figure 3.11.** In reproductively mature WT yeast that entered the non-proliferative stationary (ST) phase under CR, LCA modulates mitochondrial morphology and functions, enhances stress resistance, attenuates mitochondria-controlled apoptosis, and increases stability of nuclear and mitochondrial DNA. (A) Percent of WT cells grown in medium with or without LCA and exhibiting a tubular mitochondrial network or fragmented mitochondria. Mitochondria were visualized by indirect immunofluorescence microscopy using monoclonal anti-porin primary antibodies and Alexa Fluor 568-conjugated goat anti-mouse IgG secondary antibodies. (B - D) Oxygen consumption by WT cells grown in medium with or without LCA (B), their mitochondrial membrane potential ΔΨ (C) and their ROS levels (D). ΔΨ and ROS were visualized in living cells by fluorescence microscopy using fluorescent dyes Rhodamine 123 or Dihydrorhodamine 123,

respectively. (E) The resistance of WT cells pre-grown in medium with or without LCA to chronic oxidative, thermal and osmotic stresses. (F) Viability of WT cells pre-grown in medium with or without LCA and then treated for 1 h with hydrogen peroxide or acetic acid (AcOH) to induce mitochondria-controlled apoptosis. (G - I) The frequencies of *rho*$^{-}$ and *rho*$^{0}$ mutations in mitochondrial DNA (G), *rib2* and *rib3* mutations in mitochondrial DNA (H), and of *can1* (Can$^{r}$) mutations in nuclear DNA (I) of WT cells grown in medium with or without LCA. Data in A - D and F - I are presented as means ± SEM (n = 4-17; ***p < 0.001; **p < 0.01). WT cells grown on 0.2% glucose in the presence or absence of LCA were taken for analyses at day 7, when they reached reproductive maturation by entering into ST phase.

of oxygen consumption by mitochondria (Figure 3.11B); 3) reduced the mitochondrial membrane potential (Figure 3.11C); and 4) decreased the level of intracellular ROS (Figure 3.11D) known to be generated mainly in mitochondria [276, 277].

Moreover, I also demonstrated that in WT yeast that under CR conditions on 0.2% glucose reached reproductive maturation by entering into ST phase, LCA 1) enhanced cell resistance to chronic oxidative and thermal (but not to osmotic) stresses (Figure 3.11E); 2) reduced cell susceptibility to death triggered by a short-term exposure to exogenous hydrogen peroxide or acetic acid (Figure 3.11F) known to be caused by mitochondria-controlled apoptosis [294, 312]; and 3) decreased the frequencies of deletions and point mutations in mitochondrial and nuclear DNA (Figures 3.11G to 3.11I).

### 3.4.6 LCA extends yeast CLS independent of TOR, by modulating housekeeping longevity assurance pathways

My chemical genetic screen was aimed at identifying small molecules that can increase the CLS of yeast under CR by modulating housekeeping longevity pathways. Such pathways may regulate yeast longevity irrespective of the number of available

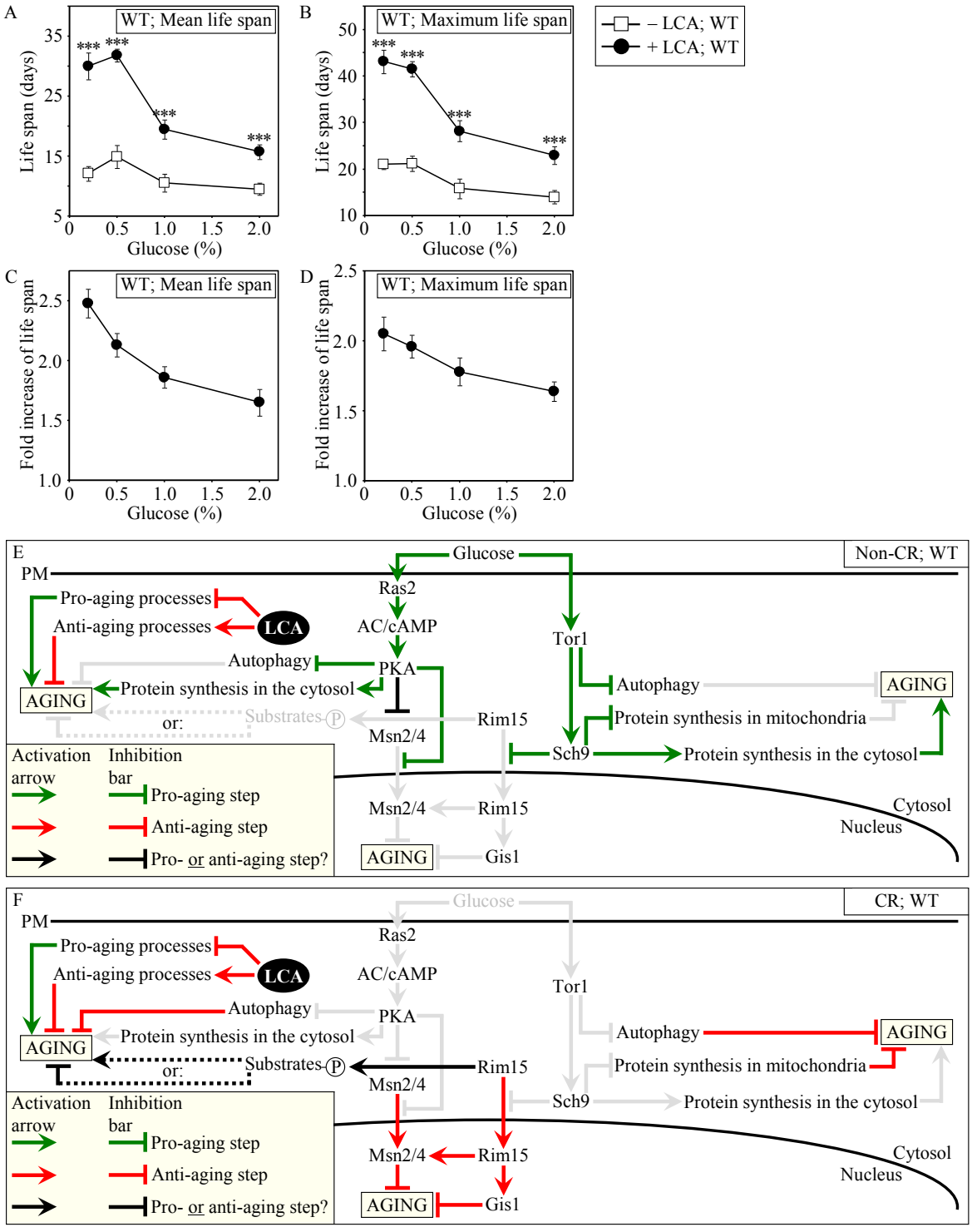


**Figure 3.12.** LCA increases the CLS of WT strain to the highest extent under CR conditions. (A and B) Effect of LCA on the mean (A) and maximum (B) life spans of chronologically aging WT strain. Data are presented as means ± SEM (n = 12-28; ***p < 0.001). (C - E) Effect of LCA on the fold increase in the mean (C) or maximum (D) life span of chronologically aging WT strain. Data are presented as means ±

SEM (n = 12-28). Cells in A to D were cultured in medium initially containing 0.2%, 0.5%, 1% or 2% glucose in the presence of LCA (50 μM) or in its absence. Survival data are provided in Figure 3.13 below. (E and F) Outline of pro- and anti-aging processes that are controlled by the TOR and/or cAMP/PKA signaling pathways and are modulated by LCA in WT cells grown under non-CR (E) or CR (F) conditions. Activation arrows and inhibition bars denote pro-aging processes (displayed in green color), anti-aging processes (displayed in red color) or processes whose role in longevity regulation is presently unknown (displayed in black color). Doted lines denote hypothetical processes. Abbreviations: PM, plasma membrane.

calories and may not necessarily overlap (or may only partially overlap) with the adaptable longevity pathways that are under the stringent control of calorie availability. In chronologically aging yeast, the TOR and cAMP/PKA signaling pathways are the two adaptable longevity pathways that govern the life-extending effect of CR (Figure 3.16A) [10, 35, 44, 45, 58]. Reduction of the Tor1p protein kinase activity in yeast placed on a CR diet or exposed to rapamycin prevents inhibitory phosphorylation of Atg13p, a key positive regulator of autophagy, thereby activating this essential anti-aging process (Figure 3.16A) [315, 316]. Under CR conditions or in response to rapamycin, Tor1p is also unable to phosphorylate and activate the nutrient-sensory protein kinase Sch9p [44, 317]. The resulting inhibition of the Sch9p kinase activity suppresses its ability to attenuate protein synthesis in mitochondria, thus turning on this essential anti-aging process [45]. Furthermore, by inhibiting the Sch9p kinase activity, CR restrains Sch9p from activating protein synthesis in the cytosol, thereby slowing down this essential pro-aging process [44, 58, 317]. Moreover, the attenuation of the Sch9p kinase activity in CR yeast prevents the retention of Rim15p in the cytosol, hence allowing this nutrient-sensory protein kinase to enter the nucleus where it orchestrates an anti-aging transcriptional program by activating the stress response transcriptional activators Msn2p,

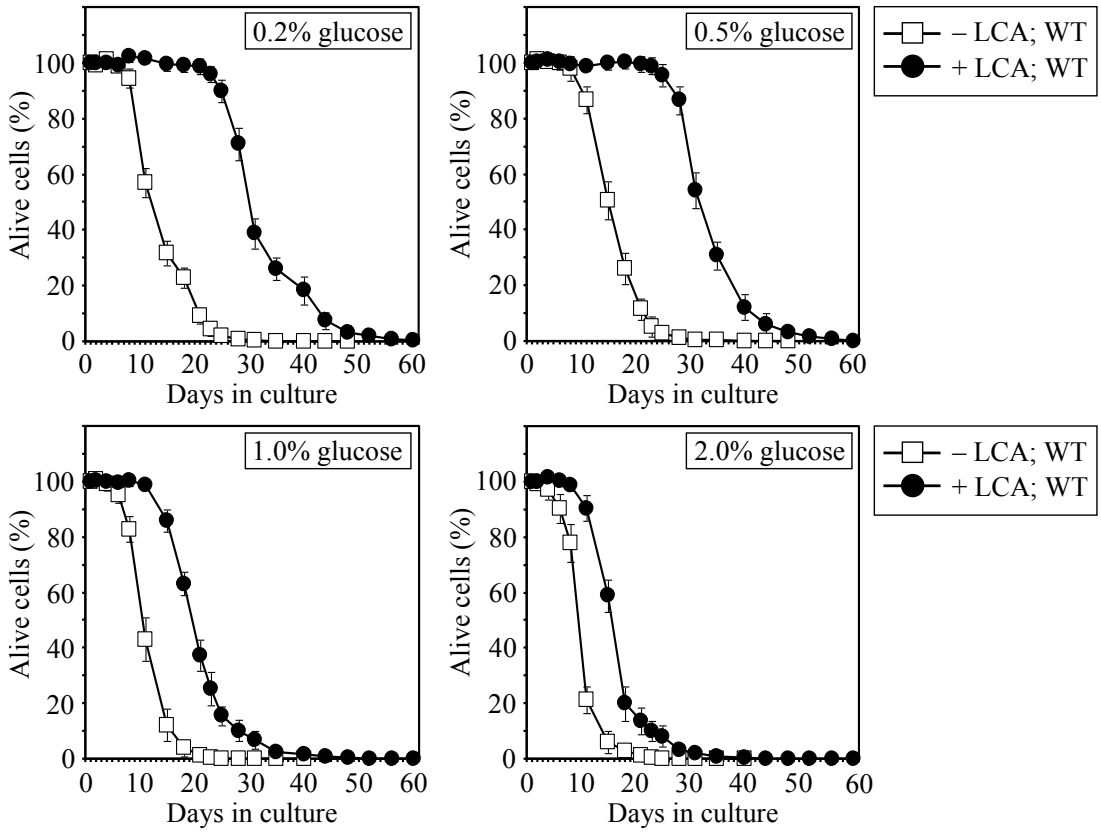


**Figure 3.13.** Chronological survival data for WT strain cultured in medium initially containing 0.2%, 0.5%, 1% or 2% glucose in the presence of LCA (50 μM) or in its absence. Dataset for Figure 3.12.

Msn4p and Gis1p [58, 101]. The longevity benefit associated with CR in chronologically aging yeast is also due to the attenuation of signaling through the cAMP/PKA pathway, which is driven by glucose deprivation [10, 35, 58]. By preventing inhibitory phosphorylation of Atg13p, the reduction of the PKA kinase activity in CR yeast results in activation of autophagy (Figure 10A) [315, 318]. In addition, by inhibiting the PKA kinase activity, CR suppresses the ability of PKA to activate protein synthesis in the cytosol [58]. Moreover, reduced PKA kinase activity in CR yeast enables nuclear import of Msn2p and Msn4p, thus turning on an anti-aging transcriptional program driven - in a Rim15p-dependent fashion - by these two transcriptional activators [58, 115, 319].

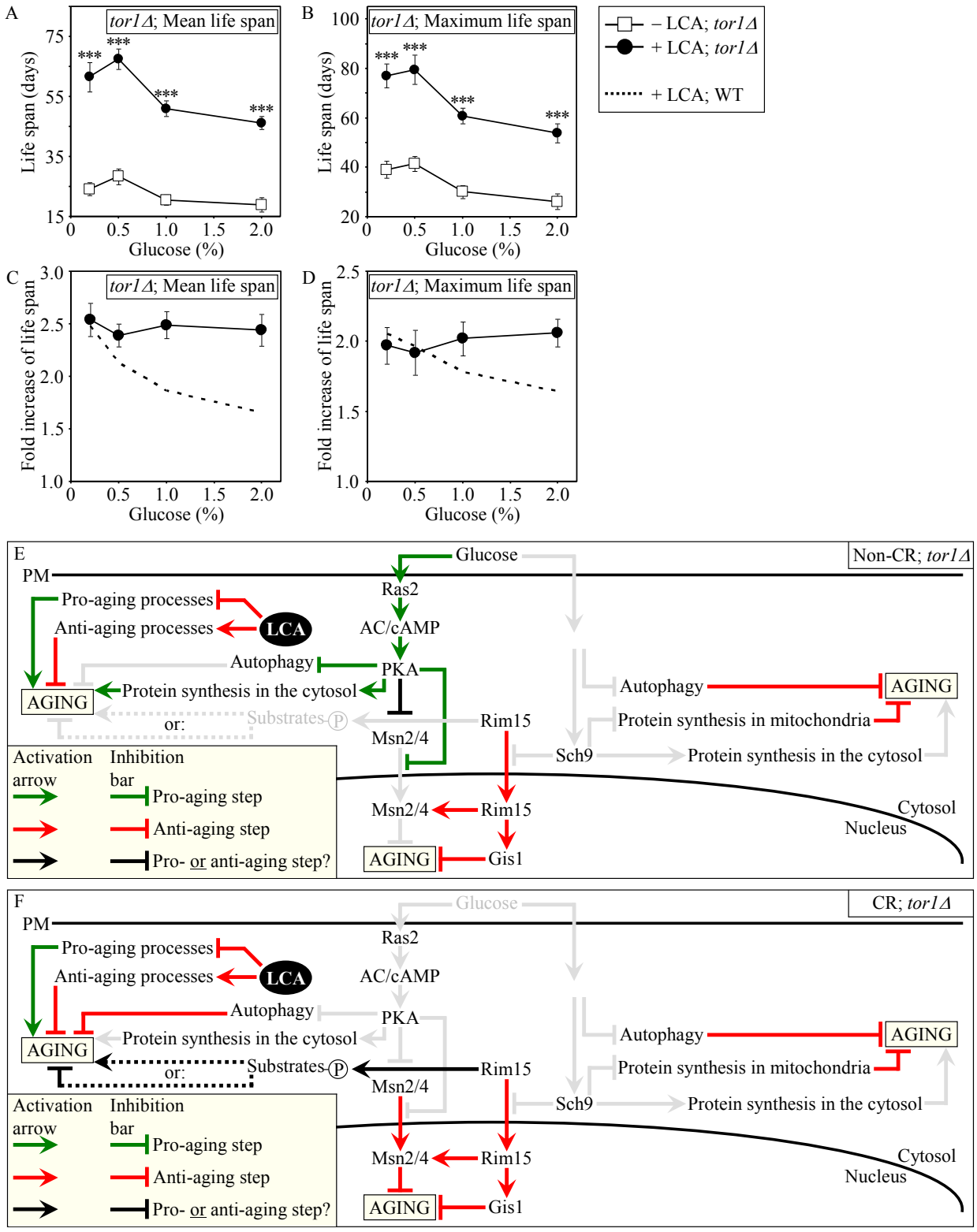


**Figure 3.14.** Lack of Tor1p does not impair the life-extending effect of LCA and abolishes the dependence of the anti-aging efficacy of LCA on the number of available calories. (A and B) Effect of LCA on the mean (A) and maximum (B) life spans of chronologically aging *tor1Δ* strain. Data are presented as means ±

SEM (n = 4-7; ***p < 0.001). (C and D) Effect of LCA on the fold increase in the mean (C) or maximum (D) life spans of chronologically aging *tor1Δ* and WT strains. Data are presented as means ± SEM (n = 4-7). Cells in A to D were cultured in medium initially containing 0.2%, 0.5%, 1% or 2% glucose in the presence of LCA (50 μM) or in its absence. Survival data are provided in Figure 3.15 below. (E and F) Outline of pro- and anti-aging processes that are controlled by the TOR and/or cAMP/PKA signaling pathways and are modulated by LCA in *tor1Δ* cells grown under non-CR (E) or CR (F) conditions.

Noteworthy, the kinase activity of the cytosolic pool of Rim15p is inactivated through PKA-dependent phosphorylation (Figure 3.16A) [58]. Although some of the Rim15p phosphorylation targets are involved in longevity regulation and reside outside the nucleus [320], a role of such phosphorylation in the life-extending effect of CR in yeast remains to be established.

My evaluation of the life-extending efficacy of LCA in WT strain on a high- or low-calorie diet revealed that this compound increased CLS irrespective of the number of available calories (Figures 3.12A and 3.12B). Intriguingly, I found that the extent to which LCA extended longevity was highest under CR conditions (Figures 3.12C and 3.12D), when the pro-aging processes modulated by the adaptable TOR and cAMP/PKA pathways are suppressed and the anti-aging processes are activated (Figure 3.12F). The life-extending efficacy of LCA in CR yeast significantly exceeded that in yeast on a high-calorie diet (Figures 3.12C and 3.12D), in which the adaptable TOR and cAMP/PKA pathways greatly activate the pro-aging processes and suppress the anti-aging processes (Figure 3.12E). Altogether, these findings suggest that, consistent with its sought-after effect on a longevity signaling network, LCA mostly targets certain housekeeping longevity assurance pathways that do not overlap (or only partially overlap) with the adaptable TOR and cAMP/PKA pathways modulated by calorie availability (Figures 3.12E and 3.12F).

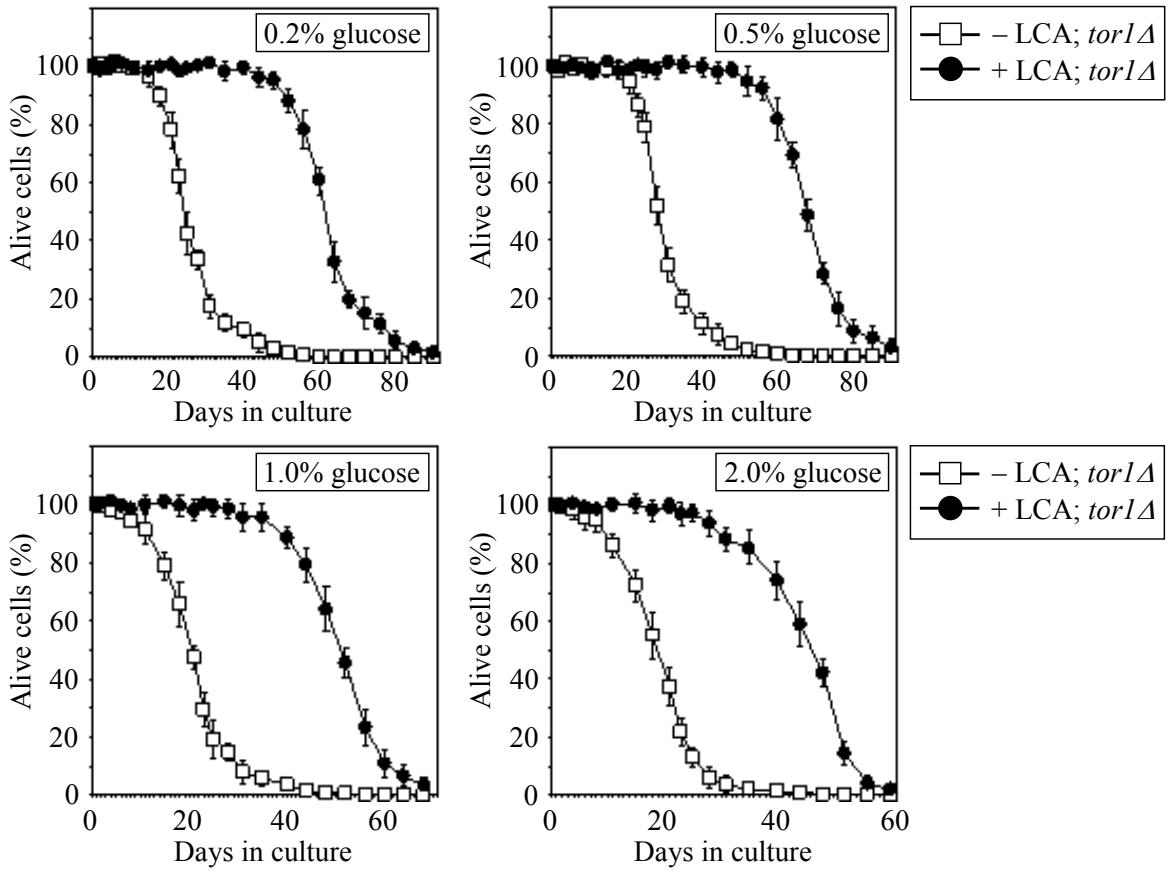


**Figure 3.15.** Chronological survival data for *tor1Δ* strain cultured in medium initially containing 0.2%, 0.5%, 1% or 2% glucose in the presence of LCA (50 μM) or in its absence. Dataset for Figure 3.14.

Consistent with my assumption that LCA extends longevity not by modulating the adaptable TOR pathway (Figures 3.14E and 3.14F), I found that lack of Tor1p did not impair the life-extending efficacy of LCA under CR (Figures 3.14A to 3.14D). Importantly, by eliminating a master regulator of this key adaptable pathway that shortens the CLS of yeast on a high-calorie diet, the *tor1Δ* mutation abolished the dependence of the anti-aging efficacy of LCA on the number of available calories. In fact, LCA extended longevity of the *tor1Δ* mutant strain to a very similar degree under CR and non-CR conditions (Figures 3.14C and 3.14D).

Vincent Richard, a graduate student in Dr. Titorenko's laboratory, then assessed

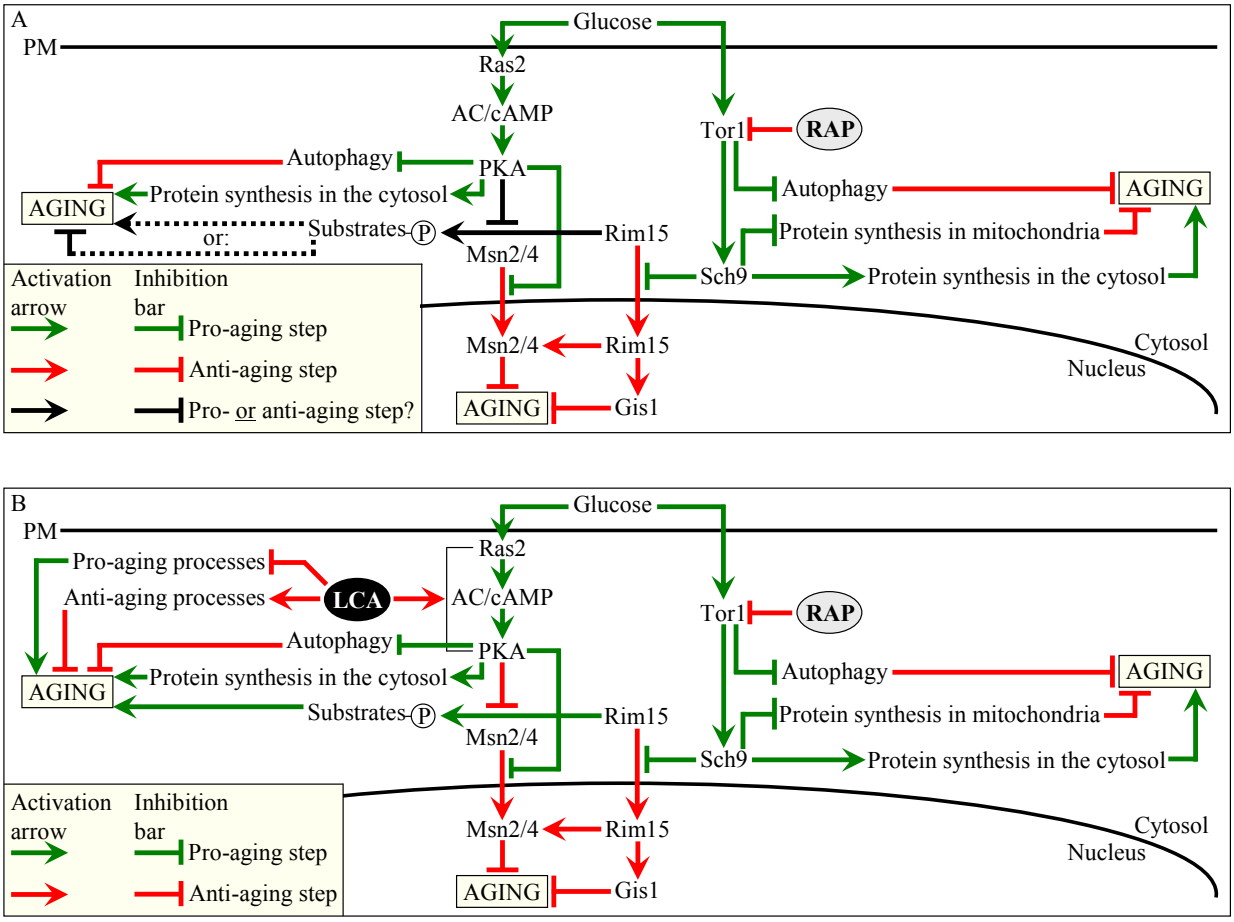


**Figure 3.16.** Outline of pro- and anti-aging processes that are controlled by the TOR and/or cAMP/PKA signaling pathways and are modulated by LCA or rapamycin (RAP) in chronologically aging yeast. The currently accepted (A) and updated, based on this study (B), outlines of pro- and anti-aging processes are shown. Activation arrows and inhibition bars denote pro-aging processes (displayed in green color), anti-aging processes (displayed in red color) or processes whose role in longevity regulation was unknown (displayed in black color). Doted lines denote hypothetical, until this study, processes. See text for details.

how the adaptable cAMP/PKA pathway influences the life-extending efficacy of LCA in yeast on a high- or low-calorie diet. He found that: 1) although the *ras2Δ* mutation greatly decreases the PKA protein kinase activity by eliminating a GTP-binding protein that activates adenylate cyclase responsible for the synthesis of the PKA activator cAMP [58], it did not abolish the ability of LCA to extend CLS under CR and non-CR conditions [247]; 2) the life-extending efficacy of LCA was decreased by the *ras2Δ*

mutation, as compared to that seen in WT cells exposed to this compound [247]; and 3) in spite of such partial reduction of the anti-aging potential of LCA in *ras2Δ*, LCA still significantly increased its CLS under CR and non-CR conditions [247].

The TOR and cAMP/PKA pathways converge on Rim15p whose nuclear pool plays a pivotal role in governing the life-extending effect of CR by enabling the establishment of an anti-aging transcriptional program driven by Msn2p, Msn4p and Gis1p (Figure 3.16A) [10, 35, 58, 115]. Vincent Richard (a graduate student in Dr. Titorenko's laboratory) evaluated the life-extending efficacy of LCA in yeast lacking Rim15p. His findings supported the notion that one of the two mechanisms underlying the anti-aging effect of this bile acid involves its ability to modulate certain housekeeping longevity assurance pathways that are not centered on Rim15p and do not overlap with the adaptable TOR and cAMP/PKA pathways [247]. In fact, he found that: 1) although the life-extending potential of LCA in *rim15Δ* was partially reduced due to the impairment of the Rim15p-centered mechanism of its anti-aging action, LCA still significantly increased the CLS of *rim15Δ* under CR and non-CR conditions [247]; and 2) by eliminating a key nutrient-sensory protein kinase on which the adaptable TOR and cAMP/PKA pathways converge to regulate longevity in a calorie availability-dependent fashion, the *rim15Δ* mutation abolished the dependence of the anti-aging efficacy of LCA on the number of available calories [247].

## 3.5 Discussion

In studies described in this chapter of my thesis, I designed a chemical genetic screen for small molecules that increase the CLS of yeast under CR conditions by

targeting lipid metabolism and modulating housekeeping longevity pathways that regulate longevity irrespective of the number of available calories. My screen identified LCA as one of such molecules. My analysis of how LCA influences various longevity-related processes and how it affects the CLS of yeast mutants impaired in the adaptable TOR longevity pathway provided important new insights into mechanisms of longevity regulation, as outlined below.

My findings described in this chapter of the thesis, along with some recently published data from Dr. Titorenko's laboratory [247], imply that LCA extends yeast CLS by modulating housekeeping longevity assurance processes that are not regulated by the adaptable TOR and cAMP/PKA signaling pathways. Based on these findings, I concluded that LCA extends longevity of chronologically aging yeast by targeting two different mechanisms. One mechanism extends longevity regardless of the number of available calories. This mechanism involves the LCA-governed modulation of certain housekeeping longevity assurance pathways that do not overlap with the adaptable TOR and cAMP/PKA pathways (Figure 3.16B). My findings presented in this chapter, together with some recently published data from Dr. Titorenko's laboratory [247], identify a compendium of processes that compose LCA-targeted housekeeping longevity assurance pathways. These findings imply that LCA modulates such pathways by 1) suppressing the pro-aging process [24, 246, 310] of lipid-induced necrotic cell death, perhaps due to its observed ability to reduce the intracellular levels of FFA and DAG that trigger such death; 2) attenuating the pro-aging process [321, 322] of mitochondrial fragmentation, a hallmark event of age-related cell death; 3) altering oxidation-reduction processes in mitochondria - such as oxygen consumption, the maintenance of membrane potential and

ROS production - known to be essential for longevity regulation [73, 75, 132, 147]; 4) enhancing cell resistance to oxidative and thermal stresses, thereby activating the anti-aging process [24, 147, 246, 299, 323] of stress response; 5) suppressing the pro-aging process [321, 322] of mitochondria-controlled apoptosis; and 6) enhancing stability of nuclear and mitochondrial DNA, thus activating the anti-aging process [324, 325] of genome maintenance. The observed pleiotropic effect of LCA on a compendium of housekeeping longevity assurance processes implies that this bile acid is a multi-target life-extending compound that increases CLS in yeast by modulating a network of the highly integrated processes that are not controlled by the adaptable TOR and cAMP/PKA pathways. The major challenge now is to define the molecular mechanisms by which LCA modulates each of these pro- and anti-aging housekeeping processes and integrates them in chronologically aging yeast.

The other mechanism underlying the life-extending effect of LCA in chronologically aging yeast increases life span only under non-CR conditions. This mechanism consists in LCA-driven unmasking of the previously unknown anti-aging potential of PKA, a key player in the adaptable cAMP/PKA pathway. I propose that LCA unveils the anti-aging potential of PKA by activating PKA-dependent phosphorylation of the cytosolic pool of Rim15p, a key nutrient-sensory protein kinase on which the adaptable TOR and cAMP/PKA pathways converge to regulate longevity in a calorie availability-dependent fashion (Figure 3.16B). Of note, the nuclear pool of Rim15p is well known for its anti-aging role in governing the life-extending effect of CR by enabling a pro-longevity transcriptional program driven by Msn2p, Msn4p and Gis1p (Figure 3.16B) [35, 58]. In my hypothesis 1) unlike its nuclear pool, the cytosolic pool of

Rim15p has an essential pro-aging function in phosphorylating a compendium of its cytosolic target proteins [320] some of which promote aging only if phosphorylated (Figure 3.16B); 2) under non-CR conditions LCA activates the PKA-dependent phosphorylation of Rim15p (Figure 3.16B); and 3) because the phosphorylation of Rim15p inactivates its protein kinase activity [58], the dephosphorylation of pro-aging target proteins of Rim15p in the cytosol by phosphatases inhibits the ability of these target proteins to promote aging (Figure 3.16B). To test the validity of this hypothesis, Dr. Titorenko laboratory is currently evaluating how genetic manipulations that alter the abundance of various extra-nuclear target proteins of Rim15p or affect their phosphorylation status influence the life-extending efficacy of LCA.

It should be stressed that, although I found that LCA greatly extends yeast longevity, yeast do not synthesize this or any other bile acid found in mammals [314, 326]; a recent mass spectrometry-based analysis of the total yeast lipidome conducted by Simon Bourque and Adam Beach in Dr. Titorenko's laboratory has confirmed lack of endogenous bile acids. One could envision that during evolution yeast have lost the ability to synthesize bile acids but have maintained the life-extending response to these biologically active molecules by retaining certain longevity-related processes that are sensitive to regulation by bile acids. Alternatively, one could think that during evolution yeast have developed the ability to sense bile acids produced by mammals (and/or bile acid-like lipids synthesized by worms), recognize these mildly toxic molecules as environmental stressors providing hormetic benefits and/or as indicators of the state of the environment or food supply, and then to respond by undergoing certain life-extending changes to their physiology that ultimately increase their chances of survival. It is

conceivable therefore that the life-extending potential of LCA and other bile acids as well as, probably, the mechanisms underlying their anti-aging action are evolutionarily conserved.

In fact, following their synthesis from cholesterol in the intestine, hypodermis, spermatheca and sensory neurons of worms, bile acid-like dafachronic acids (including 3-keto-LCA) have been shown to be delivered to other tissues where they activate the DAF-12/DAF-16 signaling cascade that in turn orchestrates an anti-aging transcriptional program, thereby increasing the life span of the entire organism [302]. Bile acids also provide health benefits to mammals. Synthesized from cholesterol in hepatocytes of the liver, these amphipathic molecules have been for a long time considered to function only as trophic factors for the enteric epithelium and as detergents for the emulsification and absorption of dietary lipids and fat-soluble vitamins [314, 326, 327]. Recent years have been marked by a significant progress in our understanding of the essential role that bile acids play as signaling molecules regulating lipid, glucose and energy homeostasis and activating detoxification of xenobiotics [314, 327, 328]. By stimulating the G-protein-coupled receptor TGR5, bile acids activate the cAMP/PKA signaling pathway that 1) enhances energy expenditure in brown adipose tissue and muscle by stimulating mitochondrial oxidative phosphorylation and uncoupling; 2) improves liver and pancreatic function by activating the endothelial nitric oxide synthase; and 3) enhances glucose tolerance in obese mice by inducing intestinal glucagon-like peptide-1 release [314, 327, 328]. Furthermore, by activating the farnesoid X receptor (FXR) and several other nuclear hormone receptors inside mammalian cells, bile acids 1) modulate the intracellular homeostasis of cholesterol, neutral lipids and fatty acids; 2) regulate glucose

metabolism by enhancing glycogenesis and attenuating gluconeogenesis; and 3) stimulate clearance of xenobiotic and endobiotic toxins by activating transcription of numerous xenobiotic detoxification genes [314, 326 - 329]. All these health-improving, beneficial metabolic effects of bile acids prevent the development of obesity following administration of high-fat diet [314, 326, 327]. Thus, bile acids have a great potential as pharmaceutical agents for the treatment of diabetes, obesity and various associated metabolic disorders, all of which are age-related [314, 326]. Moreover, bile acids have been shown to inhibit neuronal apoptosis in experimental rodent models of neurodegenerative disorders by promoting mitochondrial membrane stability, preventing the release of cytochrome c from mitochondria, reducing activities of various caspases, and activating the NF-κB, PI3K and MAPK survival pathways [329, 330].

It should be stressed that many of the metabolic, stress response and apoptotic processes modulated by bile acids in mammals are essential for healthy aging and longevity regulation. Importantly, I found that, by modulating several of these health- and longevity-related processes in chronologically aging yeast, LCA increases their life span. Moreover, the long-lived $Ghrhr^{lit/lit}$ mice displayed elevated levels of several bile acids and exhibited increased FXR-dependent transcription of numerous xenobiotic detoxification genes; if administered to food consumed by wild-type mice, cholic acid - one of these bile acids - mimicked the FXR-governed gene expression pattern observed in $Ghrhr^{lit/lit}$ mice [331, 332]. It has been therefore proposed that, by promoting chemical hormesis in mammals, these mildly toxic molecules with detergent-like properties may extend their longevity by acting as endobiotic regulators of aging [323, 332, 333].

Altogether, these findings support the notion that bile acids act as endobiotic and xenobiotic regulators of aging that are beneficial to health and longevity across phyla. A comparative analysis of the mechanisms underlying such health-improving and life-extending action of bile acids implies that these mechanisms are likely to be evolutionarily conserved.

## 3.6 Conclusions

My high-throughput chemical genetic screen identified LCA as a novel anti-aging compound that extends yeast chronological life span under CR conditions by targeting lipid metabolism and modulating housekeeping longevity assurance pathways. My analysis of how LCA influences various longevity-related processes and how it affects the chronological life span of yeast mutants impaired in the adaptable longevity pathways provided important new insights into mechanisms of longevity regulation. I revealed two mechanisms underlying the life-extending effect of LCA in chronologically aging yeast. One mechanism operates in a calorie availability-independent fashion and involves the LCA-governed modulation of housekeeping longevity assurance pathways that do not overlap with the adaptable TOR and cAMP/PKA pathways. The other mechanism extends yeast longevity under non-CR conditions and consists in LCA-driven unmasking of the previously unknown anti-aging potential of PKA. I provided evidence that LCA modulates housekeeping longevity assurance pathways by 1) attenuating mitochondrial fragmentation, a hallmark event of age-related cell death; 2) altering oxidation-reduction processes in mitochondria, including oxygen consumption, the maintenance of membrane potential, and reactive oxygen species production; 3) enhancing resistance to oxidative

and thermal stresses; 4) suppressing mitochondria-controlled apoptosis; and 5) enhancing stability of nuclear and mitochondrial DNA. I expect that this knowledge will be instrumental for defining molecular mechanisms underlying the ability of LCA to extend longevity by impacting these various housekeeping longevity assurance processes and by modulating signaling pathways governing them.

# 4 Xenohormetic, hormetic, and cytostatic forces may drive the evolution of longevity regulation mechanisms within ecosystems: A hypothesis and its empirical verification

## 4.1 Abstract

In my chemical genetic screen described in chapter 3, I identified lithocholic acid (LCA), as a novel anti-aging molecule that extends yeast longevity. Yeast do not synthesize this or any other bile acids produced by mammals [314, 326]; a recent mass spectrometry-based analysis of the total yeast lipidome conducted in Dr. Titorenko's laboratory has confirmed lack of endogenous bile acids. Therefore, I propose here that bile acids released into the environment by mammals may act as interspecies chemical signals providing longevity benefits to yeast and, perhaps, other species within an ecosystem. I hypothesize that, because bile acids are known to be mildly toxic compounds, they may create selective pressure for the evolution of yeast species that can respond to the bile acids-induced mild cellular damage by developing the most efficient stress protective mechanisms. It is likely that such mechanisms may provide effective protection of yeast against molecular and cellular damage accumulated with age. Thus, I propose that yeast species that have been selected for the most effective mechanisms providing protection against bile acids may evolve the most effective anti-aging mechanisms that are sensitive to regulation by bile acids. I extend my hypothesis on longevity regulation by bile acids by suggesting a hypothesis of the xenohormetic, hormetic and cytostatic selective forces driving the evolution of longevity regulation mechanisms at the ecosystemic level.

To verify my hypothesis empirically, I carried out the LCA-driven multistep selection of long-lived yeast species under laboratory conditions. I found that a lasting exposure of wild-type yeast to LCA results in selection of yeast species that live longer in the absence of this bile acid than their ancestor. My data enabled to rank different concentrations of LCA with respect to the efficiency with which they cause the appearance of long-lived yeast species. I revealed that, if used at the most efficient concentration of 5 μM, this bile acid induced life-extending mutations with the frequency of about $4 \times 10^8$/generation. At the concentration of 50 μM, LCA caused the appearance of long-lived species with the frequency of $1 \times 10^8$/generation, whereas a lasting exposure of yeast to 250 μM LCA did not result in selection of such species. Because the lowest used concentration of LCA resulted in the highest frequency of long-lived species appearance, I believe that it is unlikely that the life-extending mutations they carry are due to mutagenic action of this bile acid.

I outline here the most critical questions needed to be addressed empirically in the near future to test the validity of other aspects of my hypothesis on the ecosystemic evolution of longevity regulation mechanisms.

## 4.2 Introduction

I recently found that LCA greatly (and some other bile acids to a lesser degree) increases the chronological life span of yeast under caloric restriction (CR) conditions [247]. My findings provided evidence that LCA extends longevity of chronologically aging yeast through two different mechanisms (see chapter 3 for a detailed discussion of this topic) (Figure 4.1). In one mechanism, this bile acid targets longevity pathways that

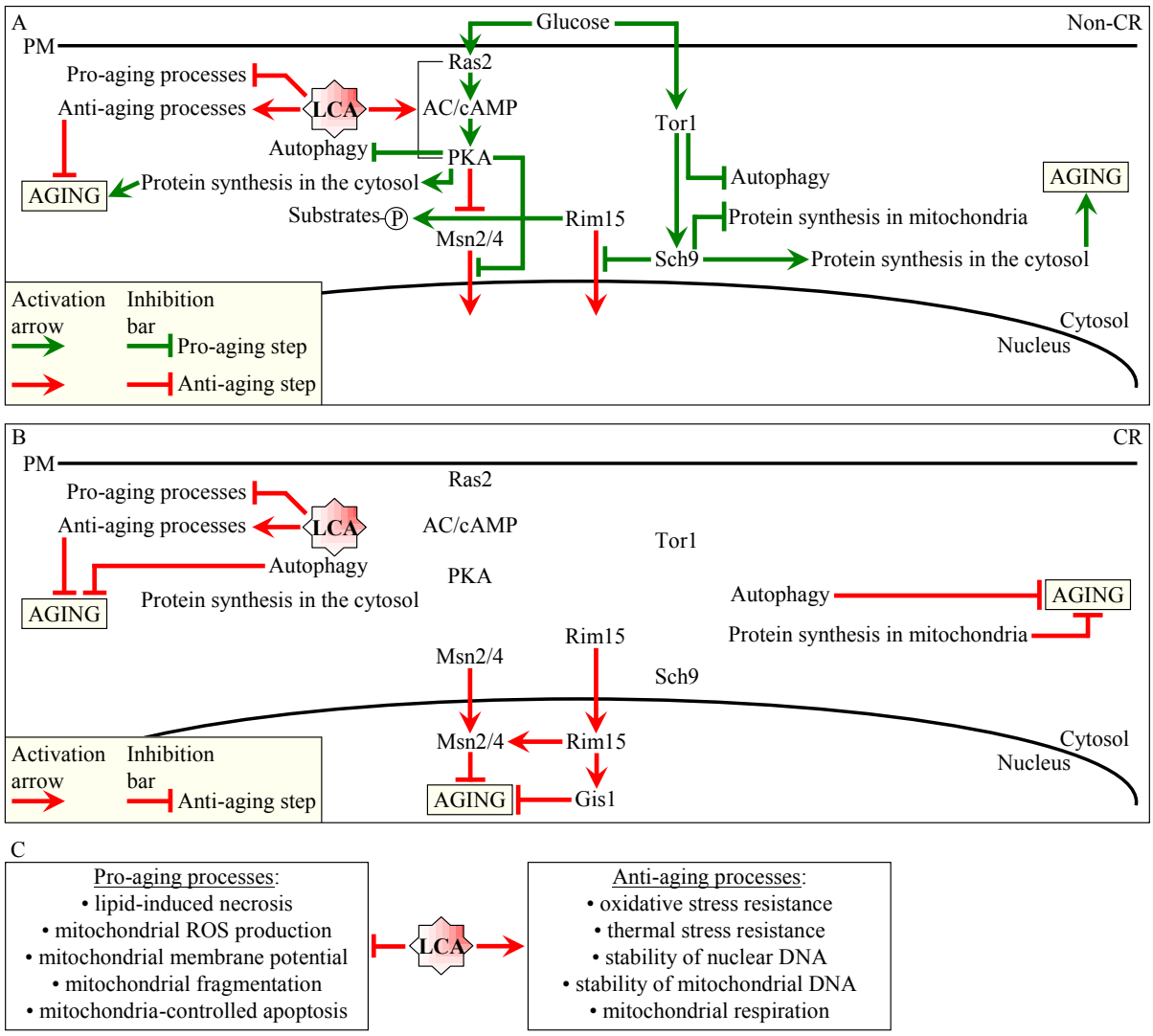


**Figure 4.1.** Lithocholic acid (LCA) extends longevity of chronologically aging yeast through two different mechanisms. (A and B) Outline of pro- and anti-aging processes that are controlled by the TOR and/or cAMP/PKA signaling pathways and are modulated by LCA in yeast cells grown under non-CR (A) or CR (B) conditions. Activation arrows and inhibition bars denote pro-aging (displayed in green color) or anti-aging (displayed in red color) processes. Under both non-CR and CR conditions, LCA targets housekeeping longevity assurance processes listed in (C). Under non-CR conditions only, LCA also targets the adaptable cAMP/PKA pathway. By activating PKA-dependent phosphorylation of the cytosolic pool of the key nutrient-sensory protein kinase Rim15p, LCA causes the inactivation of Rim15p. The resulting reduction of the phosphorylation status of several Rim15p target proteins in the cytosol lowers their pro-aging efficacy. Abbreviations: CR, caloric restriction; PM, plasma membrane.

control chronological aging irrespective of the number of calories available to yeast. Because these pathways modulate longevity regardless of calorie availability, I called them "constitutive" or "housekeeping" (see chapter 3) [247]. LCA modulates these housekeeping longevity assurance pathways by suppressing lipid-induced necrosis, attenuating mitochondrial fragmentation, altering oxidation-reduction processes in mitochondria, enhancing resistance to oxidative and thermal stresses, suppressing mitochondria-controlled apoptosis, and enhancing stability of nuclear and mitochondrial DNA ([247]; Figure 4.1C). The housekeeping longevity pathways do not overlap with the TOR (target of rapamycin) and cAMP/PKA (cAMP/protein kinase A) signaling pathways ([247]; Figure 4.1A), both of which are "adaptable" by nature because they are under the stringent control of calorie and/or nutrient availability ([4, 7, 10, 36, 334, 335]; Figure 4.1B). In the other mechanism, LCA targets the adaptable cAMP/PKA pathway by unmasking an anti-aging potential of PKA under non-CR conditions, perhaps by activating PKA-dependent phosphorylation of the cytosolic pool of the key nutrient-sensory protein kinase Rim15p (see chapter 3) [247]. The phosphorylation of Rim15p by PKA inactivates its protein kinase activity [58]. Hence, the LCA-driven inactivation of Rim15p may reduce the phosphorylation status of its known [320] target proteins in the cytosol, thereby lowering their pro-aging efficacy ([247]; Figure 4.1A).

Although bile acids in mammals have been traditionally considered only as trophic factors for the enteric epithelium and detergents for the emulsification and absorption of dietary lipids [314, 326, 327], they are now also recognized for their essential role as signaling molecules regulating lipid, glucose and energy homeostasis and activating detoxification of xenobiotics ([314, 326 - 330]; Figure 4.2A). Many of the

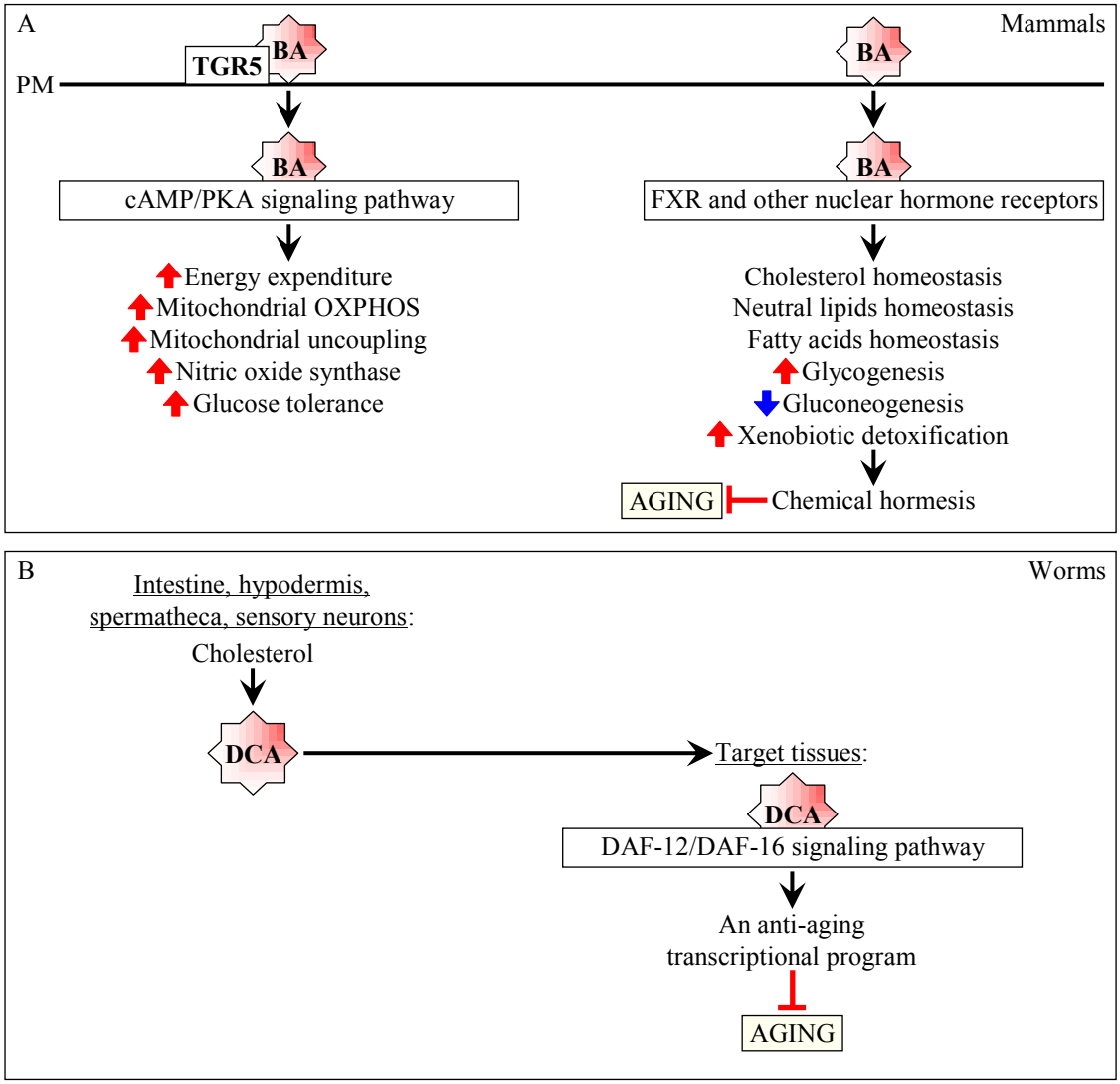


**Figure 4.2.** Bile acids are beneficial to health and longevity in animals. (A) In mammals, bile acids (BA) function not only as trophic factors for the enteric epithelium and detergents for the emulsification and absorption of dietary lipids, but also as signaling molecules that regulate lipid, glucose and energy homeostasis and activate detoxification of xenobiotics. By improving overall health, BA may delay the onset of age-related diseases and have beneficial effect on longevity. By activating transcription of numerous xenobiotic detoxification genes and thus promoting chemical hormesis, BA may extend their longevity by acting as endobiotic regulators of aging. (B) In worms, following their synthesis from cholesterol in the intestine, hypodermis, spermatheca and sensory neurons, bile acid-like dafachronic acids (DCA) are delivered to other tissues where they activate the DAF-12/DAF-16 signaling cascade, thereby orchestrating an anti-aging transcriptional program and increasing the life span of the entire organism.

numerous health-improving metabolic effects caused by bile acids and their demonstrated ability to protect mammals from xenobiotic toxins ([326 - 330]; Figure 4.2A) suggest that, by improving overall health, these amphipathic molecules may delay the onset of age-related diseases and have beneficial effect on longevity. Furthermore, because of the elevated levels of several bile acids in the long-lived $Ghrhr^{lit/lit}$ mice and due to the ability of cholic acid administered to food of wild-type mice to activate transcription of numerous xenobiotic detoxification genes, it has been proposed that, by promoting chemical hormesis in mammals, these mildly toxic molecules with detergent-like properties may extend their longevity by acting as endobiotic regulators of aging [323, 331 - 333]. Moreover, bile acid-like dafachronic acids (including 3-keto-LCA) in worms function as endocrine regulators of aging by activating an anti-aging transcriptional program governed by the DAF-12/DAF-16 signaling cascade ([302, 336, 337]; Figure 4.2B). Altogether, these findings support the notion that bile acids are beneficial to health and longevity in animals because of their ability to operate as potent signaling molecules that modulate a compendium health- and longevity-related processes. Noteworthy, by modulating many of these processes also in yeast, LCA extends their longevity [247]. It is likely therefore that the life-extending capacity of LCA and other bile acids as well as, perhaps, the mechanisms underlying their anti-aging action are conserved across animal species and other phyla.

## 4.3 Materials and Methods

### Strains and media

The wild type strain *Saccharomyces cerevisiae* BY4742 (*MATα, his3Δ leu2Δ0 lys2Δ ura3Δ0)* was cultured in liquid YP medium (1% yeast extract, 2% peptone) contained 0.2% glucose as a carbon source, with or without LCA, as detailed in the "Results" section. Cell cultures were incubated at 30°C with rotational shaking at 200 rpm in Erlenmeyer flasks at a "flask volume/medium volume" ratio of 5:1. For a spot assay of cell viability, serial 10-fold dilutions of cell cultures were spotted onto plates with solid YP medium (1% yeast extract, 2% peptone) containing 2% glucose.

## 4.4 Results

### 4.4.1 Bile acids may function as interspecies chemical signals extending yeast longevity within ecosystems

As I mentioned in section 4.1, yeast do not synthesize LCA or any other bile acid found in mammals [247, 326, 329]. Therefore, I hypothesize that bile acids released into the environment by mammals may act as interspecies chemical signals providing longevity benefits to yeast. In my hypothesis, these mildly toxic compounds released into the environment by mammals may create selective pressure for the evolution of yeast species that can respond to the resulting mild cellular damage by developing the most efficient stress protective mechanisms. Such mechanisms may provide effective protection of yeast not only against cellular damage caused by bile acids (and, perhaps, by other environmental xenobiotics) but also against molecular and cellular damage accumulated with age. In my hypothesis, yeast species that have been selected for the most effective mechanisms providing protection against bile acids (and other

environmental xenobiotics) are expected to evolve the most effective anti-aging mechanisms that are sensitive to regulation by bile acids (and, perhaps, by other environmental xenobiotics). Thus, the ability of yeast to sense bile acids produced by mammals and then to respond by undergoing certain life-extending changes to their physiology (Figure 4.1) is expected to increase their chances of survival, thereby creating selective force aimed at maintaining such ability.

### 4.4.2 Natural variations of bile acid levels within ecosystems may modulate both housekeeping and adaptable longevity pathways in yeast

Of note, the bulk quantity of bile acids in mammals exists as an organismal pool which cycles between intestine and liver in the enterohepatic circulation due to the efficient reabsorption of bile acids in the terminal ileum [326, 327]. However, about 5% (up to 600 mg/day) of this pool escapes each reabsorption cycle, being continuously released into the large intestine and ultimately into the environment [326, 327]. Thus, yeast are permanently exposed to bile acids due to their fecal loss by mammals. It is conceivable therefore that, in yeast exposed to bile acids released by mammals, these interspecies chemical signals modulate housekeeping longevity assurance pathways that 1) regulate yeast longevity irrespective of the state of the environment or food supply (*i.e.*, the number of available calories and nutrients); and 2) do not overlap (or only partially overlap) with the adaptable TOR and cAMP/PKA longevity pathways that are under the stringent control of calorie and nutrient availability.

It should be stressed, however, that the quantity of bile acids released into the environment by mammals could vary due to changes in the density of mammalian

population and, perhaps, due to other environmental factors (including the abundance of food available to mammals, its nutrient and caloric content, and its fat mass and quality). In fact, the organismal pool of bile acids in mammals is under the stringent control of regulatory mechanisms operating in the liver during the fasting-refeeding transition [314, 326, 327]. Hence, it is likely that, in addition to the ability of yeast to respond to the permanently available exogenous pool of bile acids by modulating some housekeeping longevity assurance pathways, they have also evolved the ability to sense the environmental status-dependent variations of bile acids abundance by modulating the adaptable TOR and cAMP/PKA longevity pathways. Importantly, my recent study provided evidence for two mechanisms underlying the life-extending effect of LCA in yeast (see chapter 3 of my thesis); one mechanism involves the calorie supply-independent modulation of a compendium of housekeeping longevity assurance processes that are not regulated by the TOR and cAMP/PKA pathways, whereas the other mechanism operates only in yeast on a calorie-rich diet by unmasking the previously unknown anti-aging potential of the calorie supply-dependent PKA [247].

It remains to be seen if my hypothesis on the essential role of bile acids as interspecies chemical signals regulating longevity in yeast is applicable to other species routinely exposed to bile acids within an ecosystem, such as plants and bacteria.

### 4.4.3 Rapamycin may also act as an interspecies chemical signal modulating longevity at the ecosystemic level

My hypothesis on longevity regulation by bile acids within ecosystems may explain the evolutionary origin of the life-extending effect of another anti-aging

compound, called rapamycin. Synthesized by soil bacteria to inhibit growth of fungal competitors, this macrocyclic lactone provides longevity benefit to yeast, fruit flies and mice by specifically inhibiting TOR (Tor1p in yeast), a nutrient-sensory protein kinase that operates as a master negative regulator of the key adaptable longevity pathway [110, 113, 116, 334, 335]. Because rapamycin delays proliferative growth of organisms across phyla by causing G1 cell cycle arrest [102, 334, 335], it could be considered as a mildly cytotoxic compound, akin to bile acids (recent unpublished data from Dr. Titorenko's laboratory revealed that rapamycin is a more toxic hormetic molecule than LCA and other bile acids). Therefore, I propose that, following its release into the environment by soil bacteria, rapamycin may create selective pressure for the evolution of new yeast, fly and mammalian species. These new species can respond to rapamycin-induced growth retardation by developing certain mechanisms aimed at such remodeling of their anabolic and catabolic processes that would increase their chances of survival under conditions of slow growth. It is plausible that some of these mechanisms delay aging by optimizing essential longevity-related processes and remain sensitive to modulation by rapamycin. Hence, the ability of yeast, fruit flies and mice to sense rapamycin produced by soil bacteria and then to respond by undergoing certain life-extending changes to their physiology is expected to increase their chances of survival, thereby creating selective force for maintaining such ability.

Interestingly, rapamycin has been shown to increase life span in fruit flies under dietary restriction conditions [113], when the TOR-governed adaptable pro-aging pathways are fully suppressed and the TOR-governed adaptable anti-aging pathways are fully activated [334, 335]. It is plausible therefore that - similar to the proposed above

anti-aging mechanism of LCA in yeast - rapamycin in fruit flies can modulate both the housekeeping (TOR-independent) and adaptable (TOR-dependent) longevity pathways. Hence, it is tempting to speculate that, in addition to the ability of fruit flies to respond to the permanently available exogenous pool of rapamycin by modulating some housekeeping longevity assurance pathways, they have also evolved the ability to sense the environmental status-dependent variations of rapamycin abundance (due to, *e.g.*, changes in the density of soil bacteria population) by modulating the TOR-governed adaptable longevity pathways. Of note, recent findings in yeast imply that - in addition to its role as a master negative regulator of the key adaptable longevity pathway - Tor1p may also operate as a positive longevity regulator, in particular by stimulating nuclear import of the transcriptional factors Sfp1p, Rtg1 and Rtg3 in response to partial mitochondrial dysfunction or changes in the exogenous and endogenous levels of glutamate and glutamine [338 - 340]. The ability of these transcriptional factors to regulate metabolism, ribosome biogenesis and growth is crucial for longevity [339 - 342].

### 4.4.4 The "xenohormesis" hypothesis: a case of xenohormetic phytochemicals

My hypothesis on longevity regulation by bile acids and rapamycin within ecosystems complements the "xenohormesis" hypothesis, in which plants and other autotrophic organisms respond to various environmental stresses (*i.e.*, UV light, dehydration, infection, predation, cellular damage and nutrient deprivation) by synthesizing a compendium of secondary metabolites [119, 343, 344]. Within plants and other autotrophs producing these phytochemicals in response to environmental stresses, they activate defence systems protecting the host organisms against such stresses. In

addition, these phytochemicals constitute a chemical signature of the environmental status of an ecosystem. As such, they provide to heterotrophic organisms (*i.e.*, animals and fungi) within the ecosystem an advance warning about deteriorating environmental conditions [343]. By operating as interspecies chemical signals, they could create selective pressure for the evolution of heterotrophic organisms that can sense these signals and then to respond by altering their metabolism in defensive preparation for the imminent adversity while conditions are still favourable. The resulting metabolic remodeling causes such specific changes in physiology of heterotrophs that are beneficial to their health and longevity [343]. Although xenohormetic phytochemicals are produced by autotrophic organisms only in response to hormetic environmental stresses, it is unlikely that they function as mildly toxic hormetic molecules within heterotrophic organisms; rather, the xenohormesis hypothesis proposes that the beneficial to health and longevity effects of xenohormetic phytochemicals are due to their well known ability to modulate the key enzymes of stress-response pathways governing numerous longevity-related processes in heterotrophic organisms [343 - 352]. The xenohormetic mode of positive selection for the most efficient longevity regulation mechanisms has been proposed to be driven by such phytochemicals as resveratrol, butein, fisetin and other polyphenols, as well as by curcumin [119, 343, 344]. The ability of caffeine to increase yeast chronological life span by decreasing the catalytic activity of Tor1p [101] suggests that this xanthine alkaloid could also operate as a xenohormetic phytochemical signal providing an advance warning about deteriorating environmental conditions to yeast, thereby driving the evolution of their longevity regulation mechanisms.

### 4.4.5 The "anti-aging side effect" hypothesis: delaying aging by attenuating the growth-promoting TOR signaling pathway

A common feature of many anti-aging compounds - some of which are mildly toxic hormetic molecules, whereas the others are non-toxic xenohormetic phytochemicals - is that they exhibit a cytostatic effect by inhibiting TOR, a nutrient-sensing signaling pathway that promotes proliferative growth in all heterotrophic organisms. A recently proposed "anti-aging side effect" hypothesis envisions that the primary objective for the synthesis of these cytostatic compounds by a group of the organisms composing an ecosystem is to suppress growth of other group(s) of organisms within this ecosystem, thereby killing competitors and/or protecting themselves from predators [349]. Due to its central role in promoting proliferative growth of all heterotrophic organisms, the TOR signaling pathway is a preferable target of such cytostatic compounds [102, 334, 349, 353, 354]. Because the TOR pathway provides a molecular link between growth and aging by driving a so-called quasi-programmed aging [334, 353, 354], these compounds exhibit a side effect of suppressing aging [349]. In fact, soil bacteria synthesize rapamycin to suppress growth of fungal competitors by inhibiting the TOR protein kinase, a master positive regulator of the TOR signaling pathway that drives developmental growth of young organisms [110, 113, 116, 334]. However, since - according to the anti-aging side effect hypothesis - in heterotrophic organisms across phyla this pathway also drives aging after their developmental growth is completed [353, 354], rapamycin has a side effect of suppressing aging of all groups of heterotrophic organisms within an ecosystem [349]. Moreover, the anti-aging side effect hypothesis predicts that plants synthesize resveratrol in part to protect their grapes by inhibiting

fungal growth [349]. Yet, because this small polyphenol attenuates the TOR signaling pathway by modulating key upstream regulators and downstream targets of the TOR protein kinase [345 - 352], resveratrol also displays a side effect of slowing down quasi-programmed TOR-driven aging of various species of heterotrophic organisms within an ecosystem [349].

In the anti-aging side effect hypothesis, cytostatic compounds attenuating the TOR pathway operate as interspecies chemical signals that provide longevity benefits to a range of heterotrophic organisms composing an ecosystem [349]. I propose that, following their release into the environment by soil bacteria or plants, these growth suppressing chemical compounds may create selective pressure for the evolution of yeast, worm, fly and mammalian species that can respond to the resulting retardation of their growth by developing certain mechanisms aimed at specific remodeling of the TOR-governed signaling network. By targeting the TOR protein kinase itself and/or its numerous upstream regulators and downstream targets, such mechanisms may attenuate the hyper-activation of TOR-governed cellular signaling pathways and cellular functions that - according to the concept of quasi-programmed TOR-driven aging [353, 354] - are initiated after developmental growth of a heterotrophic organism is completed. In my hypothesis, the species of heterotrophic organisms that have been selected for the most efficient mechanisms preventing the hyper-activation of TOR-governed cellular signaling pathways and cellular functions following the completion of developmental growth are expected to evolve the most effective anti-aging mechanisms. Such mechanisms may be sensitive to various environmental factors, including the density of organism population and abundance of nutrients within an ecosystem.

### 4.4.6 The xenohormetic, hormetic and cytostatic selective forces may drive the evolution of longevity regulation mechanisms within ecosystems

Unlike xenohormetic phytochemicals that are non-toxic compounds transiently synthesized and released by autotrophs only in response to environmental stresses [343, 344], bile acids are mildly toxic hormetic molecules that are permanently synthesized and released by mammals [314, 323, 326 - 328, 331 - 333]. Furthermore, rapamycin is a more toxic hormetic molecule than bile acids (recent unpublished data from Dr. Titorenko's laboratory) that is permanently synthesized and released by soil bacteria [355]. Moreover, many xenohormetic phytochemicals and mildly toxic hormetic molecules exhibit a cytostatic effect by attenuating TOR-governed cellular signaling pathways and cellular functions [349]. Therefore, by fusing the xenohormesis hypothesis [119, 343, 344], the anti-aging side effect hypothesis [349] and the proposed here hypothesis on longevity regulation by bile acids and rapamycin within ecosystems, I put forward a unified hypothesis of the xenohormetic, hormetic and cytostatic selective forces driving the evolution of longevity regulation mechanisms at the ecosystemic level.

In my unified hypothesis (Figure 4.3), organisms from all domains of life (*i.e.*, bacteria, fungi, plants and animals) within an ecosystem are able to synthesize chemical compounds that 1) are produced and then released into the environment permanently or only in response to deteriorating environmental conditions, increased population density of competitors and/or predators, or changes in food availability and its nutrient and/or caloric content; 2) are mildly toxic compounds that trigger a hormetic response in an organism that senses them or, alternatively, are not toxic for any organism within the ecosystem and do not cause a hormetic response; 3) are cytostatic compounds that

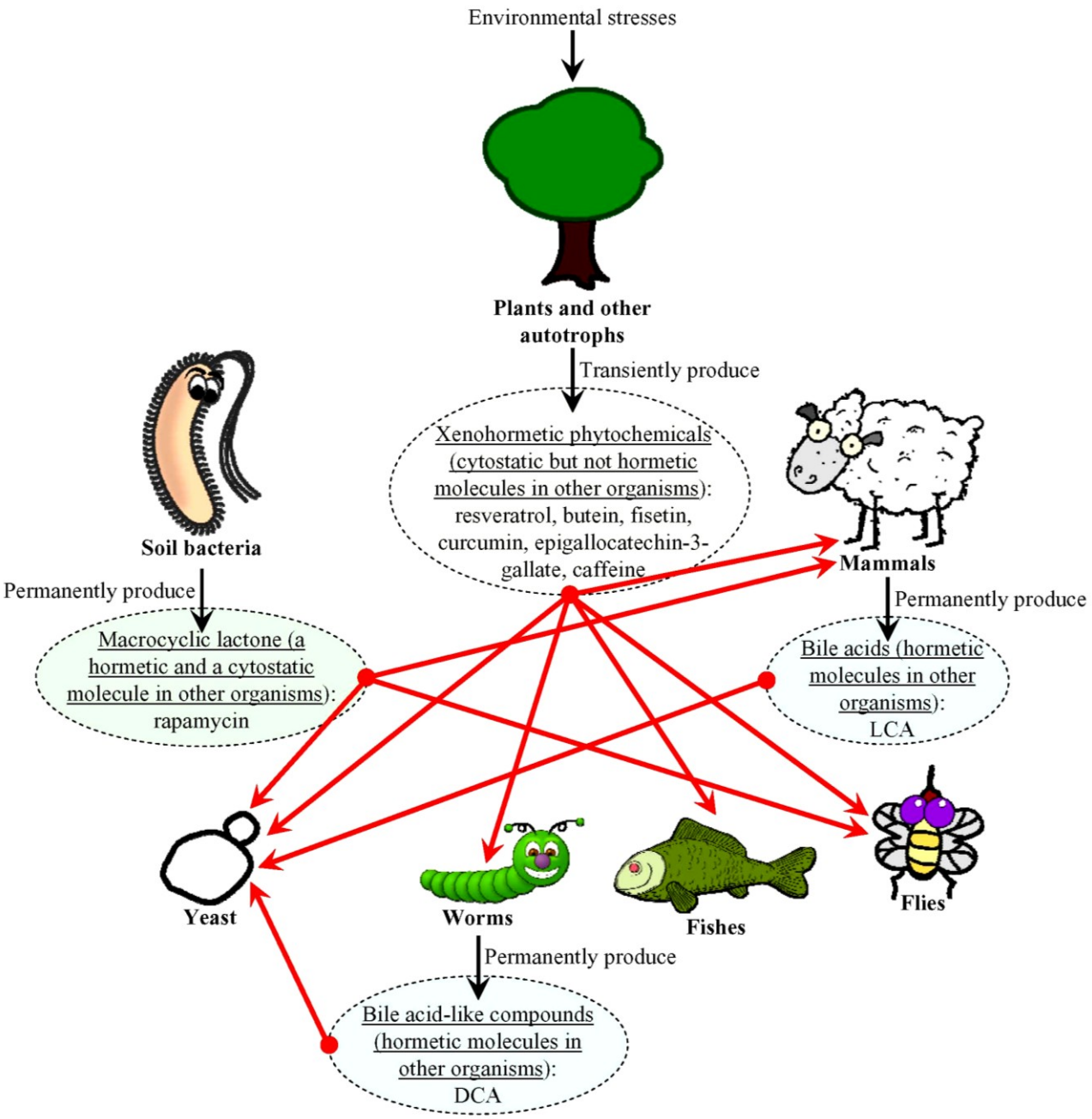


**Figure 4.3.** The xenohormetic, hormetic and cytostatic selective forces may drive the evolution of longevity regulation mechanisms within an ecosystem. I propose that organisms from all domains of life within an ecosystem synthesize chemical compounds that 1) are produced and then released into the environment permanently or only in response to deteriorating environmental conditions, increased population density of competitors and/or predators, or changes in food availability and its nutrient and/or caloric content; 2) are mildly toxic compounds that trigger a hormetic response in an organism that senses them or, alternatively, are not toxic for any organism within the ecosystem and do not cause a hormetic response; 3) are cytostatic compounds that attenuate the TOR-governed signaling network or, alternatively,

do not modulate this growth-promoting network; and 4) extend longevity of organisms that can sense these compounds (red arrows), thereby increasing their chances of survival and creating selective force aimed at maintaining the ability of organisms composing the ecosystem to respond to these compounds by undergoing specific life-extending changes to their physiology. In my hypothesis, the evolution of longevity regulation mechanisms in each group of the organisms composing an ecosystem is driven by the ability of this group of organisms to undergo specific life-extending changes to their physiology in response to a compendium of "critical" chemical compounds that are permanently or transiently released to the ecosystem by other groups of organisms. Abbreviations: LCA, lithocholic acid; DCA, bile acid-like dafachronic acids.

attenuate the TOR-governed signaling network (*e.g.*, rapamycin and resveratrol) or, alternatively, do not modulate this growth-promoting network (*e.g.*, LCA and other bile acid) and 4) extend longevity of organisms that can sense these compounds, thereby increasing their chances of survival and creating selective force aimed at maintaining the ability of organisms composing the ecosystem to respond to these compounds by undergoing specific life-extending changes to their physiology. My hypothesis implies that the evolution of longevity regulation mechanisms in each group of the organisms composing an ecosystem is driven by the ability of this group of organisms to undergo specific life-extending physiological changes in response to a compendium of "critical" chemical compounds that are permanently or transiently released to the ecosystem by other groups of organisms.

### 4.4.7 The empirical verification of my hypothesis of the xenohormetic, hormetic and cytostatic selective forces driving the evolution of longevity regulation mechanisms at the ecosystemic level

To empirically verify my hypothesis of the xenohormetic, hormetic and cytostatic selective forces driving the evolution of longevity regulation mechanisms at the

ecosystemic level, I carried out a 3-step selection of long-lived yeast species by a lasting exposure to LCA under laboratory conditions. For the first step of such selection, yeast cells from an overnight culture were inoculated into a fresh YP medium (with or without LCA) containing 0.2% glucose to the initial cell titre of 1 x $10^5$ cells/ml (Figure 4.4). After one week of the incubation in this medium and following approximately 45 cell generations, yeast entered into a non-proliferative state by reaching stationary (ST) growth phase at the cell titre of 2 x $10^8$ cells/ml (Figure 4.5). Following their entry into a non-proliferative state, yeast cells were cultured for additional 5 weeks. By the end of this cultivation, only ~ 0.02% of cells in the medium without LCA remained viable. In the cell cultures that were supplemented with LCA, ~ 1% of cells remained viable – due to the ability of LCA to increase the chronological life span (CLS) of non-dividing (senescent) yeast cells. Thus, the enrichment factor for long-lived mutants by the end of each selection step was $10^2$ (Figure 4.6). Five cultures were used to carry out the selection of long-lived yeast species: the first culture lacked LCA; the second culture contained 5 μM LCA added at the moment of cell inoculation; the third culture contained 50 μM LCA added at the moment of cell inoculation; the fourth culture contained 250 μM LCA added at the moment of cell inoculation; and the fifth culture was supplemented with 10 doses of 5 μM LCA each by adding this bile acid every 3 or 4 days (Figure 4.7). At the end of the first selection step, aliquots of each of the five cultures were plated onto plates with solid YP medium containing 2% glucose. After 2 days, each of the 10 randomly chosen colonies was inoculated into a liquid medium without LCA to carry out a viability testing step (Figure 4.4). Every week, an aliquot of each culture was used for a spot assay of cell viability to identify long-lived mutants (if any) induced due to a lasting

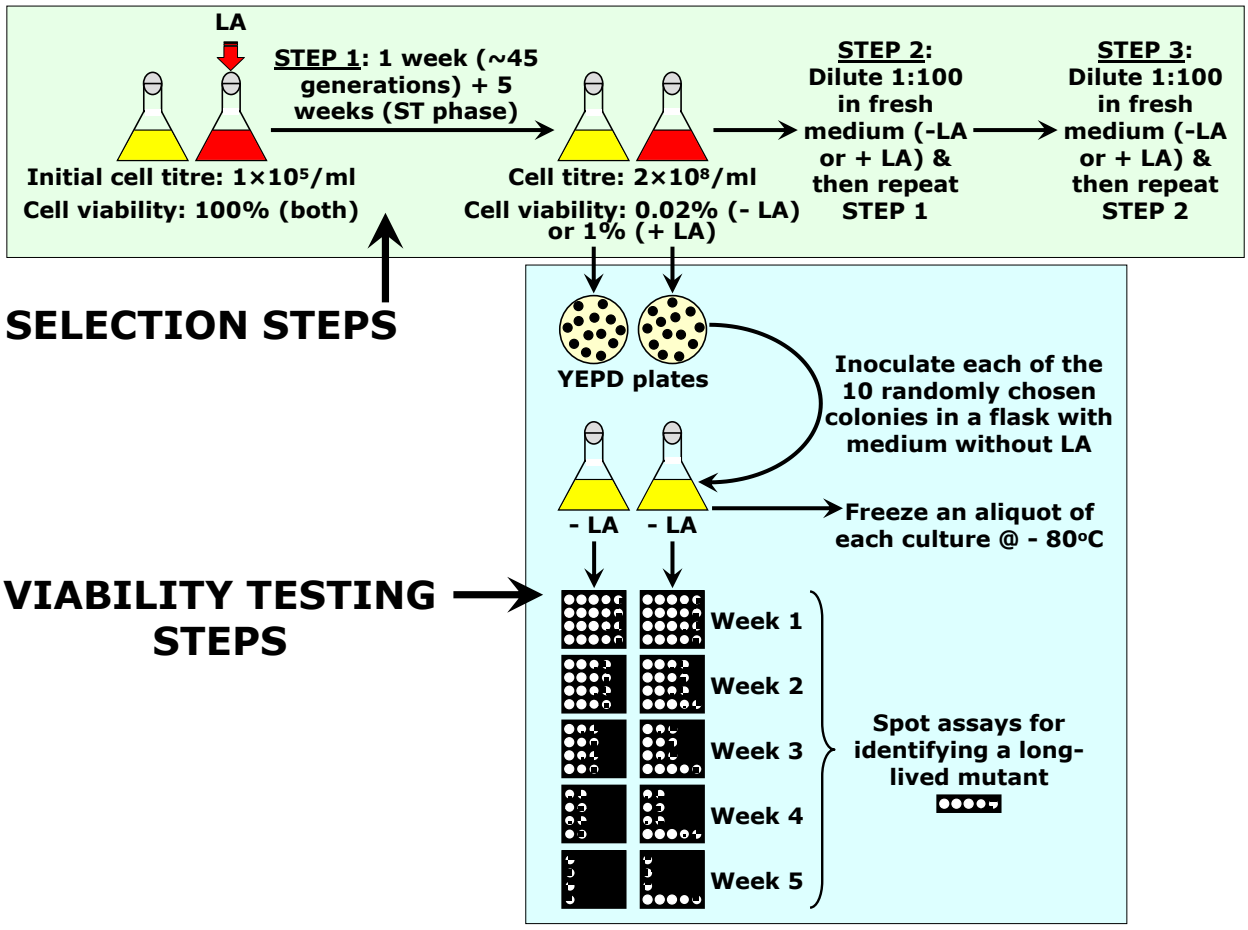


**Figure 4.4.** A 3-step process of the LCA-driven experimental evolution of longevity regulation mechanisms by conducting selection of long-lived yeast species through a lasting exposure to LCA. See text for details.

exposure of yeast to LCA during the selection step (Figure 4.4). If such mutants were detected, an aliquot of their culture in medium lacking LCA was frozen at -80°C. To conduct the second selection step, an aliquot of the culture recovered at the end of the first step of selection was diluted 100 folds in a fresh YP medium containing 0.2% glucose, with or without LCA; if added to a culture for the second selection step, LCA was present at the same final concentration as that in the medium used for the first step of selection (Figure 4.4). From that point, the second selection step was carried out exactly

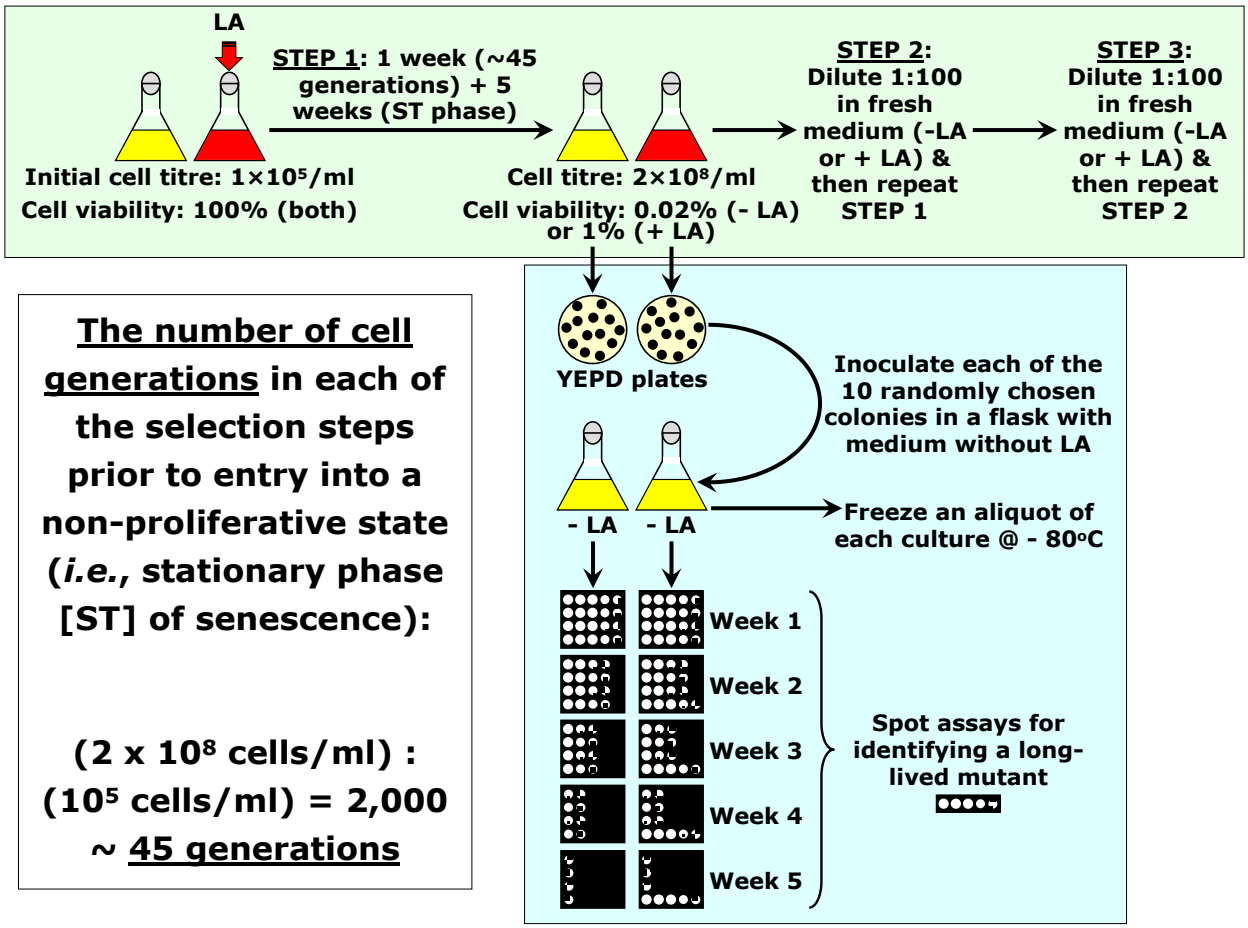


**Figure 4.5.** A 3-step process of the LCA-driven experimental evolution of longevity regulation mechanisms by conducting selection of long-lived yeast species through a lasting exposure to LCA. The number of cell generations in each of the selection steps prior to entry into a non-proliferative state is calculated. See text for details.

as the first one and was followed by a spot-assay viability step described above (Figure 4.4). The second selection step was followed by the third selection step and then by a spot-assay viability step, both conducted as described previously (Figure 4.4).

The 3-step selection of long-lived yeast species depicted in Figures 4.4 to 4.7 was expected to result in the increased fraction of long-lived mutants in a population of yeast exposed to LCA (Figure 4.8). Moreover, the fraction of such long-lived mutants in a

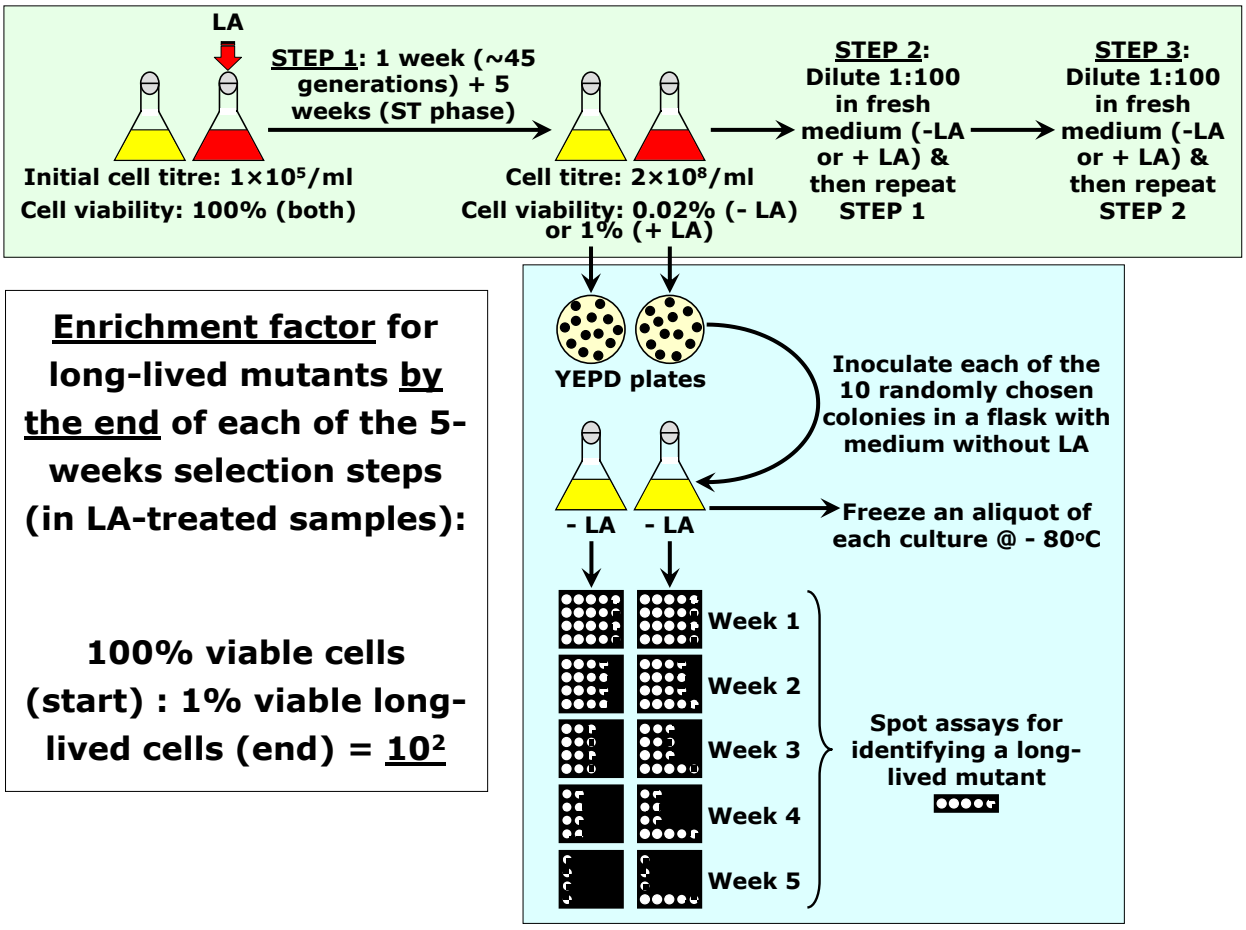


**Figure 4.6.** A 3-step process of the LCA-driven experimental evolution of longevity regulation mechanisms by conducting selection of long-lived yeast species through a lasting exposure to LCA. The enrichment factor for long-lived mutants by the end of each of the selection steps is calculated. See text for details.

population was anticipated to progressively increase at each of the consecutive selection steps (Figure 4.8 and Table 4.1). By carrying out this 3-step selection of long-lived yeast species under laboratory conditions, I found no such mutants at the end of the first selection step, one mutant at the end of the second selection step, and several mutants at the end of the third selection step (Figures 4.9, 4.10 and 4.11, respectively). I therefore concluded that a long-term exposure of wild-type yeast to LCA following the 3 selection

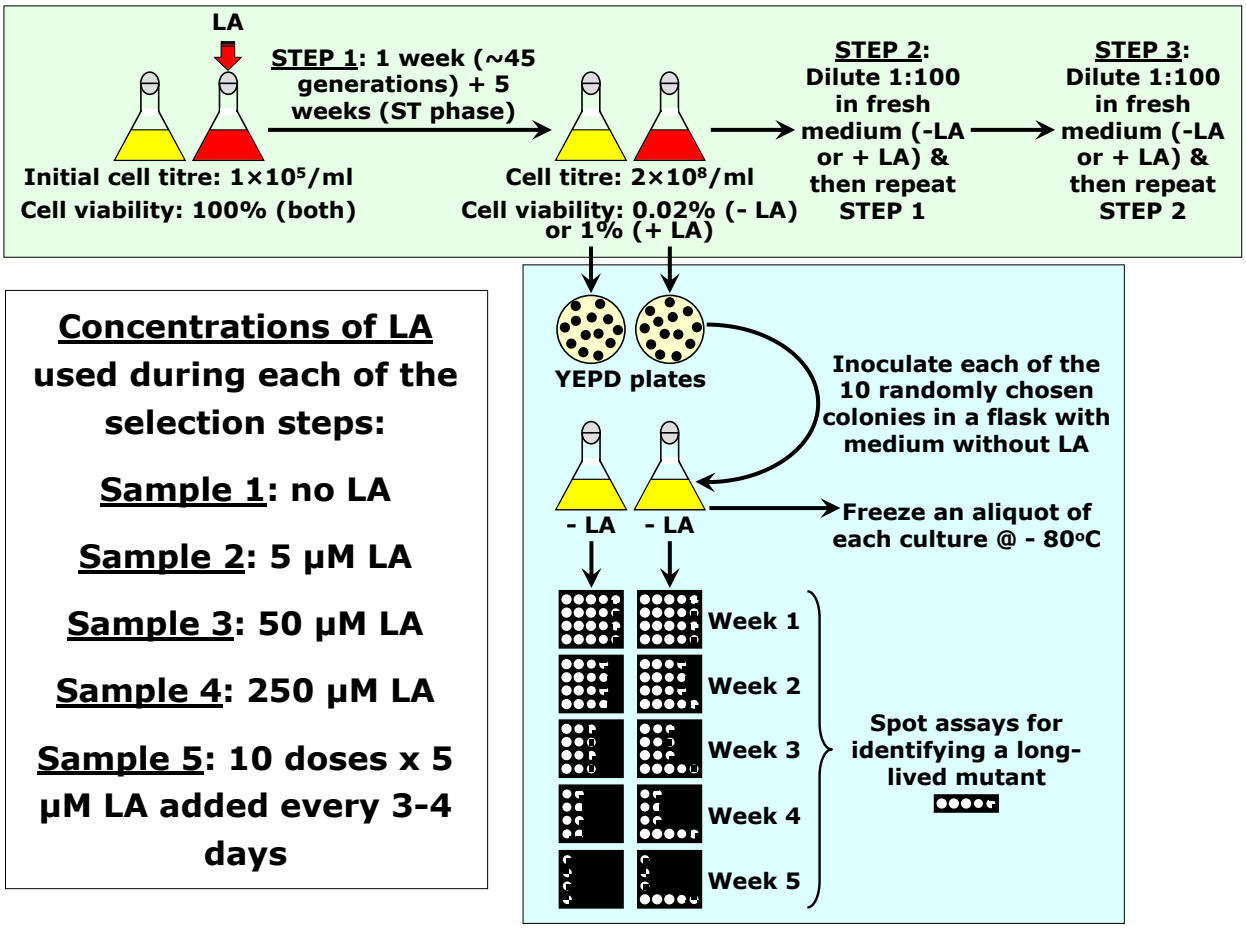


**Figure 4.7.** A 3-step process of the LCA-driven experimental evolution of longevity regulation mechanisms by conducting selection of long-lived yeast species through a lasting exposure to LCA. Concentrations of LCA used during each of the selection steps are shown. See text for details.

steps did result in selection of yeast species that live longer in the absence of LCA than their ancestor. My findings revealed the following order of different LCA concentrations ranked by the efficiency with which they cause the appearance of long-lived species (frequencies of such appearance are shown): 5 µM LCA (~4 x $10^{-8}$/generation) > 10 doses x 5 µM LCA (~3 x $10^{-8}$/generation) > 50 µM LCA (~1 x $10^{-8}$/generation) > 250 µM LCA (no long-lived species found). It should be stressed that, because the lowest used concentration of LCA resulted in the highest frequency of long-lived species appearance,

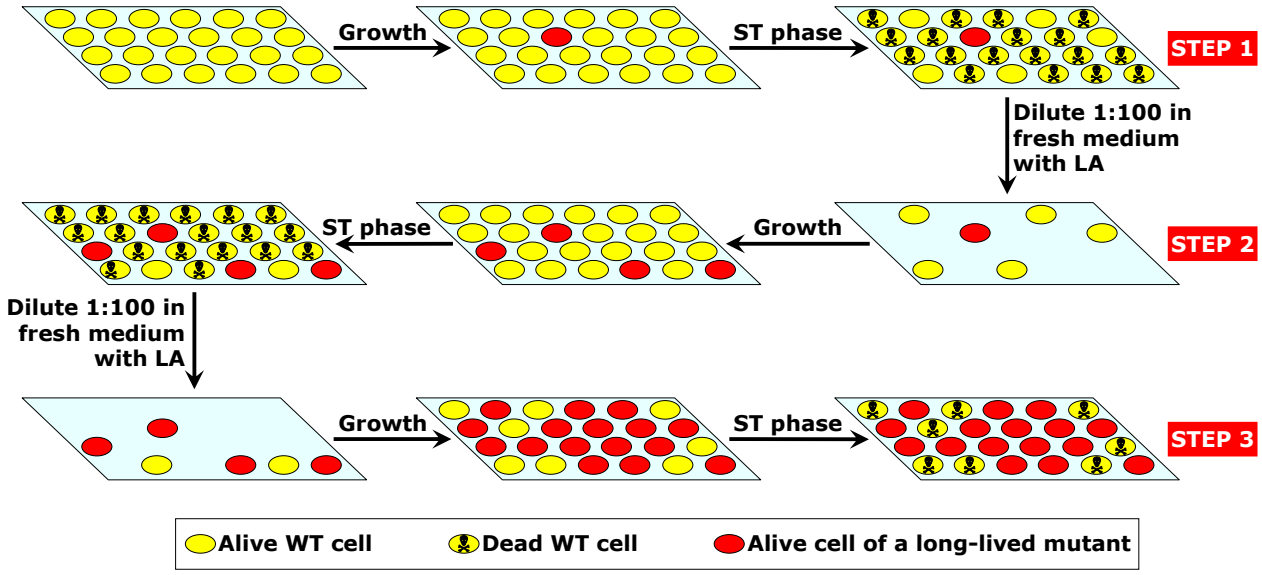


**Figure 4.8.** The fraction of long-lived mutants in a population of yeast is increased by the end of each of the 3 steps of the LCA-driven experimental evolution of longevity regulation mechanisms.

it is unlikely that the life-extending mutations they carry are due to mutagenic action of LCA.

## 4.5 Discussion

By fusing the xenohormesis hypothesis [119, 343, 344], the "anti-aging side effect" hypothesis [349] and the proposed in this chapter my hypothesis on longevity regulation by bile acids and rapamycin within ecosystems, I put forward a unified hypothesis of the xenohormetic, hormetic and cytostatic selective forces that may drive the evolution of longevity regulation mechanisms at the ecosystemic level. In my unified hypothesis (Figure 4.3), organisms from all domains of life (*i.e.*, bacteria, fungi, plants and animals) within an ecosystem are able to synthesize chemical compounds that 1) are produced and then released into the environment permanently or only in response to

**Table 4.1.** The fraction of long-lived mutants in a population of yeast is increased by the end of each of the 3 steps of the LCA-driven experimental evolution of longevity regulation mechanisms.

| If the frequency of mutations is: | Enrichment factor for long-lived mutants | The fraction of long-lived mutants & their number in a population of yeast by the end of each of the 3 steps of LA-driven experimental evolution | |
|---|---|---|---|
| | | **Fraction** | **Number** |
| $10^{-8}$/ generation | $10^2$ | **STEP 1**: $(10^{-8} \times 45 \text{ generations}) \times 10^2 = 4.5 \times 10^{-5}$ | 4-5 out of 100,000 |
| | | **STEP 2**: $[(4.5 \times 10^{-5}) + (10^{-8} \times 45 \text{ gen.})] \times 10^2 \sim 4.5 \times 10^{-3}$ | 4-5 out of 1,000 |
| | | **STEP 3**: $[(4.5 \times 10^{-3}) + (10^{-8} \times 45 \text{ gen.})] \times 10^2 \sim 4.5 \times 10^{-1}$ | 4-5 out of 10 |
| $10^{-7}$/ generation | $10^2$ | **STEP 1**: $(10^{-7} \times 45 \text{ generations}) \times 10^2 = 4.5 \times 10^{-4}$ | 4-5 out of 10,000 |
| | | **STEP 2**: $[(4.5 \times 10^{-4}) + (10^{-7} \times 45 \text{ gen.})] \times 10^2 \sim 4.5 \times 10^{-2}$ | 4-5 out of 100 |
| | | **STEP 3**: $[(4.5 \times 10^{-2}) + (10^{-7} \times 45 \text{ gen.})] \times 10^2 \sim 4.5 \times 10^{0}$ | ALL |
| $10^{-6}$/ generation | $10^2$ | **STEP 1**: $(10^{-6} \times 45 \text{ generations}) \times 10^2 = 4.5 \times 10^{-3}$ | 4-5 out of 1,000 |
| | | **STEP 2**: $[(4.5 \times 10^{-3}) + (10^{-6} \times 45 \text{ gen.})] \times 10^2 \sim 4.5 \times 10^{-1}$ | 4-5 out of 10 |
| | | **STEP 3**: $[(4.5 \times 10^{-1}) + (10^{-6} \times 30 \text{ gen.})] \times 10^2 \sim 4.5 \times 10^{1}$ | ALL |

deteriorating environmental conditions, increased population density of competitors and/or predators, or changes in food availability and its nutrient and/or caloric content; 2) are mildly toxic compounds that trigger a hormetic response in an organism that senses them or, alternatively, are not toxic for any organism within the ecosystem and do not cause a hormetic response; 3) are cytostatic compounds that attenuate the TOR-governed signaling network (*e.g.*, rapamycin and resveratrol) or, alternatively, do not modulate this growth-promoting network (*e.g.*, LCA and other bile acid); and 4) extend longevity of organisms that can sense these compounds, thereby increasing their chances of survival and creating selective force aimed at maintaining the ability of organisms composing the ecosystem to respond to these compounds by undergoing specific life-extending changes to their physiology. My hypothesis implies that the evolution of

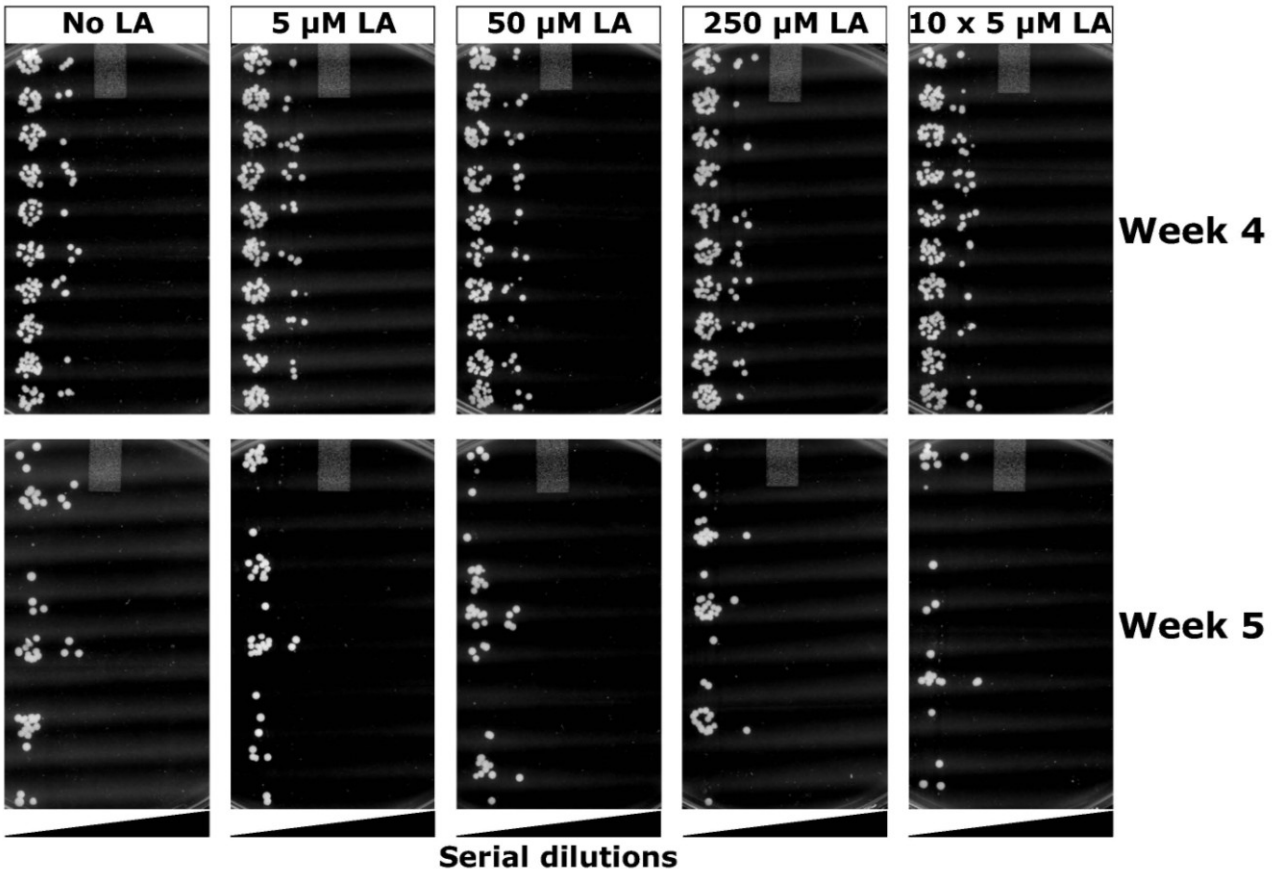


**Figure 4.9.** A spot-assay of cell survival for the 1st step of the LCA-driven experimental evolution of longevity regulation mechanism.

longevity regulation mechanisms in each group of the organisms composing an ecosystem is driven by the ability of this group of organisms to undergo specific life-extending physiological changes in response to a compendium of "critical" chemical compounds that are permanently or transiently released to the ecosystem by other groups of organisms.

To verify my hypothesis empirically, I carried out the LCA-driven multistep selection of long-lived yeast species under laboratory conditions. I found that a lasting exposure of wild-type yeast to LCA results in selection of yeast species that live longer in the absence of this bile acid than their ancestor. My data enabled to rank different

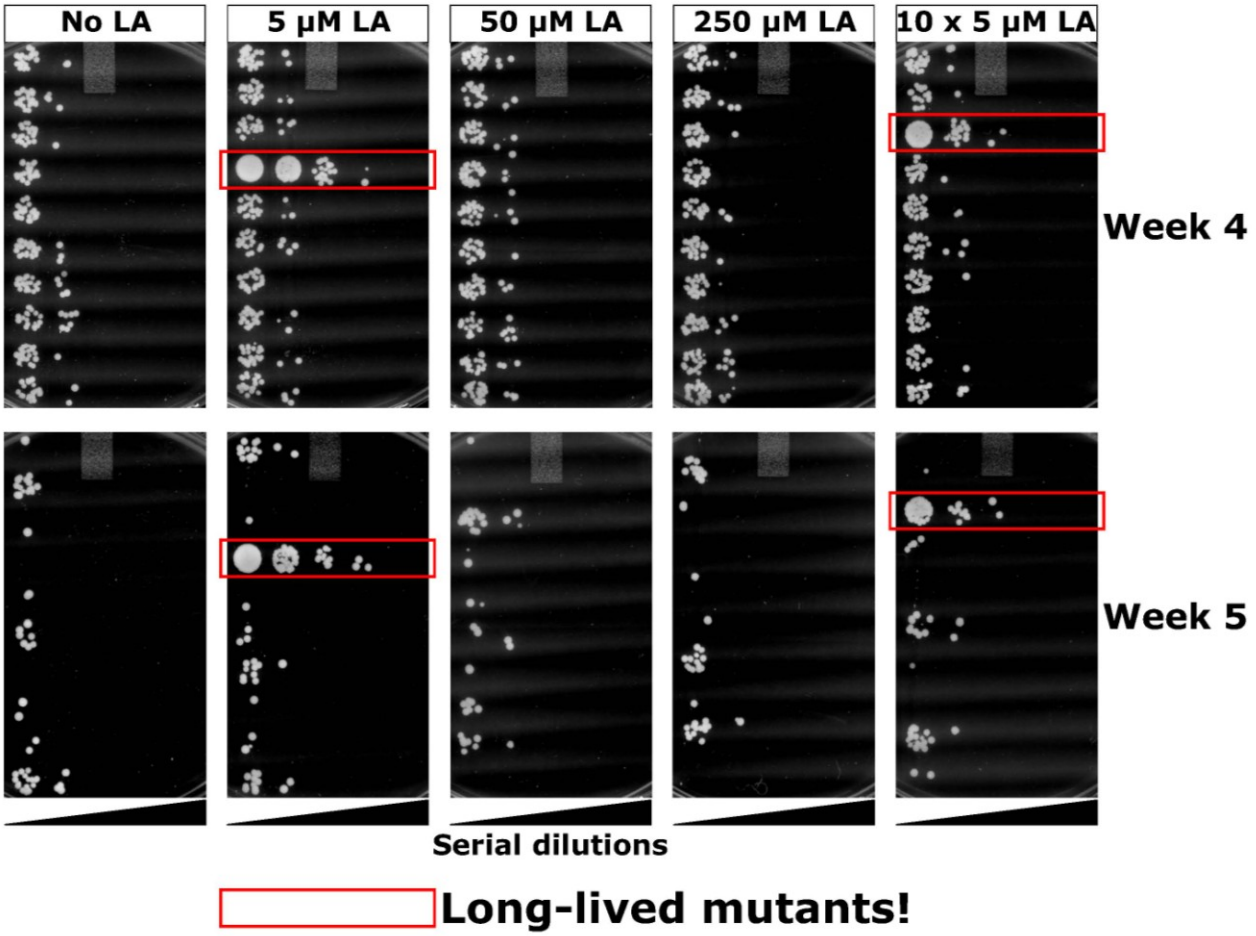


**Figure 4.10.** A spot-assay of cell survival for the 2nd step of the LCA-driven experimental evolution of longevity regulation mechanism.

concentrations of LCA with respect to the efficiency with which they cause the appearance of long-lived yeast species. Because the lowest used concentration of LCA resulted in the highest frequency of long-lived species appearance, I believe that it is unlikely that the life-extending mutations they carry are due to mutagenic action of this bile acid.

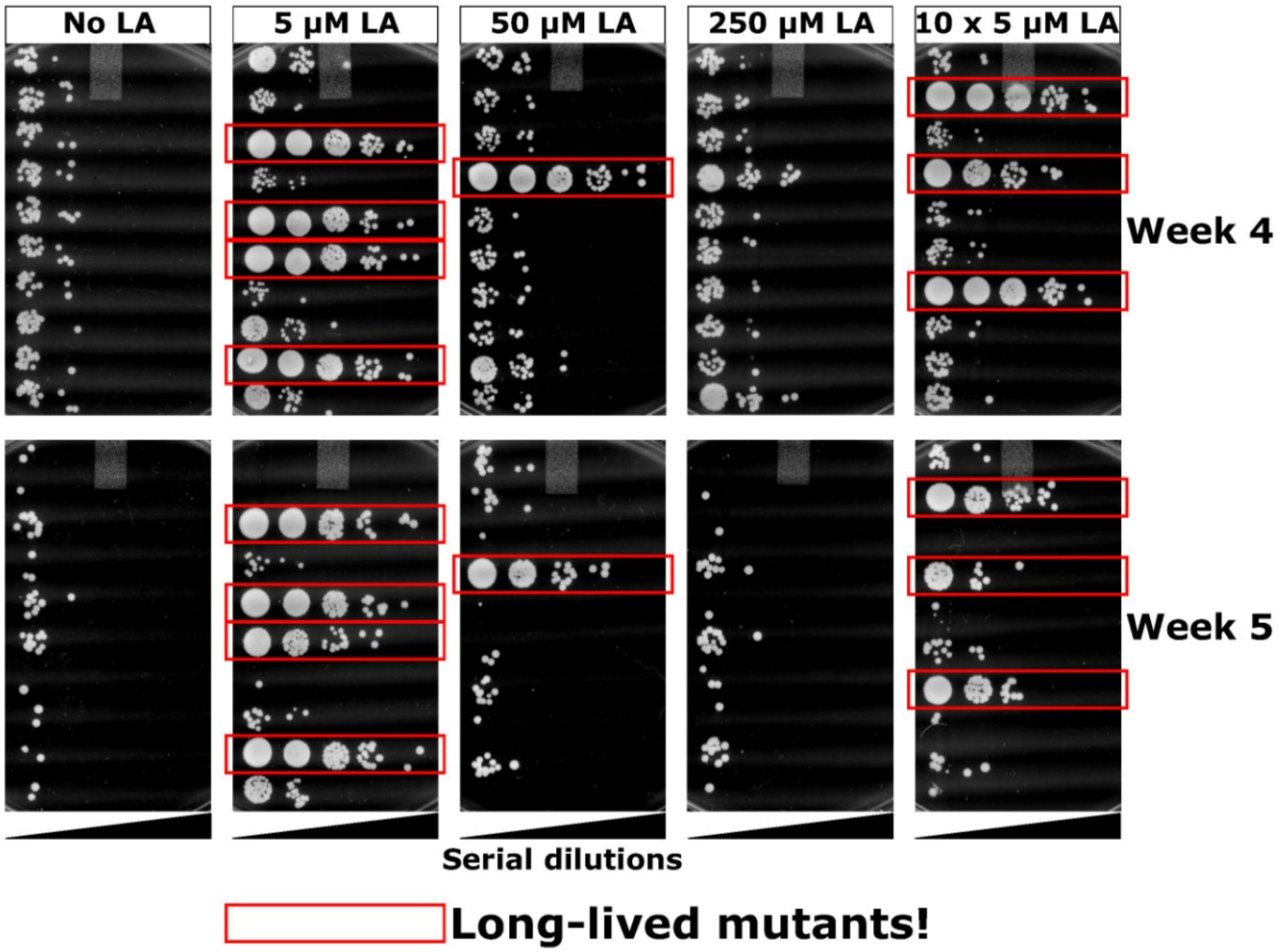


**Figure 4.11.** A spot-assay of cell survival for the 3rd step of the LCA-driven experimental evolution of longevity regulation mechanism.

## 4.6 Conclusions

To test the validity of other aspects of my hypothesis on the ecosystemic evolution of longevity regulation mechanisms, future studies need to address the following most critical questions: 1) what genes are affected by mutations responsible for the extended longevity of selected long-lived yeast species? 2) how these mutations influence a compendium of the housekeeping longevity-related processes modulated by LCA in chronologically aging yeast ([247]; Figure 4.1)?; 3) 3) will these mutations affect

the growth rate of yeast in media with or without LCA? 4) will selected long-lived yeast species be able to maintain their ability to live longer than wild-type yeast if they undergo several successive passages in medium without LCA? - and, thus, is there selective pressure aimed at maintaining of an "optimal" rather than a "maximal" chronological life span of yeast (due to, *e.g.*, a proposed selective advantage of the envisioned "altruistic" program [356 - 361] of chronological aging in yeast)? and 5) if mixed with an equal number of wild-type yeast cells, will selected long-lived yeast species out-grow and/or out-live them in medium without LCA or the opposite will happen (due to selective pressure on yeast aimed at maintaining of the so-called "altruistic" program [356 - 361] of their chronological aging)?

# 5 Lithocholic acid exhibits a potent and selective anti-tumor effect in cultured human neuroblastoma cells by activating both intrinsic and extrinsic pathways of their apoptotic death, sensitizing them to hydrogen peroxide-induced apoptotic death, and preventing growth and proliferation of their neighboring neuroblastoma cells in the culture

## 5.1 Abstract

Aging is one of the major risk factors in the onset and incidence of cancer [154 - 156], and cancer is considered as one of the numerous age-associated diseases whose onset can be delayed and incidence reduced by anti-aging interventions [157 - 162]. As I mentioned in chapter 1, the interplay between aging and cancer is intricate as these two complex and dynamic biological phenomena have both convergent and divergent underlying mechanisms [157 - 223]. One of the major objectives of my thesis was to examine if lithocholic acid (LCA), a novel anti-aging compound that I identified in a high-throughput chemical genetic screen (see chapter 3), also exhibits an anti-tumor effect in cultured human cancer cells by activating certain anti-cancer processes that may (or may not) play an essential role in cellular aging. As a model system for addressing this important question (and if LCA indeed displays an anti-tumor effect, for establishing the mechanism underlying such effect), I choose several cell lines of the human neuroblastoma (NB) tumor.

In this chapter of my thesis, I describe findings providing strong evidence that LCA exhibits a potent anti-tumor effect in cultured human NB cells by: 1) activating both intrinsic (mitochondrial) and extrinsic (death receptor) pathways of apoptotic death in

these cells; 2) sensitizing them to hydrogen peroxide-induced apoptotic death; and 3) preventing growth and proliferation of their neighbouring NB cells in the culture. Importantly, my findings imply that LCA does not display any of these deleterious effects in human neurons and, therefore, is a selective anti-tumor compound. Moreover, my mass spectrometry-based measurement of intracellular and extracellular levels of exogenously added LCA revealed that this bile acid does not enter cultured NB cells. Thus, LCA prevents proliferation of human NB cells and selectively kills these cancer cells by binding to their surface and then initiating intracellular signaling cascades that not only impair their growth and division, but also cause their apoptotic death. The demonstrated inability of LCA to enter cultured human NB cells suggests that this potent and selective anti-cancer compound is unlikely to display undesirable side effects in non-cancerous human neurons.

Of note, a recent collaborative effort of the laboratories of Dr. Troy Harkness (Department of Anatomy and Cell Biology, University of Saskatchewan) and Dr. Vladimir Titorenko has revealed that in low concentrations LCA kills cultured MCF7 human breast cancer cells and F98 rat glioblastoma cells. Thus, LCA exhibits a universal anti-tumor effect, as it has a very broad cytotoxic effect on cancer cells derived from different tissues and from different organisms.

## 5.2 Introduction

In the commonly accepted paradigm of the relationship between aging and cancer, these two complex and dynamic biological phenomena share common aetiology (*i.e.*, an age-related progressive accumulation of cellular damage) and have coalescent underlying

mechanisms [157 - 159]. In this paradigm: 1) genetic interventions that accelerate the age-related accumulation of cellular damage (or hasten some other common aetiologies of aging and cancer) and target some of the common mechanisms underlying aging and cancer are expected to exhibit both pro-aging and pro-cancer effects; and 2) genetic, pharmacological and/or dietary interventions that reduce the age-related accumulation of cellular damage (or attenuate some other common aetiologies of aging and cancer) and target some of the common mechanisms underlying aging and cancer are expected to exhibit both anti-aging and anti-cancer effects [157 - 159]. A body of evidence supports the validity of this hypothesis (see chapter 1 of my thesis for a detailed discussion of this topic). The predicted by the commonly accepted paradigm of the relationship between aging and cancer convergent underlying mechanisms linking these two biological phenomena include: 1) a longevity-defining signaling network that integrates the pro-aging AMP-activated protein kinase/target of rapamycin (AMPK/TOR), cAMP/protein kinase A (cAMP/PKA) and insulin/insulin-like growth factor 1 (IGF-1) signaling pathways and also includes a sirtuin-governed protein deacetylation module [156 - 208]; 2) autophagy, a cytoprotective process in which old and damaged cellular proteins and organelles are delivered to the lysosome for degradation that allows cells to recycle their damaged components under various cellular stress conditions [157, 158, 364 - 378]; and 3) mitochondrial TCA cycle and respiration as well as ROS production and detoxification in mitochondria [157, 158, 379 - 389].

In the conceptual framework of the above paradigm of the relationship between aging and cancer, pharmacological interventions that attenuate common aetiologies of these complex biological phenomena and target their common underlying mechanisms

are expected to exhibit both anti-aging and anti-cancer effects [157 - 159]. In a series of experiments described in this chapter of my thesis, I examined if the recently discovered anti-aging compound LCA (see chapter 3) also exhibits an anti-tumor effect in cultured human NB cancer cells. As I found, this bile acid indeed displays a potent and specific anti-tumor effect. My elucidation of mechanisms underlying such effect of LCA provided strong evidence that this bile acid: 1) activates both intrinsic (mitochondrial) and extrinsic (death receptor) pathways of apoptotic death in cultured human NB cancer cells; 2) sensitizes these cells to hydrogen peroxide-induced death; and 3) prevents growth and proliferation of their neighbouring NB cells in the culture.

## 5.3 Materials and Methods

### Cell cultures

Human NB cell lines SK-n-MCIXC, BE(2)-m17 and SH-SY5Y were cultured in a mixture (ratio 1:1) of Dulbecco's modified Eagle's medium (DMEM) and Hamm's F12 nutrient mixture (Gibco, Carlsbad, CA) with 10% fetal bovine serum (FBS) (HyClone, Logan, UT), while SK-n-SH cells were cultured in Eagle's minimal essential medium (MEM) (Gibco) with 10% FBS. Lan-1 cells were cultured in DMEM (Gibco) with 10% bovine calf serum (BCS) (HyClone). Human primary neurons were prepared from fetal cerebrum tissue and cultured as previously described [362], in accordance with the Canadian Institute of Health Research regulations and as approved by the McGill University Institutional Review Board. All cell lines were cultured at 37°C with 5% $CO_2$.

### Treatment of cells with LCA, hydrogen peroxide and z-DEVD-fmk

Stock solutions of LCA (Sigma-Aldrich, St Louis, MI) in varying concentrations were first made in 100% dimethyl sulfoxide (DMSO) (Sigma-Aldrich, St Louis, MI). These stock solutions were then diluted to a certain final concentration of LCA (the final concentration of DMSO was always kept at 1%) in either DMEM/Hamm's F12 mixture with 10% FBS (for SK-n-MXIXC and BE(2)-m17 cells), MEM with 10% FBS (for SK-n-SH cells) or DMEM with 10% BCS (for Lan-1 cells). For treatment of human primary neurons, stock solutions of LCA in varying concentrations made in 100% DMSO were diluted in MEM containing 0.225% sodium bicarbonate, 1 mM sodium pyruvate, 2 mM L-glutamine, 0.1% dextrose (all from Life Technologies, Gaithersburg, MD) and 5% FBS (HyClone, Logan, UT) to a certain final concentration of LCA (the final concentration of DMSO was always kept at 1%). In experiments involving cell treatment with z-DEVD-fmk, this caspase-3 inhibitor was added to a final concentration of 5 μM simultaneously with LCA.

For hydrogen peroxide treatment, 30% hydrogen peroxide (Fisher Scientific, Waltham, MA) was diluted in sterile $H_2O$ and added directly to the cultures after 24 h of pre-treatment with LCA. Cell cultures supplemented with hydrogen peroxide were incubated for 24 h.

**Cell viability assays**

Chromatin in cells exposed to LCA and/or hydrogen peroxide was visualized with the fluorescent dye Hoechst used at a final concentration of 4 μM in culture media and viewed using fluorescence microscopy. For each cell culture, the percentage of viable non-apoptotic cells carrying intact, non-fragmented nuclei containing non-condensed

chromatin was calculated. Dead apoptotic cells carried fragmented nuclei containing condensed chromatin, a hallmark event of apoptotic death.

The number of viable cells in cultures exposed to LCA was measured using the MTT (3-(4,5-dimethylthiozol-2-yl)-2,5-diphenyltetrazolium bromide)-based CellTiter 96 Non-Radioactive Cell Proliferation Assay (Promega, Madison, WI). In this assay, only viable, metabolically active cells were able to reduce the yellow tetrazolium salt of MTT to form a purple formazan product. This insoluble product was solubilized by the addition of a detergent. The resulting intracellular purple formazan was then detected spectrophotometrically using a 96-well plate reader at a wavelength of 570 nm. The signal was corrected to account for cellular debris using a wavelength of 630 nm.

**Visualization of mitochondria and measurement of the mitochondrial membrane potential by fluorescence microscopy**

Mitochondrial morphology of cells treated with LCA was visualized using MitoTracker Red CMXRos (Molecular Probes, San Diego, CA) used at a concentration of 125 nM in the culture media. Cells were viewed using fluorescence microscopy, and the percentage of cells displaying fragmented mitochondria was calculated.

The mitochondrial membrane potential ($\Delta\Psi$) was measured using tetramethylrhodamine ethyl ester (TMRE), a cell-permeant, cationic fluorescent dye. The extent of reversible sequestration of TMRE by mitochondria is proportional to the value of $\Delta\Psi$. Cells were incubated in 50 nM of TMRE for 20 minutes and directly viewed using fluorescence microscopy. The percentage of TMRE-positive cells displaying a detectable level of $\Delta\Psi$ was calculated.

**Fluorescence microscopy**

For all cells and fluorescent dyes, images were collected with a Nikon Eclipse (TE2000-U) inverted fluorescence microscope under 20 × magnification. A filter cube with an excitation wavelength of 330-380 nm was used to visualize Hoechst-stained cells. Cells stained with MitoTracker Red CMXRos and TMRE were visualized using filter cubes with excitations of 590-650 nm and 532-587 nm, respectively.

**Subcellular fractionation, isolation of the crude mitochondrial fraction, protein separation by SDS-PAGE and immunoblotting**

Cells were washed with PBS, resuspended in homogenization buffer (8% sucrose, 20 mM Tricine pH 7.8, 1 mM EDTA) and homogenized with a dounce homogenizer (VWR, Mississauga, ON). Cell debris was sedimented by centrifugation for 10 min at 2000 rpm. The resulting supernatant was then centrifuged for 10 min at 13000 rpm at 4$^{o}$C. The pellet containing the crude mitochondrial fraction was resuspended in lysis buffer (150 mM NaCl, 2 mM EDTA, 0.5% Triton X-100 (v/v), 0.5% sodium deoxycholate (w/v) and 50 mM Tris-HCl pH 7.5).

Proteins recovered in the mitochondrial (pellet) and cytoplasmic (supernatant) fractions were resolved by SDS-PAGE in a 15% polyacrylamide gel and then transferred to a PVDF Immobilon-P membrane. Following wash with 5% milk, blots were incubated with 1/500 anti-cytochrome-c antibody (Pharmingen, San Diego, CA) or 1/500 anti-mitoHsp70 antibody (ABR Affinity BioReagents, Golden, CO). Immunoreactivity was detected using 1/1000 anti-mouse horseradish peroxidase-conjugated antibody

(Amersham, Oakville, ON). Antigen-antibody complexes were visualized by enhanced chemiluminescence using an ECL plus chemiluminescence Western blotting detection reagents (Amersham Pharmacia Biotech, Piscataway, NJ).

**Caspase activity assays**

Proteins were extracted from harvested cells using an ice-cold lysis buffer containing 50 mM HEPES, 0.1% CHAPS, 0.1 mM EDTA and protease inhibitors (0.1μg/ml TLCK, 0.5 μg/ml leupeptin, 38 mg/ml AEBSF and 0.1 μg/ml pepstatin A). The cell lysate was centrifuged at 13000 × g for 5 min at 4$^{o}$C to remove cell debris and any detergent-insoluble proteins. The supernatant was collected and frozen at -80$^{o}$C. Extracts were thawed and protein concentrations were quantified with the Pierce BCA assay (Thermo Scientific, Waltham, MA). The extracts were then assayed for caspase activities using fluorogenic substrates specific for caspase-1 (10 μM Ac-YVAD-AFC), caspase-3 (5 μM Ac-DEVD-AFC), caspase-6 (10 μM Ac-VEID-AFC), caspase-8 (10 μM Ac-IETD-AFC) or caspase-9 (10 μM Ac-LEHD-AFC) in caspase reaction buffer (20 mM PIPES, 30 mM NaCl, 10 mM DTT, 1 mM EDTA, 0.1% CHAPS and 10% sucrose, pH 7.2). The time-dependent release of the fluorescent compound 7-amino-4-trifluoromethyl coumarin (AFC) was monitored using a Bio-Rad Fluoromark fluorometer (Hercules, CA) at an excitation wavelength of 390 nm and an emission wavelength of 538 nm. Measurements were recorded at 2 min intervals for 1 h. A standard curve of AFC fluorescence was used to calculate AFC (in picomoles) released in the reactions. Specific activities were expressed as picomoles of AFC released per microgram of protein per minute, based on the linear range of the curve.

**Pro-caspase-3 and pro-caspase-6 cleavage assays**

50 μg of protein from crude cellular extracts were resolved by SDS-PAGE in a 15% polyacrylamide gel and then transferred to a PVDF Immobilon-P membrane (Millipore, Bedford, MA). Following wash with 5% milk, blots were incubated with antibodies used at the following dilutions: 1/500 anti-cleaved-caspase-3 p17 (Cell Signaling, Beverly, MA), 1/250 anti-cleaved-caspase-6 p10 (Pharmingen, San Diego, CA) and 1/5000 anti-β-Actin (Sigma-Aldrich, St Louis, MI). Immunoreactivity was detected using 1/2000 (for anti-rabbit) and 1/5000 (for anti-mouse) horseradish peroxidase-conjugated secondary antibodies (Amersham, Oakville, ON). Antigen-antibody complexes were detected by enhanced chemiluminescence using an ECL plus chemiluminescence Western blotting detection reagents (Amersham Pharmacia Biotech, Piscataway, NJ).

**Mass spectrometric measurement of LCA**

Mass spectrometry-based quantitative analysis of LCA was performed as previously reported [363]. In brief, lipids were extracted by a modified Bligh and Dyer method [363] from cells pelleted by centrifugation for 16000 × g for 5 min at 4$^{o}$C and from the supernatant of cultural medium. The extracted lipids were dried under nitrogen and resuspended in chloroform. Immediately prior to injection the extracted lipids were combined with 2:1 methanol:chloroform with 0.1% (v/v) ammonium hydroxide. This was injected directly into a Q-TOF 2 mass spectrometer (Waters, Milford, MA) using a nano-ESI spray source at 1 μl/min. Spectra were obtained in a negative-ion mode. Acquired

spectra were centroided using the Masslynx software then deconvoluted and deisotoped with Excel macros.

**Statistical analysis**

Statistical analysis was performed using Systat (version 10.2) and Microsoft Excel's (2007) Analysis ToolPack-VBA. Comparisons between multiple groups were done using multiple t-tests followed by a Bonferroni correction. All data are presented as group means ± SEM. In all statistical tests, values of $p < 0.05$ were considered significant.

## 5.4 Results

### 5.4.1 LCA selectively kills cultured human NB cells by causing their apoptotic death if used at concentrations that are not cytotoxic to primary cultures of human neurons

In addition to its great life-extending efficacy in yeast, LCA also exhibits a potent and selective anti-tumor effect in several lines of cultured human NB cells. In fact, I found that this bile acid kills cultured human NB cell lines BE(2)-m17, Lan-1, SK-n-SH and SK-n-MCIXC if used at concentrations that are not cytotoxic or only mildly cytotoxic (as in case of Lan-1 cells) to primary cultures of human neurons (Figures 5.1 - 5.4). The percentage of viable cells in these cell viability experiments was calculated as a portion of their population displaying a detectable level of redox potential which was visualized using the yellow tetrazolium salt of MTT (3-(4,5-dimethylthiozol-2-yl)-2,5-diphenyltetrazolium bromide). In this assay, only viable, metabolically active cells were

able to reduce the yellow tetrazolium salt of MTT to form a purple formazan product, which was detected spectrophotometrically at a wavelength of 570 nm [397 - 400].

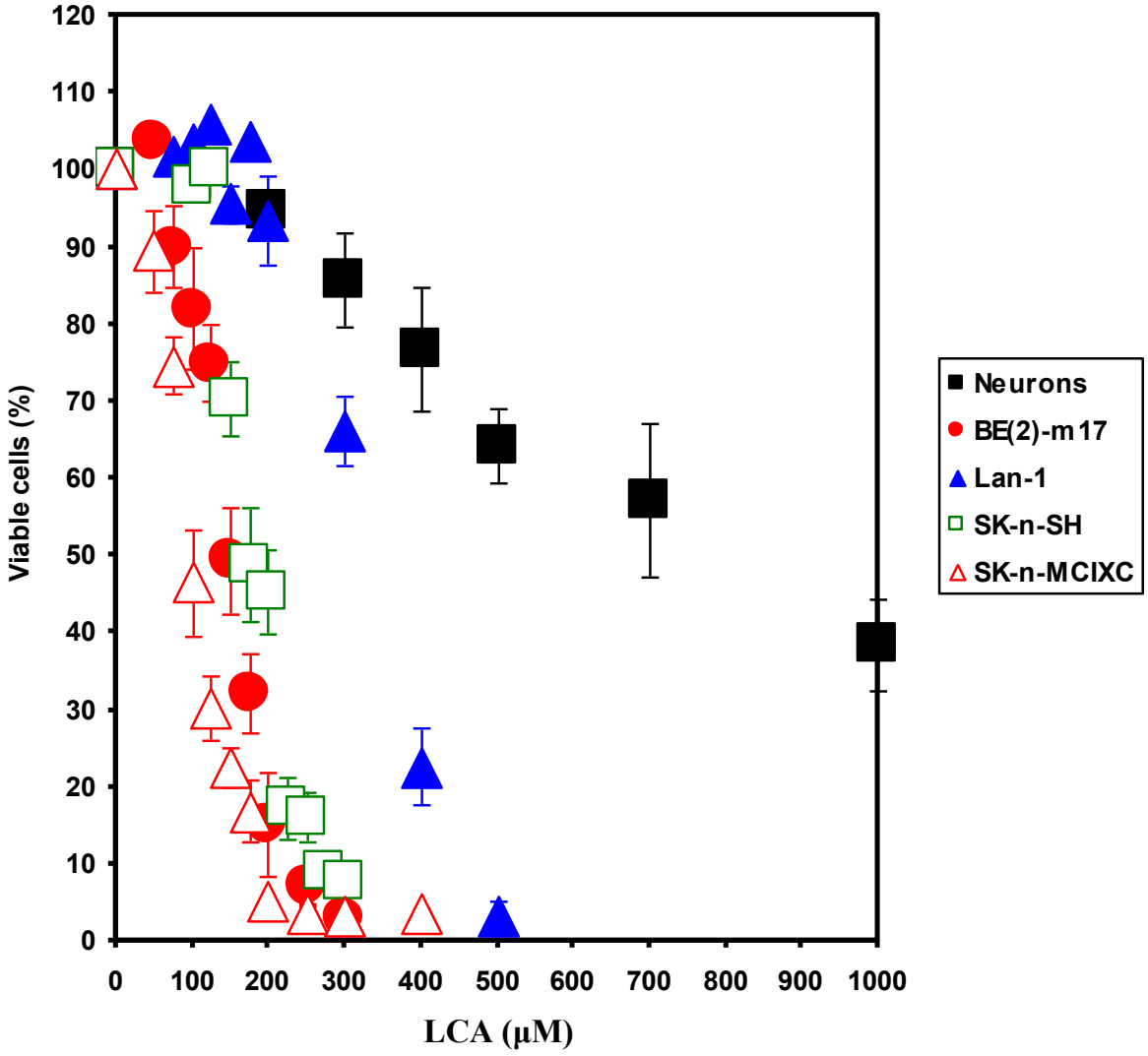


**Figure 5.1.** LCA kills cultured human NB cell lines BE(2)-m17, Lan-1, SK-n-SH and SK-n-MCIXC if used at concentrations that are not cytotoxic or only mildly cytotoxic (as in case of Lan-1 cells) to primary cultures of human neurons. The percentage of viable cells was calculated as a portion of their population displaying a detectable level of redox potential which was visualized using the MTT (3-(4,5-dimethylthiozol-2-yl)-2,5-diphenyltetrazolium bromide)-based CellTiter 96 Non-Radioactive Cell Proliferation Assay. In this assay, only viable, metabolically active cells were able to reduce the yellow tetrazolium salt of MTT to form a purple formazan product, which was detected spectrophotometrically at a wavelength of 570 nm. Data are presented as means ± SD (n = 4-6).

The NB cell line SK-n-MCIXC was the most sensitive (as compared to other NB cell lines tested and especially as compared to primary cultures of human neurons) to the cytotoxic effect of LCA; I found that less than 10% of SK-n-MCIXC cells remain viable when exposed to 200 μM LCA, a concentration which was not cytotoxic to primary cultures of human neurons (Figure 5.2).

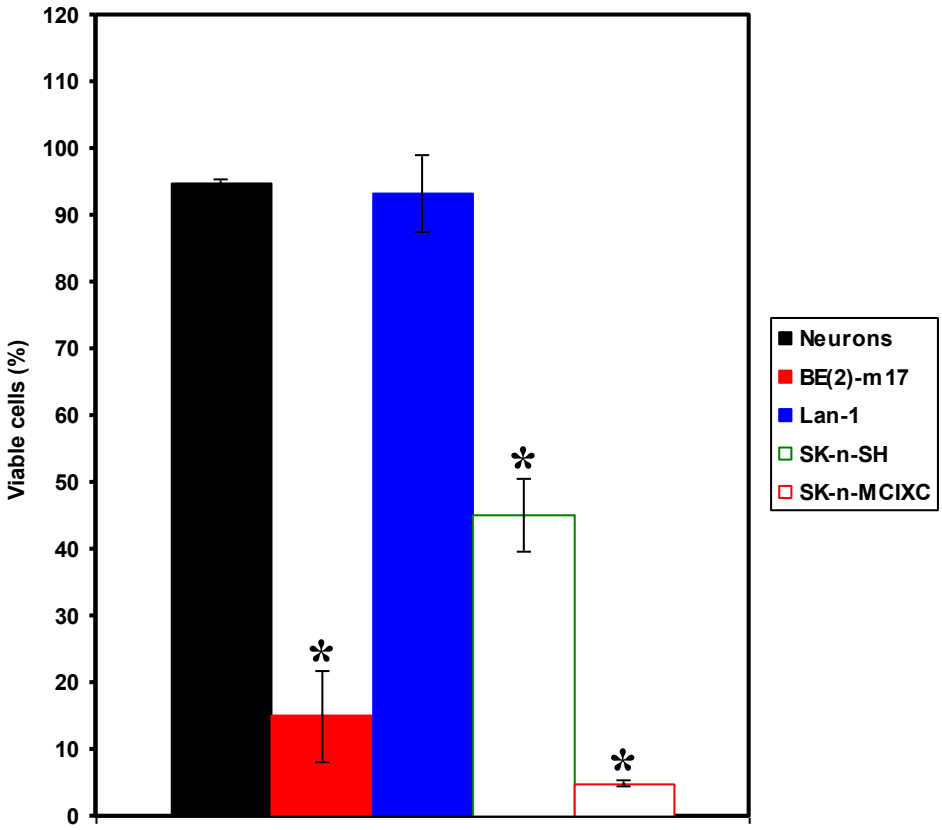


**Figure 5.2.** The NB cell line SK-n-MCIXC is the most sensitive (as compared to other NB cell lines tested and especially as compared to primary cultures of human neurons) to the cytotoxic effect of LCA. Less than 10% of SK-n-MCIXC cells remain viable when exposed to 200 μM LCA, a concentration which is not cytotoxic to primary cultures of human neurons (Figure 5.2). The percentage of viable cells was calculated as a portion of their population displaying a detectable level of redox potential which was visualized using the MTT (3-(4,5-dimethylthiozol-2-yl)-2,5-diphenyltetrazolium bromide)-based CellTiter 96 Non-Radioactive Cell Proliferation Assay. In this assay, only viable, metabolically active cells were able to reduce the yellow tetrazolium salt of MTT to form a purple formazan product, which was detected spectrophotometrically at a wavelength of 570 nm. Data are presented as means ± SD (n = 4-6); *$p < 0.05$.

Two NB cell lines, BE(2)-m17 and SK-n-SH, exhibited much higher sensitivity to LCA than primary cultures of human neurons (or than the NB cell line Lan-1); in fact, I found that less than 10% of BE(2)-m17 and SK-n-SH cells remain viable when exposed to 300 μM LCA, a concentration which was not cytotoxic to primary cultures of human neurons and only mildly cytotoxic to Lan-1 cells (Figure 5.3).

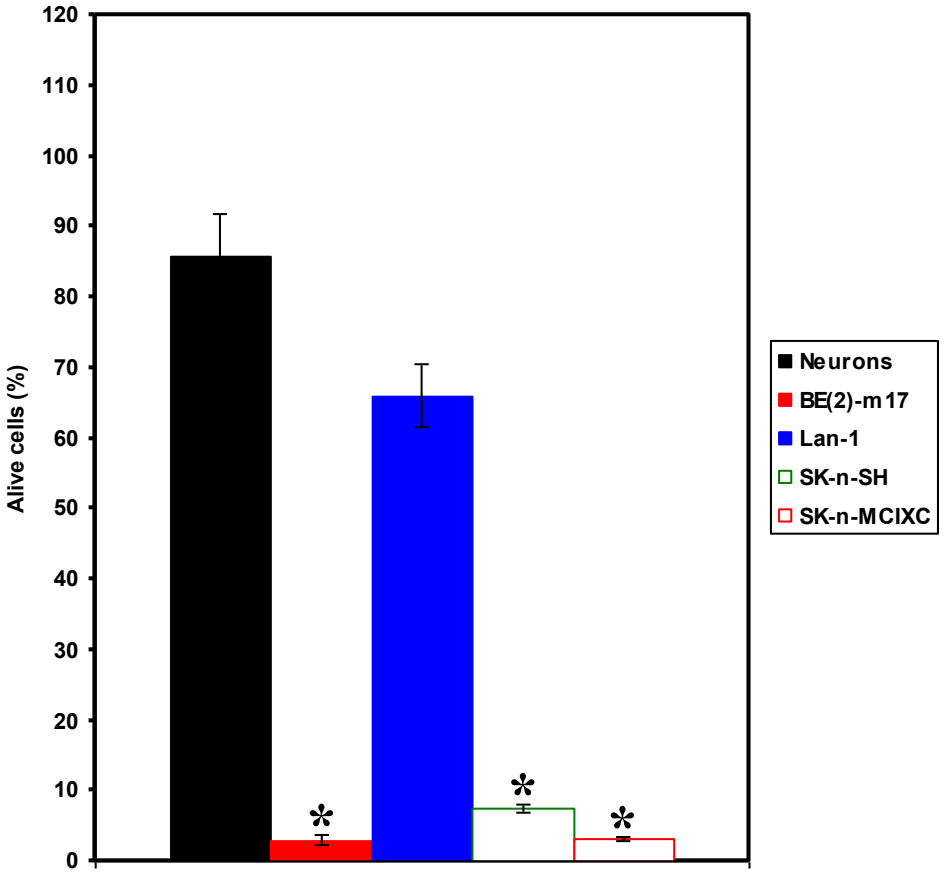


**Figure 5.3.** The NB cell lines BE(2)-m17 and SK-n-SH exhibit much higher sensitivity to LCA than primary cultures of human neurons (or than the NB cell line Lan-1). Less than 10% of BE(2)-m17 and SK-n-SH cells remain viable when exposed to 300 μM LCA, a concentration which is not cytotoxic to primary cultures of human neurons and only mildly cytotoxic to Lan-1 cells. The percentage of viable cells was calculated as a portion of their population displaying a detectable level of redox potential which was visualized using the MTT (3-(4,5-dimethylthiozol-2-yl)-2,5-diphenyltetrazolium bromide)-based CellTiter 96 Non-Radioactive Cell Proliferation Assay. In this assay, only viable, metabolically active cells were able to reduce the yellow tetrazolium salt of MTT to form a purple formazan product, which was detected spectrophotometrically at a wavelength of 570 nm. Data are presented as means ± SD (n = 4-6); *$p < 0.05$.

Although being less sensitive to the cytotoxic effect of LCA than the three other NB cell lines tested, the NB cell line Lan-1 was significantly more sensitive to LCA than primary cultures of human neurons; I found that less than 10% of Lan-1 cells remain viable when exposed to 500 μM LCA, a concentration which was only mildly cytotoxic to primary cultures of human neurons (Figure 5.4).

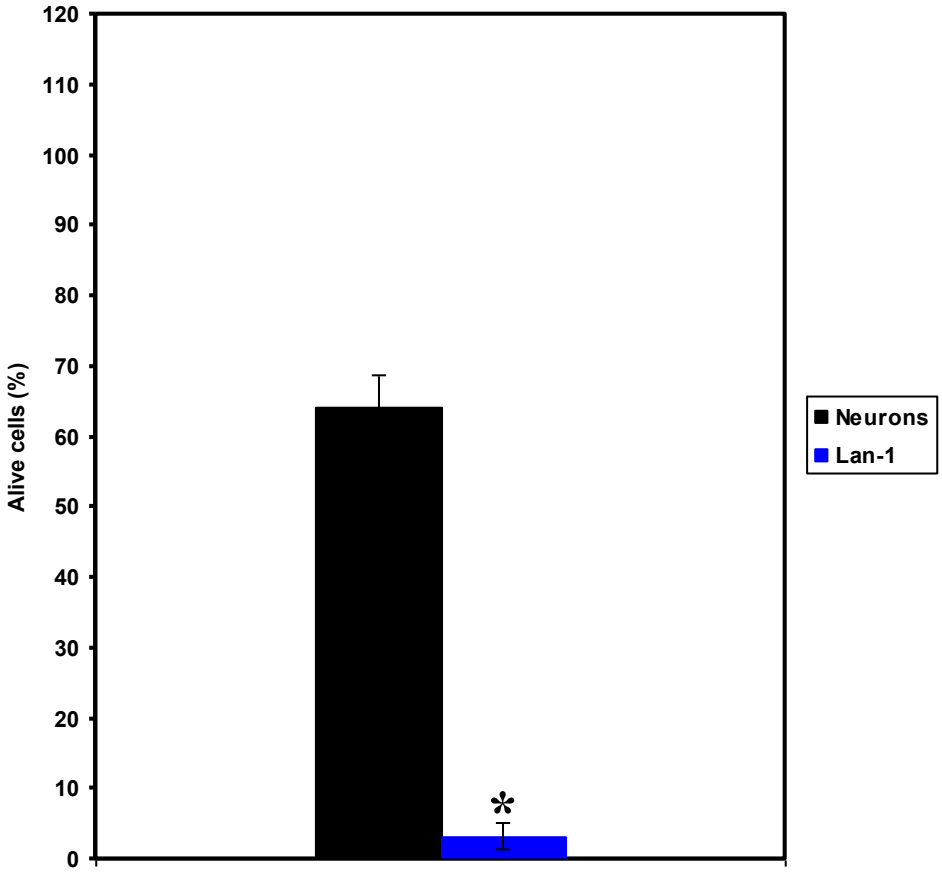


**Figure 5.4.** Although the NB cell line Lan-1 is less sensitive to the cytotoxic effect of LCA than the three other NB cell lines tested (see Figures 5.1 to 5.3), it is significantly more sensitive to LCA than primary cultures of human neurons. Less than 10% of Lan-1 cells remain viable when exposed to 500 μM LCA, a concentration which is only mildly cytotoxic to primary cultures of human neurons. The percentage of viable cells was calculated as a portion of their population displaying a detectable level of redox potential which was visualized using the MTT (3-(4,5-dimethylthiozol-2-yl)-2,5-diphenyltetrazolium bromide)-based CellTiter 96 Non-Radioactive Cell Proliferation Assay. In this assay, only viable, metabolically

active cells were able to reduce the yellow tetrazolium salt of MTT to form a purple formazan product, which was detected spectrophotometrically at a wavelength of 570 nm. Data are presented as means ± SD (n = 4-5); *$p < 0.05$.

My data imply that if LCA is used at concentrations that are not cytotoxic to primary cultures of human neurons, it selectively kills the NB cell lines BE(2)-m17, SK-n-SH and SK-n-MCIXC by causing their apoptotic death. In experiments that support this notion, I used the fluorescent dye Hoechst to visualize chromatin in various NB cell cultures and in primary cultures of human neurons exposed to LCA or remained untreated. For each cell culture, I calculated the percentage of viable non-apoptotic cells carrying intact, non-fragmented nuclei containing non-condensed chromatin. Dead apoptotic cells carried condensed and/or fragmented nuclei, a major hallmark event of apoptotic death that is not seen under any other modes of cell death [401 - 403]. I found that the NB cell line SK-n-MCIXC is the most sensitive (as compared to other NB cell lines tested and especially as compared to primary cultures of human neurons) to LCA-induced apoptotic death (Figures 5.5 and 5.6). Furthermore, my findings imply that two NB cell lines, BE(2)-m17 and SK-n-SH, exhibit much higher sensitivity to LCA-induced apoptotic death than primary cultures of human neurons (or than the NB cell line Lan-1); however, these two NB cell lines are less sensitive to LCA-induced apoptotic cell death than the NB cell line SK-n-MCIXC (Figures 5.5 and 5.6).

Moreover, although at certain concentrations of LCA the NB cell line Lan-1 was more sensitive to the MTT-monitored cytotoxic effect of this bile acid than primary

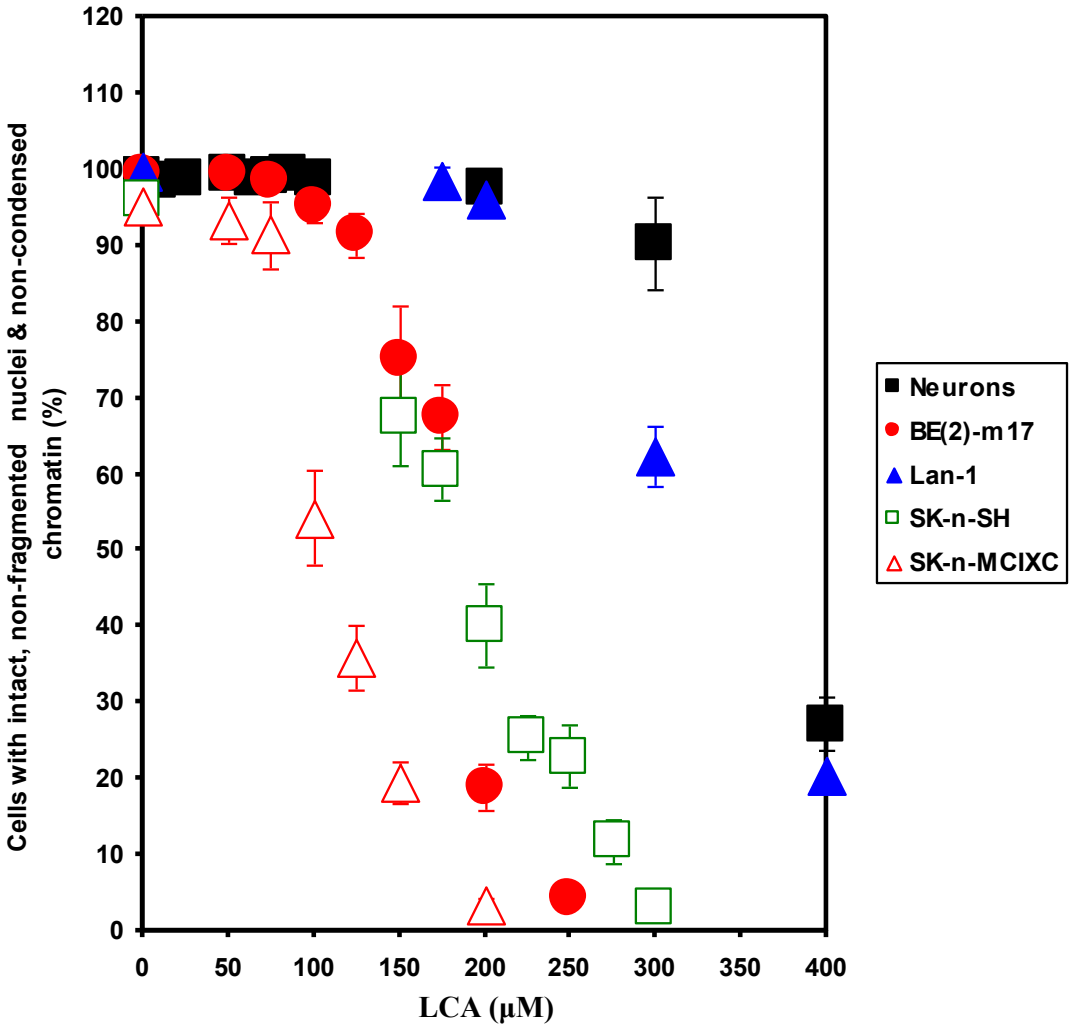


**Figure 5.5.** If used at concentrations that are not cytotoxic to primary cultures of human neurons (see Figure 5.1 to 5.4), LCA selectively kills the NB cell lines BE(2)-m17, SK-n-SH and SK-n-MCIXC by causing their apoptotic death. The fluorescent dye Hoechst was used to visualize chromatin in various NB cell cultures and in primary cultures of human neurons exposed to LCA or remained untreated. For each cell culture, the percentage of viable non-apoptotic cells carrying intact, non-fragmented nuclei containing non-condensed chromatin was calculated. Dead apoptotic cells carried fragmented nuclei containing condensed chromatin, a hallmark event of apoptotic death. Data are presented as means ± SD (n = 4-6).

cultures of human neurons (Figure 5.4), this cell line did not exhibit higher sensitivity to LCA-induced apoptotic cell death than primary cultures of human neurons did (Figures 5.5 and 5.6). Thus, if LCA is used at concentrations that are not cytotoxic to primary

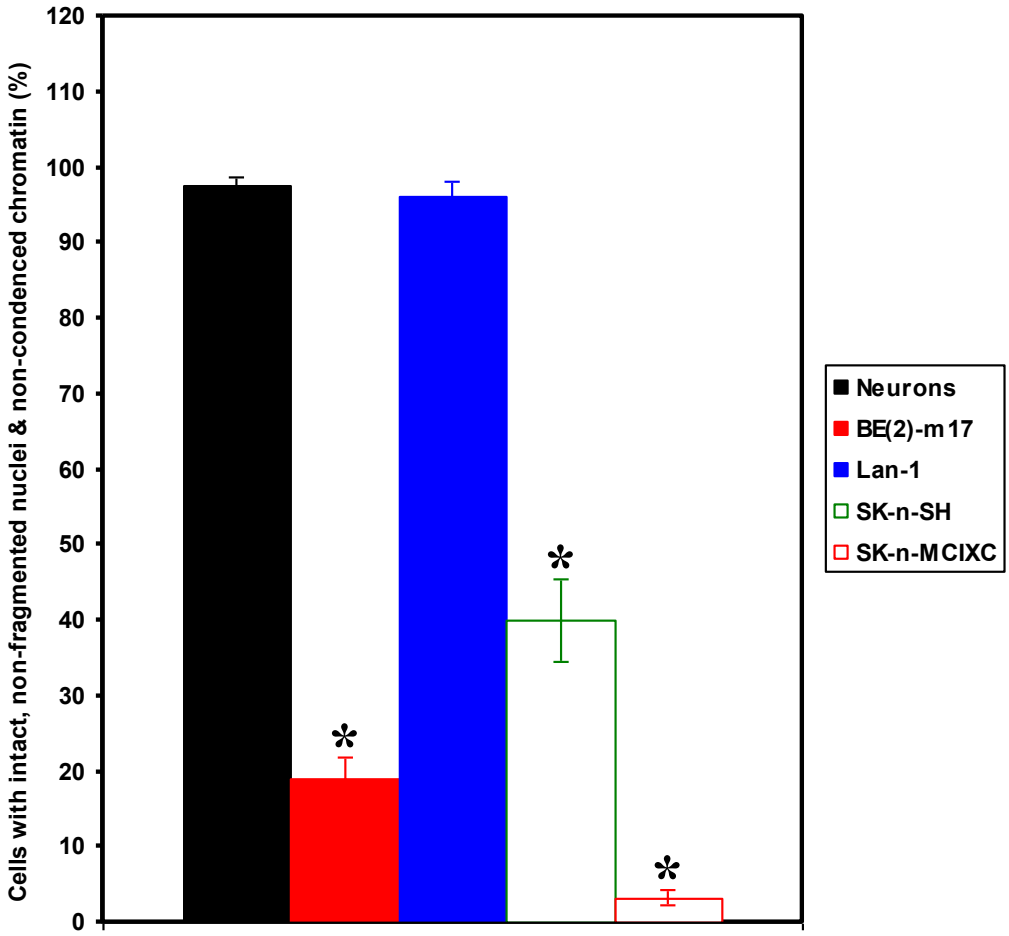


**Figure 5.6.** The NB cell line SK-n-MCIXC is the most sensitive (as compared to other NB cell lines tested and especially as compared to primary cultures of human neurons) to LCA-induced apoptotic death. Two other NB cell lines, BE(2)-m17 and SK-n-SH, exhibit much higher sensitivity to LCA-induced apoptotic death than primary cultures of human neurons (or than the NB cell line Lan-1); however, these two NB cell lines are less sensitive to LCA-induced apoptotic cell death than the NB cell line SK-n-MCIXC. The fluorescent dye Hoechst was used to visualize chromatin in various NB cell cultures and in primary cultures of human neurons exposed to LCA or remained untreated. For each cell culture, the percentage of viable non-apoptotic cells carrying intact, non-fragmented nuclei containing non-condensed chromatin was calculated. Dead apoptotic cells carried fragmented nuclei containing condensed chromatin, a hallmark event of apoptotic death. Data are presented as means ± SD (n = 4-6); *$p < 0.05$.

cultures of human neurons but exhibit strong MTT-monitored cytotoxic effect in Lan-1 cells (Figure 5.4), it selectively kills this NB cell line not by causing its apoptotic death.

One could speculate that LCA selectively kills Lan-1 cells by causing their necrotic or some other non-apoptotic kind of death, which is not characterized by such major distinctive (*i.e.*, not seen under any other modes of cell death) event of apoptotic cell death as nuclear condensation and fragmentation.

### 5.4.2 LCA sensitizes cultured human NB cells to hydrogen peroxide-induced apoptotic cell death

The exogenously added hydrogen peroxide has been shown to cause mitochondria-controlled apoptotic death in various types of cultured eukaryotic cells [390 - 396]. I found that LCA protects primary cultures of human neurons – but not cultured human NB cell lines BE(2)-m17 or SK-n-MCIXC – against mitochondria-controlled apoptosis induced in response to exogenously added 0.1 mM hydrogen peroxide (Figures 5.7 and 5.8). In these experiments, chromatin condensation and nuclear fragmentation were visualized with the fluorescent dye Hoechst and were used as a measure of the efficacy of hydrogen peroxide-induced apoptotic cell death. Importantly, I found that LCA greatly enhances the susceptibility of cultured human NB cell lines BE(2)-m17 and SK-n-MCIXC to such hydrogen peroxide-induced form of mitochondria-controlled apoptotic cell death (Figures 5.7 and 5.8), even when this bile acid was used at concentrations that in the absence of hydrogen peroxide do not compromise their viability (compare Figures 5.1 and 5.5 to Figures 5.7 and 5.8). It should be stressed that, while 75 μM LCA caused apoptotic death of all or most of the BE(2)-m17 and SK-n-MCIXC cells exposed to 0.1 mM hydrogen peroxide, in this concentration LCA greatly increased the

resistance of primary cultures of human neurons to the hydrogen peroxide-induced form of mitochondria-controlled apoptotic cell death (Figures 5.7 and 5.8). Based on these

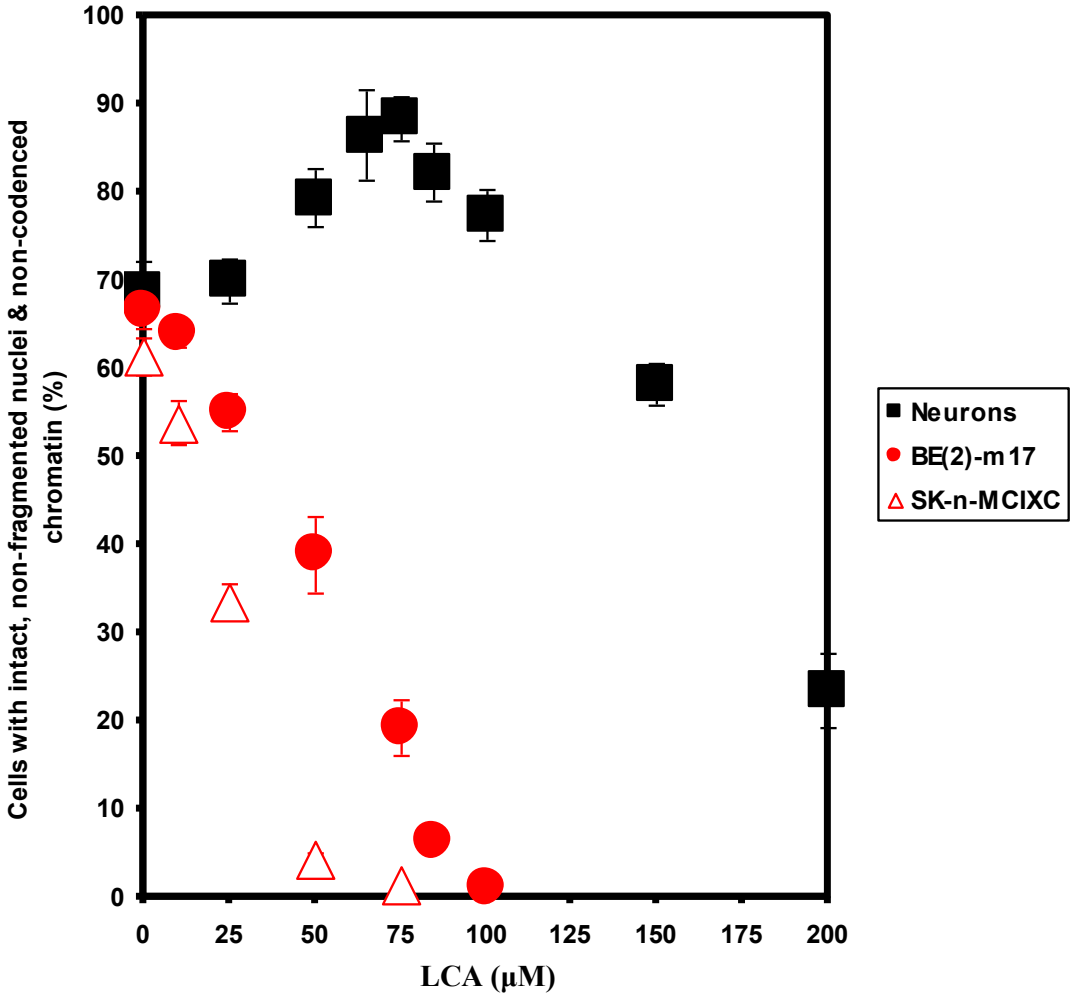


**Figure 5.7.** LCA protects primary cultures of human neurons – but not cultured human NB cell lines BE(2)-m17 or SK-n-MCIXC – against mitochondria-controlled apoptosis induced in response to exogenously added 0.1 mM hydrogen peroxide. Moreover, LCA greatly enhances the susceptibility of cultured human NB cell lines BE(2)-m17 and SK-n-MCIXC to such hydrogen peroxide-induced form of mitochondria-controlled apoptotic cell death, even when this bile acid is used at concentrations that in the absence of hydrogen peroxide do not compromise their viability (compare to Figures 5.1 and 5.5). Nuclear fragmentation and chromatin condensation were visualized with the fluorescent dye Hoechst and were used as a measure of the efficacy of hydrogen peroxide-induced apoptotic cell death. For each cell culture, the percentage of viable non-apoptotic cells carrying intact, non-fragmented nuclei containing non-condensed chromatin was calculated. Data are presented as means ± SD (n = 3-5).

observations, it seems likely that the exposure of a mixed population of various NB cell lines and non-cancerous neurons to low concentrations of simultaneously added hydrogen

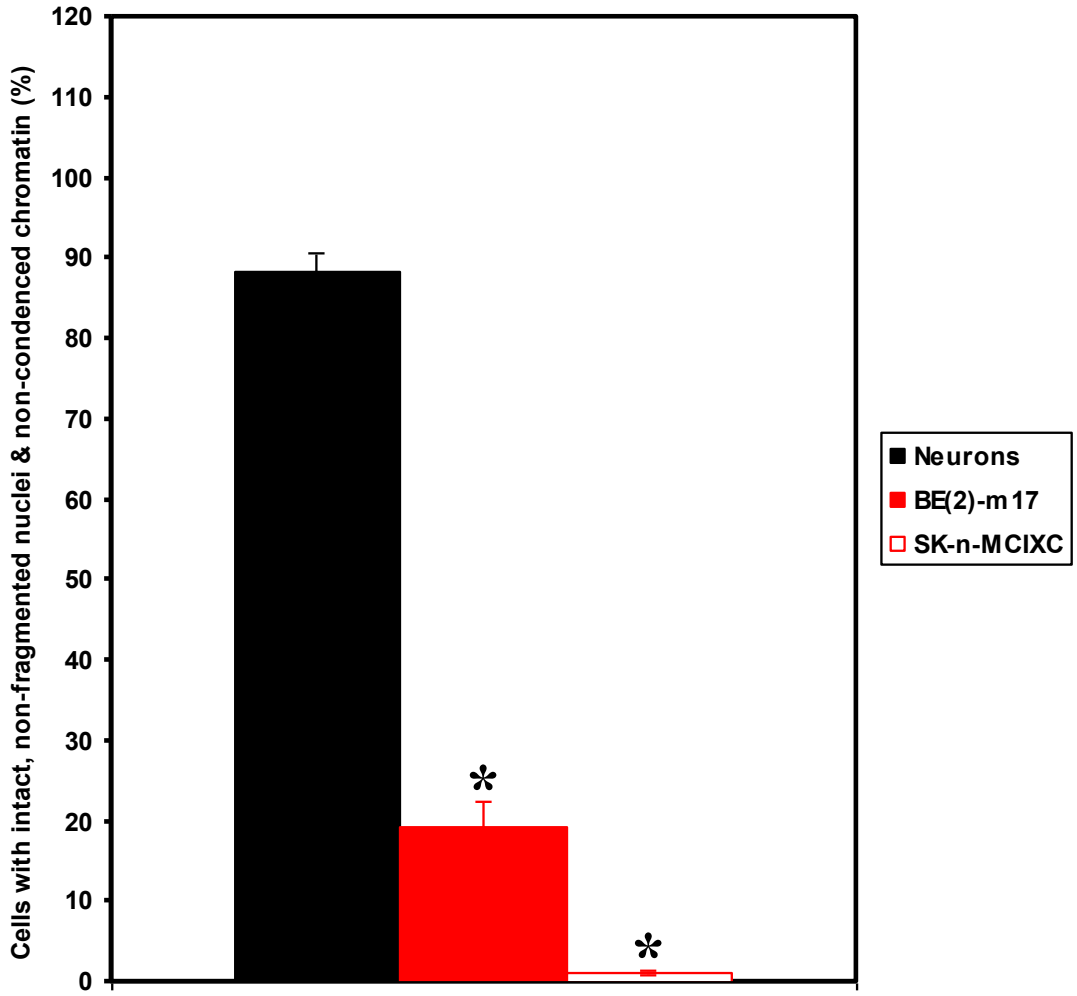


**Figure 5.8.** While 75 μM LCA causes apoptotic death of all or most of the cells of cultured human NB cell lines BE(2)-m17 and SK-n-MCIXC exposed to 0.1 mM hydrogen peroxide, in this concentration LCA greatly increases the resistance of primary cultures of human neurons to the hydrogen peroxide-induced form of mitochondria-controlled apoptotic cell death in the absence of hydrogen peroxide do not compromise their viability (compare to Figures 5.1 and 5.5). Nuclear fragmentation and chromatin condensation were visualized with the fluorescent dye Hoechst and were used as a measure of the efficacy of hydrogen peroxide-induced apoptotic cell death. For each cell culture, the percentage of viable non-apoptotic cells carrying intact, non-fragmented nuclei containing non-condensed chromatin was calculated. Data are presented as means ± SD (n = 3-5); *$p < 0.05$.

peroxide and LCA may concurrently 1) kill all NB cells by causing their apoptotic death; and 2) promote the viability of non-cancerous neurons by increasing their resistance to hydrogen peroxide-induced apoptosis.

### 5.4.3 In two NB cell lines, LCA causes the efflux of cytochrome c from mitochondria, activation of the initiator caspase-9, mitochondrial fragmentation and loss of mitochondrial transmembrane potential - all characteristic of the intrinsic (mitochondrial) apoptotic death pathway

As described above in this chapter of my thesis, I found that LCA: 1) selectively kills the NB cell lines BE(2)-m17, SK-n-SH and SK-n-MCIXC by causing nuclear condensation and fragmentation, a major hallmark event of apoptotic cell death; and 2) greatly enhances the susceptibility of cultured human NB cell lines BE(2)-m17 and SK-n-MCIXC to hydrogen peroxide-induced form of mitochondria-controlled apoptotic cell death. Therefore, I sought to investigate if LCA kills these cultured human NB cell lines by activating the intrinsic (mitochondrial) apoptotic death pathway.

The key feature of the mitochondrial pathway of apoptosis is mitochondrial outer membrane permeabilization (MOMP), which leads to the release of cytochrome c (and several other pro-apoptotic proteins) from the mitochondrial intermembrane space into the cytosol [404 - 407]. Following its efflux from mitochondria, cytochrome c binds an apoptotic protease-activating factor 1 (APAF-1) monomer whose oligomerization into the heptameric apoptosome complex recruits caspase-9 and ultimately activates this initiator caspase [403, 404, 408, 409]. I found that in cultured human NB cell line SK-n-MCIXC,

LCA triggers the release of cytochrome c from the mitochondrial intermembrane space into the cytosol (Figure 5.9).

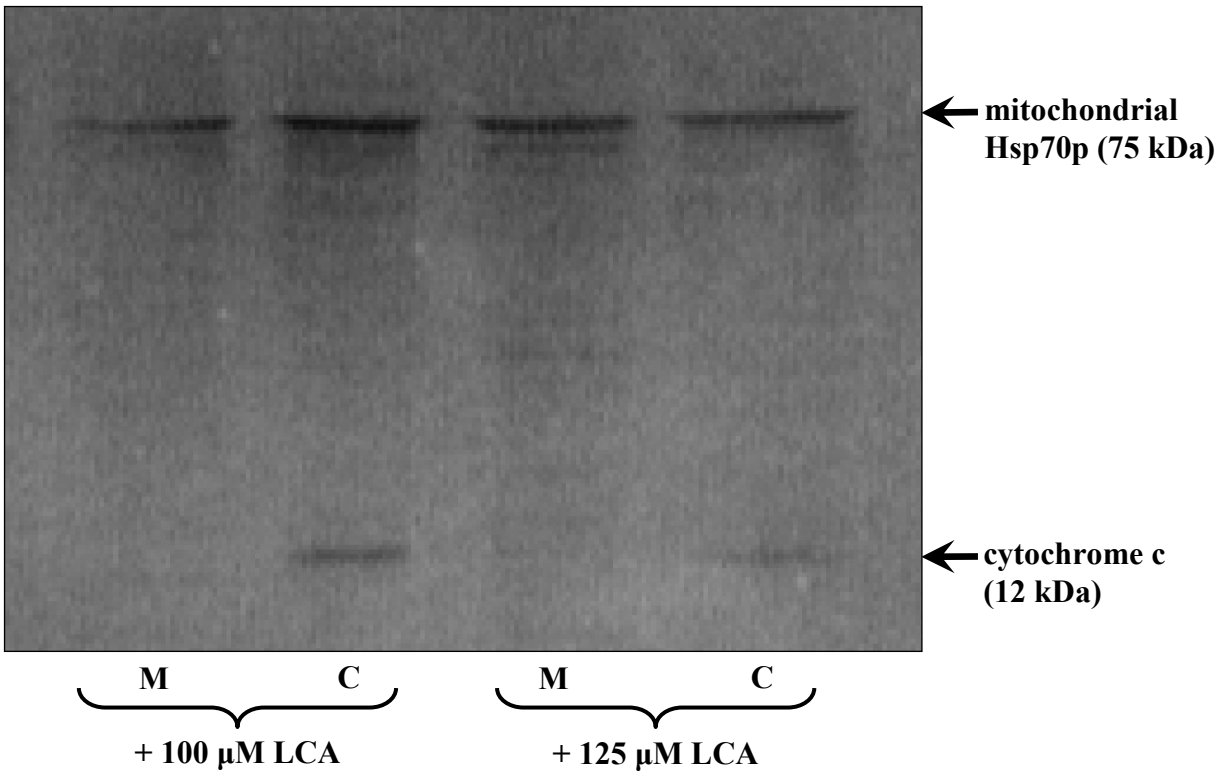


**Figure 5.9.** In cultured human NB cell line SK-n-MCIXC, LCA triggers the release of cytochrome c from the mitochondrial (M) intermembrane space into the cytosol (C). Unlike mitochondrial Hsp70p, whose significant quantities remain associated with mitochondria purified from SK-n-MCIXC cells exposed to LCA, the bulk quantities of cytochrome c exit mitochondria in these human NB cells. Proteins recovered in the mitochondrial (M) and cytoplasmic (C) fractions were resolved by SDS-PAGE in a 15% polyacrylamide gel and then transferred to a PVDF Immobilon-P membrane. Following wash with 5% milk, blots were incubated with 1/500 anti-cytochrome-c antibody or 1/500 anti-mitoHsp70 antibody. Immunoreactivity was detected using 1/1000 anti-mouse horseradish peroxidase-conjugated antibody. Antigen-antibody complexes were visualized by enhanced chemiluminescence using an ECL plus chemiluminescence Western blotting detection reagents.

The observed efflux of cytochrome c from mitochondria in LCA-treated SK-n-MCIXC cells was not an artifact of the mitochondrial purification procedure. Indeed, unlike

cytochrome c (whose bulk quantities were recovered in the cytoplasmic fraction), significant quantities of the mitochondrial protein Hsp70p remained associated with mitochondria purified from SK-n-MCIXC cells exposed to LCA (Figure 5.9).

Furthermore, I also revealed that LCA significantly increases the activity of the initiator caspase-9 in cultured human NB cell lines BE(2)-m17 and SK-n-MCIXC (Figure 5.10). Of note, the higher LCA-induced activity of caspase-9 in SK-n-MCIXC cells - as compared to that in BE(2)-m17 cells – correlated with the higher sensitivity of SK-n-MCIXC (as compared to that of BE(2)-m17) to the cytotoxic and apoptotic cell death effects of LCA on human NB cell lines in culture (compare Figures 5.1 and 5.5 to Figure 5.10). It should be stressed that, unlike the stimulating effect of LCA on caspase-9 seen in BE(2)-m17 and SK-n-MCIXC cells, this bile acid did not increase caspase-9 activity in cultured human NB cell line Lan-1 (Figure 5.10). As I mentioned above, LCA selectively kills Lan-1 cells (Figures 5.1 and 5.4) not by causing their apoptotic death (Figures 5.5 and 5.6), but perhaps by promoting their necrotic or some other non-apoptotic kind of death – the one which is not characterized by such major hallmark event of apoptotic cell death as nucleus condensation and fragmentation.

One of the earliest distinctive events of the mitochondrial pathway of apoptosis is the fragmentation of a tubular mitochondrial network into individual mitochondria (mitochondrial fragmentation) [403 - 406, 410, 411]. This hallmark event of mitochondria-dependent cell death occurs before caspase-9 activation, around the point of MOMP and cytochrome c efflux from mitochondria, and is caspase-independent [403, 404, 410, 411]. I found that LCA causes mitochondrial fragmentation in cultured human NB cell lines BE(2)-m17 and SK-n-MCIXC (Figure 5.11). Noteworthy, the higher

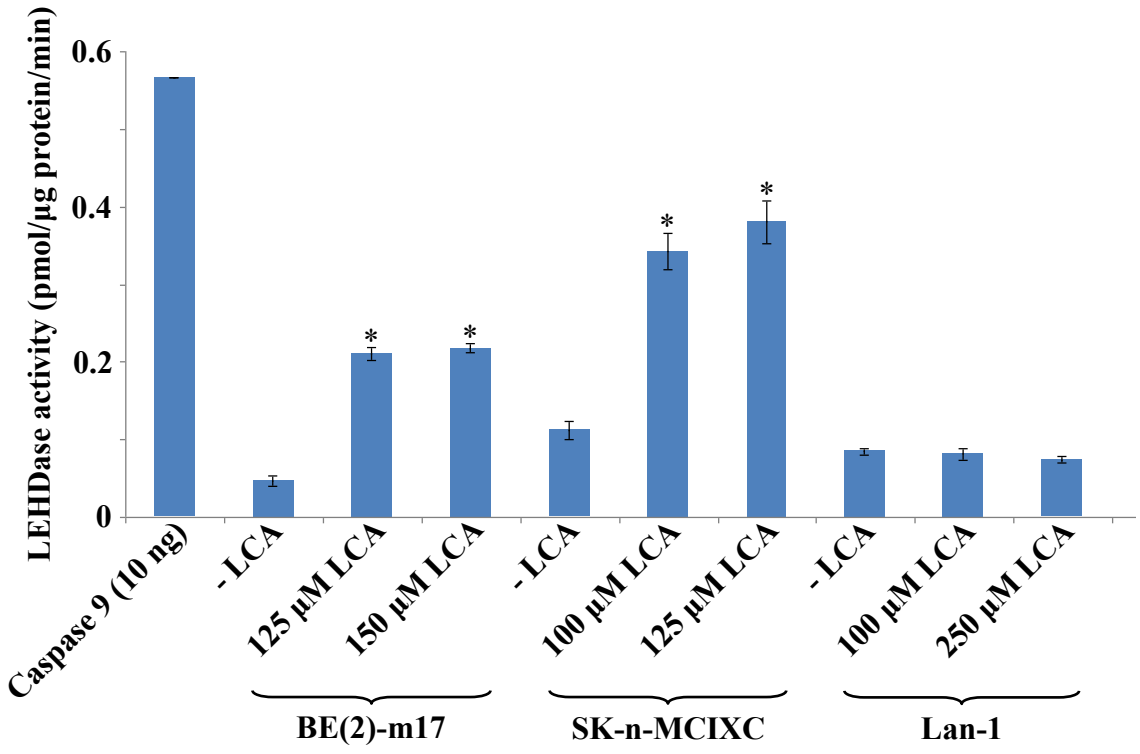


**Figure 5.10.** LCA significantly increases the activity of the initiator caspase-9 in cultured human NB cell lines BE(2)-m17 and SK-n-MCIXC. Proteins were extracted from harvested cells using an ice-cold lysis buffer. The cell lysate was centrifuged at 13000 × g for 5 min at 4°C to remove cell debris and any detergent-insoluble proteins. The supernatant was collected and frozen at -80°C. Extracts were thawed and then assayed for caspase-9 activity using 10 µM Ac-LEHD-AFC as a fluorogenic substrate specific for this caspase. The time-dependent release of the fluorescent compound 7-amino-4-trifluoromethyl coumarin (AFC) was monitored using a Bio-Rad Fluoromark fluorometer at an excitation wavelength of 390 nm and an emission wavelength of 538 nm. Measurements were recorded at 2 min intervals for 1 h.

efficacy of LCA-induced mitochondrial fragmentation observed in SK-n-MCIXC cells - as compared to that seen in BE(2)-m17 cells - correlated with the higher sensitivity of SK-n-MCIXC (as compared to that of BE(2)-m17) to the cytotoxic and apoptotic cell death effects of LCA on human NB cell lines in culture (compare Figures 5.1 and 5.5 to Figure 5.11B). Moreover, if used at a concentration that leads to fragmentation of the entire mitochondrial network (*i.e.*, 125 µM - 150 µM) in BE(2)-m17 and SK-n-MCIXC cells, LCA did not cause such mitochondrial fragmentation in cultured human NB cell

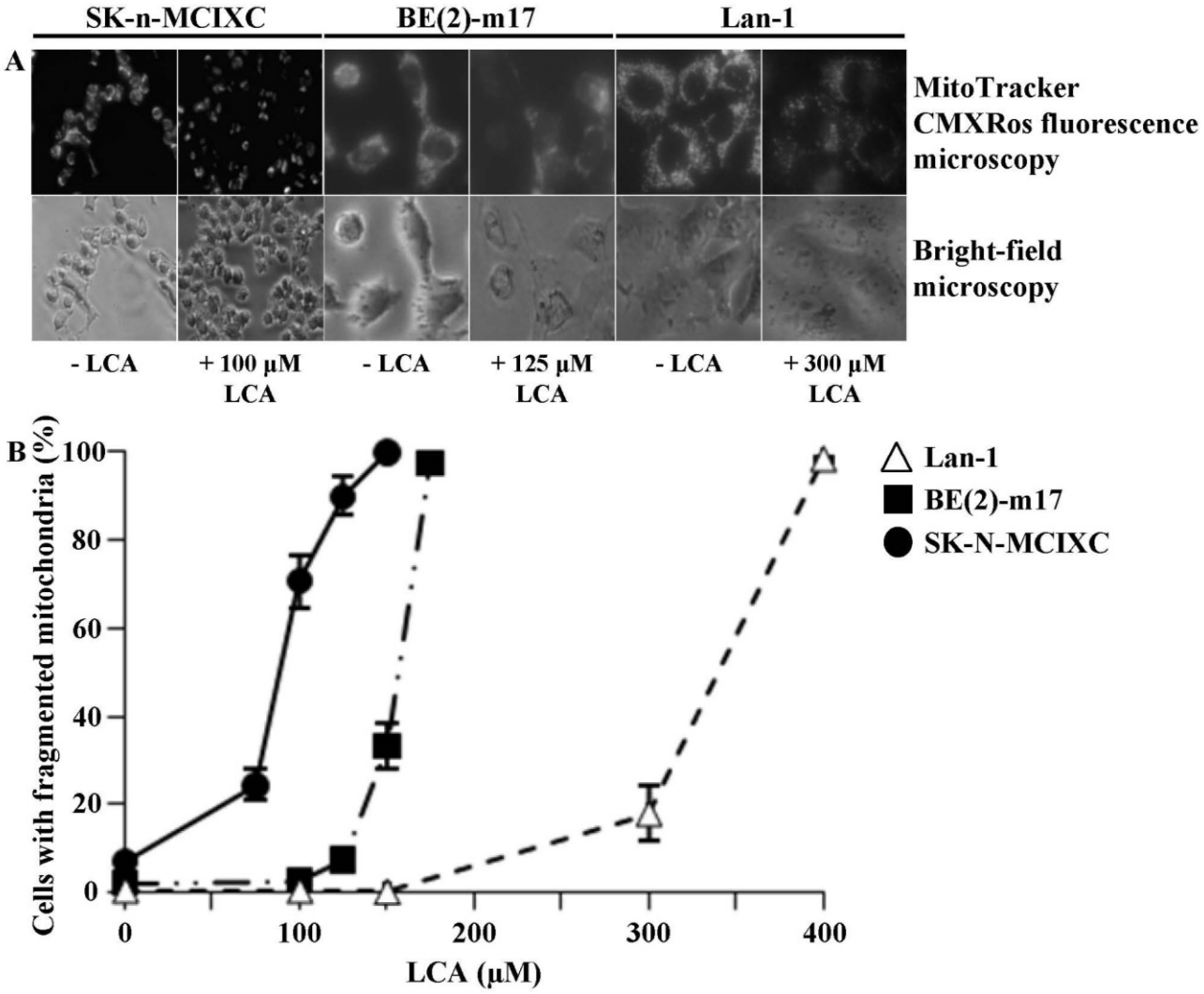


**Figure 5.11.** LCA causes mitochondrial fragmentation in cultured human NB cell lines BE(2)-m17 and SK-n-MCIXC. If used at a concentration that leads to fragmentation of the entire mitochondrial network (*i.e.*, 125 µM - 150 µM) in BE(2)-m17 and SK-n-MCIXC cells, LCA did not cause such mitochondrial fragmentation in cultured human NB cell line Lan-1 – whose LCA-induced death in culture was not due to apoptosis. Mitochondrial morphology of cells treated with LCA was visualized using MitoTracker Red CMXRos used at a concentration of 125 nM in the culture media. Cells were viewed using fluorescence microscopy, and the percentage of cells displaying fragmented mitochondria was calculated.

line Lan-1 (Figure 5.11B) – whose LCA-induced death in culture (Figures 5.1 and 5.4) was not due to apoptosis (see Figures 5.5 and 5.6 and discussion in section 5.4.1).

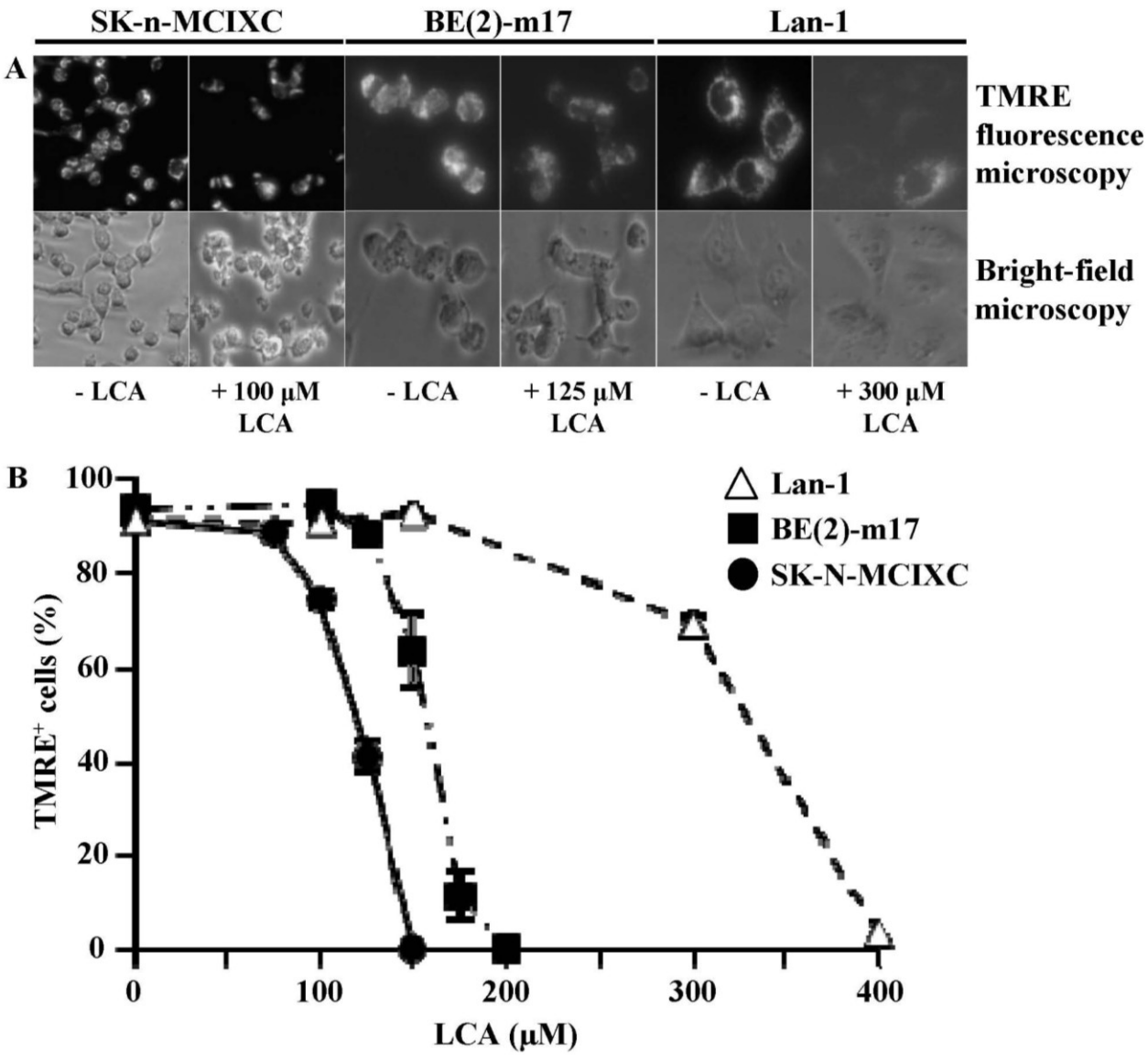


**Figure 5.12.** LCA triggers the dissipation of the electrochemical potential across the inner mitochondrial membrane in cultured human NB cell lines BE(2)-m17 and SK-n-MCIXC. The mitochondrial membrane potential ($\Delta\Psi$) was measured using tetramethylrhodamine ethyl ester (TMRE), a cell-permeant, cationic fluorescent dye. The extent of reversible sequestration of TMRE by mitochondria is proportional to the value of $\Delta\Psi$. Cells were incubated in 50 nM of TMRE for 20 minutes and directly viewed using fluorescence microscopy. The percentage of TMRE-positive cells displaying a detectable level of $\Delta\Psi$ was calculated.

A progressive decline in mitochondrial function during mitochondria-controlled apoptosis, including a gradual dissipation and eventual loss of mitochondrial

transmembrane potential, follows MOMP and occurs in both caspase-dependent and caspase-independent fashion [403 - 405, 412 - 415]. I found that LCA triggers the dissipation of the electrochemical potential across the inner mitochondrial membrane in cultured human NB cell lines BE(2)-m17 and SK-n-MCIXC (Figure 5.12). Again, the higher efficacy of LCA-induced mitochondrial inner membrane depolarization observed in SK-n-MCIXC cells - as compared to that seen in BE(2)-m17 cells - correlated with the higher sensitivity of SK-n-MCIXC (as compared to that of BE(2)-m17) to the cytotoxic and apoptotic cell death effects of LCA on human NB cell lines in culture (compare Figures 5.1 and 5.5 to Figure 5.12B). Moreover, if used at a concentration that leads to a complete loss of mitochondrial transmembrane potential (*i.e.*, 150 μM - 200 μM) in all cells of the cultured NB lines BE(2)-m17 and SK-n-MCIXC, LCA did not cause mitochondrial inner membrane depolarization or caused only minor reduction of mitochondrial transmembrane potential in cultured human NB cell line Lan-1 (Figure 5.12B) – whose LCA-induced death in culture (Figures 5.1 and 5.4) was not due to apoptosis (see Figures 5.5 and 5.6 and discussion in section 5.4.1).

### 5.4.4 In two NB cell lines, LCA triggers a proteolytic cascade of events leading to activation of two executioner caspases, caspase-3 and caspase-6

The apoptosome-driven activation of caspase-9 during mitochondria-controlled apoptosis initiates a branched cascade of events resulting in a step-wise proteolytic activation of several executioner caspases [403, 416, 417]. The caspase-9-dependent proteolytic activation of the executioner caspases-3 and -7 is followed by the caspase-3-driven proteolytic activation of the executioner caspases-2 and -6 and then by the

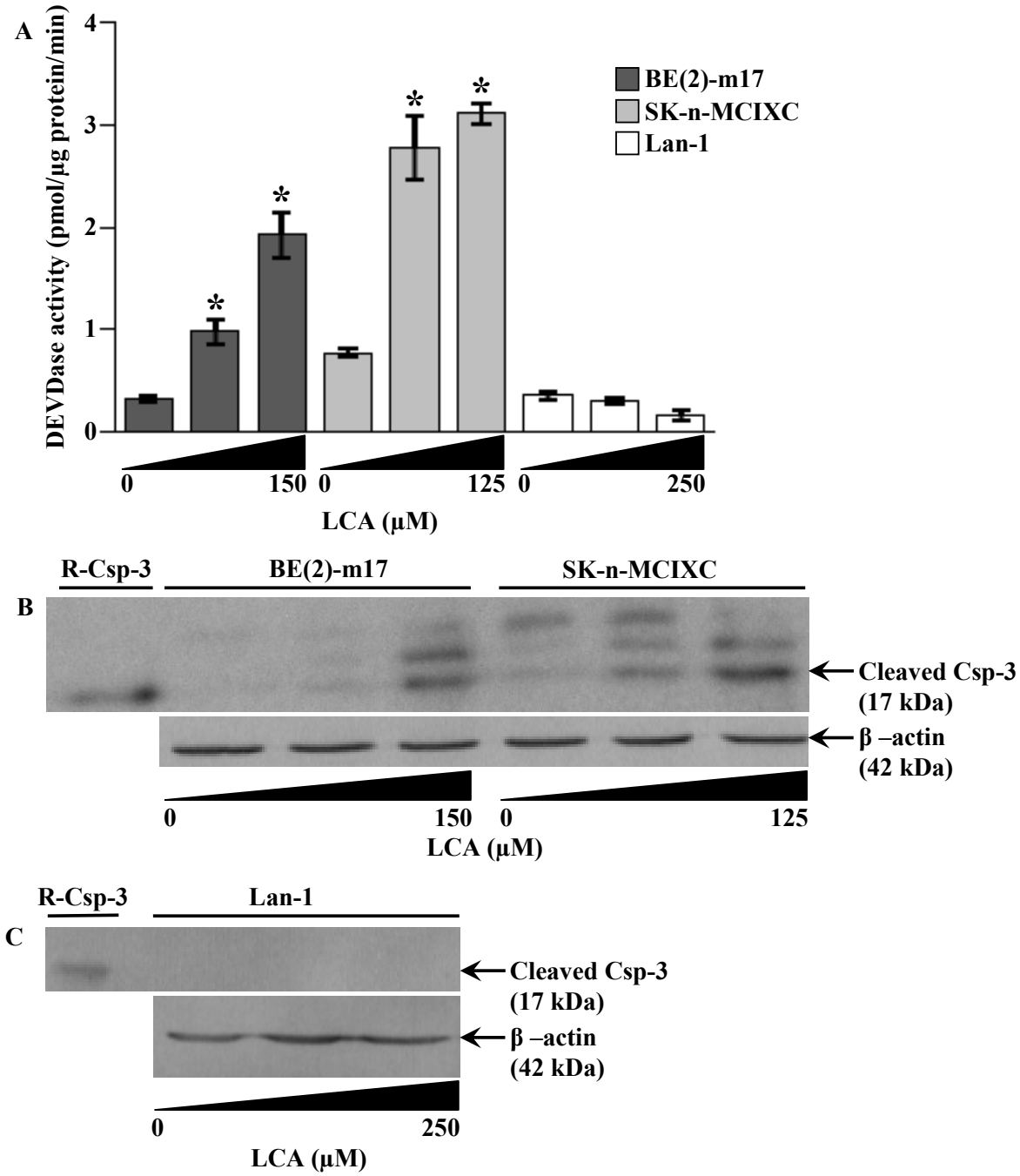


**Figure 5.13.** LCA increases the activity of caspase-3 in cultured human NB cell lines BE(2)-m17 and SK-n-MCIXC (A) by promoting a proteolytic conversion of a zymogen pro-caspase-3 form of this executioner caspase into its enzymatically active 17 kDa form (B). In contrast, if used even at a higher concentration (*i.e.*, 250 µM) than the ones causing the highest extent of the LCA-induced proteolytic activation of caspase-3 (*i.e.*, 125 µM or 150 µM) in SK-n-MCIXC and BE(2)-m17 cells, LCA does not promote its proteolysis-driven activation in cultured human NB cell line Lan-1 (C). Data in (A) are presented as means ± SD (n = 3-4); *$p < 0.05$.

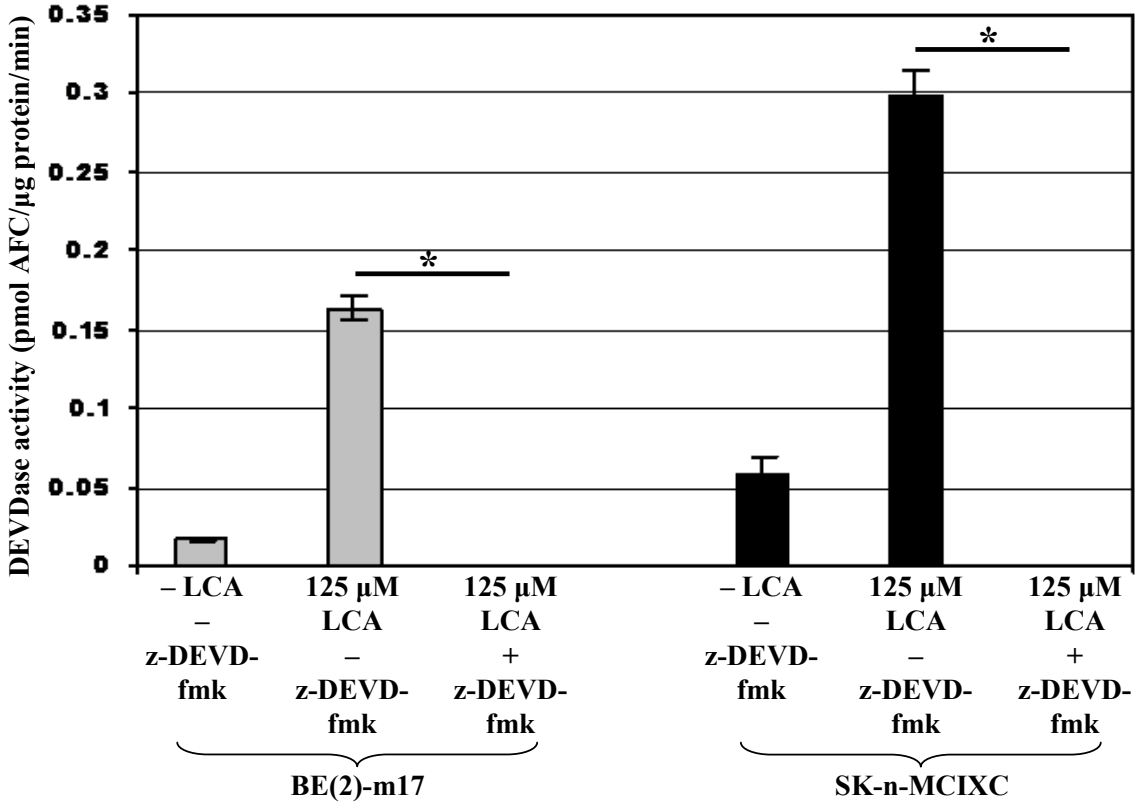


**Figure 5.14.** z-DEVD-fmk, a potent and specific inhibitor of caspase-3, completely inhibits the LCA-induced activity of this caspase in cultured human NB cell lines BE(2)-m17 and SK-n-MCIXC. z-DEVD-fmk was used at the concentration of 5 µM. DMSO was used as a solvent at the standard concentration of 1%. Data are presented as means ± SD (n = 3-4); *$p < 0.05$.

caspase-6-driven proteolytic activation of the executioner caspase-10 [403, 416, 417]. When the full complement of executioner caspases that are necessary for the proper execution of the mitochondria-controlled apoptotic program becomes activated, these caspases complete the demolition phase of the program by cleaving their respective protein substrates and producing the morphological features characteristic of apoptotic cell death [403 - 405].

I found that LCA increases the activity of caspase-3 in cultured human NB cell lines BE(2)-m17 and SK-n-MCIXC (Figure 5.13A) by promoting a proteolytic

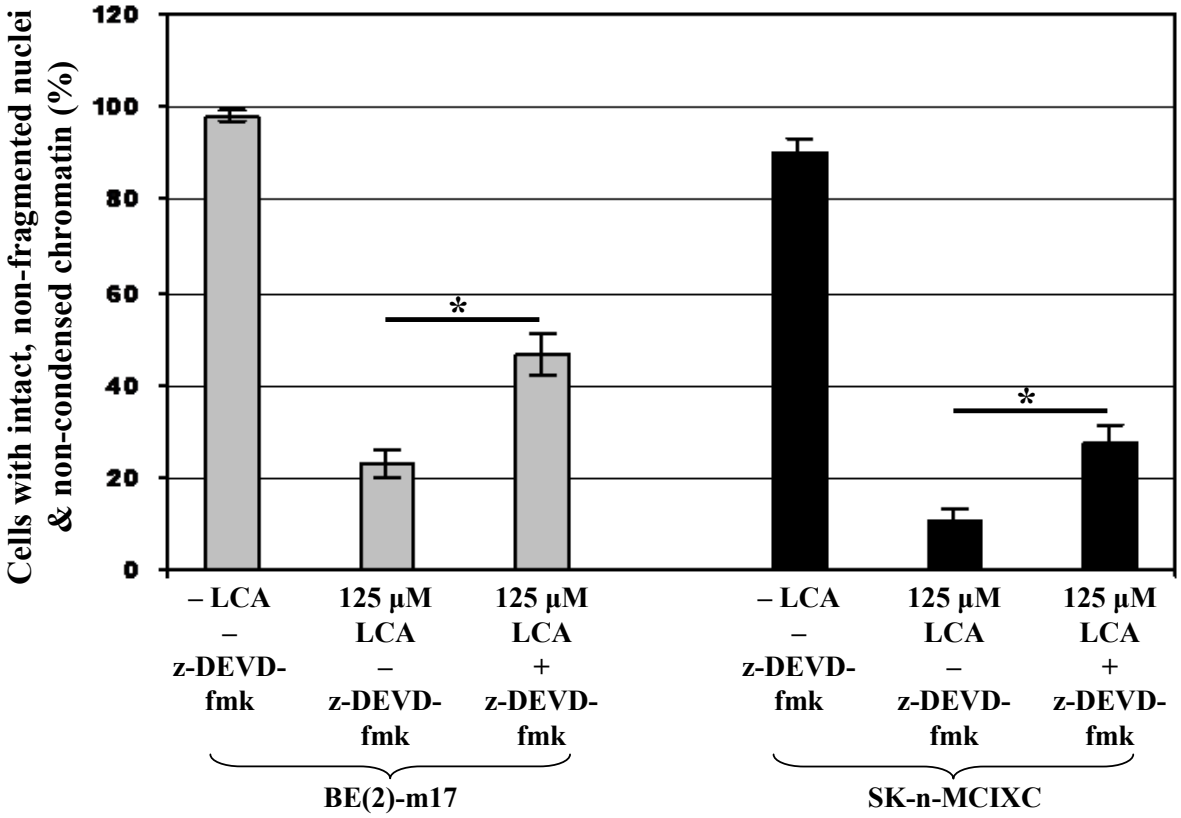


**Figure 5.15.** z-DEVD-fmk, a potent and specific inhibitor of caspase-3, weakens the anti-tumor effect of LCA in cultured human NB cell lines BE(2)-m17 and SK-n-MCIXC. z-DEVD-fmk was used at the concentration of 5 µM. DMSO was used as a solvent at the standard concentration of 1%. The percentage of alive human cells was calculated as a portion of their population carrying intact, non-fragmented nuclei containing non-condensed chromatin that were visualized using the Hoechst fluorescent dye. Dead human cells carried condensed and/or fragmented nuclei, a major hallmark event of apoptotic death that is not seen under any other modes of cell death. Data are presented as means ± SD (n = 3-4); *$p < 0.05$.

conversion of a zymogen pro-caspase-3 form of this executioner caspase into its enzymatically active 17 kDa form (Figure 5.13B). It should be stressed that the anti-tumor effect of LCA in these two NB cell lines was due, at least in part, to the ability of this bile acid to increase the activity of the executioner caspase-3. In fact, I found that z-DEVD-fmk – a potent and specific inhibitor of caspase-3 (see Figure 5.14) – significantly reduces the efficacy with which LCA causes selective killing of BE(2)-m17 and SK-n-

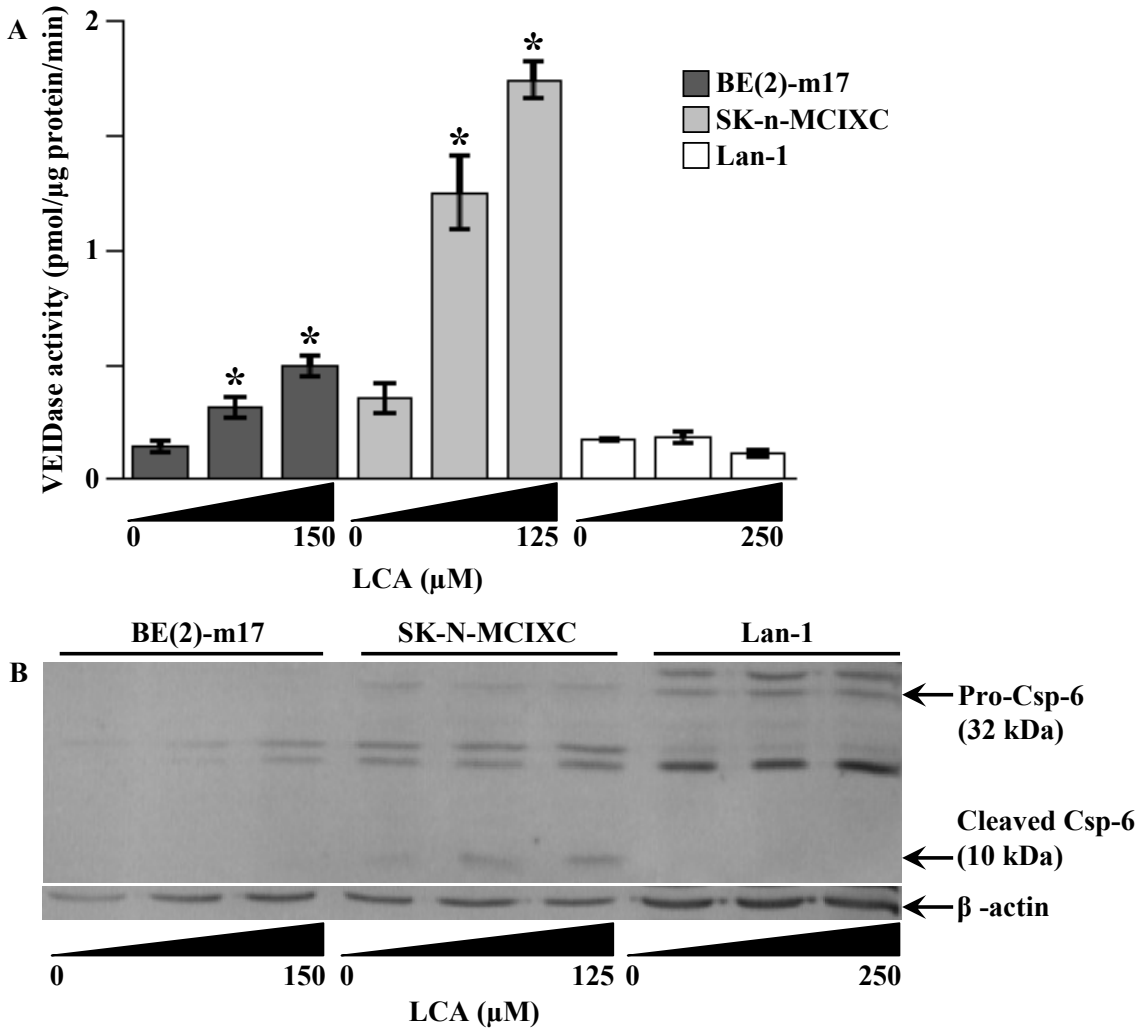


**Figure 5.16.** LCA increases the activity of caspase-6 in cultured human NB cell lines BE(2)-m17 and SK-n-MCIXC (A) by promoting a proteolytic conversion of a 32-kDa zymogen pro-caspase-6 form of this executioner caspase into its enzymatically active 10 kDa form (B). In contrast, if used even at a higher concentration (*i.e.*, 250 µM) than the ones causing the highest extent of the LCA-induced proteolytic activation of caspase-6 (*i.e.*, 125 µM or 150 µM) in SK-n-MCIXC and BE(2)-m17 cells, LCA does not promote its proteolysis-driven activation in cultured human NB cell line Lan-1 (B). Data in (A) are presented as means ± SD (n = 3-4); **p* < 0.05.

MCIXC cells in culture (Figure 5.15). The incomplete reduction by z-DEVD-fmk of the anti-tumor efficacy of LCA in cultured human NB cell lines BE(2)-m17 and SK-n-MCIXC (Figure 5.15) suggests that the LCA-triggered, mitochondria-driven selective

apoptotic death of both these NB cell lines could be due not only to a caspase-dependent mechanism, but also to a caspase-independent progressive decline in mitochondrial function - which leads to the observed LCA-dependent loss of mitochondrial transmembrane potential (Figure 5.12) among other effects.

My findings also imply that, following its LCA-driven activation in cultured human NB cell lines BE(2)-m17 and SK-n-MCIXC, the executioner caspase-3 activates the downstream executioner caspase-6 in these cell lines (Figure 5.16A). (Caspase-6 is a well established executioner caspase known to be activated *in vivo* only following the caspase-3-driven proteolytic cleavage of pro-caspase-6, an enzymatically inactive zymogen form of caspase-6 [403, 416, 417]). Indeed, in both these NB cell lines, LCA promoted such cleavage of a 32-kD form of pro-caspase-6 and induced the formation of its enzymatically active 10-kD form (Figure 5.16B).

Of note, the higher extent of the LCA-induced proteolytic activation of caspase-3 and caspase-6 observed in SK-n-MCIXC cells - as compared to that seen in BE(2)-m17 cells – correlated with the higher sensitivity of SK-n-MCIXC (as compared to that of BE(2)-m17) to the cytotoxic and apoptotic cell death effects of LCA on human NB cell lines in culture (compare Figures 5.1 and 5.5 to Figures 5.13 and 5.16).

Importantly, if used at a concentration that causes the highest extent of the LCA-induced proteolytic activation of caspase-3 and caspase-6 (*i.e.*, 125 μM - 150 μM) in SK-n-MCIXC and BE(2)-m17 cells, LCA did not promote their proteolysis-driven activation in cultured human NB cell line Lan-1 (Figures 5.13A, 5.13C and 5.16B) – whose LCA-induced death in culture (Figures 5.1 and 5.4) was not due to apoptosis (see Figures 5.5 and 5.6 and discussion in section 5.4.1).

### 5.4.5 In two NB cell lines, LCA increases the activity of caspase-8, an initiator caspase that functions in the extrinsic (death receptor) apoptotic death pathway but can also cause MOMP and trigger the intrinsic (mitochondrial) pathway of apoptosis

The proteolytic cleavage of pro-caspase-3 and the resulting increase of caspase-3 activity, which in turn cleaves pro-caspase-6 and activates the downstream executioner caspase-6, can be triggered not only through the intrinsic (mitochondrial) apoptotic death pathway but also through the extrinsic (death receptor) pathway of apoptosis [403, 404]. This extrinsic pathway is initiated when specific extracellular death ligands cause the ligation of death receptors in the plasma membrane, thus triggering a process eventually leading to activation of the initiator caspase-8 [403, 404]. In addition to its role in the proteolytic activation of caspase-3, caspase-8 can also cause MOMP and trigger the intrinsic (mitochondrial) pathway of apoptosis [418, 419]. Indeed, following its activation in response to death receptor ligation caspase-8 can cleave and activate the BH-3 only protein BH3-interacting domain death agonist (BID), thereby causing MOMP and initiating the intrinsic (mitochondrial) apoptotic death pathway [403 - 404, 418, 419].

As I found, LCA significantly increases the activity of the initiator caspase-8 in cultured human NB cell lines BE(2)-m17 and SK-n-MCIXC (Figure 5.17). Of note, the higher LCA-induced activity of caspase-8 in SK-n-MCIXC cells - as compared to that in BE(2)-m17 cells – correlated with the higher sensitivity of SK-n-MCIXC (as compared to that of BE(2)-m17) to the cytotoxic and apoptotic cell death effects of LCA on human NB cell lines in culture (compare Figures 5.1 and 5.5 to Figure 5.17). It should be stressed that, unlike the stimulating effect of LCA on caspase-8 seen in BE(2)-m17 and

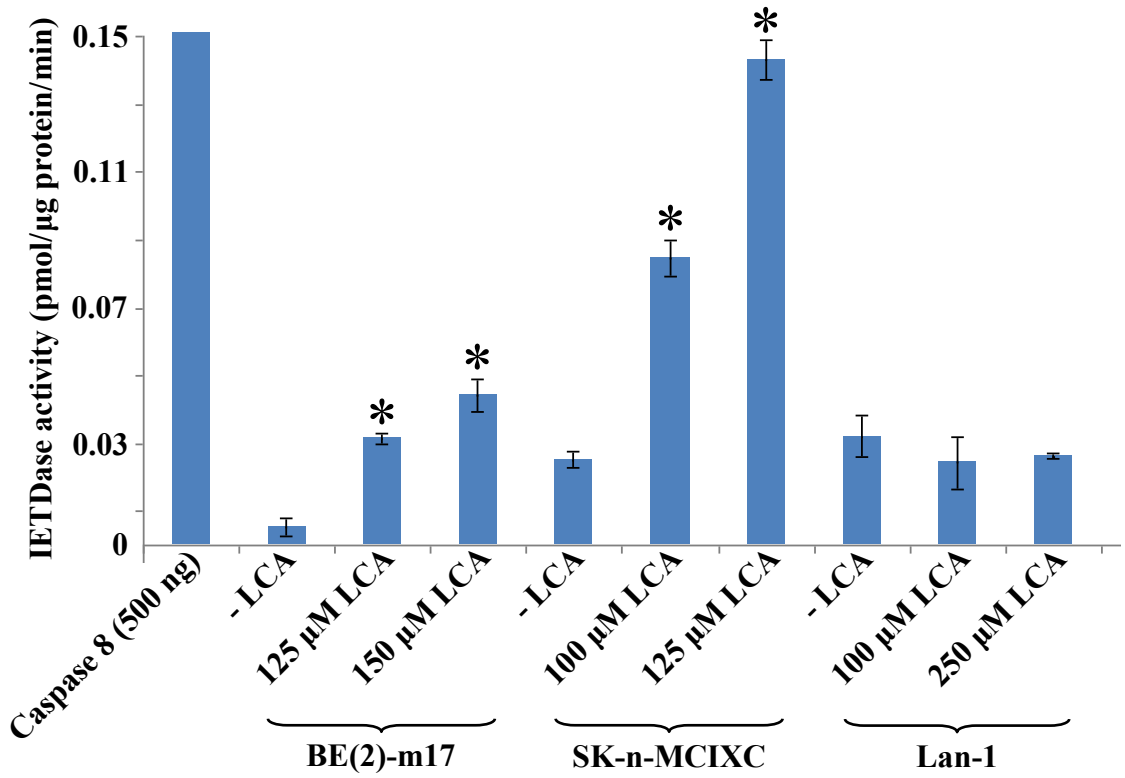


**Figure 5.17.** LCA significantly increases the activity of the initiator caspase-8 in cultured human NB cell lines BE(2)-m17 and SK-n-MCIXC. In contrast, if used even at a higher concentration (*i.e.*, 250 µM) than the ones causing the highest extent of the LCA-induced activation of caspase-8 (*i.e.*, 125 µM or 150 µM) in SK-n-MCIXC and BE(2)-m17 cells, LCA does not promote its activation in cultured human NB cell line Lan-1. Proteins were extracted from harvested cells using an ice-cold lysis buffer. The cell lysate was centrifuged at 13000 × g for 5 min at 4°C to remove cell debris and any detergent-insoluble proteins. The supernatant was collected and frozen at -80°C. Extracts were thawed and then assayed for caspase-8 activity using 10 µM Ac-IETD-AFC as a fluorogenic substrate specific for this caspase. The time-dependent release of the fluorescent compound 7-amino-4-trifluoromethyl coumarin (AFC) was monitored using a Bio-Rad Fluoromark fluorometer at an excitation wavelength of 390 nm and an emission wavelength of 538 nm. Measurements were recorded at 2 min intervals for 1 h. Data are presented as means ± SD (n = 3-4); *$p < 0.05$.

SK-n-MCIXC cells, this bile acid did not increase caspase-8 activity in cultured human NB cell line Lan-1 (Figure 5.17). As I mentioned above, LCA selectively kills Lan-1 cells (Figures 5.1 and 5.4) not by causing their apoptotic death (Figures 5.5 and 5.6), but

perhaps by promoting their necrotic or some other non-apoptotic kind of death – the one which is not characterized by such major hallmark event of apoptotic cell death as nucleus condensation and fragmentation.

These findings suggest that LCA could kill both BE(2)-m17 and SK-n-MCIXC cell lines by activating not only the intrinsic (mitochondrial) apoptotic death pathway dependent on the initiating caspase-9 (see sections 5.4.3 and 5.4.4) but also the extrinsic (death receptor) apoptotic death pathway driven by the initiator caspase-8. The LCA-dependent activation of caspase-8 in BE(2)-m17 and SK-n-MCIXC cells (Figure 5.17) could be responsible not only for the observed in these cells direct proteolytic activation of caspase-3 (Figure 5.13), but also for MOMP and the resulting efflux of cytochrome c from mitochondria of these cells (Figure 5.9). These LCA-induced, caspase-8-mediated events could ultimately trigger the intrinsic (mitochondrial) apoptotic pathway in BE(2)-m17 and SK-n-MCIXC cells, thereby enhancing the extent of LCA-driven cellular demise.

### 5.4.6 In two NB cell lines, LCA reduces the activity of caspase-1, an inflammatory caspase that drives the processing and secretion of the cytokines interleukin-1β and interleukin-18

My findings also revealed that LCA significantly reduces the activity of caspase-1 in cultured human NB cell lines BE(2)-m17 and SK-n-MCIXC, but not in cultured Lan-1 cell line (Figure 5.18). Caspase-1 is known to be an inflammatory caspase that drives the processing and unconventional secretion of the cytokines interleukin-1β and interleukin-18 [420 - 423]. Following their secretion by mammalian cells, cytokines promote the

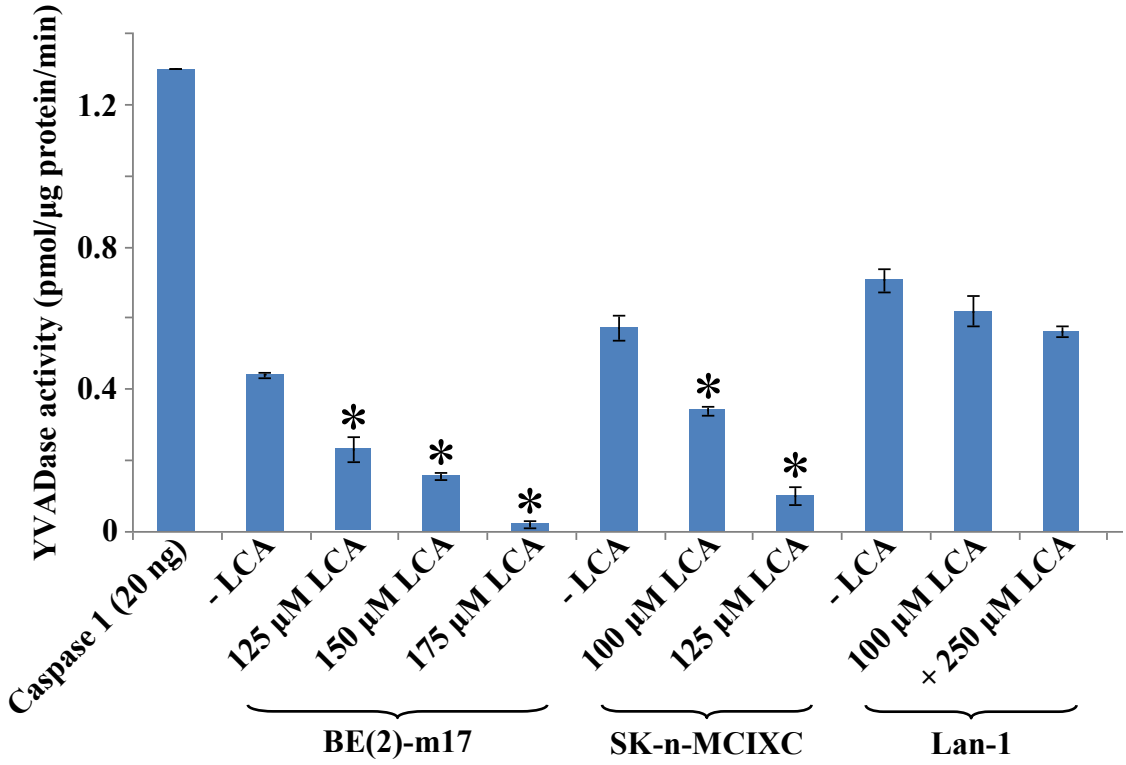


**Figure 5.18.** LCA significantly reduces the activity of the inflammatory caspase-1 in cultured human NB cell lines BE(2)-m17 and SK-n-MCIXC. In contrast, if used even at a higher concentration (*i.e.*, 250 µM) than the ones causing the highest extent of the LCA-induced inhibition of caspase-1 (*i.e.*, 125 µM or 150 µM) in SK-n-MCIXC and BE(2)-m17 cells, LCA does not promote its inhibition in cultured human NB cell line Lan-1. Proteins were extracted from harvested cells using an ice-cold lysis buffer. The cell lysate was centrifuged at 13000 × g for 5 min at 4°C to remove cell debris and any detergent-insoluble proteins. The supernatant was collected and frozen at -80°C. Extracts were thawed and then assayed for caspase-1 activity using 10 µM Ac-YVAD-AFC as a fluorogenic substrate specific for this caspase. The time-dependent release of the fluorescent compound 7-amino-4-trifluoromethyl coumarin (AFC) was monitored using a Bio-Rad Fluoromark fluorometer at an excitation wavelength of 390 nm and an emission wavelength of 538 nm. Measurements were recorded at 2 min intervals for 1 h. Data are presented as means ± SD (n = 3-4); *$p < 0.05$.

growth and proliferation of neighbouring cells in the same tissue [424 - 427]. Hence, it is tempting to speculate that, by reducing caspase-1 activity in cultured cells of NB lines

BE(2)-m17 and SK-n-MCIXC and thereby impairing their ability to process and secrete cytokines, LCA could prevent growth and proliferation of neighbouring NB cells in culture.

Of note, it has been shown that under some conditions in serum-deprived primary human neurons caspase-1 could function not as an inflammatory caspase, but as a positive regulator of a caspase-6-mediated apoptotic death [428]. Such pro-apoptotic potential of caspase-1 in primary human neurons requires an additional stress factor (a stress co-activator and/or removal of a caspase-1 inhibitor) [428]. A possible role of the observed inhibitory effect of LCA on caspase-1 activity in BE(2)-m17 and SK-n-MCIXC cells in modulating such pro-apoptotic activity of caspase-1 in these NB cell lines remains to be investigated.

### 5.4.7 LCA does not enter cultured NB cells

My mass spectrometry-based measurement of intracellular and extracellular levels of exogenously added LCA revealed that this bile acid does not enter cultured human NB cell lines BE(2)-m17 (Figure 5.19), SK-n-MCIXC (Figure 5.20) and Lan-1 (Figure 5.21). Thus, LCA prevents proliferation of human NB cells and selectively kills these cancer cells (see sections 5.4.1 to 5.4.6) by binding to their surface and then initiating intracellular signaling cascades that not only impair their growth and division, but also cause their apoptotic death. The demonstrated inability of LCA to enter cultured human NB cells suggests that this potent and selective anti-cancer compound is unlikely to display undesirable side effects in non-cancerous human neurons.

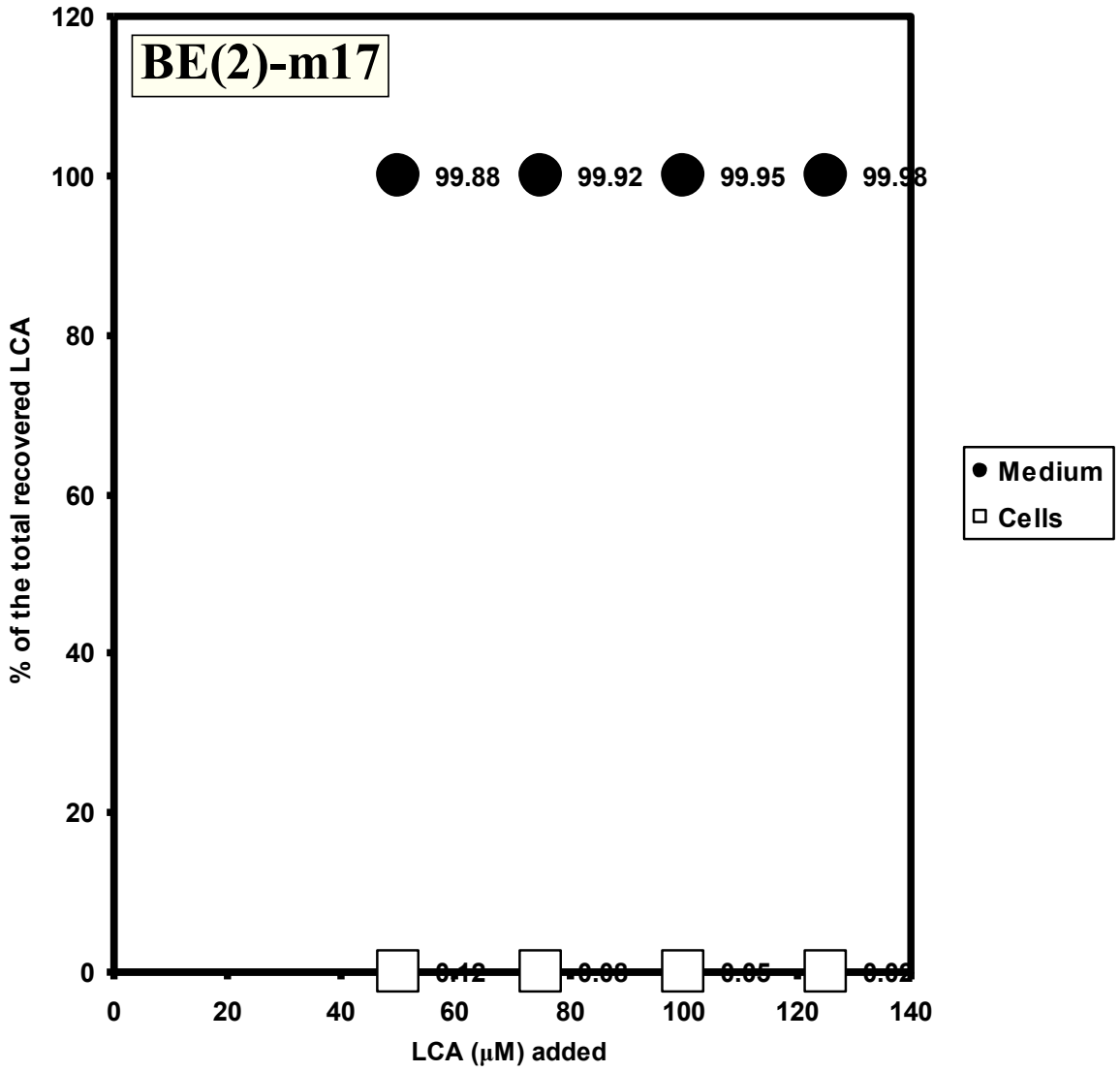


**Figure 5.19.** Exogenously added LCA does not enter cultured human NB cell lines BE(2)-m17. LCA was added to cultured cells at the indicated final concentrations. Lipids were extracted from cells pelleted by centrifugation for 16000 × g for 5 min at 4°C and from the supernatant of cultural medium. The extracted lipids were dried under nitrogen and resuspended in chloroform. Immediately prior to injection the extracted lipids were combined with 2:1 methanol:chloroform with 0.1% (v/v) ammonium hydroxide. This was injected directly into a Q-TOF 2 mass spectrometer using a nano-ESI spray source at 1 μl/min. Spectra were obtained in a negative-ion mode. Acquired spectra were centroided using the Masslynx software then deconvoluted and deisotoped with Excel macros.

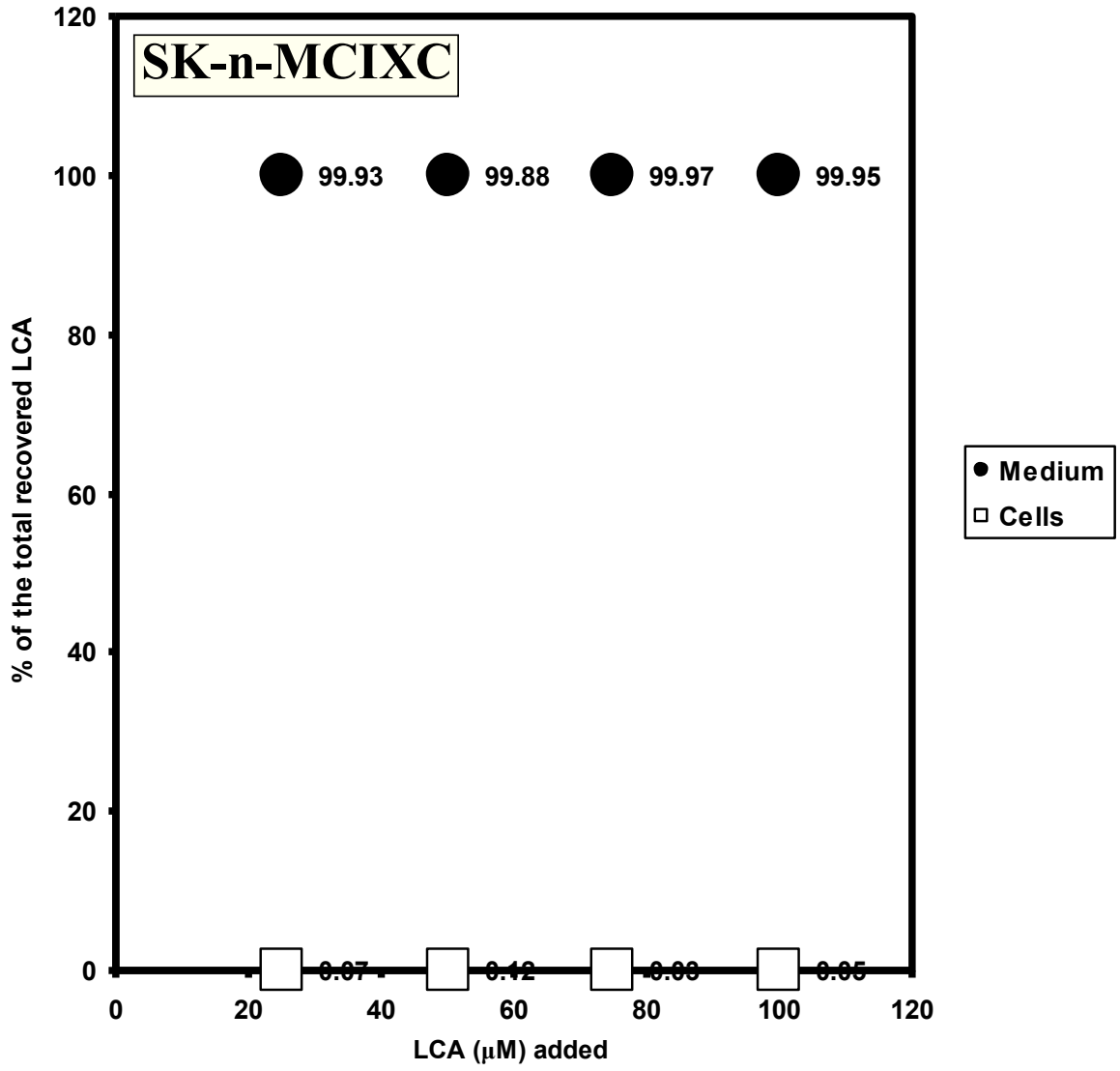


**Figure 5.20.** Exogenously added LCA does not enter cultured human NB cell lines SK-n-MCIXC. LCA was added to cultured cells at the indicated final concentrations. Lipids were extracted from cells pelleted by centrifugation for 16000 × g for 5 min at 4°C and from the supernatant of cultural medium. The extracted lipids were dried under nitrogen and resuspended in chloroform. Immediately prior to injection the extracted lipids were combined with 2:1 methanol:chloroform with 0.1% (v/v) ammonium hydroxide. This was injected directly into a Q-TOF 2 mass spectrometer using a nano-ESI spray source at 1 μl/min. Spectra were obtained in a negative-ion mode. Acquired spectra were centroided using the Masslynx software then deconvoluted and deisotoped with Excel macros.

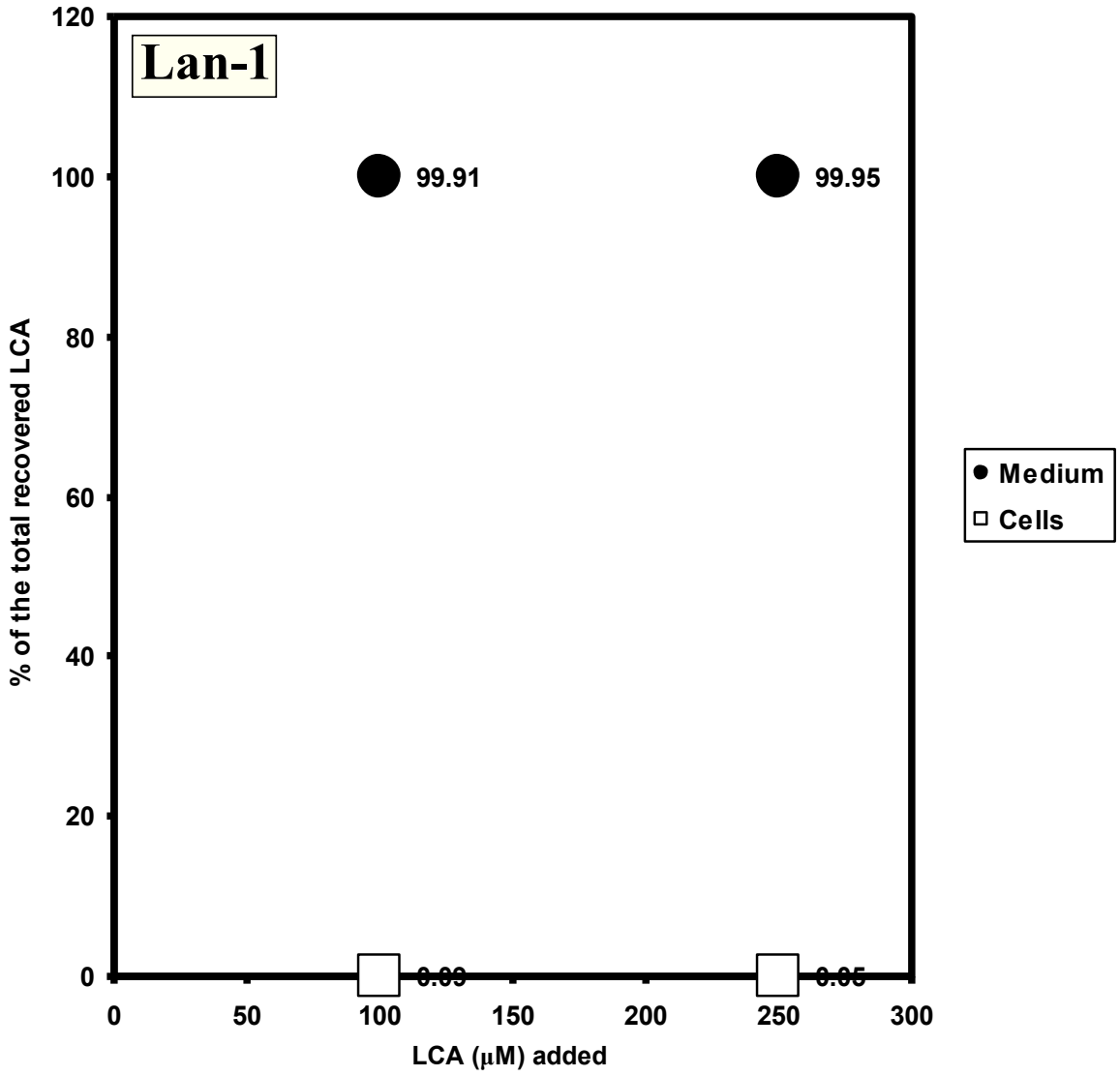


**Figure 5.21.** Exogenously added LCA does not enter cultured human NB cell lines Lan-1. LCA was added to cultured cells at the indicated final concentrations. Lipids were extracted from cells pelleted by centrifugation for 16000 × g for 5 min at 4°C and from the supernatant of cultural medium. The extracted lipids were dried under nitrogen and resuspended in chloroform. Immediately prior to injection the extracted lipids were combined with 2:1 methanol:chloroform with 0.1% (v/v) ammonium hydroxide. This was injected directly into a Q-TOF 2 mass spectrometer using a nano-ESI spray source at 1 μl/min. Spectra were obtained in a negative-ion mode. Acquired spectra were centroided using the Masslynx software then deconvoluted and deisotoped with Excel macros.

## 5.5 Discussion

Findings presented in this chapter of my thesis provide strong evidence that LCA, a bile acid that greatly extends longevity in yeast (see chapter 3), exhibits a potent anti-tumor effect in cultured human NB cells. Bile acids have been shown to provide health benefits to mammals. Synthesized from cholesterol in hepatocytes of the liver, these amphipathic molecules have been for a long time considered to function only as trophic factors for the enteric epithelium and as detergents for the emulsification and absorption of dietary lipids and fat-soluble vitamins [314, 326, 327]. Recent years have been marked by a significant progress in our understanding of the essential role that bile acids play as signaling molecules regulating lipid, glucose and energy homeostasis and activating detoxification of xenobiotics [314, 327, 328]. By stimulating the G-protein-coupled receptor TGR5, bile acids activate the cAMP/PKA signaling pathway that 1) enhances energy expenditure in brown adipose tissue and muscle by stimulating mitochondrial oxidative phosphorylation and uncoupling; 2) improves liver and pancreatic function by activating the endothelial nitric oxide synthase; and 3) enhances glucose tolerance in obese mice by inducing intestinal glucagon-like peptide-1 release [314, 327, 328]. Furthermore, by activating the farnesoid X receptor (FXR) and several other nuclear hormone receptors inside mammalian cells, bile acids 1) modulate the intracellular homeostasis of cholesterol, neutral lipids and fatty acids; 2) regulate glucose metabolism by enhancing glycogenesis and attenuating gluconeogenesis; and 3) stimulate clearance of xenobiotic and endobiotic toxins by activating transcription of numerous xenobiotic detoxification genes [314, 326 - 329]. All these health-improving, beneficial metabolic effects of bile acids prevent the development of obesity following administration of high-

fat diet [314, 326, 327]. Thus, bile acids have a great potential as pharmaceutical agents for the treatment of diabetes, obesity and various associated metabolic disorders, all of which are age-related [314, 326]. Moreover, bile acids have been shown to inhibit neuronal apoptosis in experimental rodent models of neurodegenerative disorders by promoting mitochondrial membrane stability, preventing the release of cytochrome c from mitochondria, reducing activities of various caspases, and activating the NF-κB, PI3K and MAPK survival pathways [329, 330].

My findings presented in this chapter provide the following model for a mechanism underlying a potent and selective anti-tumor effect of LCA in cultured human NB cell lines BE(2)-m17 and SK-n-MCIXC (Figure 5.22). The demonstrated in chapter 5 inability of LCA to enter these cultured human NB cells suggests that this most hydrophobic bile acid species first binds to the G-protein-coupled receptor TGR5, the only known receptor for such compounds in the plasma membrane. In response to such binding, TGR5 and its associated protein partners: 1) transmit, by a yet to be established mechanism, the signal from the plasma membrane to the mitochondrial surface to activate MOMP (process *a* in Figure 5.22); 2) activate, perhaps by a mechanism similar to the one involved in activation of the extrinsic (death receptor) pathway of apoptosis through ligation of death receptors in the plasma membrane [403, 404], the initiator caspase-8 (process *b* in Figure 5.22); and 3) inhibit the inflammatory caspase-1 (process c in Figure 5.23). The LCA/TGR5-induced MOMP results in efflux of cytochrome c from mitochondria, thereby causing apoptosome formation and initiator caspase-9 activation (process *d* in Figure 5.23). The proteolytic cleavage of pro-caspase-3 by the enzymatically active caspase-9 elevates caspase-3 activity, thereby enabling the caspase-

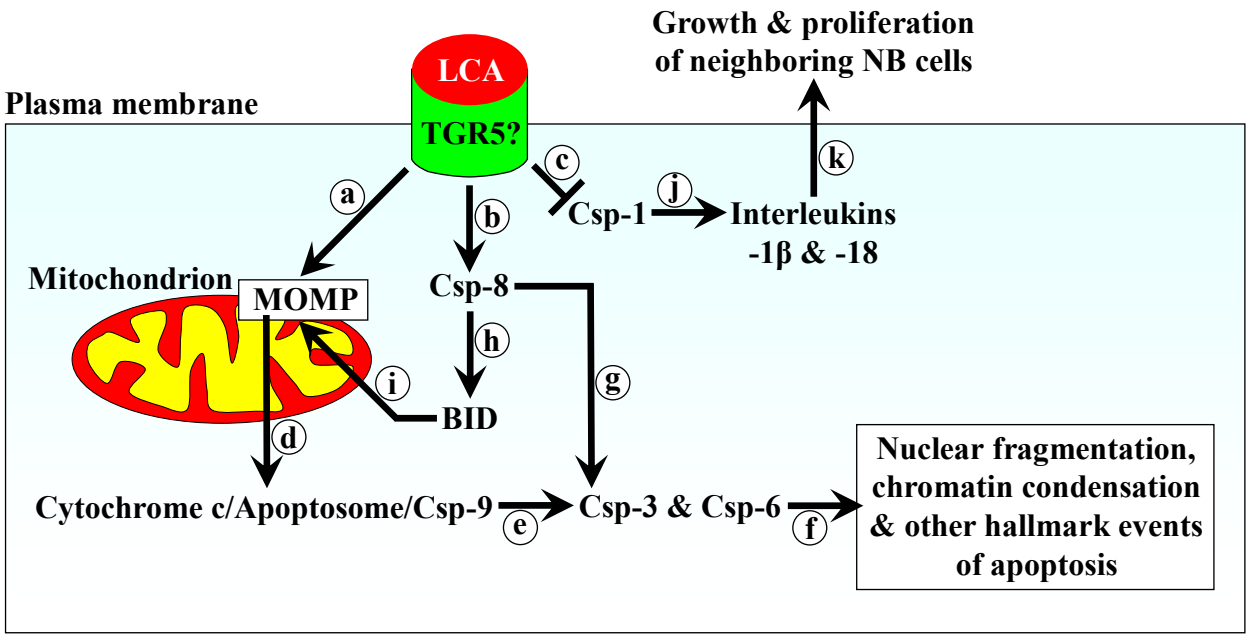


**Figure 5.22.** A model for a mechanism underlying a potent and selective anti-tumor effect of LCA in cultured human NB cell lines BE(2)-m17 and SK-n-MCIXC. See text for details.

3-driven cleavage of pro-caspase-6 and activation of the downstream executioner caspase-6 (process *e* in Figure 5.23). Together, activated caspase-3 and caspase-6 (and perhaps other executioner caspases that are necessary for the proper execution of the LCA-driven, mitochondria-mediated apoptotic program) complete the demolition phase of the program by cleaving their respective protein substrates and producing the morphological features characteristic of apoptotic cell death (process *f* in Figure 5.23). In LCA-exposed NB cells, the proteolytic cleavage of pro-caspase-3 and the resulting increase of caspase-3 activity (which in turn cleaves pro-caspase-6 and activates the downstream executioner caspase-6; process *e* in Figure 5.23) is also triggered by the initiator caspase-8 acting in the LCA-driven extrinsic pathway of apoptosis (process *g* in Figure 5.23). In addition, activated in LCA-exposed NB cells caspase-8 causes MOMP

and triggers the intrinsic (mitochondrial) pathway of apoptosis by cleaving and activating BID (processes *h* and *i* in Figure 5.23). In my model, the LCA-driven inhibition of the inflammatory caspase-1 (process *c* in Figure 5.23) contributes to the anti-tumor effect of LCA in cultured cells of NB lines BE(2)-m17 and SK-n-MCIXC by attenuating the processing and unconventional secretion of the cytokines interleukin-1β and interleukin-18 (process *j* in Figure 5.23) – thereby preventing growth and proliferation of neighbouring NB cells in culture (process *k* in Figure 5.23).

Importantly, I found that LCA greatly enhances the susceptibility of cultured human NB cell lines BE(2)-m17 and SK-n-MCIXC to a hydrogen peroxide-induced form of mitochondria-controlled apoptotic cell death, even when this bile acid was used at concentrations that in the absence of hydrogen peroxide do not compromise their viability. Furthermore, while 75 μM LCA caused apoptotic death of all or most of the BE(2)-m17 and SK-n-MCIXC cells exposed to 0.1 mM hydrogen peroxide, in this concentration LCA greatly increased the resistance of primary cultures of human neurons to the hydrogen peroxide-induced form of mitochondria-controlled apoptotic cell death. Based on these observations, I propose that the exposure of a mixed population of various NB cell lines and non-cancerous neurons to low concentrations of simultaneously added hydrogen peroxide and LCA may concurrently 1) kill all NB cells by causing their apoptotic death; and 2) promote the viability of non-cancerous neurons by increasing their resistance to hydrogen peroxide-induced apoptosis.

A different, yet to be defined mechanism underlies the observed ability of LCA to selectively kill cultured human NB cell line Lan-1. I propose that the anti-tumor effect of LCA in cultured Lan-1 cells is due to the ability of this bile acid to cause necrotic or

some other non-apoptotic kind of death, which is not characterized by such major distinctive (*i.e.*, not seen under any other modes of cell death) event of apoptotic cell death as nuclear condensation and fragmentation.

Of note, a recent collaborative effort of the laboratories of Dr. Troy Harkness (Department of Anatomy and Cell Biology, University of Saskatchewan) and Dr. Vladimir Titorenko has revealed that in low concentrations LCA kills cultured MCF7 human breast cancer cells and F98 rat glioblastoma cells. Thus, LCA exhibits a universal anti-tumor effect, as it has a very broad cytotoxic effect on cancer cells derived from different tissues and from different organisms.

## 5.6 Conclusions

My findings imply that LCA exhibits a potent anti-tumor effect in cultured human NB cells by: 1) activating both intrinsic (mitochondrial) and extrinsic (death receptor) pathways of apoptotic death in these cells; 2) sensitizing them to hydrogen peroxide-induced apoptotic death; and 3) preventing growth and proliferation of their neighbouring NB cells in the culture. Importantly, LCA does not display any of these deleterious effects in human neurons and, therefore, is a selective anti-tumor compound. Furthermore, the demonstrated here inability of LCA to enter cultured human NB cells suggests that this potent and selective anti-tumor compound is unlikely to display undesirable side effects in non-cancerous human neurons. My findings suggest a mechanism underlying a potent and selective anti-tumor effect of LCA in cultured human NB cell lines BE(2)-m17 and SK-n-MCIXC.

# 6 Conclusions and suggestions for future work

## 6.1 General conclusions

### 6.1.1 Chronological aging in yeast is the final step of a developmental program progressing through a series of checkpoints

To address the inherent complexity of aging from a systems perspective and to build an integrative spatiotemporal model of aging process, I used the concepts and methodologies of so-called metabolic control analysis [1, 8]. In studies described in chapter 2, I investigated how caloric restriction (CR) - a low-calorie dietary regimen known to extend longevity and improve health in evolutionarily distant organisms ranging from yeast to rhesus monkeys [76 - 83] - influences the metabolic history of chronologically aging yeast. I examined how CR influences the age-related dynamics of changes in the intracellular levels of numerous proteins and metabolites, carbohydrate metabolism, interorganellar metabolic flow, concentration of reactive oxygen species (ROS), mitochondrial morphology, essential oxidation-reduction processes in mitochondria, mitochondrial proteome, frequency of mitochondrial DNA mutations, dynamics of mitochondrial nucleoid, susceptibility to mitochondria-controlled apoptosis, and stress resistance. Based on my comparison of the metabolic histories of long-lived CR yeast and short-lived non-CR yeast reported in chapter 2, I concluded that yeast define their long-term viability by designing a diet-specific pattern of metabolism and organelle dynamics prior to reproductive maturation. My data imply that longevity in chronologically aging yeast is programmed by the level of metabolic capacity and organelle organization they developed, in a diet-specific fashion, prior to entry into a non-proliferative state. Therefore, my conclusion is that chronological aging in yeast is

the final step of a developmental program progressing through a series of checkpoints. By unveiling the different scenarios for a stepwise establishment of patterns of metabolism, inter-organellar communications and mitochondrial morphology in chronologically aging CR and non-CR yeast, my studies described in chapter 2 enabled to define a distinct group of cellular metabolites and processes that play an essential role in longevity regulation.

### 6.1.2 My chemical genetic screen identifies lithocholic acid as an anti-aging compound that extends yeast chronological life span in a TOR-independent manner, by modulating housekeeping longevity assurance processes

In studies described in chapter 3, I designed a chemical genetic screen for small molecules that increase the chronological life span (CLS) of yeast under CR by targeting lipid metabolism and modulating housekeeping longevity pathways that regulate longevity irrespective of the number of available calories. My screen identified lithocholic acid (LCA) as one of such molecules. My evaluation of the life-extending efficacy of LCA in WT strain on a high- or low-calorie diet revealed that this compound extends yeast CLS irrespective of the number of available calories. I found that the extent to which LCA extends longevity is highest under CR conditions, when the pro-aging processes modulated by the adaptable TOR and cAMP/PKA pathways are suppressed and the anti-aging processes are activated [6, 7, 10]. I also found that the life-extending efficacy of LCA in CR yeast significantly exceeded that in yeast on a high-calorie diet, in which the adaptable TOR and cAMP/PKA pathways greatly activate the pro-aging processes and suppress the anti-aging processes [4, 5, 7, 35, 279]. Altogether, my

findings suggest that, consistent with its sought-after effect on a longevity signaling network, LCA mostly targets certain housekeeping longevity assurance pathways that do not overlap (or only partially overlap) with the adaptable TOR and cAMP/PKA pathways modulated by calorie availability.

Consistent with my assumption that LCA extends longevity not by modulating the adaptable TOR pathway, in studies described in chapter 3 I found that lack of Tor1p does not impair the life-extending efficacy of LCA under CR. I also revealed that, LCA extends longevity of the *tor1Δ* mutant strain to a very similar degree under CR and non-CR conditions. Thus, by eliminating a master regulator of this key adaptable pathway that shortens the CLS of yeast on a high-calorie diet, the *tor1Δ* mutation abolished the dependence of the anti-aging efficacy of LCA on the number of available calories.

My findings described in chapter 3, along with some recently published data from Dr. Titorenko's laboratory, revealed two mechanisms underlying the life-extending effect of LCA in chronologically aging yeast. One mechanism operates in a calorie availability-independent fashion and involves the LCA-governed modulation of housekeeping longevity assurance pathways that do not overlap with the adaptable TOR and cAMP/PKA pathways. The other mechanism extends yeast longevity under non-CR conditions and consists in LCA-driven unmasking of the previously unknown anti-aging potential of PKA. I provide evidence that LCA modulates housekeeping longevity assurance pathways by 1) attenuating mitochondrial fragmentation, a hallmark event of age-related cell death; 2) altering oxidation-reduction processes in mitochondria, including oxygen consumption, the maintenance of membrane potential, and reactive oxygen species production; 3) enhancing resistance to oxidative and thermal stresses; 4)

suppressing mitochondria-controlled apoptosis; and 5) enhancing stability of nuclear and mitochondrial DNA.

### 6.1.3 A hypothesis on xenohormetic, hormetic and cytostatic forces driving the evolution of longevity regulation mechanisms within ecosystems and its empirical verification

In my chemical genetic screen described in chapter 3, I identified lithocholic acid (LCA), as a novel anti-aging molecule that extends yeast longevity. Yeast do not synthesize this or any other bile acids produced by mammals [314, 326]; a recent mass spectrometry-based analysis of the total yeast lipidome conducted in Dr. Titorenko's laboratory has confirmed lack of endogenous bile acids. Therefore, in chapter 4 I proposed that bile acids released into the environment by mammals may act as interspecies chemical signals providing longevity benefits to yeast and, perhaps, other species within an ecosystem. I hypothesized that, because bile acids are known to be mildly toxic compounds, they may create selective pressure for the evolution of yeast species that can respond to the bile acids-induced mild cellular damage by developing the most efficient stress protective mechanisms. It is likely that such mechanisms may provide effective protection of yeast against molecular and cellular damage accumulated with age. Thus, I proposed in chapter 4 that yeast species that have been selected for the most effective mechanisms providing protection against bile acids may evolve the most effective anti-aging mechanisms that are sensitive to regulation by bile acids. I extended my hypothesis on longevity regulation by bile acids by suggesting in chapter 4 a

hypothesis of the xenohormetic, hormetic and cytostatic selective forces driving the evolution of longevity regulation mechanisms at the ecosystemic level.

To verify my hypothesis empirically, I carried out the LCA-driven multistep selection of long-lived yeast species under laboratory conditions. As outlined in chapter 4, I found that a lasting exposure of wild-type yeast to LCA results in selection of yeast species that live longer in the absence of this bile acid than their ancestor. My data enabled to rank different concentrations of LCA with respect to the efficiency with which they cause the appearance of long-lived yeast species. I revealed that, if used at the most efficient concentration of 5 μM, this bile acid induced life-extending mutations with the frequency of about $4 \times 10^8$/generation. At the concentration of 50 μM, LCA caused the appearance of long-lived species with the frequency of $1 \times 10^8$/generation, whereas a lasting exposure of yeast to 250 μM LCA did not result in selection of such species. Because the lowest used concentration of LCA resulted in the highest frequency of long-lived species appearance, I believe that it is unlikely that the life-extending mutations they carry are due to mutagenic action of this bile acid.

### 6.1.4 The molecular mechanism underlying a potent and selective anti-tumor effect of LCA in cultured human neuroblastoma cells

Aging is one of the major risk factors in the onset and incidence of cancer [154 - 156], and cancer is considered as one of the numerous age-associated diseases whose onset can be delayed and incidence reduced by anti-aging interventions [157 - 162]. The interplay between aging and cancer is intricate as these two complex and dynamic biological phenomena have both convergent and divergent underlying mechanisms [157 -

223]. The objective of my studies described in chapter 5 was to examine if lithocholic acid (LCA), a novel anti-aging compound that I identified in a high-throughput chemical genetic screen, also exhibits an anti-tumor effect in cultured human cancer cells by activating certain anti-cancer processes that may (or may not) play an essential role in cellular aging. As a model system for addressing this important question (and if LCA indeed displays an anti-tumor effect, for establishing the mechanism underlying such effect), I choose several cell lines of the human neuroblastoma (NB) tumor.

In chapter 5 of my thesis, I described findings providing strong evidence that LCA exhibits a potent anti-tumor effect in cultured human NB cells by: 1) activating both intrinsic (mitochondrial) and extrinsic (death receptor) pathways of apoptotic death in these cells; 2) sensitizing them to hydrogen peroxide-induced apoptotic death; and 3) preventing growth and proliferation of their neighbouring NB cells in the culture. Importantly, my findings described in chapter 5 imply that LCA does not display any of these deleterious effects in human neurons and, therefore, is a selective anti-tumor compound. Moreover, my mass spectrometry-based measurement of intracellular and extracellular levels of exogenously added LCA revealed that this bile acid does not enter cultured NB cells. Thus, LCA prevents proliferation of human NB cells and selectively kills these cancer cells by binding to their surface and then initiating intracellular signaling cascades that not only impair their growth and division, but also cause their apoptotic death. The demonstrated inability of LCA to enter cultured human NB cells suggests that this potent and selective anti-cancer compound is unlikely to display undesirable side effects in non-cancerous human neurons.

## 6.2 Suggestions for future work

As my comparison of the metabolic histories of long-lived CR yeast and short-lived non-CR yeast reported in chapter 2 revealed, yeast define their long-term viability by designing a diet-specific pattern of metabolism and organelle dynamics prior to reproductive maturation. These findings imply that longevity in chronologically aging yeast is programmed by the level of metabolic capacity and organelle organization they developed, in a diet-specific fashion, prior to entry into a non-proliferative state. Therefore, my conclusion is that chronological aging in yeast is the final step of a developmental program progressing through a series of checkpoints.

The major challenges for the future research are 1) to validate my hypothesis that the longevity of chronologically aging yeast is programmed by the level of metabolic capacity and organelle organization they developed, in a diet-specific fashion, prior to reproductive maturation; and 2) to rank the relative contributions of different metabolites and processes to the chronological aging of yeast. To address these challenges, one could evaluate how genetic manipulations that alter concentrations of these critical metabolites and affect these essential processes influence yeast longevity by modulating age-related protein aggregation, mitochondria-controlled apoptosis, free fatty acid- and diacylglycerol-induced necrosis, susceptibility to oxidative stress, and frequency of mtDNA mutations. A challenge for the future will be to elucidate how a longevity regulatory network centered on the Ras2p/cAMP/PKA/Rim15p/Msn2p/Msn4p and Tor1p/Sch9p/Rim15p/Gis1p nutrient-sensing pathways [278, 296, 301] governs the development of the diet-specific pattern of metabolism and organelle dynamics in chronologically aging yeast under CR conditions. Moreover, it would be interesting to

examine whether the pattern established in yeast cells grown under CR conditions can be reversed upon their transfer to calorie-rich medium. Another challenge for the future will be to test the validity of my hypothesis that chronologically aging CR yeast protect their mitochondrial nucleoids from oxidative damage by turning on the RTG signaling pathway, which then activates transcription of *ACO1* and other genes encoding bifunctional mtDNA-binding proteins known to maintain the integrity of mtDNA under respiratory conditions.

Finally, I expect that in the near future this knowledge will be instrumental for designing high-throughput screening of novel anti-aging drugs that can extend longevity by modulating the envisioned here developmental program of chronological aging operating in yeast.

In chapter 3, I provided evidence that LCA - a novel anti-aging compound identified in my high-throughput chemical genetic screen - modulates housekeeping longevity assurance pathways by 1) attenuating mitochondrial fragmentation, a hallmark event of age-related cell death; 2) altering oxidation-reduction processes in mitochondria, including oxygen consumption, the maintenance of membrane potential, and reactive oxygen species production; 3) enhancing resistance to oxidative and thermal stresses; 4) suppressing mitochondria-controlled apoptosis; and 5) enhancing stability of nuclear and mitochondrial DNA. I expect that in the near future this knowledge will be instrumental for defining molecular mechanisms underlying the ability of LCA to extend longevity by impacting these various housekeeping longevity assurance processes and by modulating signaling pathways governing them.

In chapter 4, I suggested a hypothesis on the xenohormetic, hormetic and

cytostatic selective forces driving the evolution of longevity regulation mechanisms at the ecosystemic level. As a first step towards empirical verification of my hypothesis, I carried out the LCA-driven multistep selection of long-lived yeast species under laboratory conditions. As outlined in chapter 4, I found that a lasting exposure of wild-type yeast to LCA results in selection of yeast species that live longer in the absence of this bile acid than their ancestor. To test the validity of other aspects of my hypothesis on the ecosystemic evolution of longevity regulation mechanisms, future studies need to address the following most critical questions: 1) what genes are affected by mutations responsible for the extended longevity of selected long-lived yeast species? 2) how these mutations influence a compendium of the housekeeping longevity-related processes modulated by LCA in chronologically aging yeast and described in chapter 3?; 3) 3) will these mutations affect the growth rate of yeast in media with or without LCA? 4) will selected long-lived yeast species be able to maintain their ability to live longer than wild-type yeast if they undergo several successive passages in medium without LCA? - and, thus, is there selective pressure aimed at maintaining of an "optimal" rather than a "maximal" chronological life span of yeast (due to, *e.g.*, a proposed selective advantage of the envisioned "altruistic" program [356 - 361] of chronological aging in yeast)? and 5) if mixed with an equal number of wild-type yeast cells, will selected long-lived yeast species out-grow and/or out-live them in medium without LCA or the opposite will happen (due to selective pressure on yeast aimed at maintaining of the so-called "altruistic" program [356 - 361] of their chronological aging)?

As described in chapter 5, my findings imply that LCA exhibits a potent anti-tumor effect in cultured human neuroblastoma (NB) cells by: 1) activating both intrinsic

(mitochondrial) and extrinsic (death receptor) pathways of apoptotic death in these cells; 2) sensitizing them to hydrogen peroxide-induced apoptotic death; and 3) preventing growth and proliferation of their neighbouring NB cells in the culture. Importantly, I found that LCA does not display any of these deleterious effects in human neurons and, therefore, is a selective anti-tumor compound. Furthermore, the demonstrated in chapter 5 inability of LCA to enter cultured human NB cells suggests that this potent and selective anti-tumor compound is unlikely to display undesirable side effects in non-cancerous human neurons. My findings described in chapter 5 suggest a mechanism underlying a potent and selective anti-tumor effect of LCA in cultured human NB cell lines BE(2)-m17 and SK-n-MCIXC. In this mechanism, LCA kills these NB cells by: 1) activating both intrinsic (mitochondrial) and extrinsic (death receptor) pathways of apoptotic death in these cells; 2) sensitizing them to hydrogen peroxide-induced apoptotic death; and 3) preventing growth and proliferation of their neighbouring NB cells in the culture. Of note, a recent collaborative effort of the laboratories of Dr. Troy Harkness (Department of Anatomy and Cell Biology, University of Saskatchewan) and Dr. Vladimir Titorenko has revealed that in low concentrations LCA kills cultured MCF7 human breast cancer cells and F98 rat glioblastoma cells. Thus, LCA exhibits a universal anti-tumor ability, as it has a very broad cytotoxic effect on cancer cells derived from different tissues and from different organisms. In the future, one could use an algorithm which I developed for cultured human NB cells to define the mechanisms underlying the anti-tumor action of LCA in MCF7 human breast cancer cells and in F98 rat glioblastoma cells.

# 7 References


1. Kirkwood, T.B.L., Boys, R.J., Gillespie, C.S., Proctor, C.J., Shanley, D.P. and Wilkinson, D.J. (2003). Towards an e-biology of ageing: integrating theory and data. *Nat. Rev. Mol. Cell Biol.* 4:243-249.
2. Kirkwood, T.B.L. (2005). Understanding the odd science of aging. *Cell* 120:437-447.
3. Kirkwood, T.B.L. (2008). Understanding ageing from an evolutionary perspective. *J. Intern. Med.* 263:117-127.
4. Greer, E.L. and Brunet, A. (2008). Signaling networks in aging. *J. Cell Sci.* 121:407-412.
5. Guarente, L.P., Partridge, L. and Wallace, D.C. (Editors) (2008). *Molecular Biology of Aging*. Cold Spring Harbor Laboratory Press, Cold Spring Harbor, New York, 610 pages.
6. Lin, S.-J. and Sinclair, D. (2008). Molecular mechanisms of aging: insights from budding yeast. In: Guarente, L.P., Partridge, L., Wallace, D.C. (Eds.), *Molecular Biology of Aging*. Cold Spring Harbor Laboratory Press, Cold Spring Harbor, New York, pp. 483-516.
7. Mair, W. and Dillin, A. (2008). Aging and survival: the genetics of life span extension by dietary restriction. *Annu. Rev. Biochem.* 77:727-754.
8. Murphy, M.P. and Partridge, L. (2008). Toward a control theory analysis of aging. *Annu. Rev. Biochem*. 77:777-798.

9. Puigserver, P. and Kahn, C.R. (2008). Mammalian metabolism in aging. In: Guarente, L.P., Partridge, L., Wallace, D.C. (Eds.), *Molecular Biology of Aging*. Cold Spring Harbor Laboratory Press, Cold Spring Harbor, New York, pp. 545-574.

10. Fontana, L., Partridge, L. and Longo, V.D. (2010). Extending healthy life span - from yeast to humans. *Science* 328:321-326.

11. Tavernarkis, N. (Editor) (2010). *Protein Metabolism and Homeostasis in Aging*. Landes Bioscience and Springer Science+Business Media, New York, 249 pages.

12. Kirkwood, T.B.L. (2011). Systems biology of ageing and longevity. *Philos. Trans. R. Soc. Lond. B Biol. Sci*. 366:64-70.

13. Masoro, E.J. and Austad, S.N. (Editors) (2011). *Handbook of the Biology of Aging.* 7th Edition. Academic Press (an imrint of Elsevier), Amsterdam, 572 pages.

14. Partridge, L. (2010). The new biology of ageing. *Philos. Trans. R. Soc. Lond. B Biol. Sci*. 365:147-154.

15. Wheeler, H.E. and Kim, S.K. (2011). Genetics and genomics of human ageing. *Philos. Trans. R. Soc. Lond. B Biol. Sci*. 366:43-50.

16. Dillin, A. and Cohen, E. (2011). Ageing and protein aggregation-mediated disorders: from invertebrates to mammals. *Philos. Trans. R. Soc. Lond. B Biol. Sci*. 366:94-98.

17. Lithgow, G.J. (2006). Why aging isn't regulated: a lamentation on the use of language in aging literature. *Exp. Gerontol*. 41:890-893.

18. Antebi, A. (2005). Physiology. The tick-tock of aging? *Science* 310:1911-1913.

19. Blagosklonny, M.V. (2007). Paradoxes of aging. *Cell Cycle* 6:2997-3003.

20. Blagosklonny, M.V. (2007). Program-like aging and mitochondria: instead of random damage by free radicals. *J. Cell. Biochem.* 102:1389-1399.

21. Budovskaya, Y.V., Wu, K., Southworth, L.K., Jiang, M., Tedesco, P., Johnson, T.E. and Kim, S.K. (2008). An elt-3/elt-5/elt-6 GATA transcription circuit guides aging in *C. elegans*. *Cell* 134:291-303.

22. Longo, V.D., Mitteldorf, J. and Skulachev, V.P. (2005). Programmed and altruistic ageing. *Nat. Rev. Genet.* 6:866-872.

23. Skulachev, V.P. and Longo, V.D. (2005). Aging as a mitochondria-mediated atavistic program: can aging be switched off? *Ann. N. Y. Acad. Sci.* 1057:145-164.

24. Goldberg, A.A., Bourque, S.D., Kyryakov, P., Gregg, C., Boukh-Viner, T., Beach, A., Burstein, M.T., Machkalyan, G., Richard, V., Rampersad, S., Cyr, D., Milijevic, S. and Titorenko, V.I. Effect of calorie restriction on the metabolic history of chronologically aging yeast. (2009) *Exp. Gerontol*. 44:555-571.

25. Kenyon, C. (2001). A conserved regulatory system for aging. *Cell* 105: 165-168.

26. Kenyon, C. (2005). The plasticity of aging: insights from long-lived mutants. *Cell* 120: 449-460.

27. Kenyon, C. (2010). The genetics of ageing. *Nature* 464:504-512.

28. Kenyon, C. (2010). A pathway that links reproductive status to lifespan in *Caenorhabditis elegans*. *Ann. N. Y. Acad. Sci*. 1204:156-162.

29. Kenyon, C. (2011). The first long-lived mutants: discovery of the insulin/IGF-1 pathway for ageing. *Philos. Trans. R. Soc. Lond. B Biol. Sci*. 366:9-16.

30. Longo, V.D. and Finch, C.E. (2003). Evolutionary medicine: from dwarf model systems to healthy centenarians? *Science* 299:1342-1346.

31. Bitterman, K.J., Medvedik, O. and Sinclair, D.A. (2003). Longevity regulation in *Saccharomyces cerevisiae*: linking metabolism, genome stability, and heterochromatin. *Microbiol. Mol. Biol. Rev.* 67:376-399.

32. Kenyon, C. (2005). The plasticity of aging: insights from long-lived mutants. *Cell* 120:449-460.

33. Guarente, L. (2006). Sirtuins as potential targets for metabolic syndrome. *Nature* 444:868-874.

34. Kaeberlein, M., Burtner, C.R. and Kennedy, B.K. (2007). Recent developments in yeast aging. *PLoS Genet.* 3:e84.

35. Wei, M., Fabrizio, P., Hu, J., Ge, H., Cheng, C., Li, L. and Longo, V.D. (2008). Life span extension by calorie restriction depends on Rim15 and transcription factors downstream of Ras/PKA, Tor, and Sch9. *PLoS Genet*. 4:e13.

36. Narasimhan, S.D., Yen, K. and Tissenbaum, H.A. (2009). Converging pathways in lifespan regulation. *Curr. Biol*. 19:R657-R666.

37. Laplante, M. and Sabatini, D.M. (2009). mTOR signaling at a glance. *J. Cell Sci*. 122:3589-3594.

38. Shaw, R.J. (2009). LKB1 and AMP-activated protein kinase control of mTOR signalling and growth. *Acta Physiol*. 196:65-80.

39. Zoncu, R., Efeyan, A. and Sabatini, D.M. (2011). mTOR: from growth signal integration to cancer, diabetes and ageing. *Nat. Rev. Mol. Cell Biol*. 12:21-35.

40. Jacinto, E. (2008). What controls TOR? *IUBMB Life*. 60:483-496.

41. Kapahi, P., Chen, D., Rogers, A.N., Katewa, S.D., Li, P.W., Thomas, E.L. and Kockel L. (2010). With TOR, less is more: a key role for the conserved nutrient-sensing TOR pathway in aging. *Cell Metab*. 11:453-465.

42. Rohde, J.R., Bastidas, R., Puria, R. And Cardenas, M.E. (2008). Nutritional control via Tor signaling in *Saccharomyces cerevisiae*. *Curr. Opin. Microbiol*. 11:153-160.

43. Díaz-Troya, S., Pérez-Pérez, M.E., Florencio, F.J. and Crespo, J.L. (2008). The role of TOR in autophagy regulation from yeast to plants and mammals. *Autophagy* 4:851-865.

44. Huber, A., Bodenmiller, B., Uotila, A., Stahl, M., Wanka, S., Gerrits, B., Aebersold, R. and Loewith, R. (2009). Characterization of the rapamycin-sensitive phosphoproteome reveals that Sch9 is a central coordinator of protein synthesis. *Genes Dev*. 23:1929-1943.

45. Pan, Y. and Shadel, G.S. (2009). Extension of chronological life span by reduced TOR signaling requires down-regulation of Sch9p and involves increased mitochondrial OXPHOS complex density. *Aging* 1:131-145.

46. Kim, E., Goraksha-Hicks, P., Li, L., Neufeld, T.P. and Guan, K.L. (2008). Regulation of TORC1 by Rag GTPases in nutrient response. *Nat. Cell Biol*. 10:935-945.

47. Sancak, Y., Peterson, T.R., Shaul, Y.D., Lindquist, R.A., Thoreen, C.C., Bar-Peled, L. and Sabatini, D.M. (2008). The Rag GTPases bind raptor and mediate amino acid signaling to mTORC1. *Science* 320:1496-1501.

48. Avruch, J., Long, X., Ortiz-Vega, S., Rapley, J., Papageorgiou, A. and Dai, N. (2009). Amino acid regulation of TOR complex 1. *Am. J. Physiol. Endocrinol. Metab*. 296:E592-E602.

49. Binda, M., Péli-Gulli, M.P., Bonfils, G., Panchaud, N., Urban, J., Sturgill, T.W., Loewith, R. and De Virgilio, C. (2009). The Vam6 GEF controls TORC1 by activating the EGO complex. *Mol. Cell* 35:563-573.

50. Narbonne, P. and Roy, R. (2009). *Caenorhabditis elegans* dauers need LKB1/AMPK to ration lipid reserves and ensure long-term survival. *Nature* 457:210-214.

51. Yan, L., Vatner, D.E., O'Connor, J.P., Ivessa, A., Ge, H., Chen, W., Hirotani, S., Ishikawa, Y., Sadoshima, J. and Vatner, S.F. (2007). Type 5 adenylyl cyclase disruption increases longevity and protects against stress. *Cell* 130:247-258.

52. Enns, L.C., Morton, J.F., Mangalindan, R.S., McKnight, G.S., Schwartz, M.W., Kaeberlein, M.R., Kennedy, B.K., Rabinovitch, P.S. and Ladiges, W.C. (2009). Attenuation of age-related metabolic dysfunction in mice with a targeted disruption of the Cβ subunit of protein kinase A. *J. Gerontol. A Biol. Sci. Med. Sci*. 64:1221-1231.

53. Enns, L.C., Morton, J.F., Treuting, P.R., Emond, M.J., Wolf, N.S., McKnight, G.S., Rabinovitch, P.S. and Ladiges, W.C. (2009). Disruption of protein kinase A in mice enhances healthy aging. *PLoS One* 4:e5963.

54. Santangelo, G.M. (2006). Glucose signaling in *Saccharomyces cerevisiae*. *Microbiol. Mol. Biol. Rev*. 70:253-282.

55. Gancedo, J.M. (2008). The early steps of glucose signalling in yeast. *FEMS Microbiol. Rev*. 32:673-704.

56. Medvedik, O., Lamming, D.W., Kim, K.D. and Sinclair, D.A. (2007). MSN2 and MSN4 link calorie restriction and TOR to sirtuin-mediated lifespan extension in *Saccharomyces cerevisiae*. *PLoS Biol*. 5:e261.

57. Lee, P., Cho, B.R., Joo, H.S. and Hahn, J.S. (2008). Yeast Yak1 kinase, a bridge between PKA and stress-responsive transcription factors, Hsf1 and Msn2/Msn4. *Mol. Microbiol*. 70:882-895.

58. Smets, B., Ghillebert, R., De Snijder, P., Binda, M., Swinnen, E., De Virgilio, C. and Winderickx, J. (2010). Life in the midst of scarcity: adaptations to nutrient availability in *Saccharomyces cerevisiae*. *Curr. Genet*. 56:1-32.

59. Roosen, J., Engelen, K., Marchal, K., Mathys, J., Griffioen, G., Cameroni, E., Thevelein, J.M., De Virgilio, C., De Moor, B. and Winderickx, J. (2005). PKA and Sch9 control a molecular switch important for the proper adaptation to nutrient availability. *Mol. Microbiol*. 55:862-880.

60. Cheng, C., Fabrizio, P., Ge, H., Longo, V.D. and Li, L.M. (2007). Inference of transcription modification in long-live yeast strains from their expression profiles. *BMC Genomics* 8:219.

61. Cheng, C., Fabrizio, P., Ge, H., Wei, M., Longo, V.D. and Li, L.M. (2007). Significant and systematic expression differentiation in long-lived yeast strains. *PLoS One* 2:e1095.

62. Slattery, M.G., Liko, D. and Heideman, W. (2008). Protein kinase A, TOR, and glucose transport control the response to nutrient repletion in *Saccharomyces cerevisiae*. *Eukaryot. Cell* 7:358-367.

63. Fabrizio, P. and Longo, V.D. (2003). The chronological life span of *Saccharomyces cerevisiae*. *Aging Cell* 2:73-81.

64. Anderson, R.M., Bitterman, K.J., Wood, J.G., Medvedik, O. and Sinclair, D.A. (2003). Nicotinamide and *PNC1* govern lifespan extension by calorie restriction in *Saccharomyces cerevisiae*. *Nature* 423:181-185.

65. Yan, L., Vatner, D.E., O'Connor, J.P., Ivessa, A., Ge, H., Chen, W., Hirotani, S., Ishikawa, Y., Sadoshima, J. and Vatner, S.F. (2007). Type 5 adenylyl cyclase disruption increases longevity and protects against stress. *Cell* 130:247-258.

66. Piper, M.D., Selman, C., McElwee, J.J. and Partridge, L. (2008). Separating cause from effect: how does insulin/IGF signalling control lifespan in worms, flies and mice? *J. Intern. Med*. 263:179-191.

67. Puigserver, P. and Kahn, C.R. (2008). Mammalian metabolism in aging. In: *Molecular Biology of Aging* (Guarente LP, Partridge L, Wallace DC, eds). Cold Spring Harbor Laboratory Press, Cold Spring Harbor, New York, pp. 545-574.

68. Salih, D.A. and Brunet, A. (2008). FoxO transcription factors in the maintenance of cellular homeostasis during aging. *Curr. Opin. Cell Biol*. 20:126-136.

69. Wolff, S. and Dillin, A. (2006). The trifecta of aging in *Caenorhabditis elegans*. *Exp. Gerontol*. 41:894-903.

70. Murphy, C.T. (2006). The search for DAF-16/FOXO transcriptional targets: approaches and discoveries. *Exp. Gerontol*. 41:910-921.

71. Oh, S.W., Mukhopadhyay, A., Dixit, B.L., Raha, T., Green, M.R. and Tissenbaum, H.A. (2006). Identification of direct DAF-16 targets controlling longevity, metabolism and diapause by chromatin immunoprecipitation. *Nat. Genet*. 38:251-257.

72. Finkel, T., Deng, C.X. and Mostoslavsky, R. (2009). Recent progress in the biology and physiology of sirtuins. *Nature* 460:587-591.

73. Finley, L.W. and Haigis, M.C. (2009). The coordination of nuclear and mitochondrial communication during aging and calorie restriction. *Ageing Res. Rev*. 8:173-188.

74. Soukas, A.A., Kane, E.A., Carr, C.E., Melo, J.A. and Ruvkun, G. (2009). Rictor/TORC2 regulates fat metabolism, feeding, growth, and life span in *Caenorhabditis elegans*. *Genes Dev*. 23:496-511.

75. Giorgio, M., Trinei, M., Migliaccio, E. and Pelicci, P.G. (2007). Hydrogen peroxide: a metabolic by-product or a common mediator of ageing signals? *Nat. Rev. Mol. Cell Biol*. 8:722-728.

76. Weindruch, R. and Walford, R.L. (1988). The Retardation of Aging and Disease by Dietary Restriction. Thomas, Springfield.

77. Masoro, E.J. (2002). Caloric Restriction: A Key to Understanding and Modulating Aging. Elsevier, Amsterdam.

78. Colman, R.J., Anderson, R.M., Johnson, S.C., Kastman, E.K., Kosmatka, K.J., Beasley, T.M., Allison, D.B., Cruzen, C., Simmons, H.A., Kemnitz, J.W. and Weindruch, R. (2009). Caloric restriction delays disease onset and mortality in rhesus monkeys. *Science* 325:201-204.

79. Sinclair, D.A. (2005). Toward a unified theory of caloric restriction and longevity regulation. *Mech. Ageing Dev*. 126:987-1002.

80. Min, K.J., Flatt, T., Kulaots, I. and Tatar, M. (2007). Counting calories in *Drosophila* diet restriction. *Exp. Gerontol*. 42:247-251.

81. Zimmerman, J.A., Malloy, V., Krajcik, R. and Orentreich, N. (2003). Nutritional control of aging. *Exp. Gerontol*. 38:47-52.

82. Mair, W., Piper, M.D. and Partridge, L. (2005). Calories do not explain extension of life span by dietary restriction in *Drosophila*. *PLoS Biol*. 3:e223.

83. Piper, M.D., Mair, W. and Partridge, L. (2005). Counting the calories: the role of specific nutrients in extension of life span by food restriction. *J. Gerontol. A Biol. Sci. Med. Sci*. 60:549-555.

84. Blagosklonny, M.V. (2006). Aging and immortality: quasi-programmed senescence and its pharmacologic inhibition. *Cell Cycle* 5:2087-2102.

85. Blagosklonny, M.V. (2008). Aging: ROS or TOR. *Cell Cycle* 7:3344-3354.

86. Blagosklonny, M.V. (2009). TOR-driven aging: speeding car without brakes. *Cell Cycle* 8:4055-4059.

87. Kaeberlein, M., Powers, R.W., 3rd, Steffen, K.K., Westman, E.A., Hu, D., Dang, N., Kerr, E.O., Kirkland, K.T., Fields, S. and Kennedy, B.K. (2005). Regulation of yeast replicative life span by TOR and Sch9 in response to nutrients. *Science* 310:1193-1196.

88. Meissner, B., Boll, M., Daniel, H. and Baumeister, R. (2004). Deletion of the intestinal peptide transporter affects insulin and TOR signaling in *Caenorhabditis elegans*. *J. Biol. Chem*. 279:36739-36745.

89. Hansen, M., Taubert, S., Crawford, D., Libina, N., Lee, S.J. and Kenyon, C. (2007). Lifespan extension by conditions that inhibit translation in *Caenorhabditis elegans*. *Aging Cell* 6:95-110.

90. Clancy, D.J., Gems, D., Hafen, E., Leevers, S.J. and Partridge, L. (2002). Dietary restriction in long-lived dwarf flies. *Science* 296:319.

91. Bartke, A., Masternak, M.M., Al-Regaiey, K.A. and Bonkowski, M.S. (2007). Effects of dietary restriction on the expression of insulin-signaling-related genes in long-lived mutant mice. *Interdiscip. Top. Gerontol*. 35:69-82.

92. Greer, E.L., Dowlatshahi, D., Banko, M.R., Villen, J., Hoang, K., Blanchard, D., Gygi, S.P. and Brunet, A. (2007). An AMPK-FOXO pathway mediates longevity induced by a novel method of dietary restriction in *C. elegans*. *Curr. Biol*. 17:1646-1656.

93. Iser, W.B. and Wolkow, C.A. (2007). DAF-2/insulin-like signaling in *C. elegans* modifies effects of dietary restriction and nutrient stress on aging, stress and growth. *PLoS One* 2:e1240.

94. Lakowski, B. and Hekimi, S. (1998). The genetics of caloric restriction in *Caenorhabditis elegans*. *Proc. Natl. Acad. Sci. USA* 95:13091-13096.

95. Bartke, A., Wright, J.C., Mattison, J.A., Ingram, D.K., Miller, R.A. and Roth, G.S. (2001). Extending the lifespan of long-lived mice. *Nature* 414:412.

96. Kaeberlein, T.L., Smith, E.D., Tsuchiya, M., Welton, K.L., Thomas, J.H., Fields, S., Kennedy, B.K. and Kaeberlein, M. (2006). Lifespan extension in *Caenorhabditis elegans* by complete removal of food. *Aging Cell* 5:487-494.

97. Bishop, N.A. and Guarente, L. (2007). Two neurons mediate diet-restriction-induced longevity in *C. elegans*. *Nature* 447:545-549.

98. Houthoofd, K., Gems, D., Johnson, T.E. and Vanfleteren, J.R. (2007). Dietary restriction in the nematode *Caenorhabditis elegans*. *Interdiscip. Top. Gerontol*. 35:98-114.

99. Min, K.J., Yamamoto, R., Buch, S., Pankratz, M. and Tatar, M. (2008). Drosophila lifespan control by dietary restriction independent of insulin-like signaling. *Aging Cell* 7:199-206.

100. Greer, E.L. and Brunet, A. (2009). Different dietary restriction regimens extend lifespan by both independent and overlapping genetic pathways in *C. elegans*. *Aging Cell* 8:113-127.

101. Wanke, V., Cameroni, E., Uotila, A., Piccolis, M., Urban, J., Loewith, R. and De Virgilio, C. (2008). Caffeine extends yeast lifespan by targeting TORC1. *Mol. Microbiol*. 69:277-285.

102. Wullschleger, S., Loewith, R. and Hall, M.N. (2006). TOR signaling in growth and metabolism. *Cell* 124:471-484.

103. McColl, G., Killilea, D.W., Hubbard, A.E., Vantipalli, M.C., Melov, S. and Lithgow, G.J. (2008). Pharmacogenetic analysis of lithium-induced delayed aging in *Caenorhabditis elegans*. *J. Biol. Chem*. 283:350-357.

104. Sinclair, D.A. and Oberdoerffer, P. (2009). The ageing epigenome: damaged beyond repair? *Ageing Res. Rev*. 8:189-198.

105. Benedetti, M.G., Foster, A.L., Vantipalli, M.C., White, M.P., Sampayo, J.N., Gill, M.S., Olsen, A. and Lithgow, G.J. (2008). Compounds that confer thermal stress resistance and extended lifespan. *Exp. Gerontol*. 43:882-891.

106. Bauer, J.H., Goupil, S., Garber, G.B. and Helfand, S.L. (2004). An accelerated assay for the identification of lifespan-extending interventions in *Drosophila melanogaster*. *Proc. Natl. Acad. Sci. USA* 101:12980-12985.

107. Onken, B. and Driscoll, M. (2010). Metformin induces a dietary restriction-like state and the oxidative stress response to extend *C. elegans* healthspan via AMPK, LKB1, and SKN-1. *PLoS ONE* 5:e8758.

108. Anisimov, V.N., Berstein, L.M., Egormin, P.A., Piskunova, T.S., Popovich, I.G., Zabezhinski, M.A., Tyndyk, M.L., Yurova, M.V., Kovalenko, I.G., Poroshina, T.E. and Semenchenko, A.V. (2008). Metformin slows down aging and extends life span of female SHR mice. *Cell Cycle* 7:2769-2773.

109. Shaw, R.J., Lamia, K.A., Vasquez, D., Koo, S.H., Bardeesy, N., Depinho, R.A., Montminy, M. and Cantley, L.C. (2005). The kinase LKB1 mediates glucose homeostasis in liver and therapeutic effects of metformin. *Science* 310:1642-1646.

110. Powers, R.W. 3rd, Kaeberlein, M., Caldwell, S.D., Kennedy, B.K. and Fields, S. (2006). Extension of chronological life span in yeast by decreased TOR pathway signaling. *Genes Dev*. 20:174-184.

111. Crespo, J.L, Powers, T., Fowler, B. and Hall, M.N. (2002). The TOR-controlled transcription activators *GLN3*, *RTG1*, and *RTG3* are regulated in response to intracellular levels of glutamine. *Proc. Natl. Acad. Sci. USA* 99:6784-6789.

112. Petrascheck, M., Ye, X. and Buck, LB. (2007). An antidepressant that extends lifespan in adult *Caenorhabditis elegans*. *Nature* 450:553-556.

113. Bjedov I, Toivonen JM, Kerr F, Slack C, Jacobson J, Foley A, Partridge L. Mechanisms of life span extension by rapamycin in the fruit fly Drosophila melanogaster. *Cell Metab*. 2010; 11: 35-46.

114. Bonawitz ND, Chatenay-Lapointe M, Pan Y, Shadel GS. Reduced TOR signaling extends chronological life span via increased respiration and upregulation of mitochondrial gene expression. *Cell Metab*. 2007; 5: 265-277.

115. Medvedik O, Lamming DW, Kim KD, Sinclair DA. MSN2 and MSN4 link calorie restriction and TOR to sirtuin-mediated lifespan extension in Saccharomyces cerevisiae. *PLoS Biol*. 2007; 5: e261.

116. Harrison DE, Strong R, Sharp ZD, Nelson JF, Astle CM, Flurkey K, Nadon NL, Wilkinson JE, Frenkel K, Carter CS, Pahor M, Javors MA, Fernandez E, Miller RA. Rapamycin fed late in life extends lifespan in genetically heterogeneous mice. *Nature* 2009; 460: 392-395.

117. Demidenko ZN, Zubova SG, Bukreeva EI, Pospelov VA, Pospelova TV, Blagosklonny MV. Rapamycin decelerates cellular senescence. *Cell Cycle* 2009; 8: 1888-1895.

102. Wullschleger S, Loewith R, Hall MN. TOR signaling in growth and metabolism. *Cell* 2006; 124: 471-484.

118. Alvers AL, Wood MS, Hu D, Kaywell AC, Dunn WA Jr, Aris JP. Autophagy is required for extension of yeast chronological life span by rapamycin. *Autophagy* 2009; 5: 847-849.

119. Howitz, K.T., Bitterman, K.J., Cohen, H.Y., Lamming, D.W., Lavu, S., Wood, J.G., Zipkin, R.E., Chung, P., Kisielewski, A., Zhang, L.L., Scherer, B. and Sinclair, D.A. (2003). Small molecule activators of sirtuins extend *Saccharomyces cerevisiae* lifespan. *Nature* 425:191-196.

120. Wood, J.G., Rogina, B., Lavu, S., Howitz, K., Helfand, S.L., Tatar, M. and Sinclair, D. (2004). Sirtuin activators mimic caloric restriction and delay ageing in metazoans. *Nature* 430:686-689.

121. Baur, J.A., Pearson, K.J., Price, N.L., Jamieson, H.A., Lerin, C., Kalra, A., Prabhu, V.V., Allard, J.S., Lopez-Lluch, G., Lewis, K., Pistell, P.J., Poosala, S., Becker, K.G., Boss, O., Gwinn, D., Wang, M., Ramaswamy, S., Fishbein, K.W., Spencer, R.G., Lakatta, E.G., Le Couteur, D., Shaw, R.J., Navas, P., Puigserver, P., Ingram, D.K., de Cabo, R. and Sinclair, D.A. (2006). Resveratrol improves health and survival of mice on a high-calorie diet. *Nature* 444:337-342.

122. Valenzano, D.R., Terzibasi, E., Genade, T., Cattaneo, A., Domenici, L. and Cellerino, A. (2006). Resveratrol prolongs lifespan and retards the onset of age-related markers in a short-lived vertebrate. *Curr. Biol*. 16:296-300.

123. Demidenko, Z.N. and Blagosklonny, M.V. (2009). At concentrations that inhibit mTOR, resveratrol suppresses cellular senescence. *Cell Cycle* 8:1901-1904.

124. Pearson, K.J., Baur, J.A., Lewis, K.N., Peshkin, L., Price, N.L., Labinskyy, N., Swindell, W.R., Kamara, D., Minor, R.K., Perez, E., Jamieson, H.A., Zhang, Y., Dunn, S.R., Sharma, K., Pleshko, N., Woollett, L.A., Csiszar, A., Ikeno, Y., Le Couteur, D., Elliott, P.J., Becker, K.G., Navas, P., Ingram, D.K., Wolf, N.S., Ungvari, Z., Sinclair, D.A. and de Cabo, R. (2008). Resveratrol delays age-related

deterioration and mimics transcriptional aspects of dietary restriction without extending life span. *Cell Metab*. 8:157-168.

125. Viswanathan, M., Kim, S.K., Berdichevsky, A. and Guarente, L. (2005). A role for SIR-2.1 regulation of ER stress response genes in determining *C. elegans* life span. *Dev. Cell* 9:605-615.

126. Lagouge, M., Argmann, C., Gerhart-Hines, Z., Meziane, H., Lerin, C., Daussin, F., Messadeq, N., Milne, J., Lambert, P., Elliott, P., Geny, B., Laakso, M., Puigserver, P. and Auwerx, J. (2006). Resveratrol improves mitochondrial function and protects against metabolic disease by activating SIRT1 and PGC-1α. *Cell* 127:1109-1122.

127. Picard, F., Kurtev, M., Chung, N., Topark-Ngarm, A., Senawong, T., Machado De Oliveira, R., Leid, M., McBurney, M.W. and Guarente, L. (2004). Sirt1 promotes fat mobilization in white adipocytes by repressing PPAR-γ. *Nature* 429:771-776.

128. Blagosklonny, MV. (2009). TOR-driven aging: speeding car without brakes. *Cell Cycle* 8:4055-4059.

129. Morselli, E., Maiuri, M.C., Markaki, M., Megalou, E., Pasparaki, A., Palikaras, K., Criollo, A., Galluzzi, L., Malik, S.A., Vitale, I., Michaud, M., Madeo, F., Tavernarakis, N. and Kroemer, G. (2010). Caloric restriction and resveratrol promote longevity through the Sirtuin-1-dependent induction of autophagy. *Cell Death Dis*. 1:e10.

130. Morselli, E., Maiuri, M.C., Markaki, M., Megalou, E., Pasparaki, A., Palikaras, K., Criollo, A., Galluzzi, L., Malik, S.A., Vitale, I., Michaud, M., Madeo, F., Tavernarakis, N. and Kroemer, G. (2010). The life span-prolonging effect of sirtuin-1 is mediated by autophagy. *Autophagy* 6:186-188.

131. Morselli, E., Galluzzi, L., Kepp, O., Criollo, A., Maiuri, M.C., Tavernarakis, N., Madeo, F. and Kroemer, G. (2009). Autophagy mediates pharmacological lifespan extension by spermidine and resveratrol. *Aging* 1:961-970.

132. Skulachev, V.P., Anisimov, V.N., Antonenko, Y.N., Bakeeva, L.E., Chernyak, B.V., Erichev, V.P., Filenko, O.F., Kalinina, N.I., Kapelko, V.I., Kolosova, N.G., Kopnin, B.P., Korshunova, G.A., Lichinitser, M.R., Obukhova, L.A., Pasyukova, E.G., Pisarenko, O.I., Roginsky, V.A., Ruuge, E.K., Senin, I.I., Severina, I.I., Skulachev, M.V., Spivak, I.M., Tashlitsky, V.N., Tkachuk, V.A., Vyssokikh, M.Y., Yaguzhinsky, L.S. and Zorov, D.B. (2009). An attempt to prevent senescence: a mitochondrial approach. *Biochim. Biophys. Acta* 1787:437-461.

133. Engel, N. and Mahlknecht, U. (2008). Aging and anti-aging: unexpected side effects of everyday medication through sirtuin1 modulation. *Int. J. Mol. Med*. 21:223-232.

134. Eisenberg, T., Knauer, H., Schauer, A., Büttner, S., Ruckenstuhl, C., Carmona-Gutierrez, D., Ring, J., Schroeder, S., Magnes, C., Antonacci, L., Fussi, H., Deszcz, L., Hartl, R., Schraml, E., Criollo, A., Megalou, E., Weiskopf, D., Laun, P., Heeren, G., Breitenbach, M., Grubeck-Loebenstein, B., Herker, E., Fahrenkrog, B., Fröhlich, K.U., Sinner, F., Tavernarakis, N., Minois, N., Kroemer, G. and Madeo, F. (2009). Induction of autophagy by spermidine promotes longevity. *Nat. Cell Biol*. 11:1305-1314.

135. Evason, K., Collins, J.J., Huang, C., Hughes, S. and Kornfeld, K. (2008). Valproic acid extends *Caenorhabditis elegans* lifespan. *Aging Cell* 7:305-317.

136. Demidenko, Z.N., Shtutman, M. and Blagosklonny, M.V. (2009). Pharmacologic inhibition of MEK and PI-3K converges on the mTOR/S6 pathway to decelerate cellular senescence. *Cell Cycle* 8:1896-1900.

137. Zarse, K. and Ristow, M. (2008). Antidepressants of the serotonin-antagonist type increase body fat and decrease lifespan of adult *Caenorhabditis elegans*. *PLoS ONE* 3:e4062.

138. Kaeberlein, M., McDonagh, T., Heltweg, B., Hixon, J., Westman, E.A., Caldwell, S.D., Napper, A., Curtis, R., DiStefano, P.S., Fields, S., Bedalov, A. and Kennedy, B.K. (2005). Substrate-specific activation of sirtuins by resveratrol. *J. Biol. Chem*. 280:17038-17045.

139. Bass, T.M., Weinkove, D., Houthoofd, K., Gems, D. and Partridge, L. (2007). Effects of resveratrol on lifespan in *Drosophila melanogaster* and *Caenorhabditis elegans*. *Mech. Ageing Dev*. 128:546-552.

140. Borra, M.T., Smith, B.C. and Denu, J.M. (2005). Mechanism of human SIRT1 activation by resveratrol. *J. Biol. Chem*. 280:17187-17195.

141. Denu, J.M. (2005). The Sir 2 family of protein deacetylases. *Curr. Opin. Chem. Biol*. 9:431-440.

142. Kaeberlein, M. and Kennedy, B.K. (2007). Does resveratrol activate yeast Sir2 in vivo? *Aging Cell* 6:415-416.

143. Harikumar, K.B. and Aggarwal, B.B. (2008). Resveratrol: a multitargeted agent for age-associated chronic diseases. *Cell Cycle* 7:1020-1035.

144. Shakibaei, M., Harikumar, K.B. and Aggarwal, B.B. (2009). Resveratrol addiction: to die or not to die. *Mol. Nutr. Food Res*. 53:115-128.

145. Chen, D. and Guarente, L. (2007). SIR2: a potential target for calorie restriction mimetics. *Trends Mol. Med*. 13:64-71.

146. Pacholec, M., Chrunyk, B., Cunningham, D., Flynn, D., Griffith, D., Griffor, M., Loulakis, P., Pabst, B., Qiu, X., Stockman, B., Thanabal, V., Varghese, A., Ward, J., Withka, J. and Ahn, K. (2010). SRT1720, SRT2183, SRT1460, and resveratrol are not direct activators of SIRT1. *J. Biol. Chem*. 285:8340-8351.

147. Lapointe, J. and Hekimi, S. (2010). When a theory of aging ages badly. *Cell Mol. Life Sci*. 67:1-8.

148. Ingram, D.K., Roth, G.S., Lane, M.A., Ottinger, M.A., Zou, S., de Cabo, R. and Mattison, J.A. (2006). The potential for dietary restriction to increase longevity in humans: extrapolation from monkey studies. *Biogerontology* 7:143-148.

149. Ingram, D.K., Zhu, M., Mamczarz, J., Zou, S., Lane, M.A., Roth, G.S. and de Cabo, R. (2006). Calorie restriction mimetics: an emerging research field. *Aging Cell* 5:97-108.

150. Lane, M.A., Roth, G.S. and Ingram, D.K. (2007). Caloric restriction mimetics: a novel approach for biogerontology. *Methods Mol. Biol*. 371:143-149.

151. Kaeberlein, M. (2010). Lessons on longevity from budding yeast. *Nature* 464:513-519.

152. Longo, V.D. and Kennedy, B.K. (2006). Sirtuins in aging and age-related disease. *Cell* 126:257-268.

153. Masoro, E.J. (2005). Overview of caloric restriction and ageing. *Mech. Ageing Dev*. 126:913-922.

154. Boland, C.R. and Ricciardiello, L. (1999). How many mutations does it take to make a tumor? *Proc. Natl. Acad. Sci. USA* 96:14675-14677.

155. Karakosta, A., Golias, C., Charalabopoulos, A., Peschos, D., Batistatou, A. And Charalabopoulos, K. (2005). Genetic models of human cancer as a multistep process. Paradigm models of colorectal cancer, breast cancer, and chronic myelogenous and acute lymphoblastic leukaemia. *J. Exp. Clin. Cancer Res*. 24:505-514.

156. Weinberg, R.A. (2007). The biology of cancer. Garland Science, Taylor and Francis Group, LLC. New York, USA.

157. Finkel, T., Serrano, M. and Blasco, M.A. (2007). The common biology of cancer and ageing. *Nature* 448:767-774.

158. Serrano, M. and Blasco, M.A. (2007). Cancer and ageing: convergent and divergent mechanisms. *Nat. Rev. Mol. Cell Biol*. 8:715-722.

159. Collado, M., Blasco, M.A. and Serrano, M. (2007). Cellular senescence in cancer and aging. *Cell* 130:223-233.

160. Anisimov, V.N., Zabezhinski, M.A., Popovich, I.G., Piskunova, T.S., Semenchenko, A.V., Tyndyk, M.L., Yurova, M.N., Antoch, M.P. and Blagosklonny, M.V. (2010). Rapamycin extends maximal lifespan in cancer-prone mice. *Am. J. Pathol*. 176:2092-2097.

161. Blagosklonny, M.V. (2006). Aging and immortality: quasi-programmed senescence and its pharmacologic inhibition. *Cell Cycle* 5:2087-2102.

162. Blagosklonny, M.V. (2009). Validation of anti-aging drugs by treating age-related diseases. *Aging* 1:281-288.

163. Shackelford, D.B. and Shaw, R.J. (2009). The LKB1-AMPK pathway: metabolism and growth control in tumour suppression. *Nat. Rev. Cancer* 9:563-575.

164. Shaw, R.J. (2009). LKB1 and AMP-activated protein kinase control of mTOR signalling and growth. *Acta Physiol*. 196:65-80.

165. Inoki, K., Corradetti, M.N. and Guan, K.L. (2005). Dysregulation of the TSC-mTOR pathway in human disease. *Nat. Genet*. 37:19-24.

166. Houchens, D.P., Ovejera, A.A., Riblet, S.M. and Slagel, D.E. (1983). Human brain tumor xenografts in nude mice as a chemotherapy model. *Eur. J. Cancer Clin. Oncol*. 19:799-805.

167. Eng, C.P., Sehgal, S.N. and Vezina, C. (1984). Activity of rapamycin (AY-22,989) against transplanted tumors. *J. Antibiot*. 37:1231-1237.

168. Garber, K. (2001). Rapamycin's resurrection: a new way to target the cancer cell cycle. *J. Natl. Cancer Inst*. 93:1517-1519.

169. Blagosklonny, M.V. and Darzynkiewicz, Z. (2002). Four birds with one stone: RAPA as potential anticancer therapy. *Cancer Biol. Ther*. 1:359-361.

170. Choo, A.Y. and Blenis, J. (2006). TORgeting oncogene addiction for cancer therapy. *Cancer Cell* 9:77-79.

171. Cully, M., You, H., Levine, A.J. and Mak, T.W. (2006). Beyond PTEN mutations: the PI3K pathway as an integrator of multiple inputs during tumorigenesis. *Nat. Rev. Cancer* 6:184-192.

172. Huang, S., Liu, L.N., Hosoi, H., Dilling, M.B., Shikata, T. and Houghton, P.J. (2001). p53/p21(CIP1) cooperate in enforcing rapamycin-induced G(1) arrest and determine the cellular response to rapamycin. *Cancer Res*. 61:3373-3381.

173. Majumder, P.K., Febbo, P.G., Bikoff, R., Berger, R., Xue, Q., McMahon, L.M., Manola, J., Brugarolas, J., McDonnell, T.J., Golub, T.R., Loda, M., Lane, H.A. and Sellers, W.R. (2004). mTOR inhibition reverses Akt-dependent prostate intraepithelial neoplasia through regulation of apoptotic and HIF-1-dependent pathways. *Nat. Med*. 10:594-601.

174. Wahl, P.R., Serra, A.L., Le Hir, M., Molle, K.D., Hall, M.N. and Wuthrich, R.P. (2006). Inhibition of mTOR with sirolimus slows disease progression in Han:SPRD rats with autosomal dominant polycystic kidney disease (ADPKD). *Nephrol. Dial. Transplant*. 21:598-604.

175. Dilman, V.M., Berstein, L.M., Zabezhinski, M.A., Alexandrov, V.A., Bobrov, J.F. and Pliss, G.B. (1978). Inhibition of DMBA-induced carcinogenesis by phenformin in the mammary gland of rats. *Arch. Geschwulstforsch*. 48:1-8.

176. Dilman, V.M. and Anisimov, V.N. (1980). Effect of treatment with phenformin, diphenylhydantoin or L-dopa on life span and tumour incidence in C3H/Sn mice. *Gerontology* 26:241-246.

177. Anisimov, V.N., Egormin, P.A., Bershtein, L.M., Zabezhinskii, M.A., Piskunova, T.S., Popovich, I.G. and Semenchenko, A.V. (2005). Metformin decelerates aging and development of mammary tumors in HER-2/neu transgenic mice. *Bull. Exp. Biol. Med*. 139:721-723.

178. Anisimov, V.N., Berstein, L.M., Egormin, P.A., Piskunova, T.S., Popovich, I.G., Zabezhinski, M.A., Kovalenko, I.G., Poroshina, T.E., Semenchenko, A.V., Provinciali, M., Re, F. and Franceschi, C. (2005). Effect of metformin on life span

and on the development of spontaneous mammary tumors in HER-2/neu transgenic mice. *Exp. Gerontol*. 40:685-693.

179. Buzzai, M., Jones, R.G., Amaravadi, R.K., Lum, J.J., DeBerardinis, R.J., Zhao, F., Viollet, B. and Thompson, C.B. (2007). Systemic treatment with the anti-diabetic drug metformin selectively impairs p53-deficient tumor cell growth. *Cancer Res*. 67:6745–6752.

180. Huang, X., Wullschleger, S., Shpiro, N., McGuire, V.A., Sakamoto, K., Woods, Y.L., McBurnie, W., Fleming, S. and Alessi, D.R. (2008). Important role of the LKB1-AMPK pathway in suppressing tumorigenesis in PTEN-deficient mice. *Biochem. J*. 412:211-221.

181. Schneider, M.B., Matsuzaki, H., Haorah, J., Ulrich, A., Standop, J., Ding, X.Z., Adrian, T.E. and Pour, P.M. (2001). Prevention of pancreatic cancer induction in hamsters by metformin. *Gastroenterology* 120:1263-1270.

182. Schneider, M.B., Matsuzaki, H., Haorah, J., Ulrich, A., Standop, J., Ding, X.Z., Adrian, T.E. and Pour, P.M. (2001). Prevention of pancreatic cancer induction in hamsters by metformin. *Gastroenterology* 120:1263-1270.

183. Zakikhani, M., Dowling, R., Fantus, I.G., Sonenberg, N. and Pollak, M. (2006). Metformin is an AMP kinase-dependent growth inhibitor for breast cancer cells. *Cancer Res*. 66:10269-10273.

184. Zakikhani, M., Dowling, R.J., Sonenberg, N. and Pollak, M.N. (2008). The effects of adiponectin and metformin on prostate and colon neoplasia involve activation of AMP-activated protein kinase. *Cancer Prev. Res*. 1:369-375.

185. Swinnen, J.V., Beckers, A., Brusselmans, K., Organe, S., Segers, J., Timmermans, L., Vanderhoydonc, F., Deboel, L., Derua, R., Waelkens, E., De Schrijver, E., Van de Sande, T., Noël, A., Foufelle, F. and Verhoeven, G. (2005). Mimicry of a cellular low energy status blocks tumor cell anabolism and suppresses the malignant phenotype. *Cancer Res*. 65:2441-2448.

186. Algire, C., Zakikhani, M., Blouin, M.J., Shuai, J.H. and Pollak, M. (2008). Metformin attenuates the stimulatory effect of a high-energy diet on in vivo LLC1 carcinoma growth. *Endocr. Relat. Cancer* 15:833-839.

187. Scott, J.W., van Denderen, B.J., Jorgensen, S.B., Honeyman, J.E., Steinberg, G.R., Oakhill, J.S., Iseli, T.J., Koay, A., Gooley, P.R., Stapleton, D. and Kemp, B.E. (2008). Thienopyridone drugs are selective activators of AMP-activated protein kinase beta1-containing complexes. *Chem. Biol*. 15:1220-1230.

188. Cool, B., Zinker, B., Chiou, W., Kifle, L., Cao, N., Perham, M., Dickinson, R., Adler, A., Gagne, G., Iyengar, R., Zhao, G., Marsh, K., Kym, P., Jung, P., Camp, H.S. and Frevert, E. (2006). Identification and characterization of a small molecule AMPK activator that treats key components of type 2 diabetes and the metabolic syndrome. *Cell Metab*. 3:403-416.

189. Evans, J.M., Donnelly, L.A., Emslie-Smith, A.M., Alessi, D.R. and Morris, A.D. (2005). Metformin and reduced risk of cancer in diabetic patients. *BMJ* 330:1304-1305.

190. Bowker, S.L., Majumdar, S.R., Veugelers, P. and Johnson, J.A. (2006). Increased cancer-related mortality for patients with type 2 diabetes who use sulfonylureas or insulin. *Diabetes Care* 29:254-258.

191. Jiralerspong, S., Palla, S.L., Giordano, S.H., Meric-Bernstam, F., Liedtke, C., Barnett, C.M., Hsu, L., Hung, M.C., Hortobagyi, G.N. and Gonzalez-Angulo, A.M. (2009). Metformin and pathologic complete responses to neoadjuvant chemotherapy in diabetic patients with breast cancer. *J. Clin. Oncol*. 27:3297-3302.

192. Goodwin, P.J., Ligibel, J.A. and Stambolic, V. (2009). Metformin in Breast Cancer: Time for Action. *J. Clin. Oncol*. 27:3271-3273.

193. Enns, L.C., Morton, J.F., Treuting, P.R., Emond, M.J., Wolf, N.S., Dai, D.F., McKnight, G.S., Rabinovitch, P.S. and Ladiges, W.C. (2009). Disruption of protein kinase A in mice enhances healthy aging. *PLoS One* 4:e5963.

194. Shevah, O. and Laron, Z. (2007). Patients with congenital deficiency of IGF-I seem protected from the development of malignancies: a preliminary report. *Growth Horm. IGF Res*. 17:54-57.

195. Suh, Y., Atzmon, G., Cho, M.O., Hwang, D., Liu, B., Leahy, D.J., Barzilai, N. and Cohen, P. (2008). Functionally significant insulin-like growth factor I receptor mutations in centenarians. *Proc. Natl. Acad. Sci. USA* 105:3438-3442.

196. Baur, J.A. and Sinclair, D.A. (2006). Therapeutic potential of resveratrol: the in vivo evidence. *Nat. Rev. Drug Discov*. 5:493-506.

197. Harikumar, K.B. and Aggarwal, B.B. (2008). Resveratrol: a multitargeted agent for age-associated chronic diseases. *Cell Cycle* 7:1020-1035.

198. Shakibaei, M., Harikumar, K.B. and Aggarwal, B.B. (2009). Resveratrol addiction: to die or not to die. *Mol. Nutr. Food Res*. 53:115-128.

199. Howell, A., Chapman, M. and Harvie, M. (2009). Energy restriction for breast cancer prevention. *Recent Results Cancer Res*. 181:97-111.

200. Hursting, S.D., Perkins, S.N. and Phang, J.M. (1994). Calorie restriction delays spontaneous tumorigenesis in p53-knockout transgenic mice. *Proc. Natl. Acad. Sci. USA* 91:7036-7040.

201. Hursting, S.D., Perkins, S.N., Brown, C.C., Haines, D.C. and Phang, J.M. (1997). Calorie restriction induces a p53-independent delay of spontaneous carcinogenesis in p53-deficient and wild-type mice. *Cancer Res*. 57:2843-2846.

202. Mai, V., Colbert, L.H., Berrigan, D., Perkins, S.N., Pfeiffer, R., Lavigne, J.A., Lanza, E., Haines, D.C., Schatzkin, A. and Hursting, S.D. (2003). Calorie restriction and diet composition modulate spontaneous intestinal tumorigenesis in Apc(Min) mice through different mechanisms. *Cancer Res*. 63:1752-1755.

203. Kalaany, N.Y. and Sabatini, D.M. (2009). Tumours with PI3K activation are resistant to dietary restriction. *Nature* 458:725-731.

204. Hursting, S.D., Lavigne, J.A., Berrigan, D., Perkins, S.N. and Barrett, J.C. (2003). Calorie restriction, aging, and cancer prevention: mechanisms of action and applicability to humans. *Annu. Rev. Med*. 54:131-152.

205. Hursting, S.D., Smith, S.M., Lashinger, L.M., Harvey, A.E. and Perkins, S.N. (2010). Calories and carcinogenesis: lessons learned from 30 years of calorie restriction research. *Carcinogenesis* 31:83-89.

206. Longo, V.D. and Fontana, L. (2010). Calorie restriction and cancer prevention: metabolic and molecular mechanisms. *Trends Pharmacol. Sci*. 31:89-98.

207. Raffaghello, L., Lee, C., Safdie, F.M., Wei, M., Madia, F., Bianchi, G. and Longo, V.D. (2008). Starvation-dependent differential stress resistance protects normal but

not cancer cells against high-dose chemotherapy. *Proc. Natl. Acad. Sci. USA* 105:8215-8220.

208. Colman, R.J., Anderson, R.M., Johnson, S.C., Kastman, E.K., Kosmatka, K.J., Beasley, T.M., Allison, D.B., Cruzen, C., Simmons, H.A., Kemnitz, J.W. and Weindruch, R. (2009). Caloric restriction delays disease onset and mortality in rhesus monkeys. *Science* 325:201-204.

209. Benz, C.C. and Yau, C. (2008). Ageing, oxidative stress and cancer: paradigms in parallax. *Nat. Rev. Cancer* 8:875-879.

210. Sharpless, N.E. and DePinho, R.A. (2007). How stem cells age and why this makes us grow old. *Nat. Rev. Mol. Cell Biol*. 8:703-713.

211. Blasco, M.A. (2007). Telomere length, stem cells and aging. *Nat. Chem. Biol*. 3:640-649.

212. Krtolica, A. (2005). Stem cell: balancing aging and cancer. *Int. J. Biochem. Cell Biol*. 37:935-941.

213. Vergel, M., Marin, J.J., Estevez, P. and Carnero, A. (2010). Cellular senescence as a target in cancer control. *J. Aging Res*. 2011:725365.

214. Ohtani, N., Mann, D.J. and Hara, E. (2009). Cellular senescence: its role in tumor suppression and aging. *Cancer Sci*. 100:792-797.

215. Pelicci, P.G. (2004). Do tumor-suppressive mechanisms contribute to organism aging by inducing stem cell senescence? *J. Clin. Invest*. 113:4-7.

216. Sharpless, N.E. and DePinho, R.A. (2004). Telomeres, stem cells, senescence, and cancer. *J. Clin. Invest*. 113:160-168.

217. Sharpless, N.E. (2004). Ink4a/Arf links senescence and aging. *Exp. Gerontol*. 39:1751-1759.

218. Campisi, J. And d'Adda di Fagagna, F. (2007). Cellular senescence: when bad things happen to good cells. *Nat. Rev. Mol. Cell Biol*. 8:729-740.

219. Campisi, J. (2005). Senescent cells, tumor suppression, and organismal aging: good citizens, bad neighbors. *Cell* 120:513-522.

220. Kong Y, Cui H, Ramkumar C, Zhang H. (2011). Regulation of senescence in cancer and aging. *J Aging Res*. 2011:963172.

221. Grimes, A. and Chandra, S.B. (2009). Significance of cellular senescence in aging and cancer. *Cancer Res. Treat*. 41:187-195.

222. Campisi, J. (2003). Cancer and ageing: rival demons? *Nat. Rev. Cancer*. 3:339-349.

223. Rodier, F., Campisi, J. and Bhaumik, D. (2007). Two faces of p53: aging and tumor suppression. *Nucleic Acids Res*. 35:7475-7484.

224. Esiashvili, N., Anderson, C. and Katzenstein, H.M. (2009). Neuroblastoma. *Curr. Probl. Cancer* 33:333-360.

225. Park, J.R., Eggert, A. and Caron, H. (2010). Neuroblastoma: biology, prognosis, and treatment. *Hematol. Oncol. Clin. North Am*. 24:65-86.

226. Astigarraga, I., Lejarreta, R., Navajas, A., Fernandez-Teijeiro, A., Imaz, I. And Bezanilla, J.L. (1996). Secondary central nervous system metastases in children with neuroblastoma. *Med. Pediatr. Oncol.* 27:529-533.

227. DuBois SG, Kalika Y, Lukens JN, et al. Metastatic sites in Stage IV and IVS neuroblastoma correlate with age, tumor biology, and survival [see comments]. *J Pediatr Hematol Oncol.* 1999;21:181-189.

228. Blatt J, Fitz C, Mirro J Jr. Recognition of central nervous system metastases in children with metastatic primary extracranial neuroblastoma. *Pediatr Hematol Oncol.* 1997;14:233-241.

229. Matthay, K.K., Brisse, H., Couanet, D., Couturier, J., Bénard, J., Mosseri, V., Edeline, V., Lumbroso, J., Valteau-Couanet, D. and Michon. J. (2003). Central nervous system metastases in neuroblastoma: radiologic, clinical, and biologic features in 23 patients. *Cancer* 98:155-165.

230. Maris, J.M. The biologic basis for neuroblastoma heterogeneity and risk stratification. Curr Opin Pediatr 2005; 17:7-13.

231. Seeger, R.C., Brodeur, G.M., Sather, H., Dalton, A, Siegel, S.E., Wong, K.Y. and Hammond, D. (1985). Association of multiple copies of the N-*myc* oncogene with rapid progression of neuroblastomas. *N. Engl. J. Med.* 313:1111-1116.

232. Brodeur, G.M., Seeger, R.C., Schwab, M., Varmus, H.E. and Bishop, J.M. (1984). Amplification of N-myc in untreated human neuroblastomas correlates with advanced disease stage. *Science* 224:1121-1124.

233. Lee, L.A. and Dang, C.V. (2006). Myc target transcriptomes. *Curr. Top. Microbiol. Immunol.* 302:145-167.

234. Gilbert, F., Feder, M., Balaban, G., Brangman, D., Lurie, D.K., Podolsky, R., Rinaldt, V., Vinikoor, N. and Weisband, J. (1984). Human neuroblastomas and abnormalities of chromosomes 1 and 17. *Cancer Res*. 44:5444-5449.

235. Liu, Z., Yang, X., Li, Z., McMahon, C., Sizer, C., Barenboim-Stapleton, L., Bliskovsky, V., Mock, B., Ried, T., London, W.B., Maris, J., Khan, J. and Thiele, C.J. (2011). CASZ1, a candidate tumor-suppressor gene, suppresses neuroblastoma

tumor growth through reprogramming gene expression. *Cell Death Differ*. Jan 21; Epub. ahead of print.

236. Geli, J., Kiss, N., Kogner, P. and Larsson, C. (2010). Suppression of RIZ in biologically unfavourable neuroblastomas. *Int. J. Oncol*. 37:1323-1330.

237. Fujita, T., Igarashi, J., Okawa, E.R., Gotoh, T., Manne, J., Kolla, V., Kim, J., Zhao, H., Pawel, B.R., London, W.B., Maris, J.M., White, P.S. and Brodeur, G.M. (2008). CHD5, a tumor suppressor gene deleted from 1p36.31 in neuroblastomas. *J. Natl. Cancer Inst*. 100:940-949.

238. Look, A.T., Meyerson, M., Peeper, D.S., Carter, B.D. and Kaelin, W.G. Jr. (2008). The kinesin KIF1Bbeta acts downstream from EglN3 to induce apoptosis and is a potential 1p36 tumor suppressor. *Genes Dev*. 22:884-893.

239. Modak, S. and Cheung, N.K. (2010). Neuroblastoma: Therapeutic strategies for a clinical enigma. *Cancer Treat. Rev*. 36:307-317.

240. George, R.E., Diller, L. and Bernstein, M.L. (2010). Pharmacotherapy of neuroblastoma. *Expert Opin. Pharmacother*. 11:1467-1478.

241. Tsang, W.P., Chau, S.P., Kong, S.K., Fung, K.P. and Kwok, T.T. (2003). Reactive oxygen species mediate doxorubicin induced p53-independent apoptosis. *Life Sci*. 73:2047-2058.

242. Sodhi, A. and Gupta, P. (1986). Increased release of hydrogen peroxide ($H_2O_2$) and superoxide anion ($O^-_2$) by murine macrophages in vitro after cis-platin treatment. *Int. J. Immunopharmacol*. 8:709-714.

243. Strauss, G., Westhoff, M.A., Fischer-Posovszky, P., Fulda, S., Schanbacher, M., Eckhoff, S.M., Stahnke, K., Vahsen, N., Kroemer, G. and Debatin, K.M. 4-

hydroperoxy-cyclophosphamide mediates caspase-independent T-cell apoptosis involving oxidative stress-induced nuclear relocation of mitochondrial apoptogenic factors AIF and EndoG. *Cell Death Differ*. 15:332-343.

244. Timur, M., Akbas, S.H. and Ozben, T. (2005). The effect of Topotecan on oxidative stress in MCF-7 human breast cancer cell line. *Acta Biochim. Pol*. 52:897-902.

245. Woiniak, A., Drewa, G., Woźniak, B., Schachtschabel, D.O., Mila-Kierzenkowska, C., Drewa, T., Olszewska-Słonina, D. and Sopońska, M. (2005). The effect of antitumor drugs on oxidative stress in B16 and S91 melanoma cells in vitro. *Med. Sci. Monit*. 11:BR22-29.

246. Goldberg, A.A., Bourque, S.D., Kyryakov, P., Boukh-Viner, T., Gregg, C., Beach, A., Burstein, M.T., Machkalyan, G., Richard, V., Rampersad, S. and Titorenko, V.I. (2009). A novel function of lipid droplets in regulating longevity. *Biochem. Soc. Trans.* 37:1050-1055.

247. Goldberg, A.A., Richard, V.R., Kyryakov, P., Bourque, S.D., Beach, A., Burstein, M.T., Glebov, A., Koupaki, O., Boukh-Viner, T., Gregg, C., Juneau, M., English, A.M., Thomas, D.Y. and Titorenko, V.I. (2010). Chemical genetic screen identifies lithocholic acid as an anti-aging compound that extends yeast chronological life span in a TOR-independent manner, by modulating housekeeping longevity assurance processes. *Aging* 2:393-414.

248. Goldberg, A.A., Kyryakov, P., Bourque, S.D. and Titorenko, V.I. (2010). Xenohormetic, hormetic and cytostatic selective forces driving longevity at the ecosystemic level. *Aging* 2:361-370.

249. Pringle, J.R., Adams, A.E., Drubin, D.G. and Haarer, B.K. (1991). Immunofluorescence methods for yeast. *Methods Enzymol*. 194:565-602.

250. Sherman, F. (2002). Getting started with yeast. *Methods Enzymol*. 350:3-41.

251. Doudican, N.A., Song, B., Shadel, G.S. and Doetsch, P.W. (2005). Oxidative DNA damage causes mitochondrial genomic instability in *Saccharomyces cerevisiae*. *Mol. Cell. Biol*. 25:5196-5204.

252. Chi, N.W. and Kolodner, R.D. (1994). Purification and characterization of MSH1, a yeast mitochondrial protein that binds to DNA mismatches. *J. Biol. Chem*. 269:29984-29992.

253. Cui, Z. and Mason, T.L. (1989). A single nucleotide substitution at the *rib2* locus of the yeast mitochondrial gene for 21S rRNA confers resistance to erythromycin and cold-sensitive ribosome assembly. *Curr. Genet*. 16:273-279.

254. Shevchenko, A., Jensen, O.N., Podtelejnikov, A.V., Sagliocco, F., Mortensen, P., Shevchenko, A., Boucherie, H. and Mann, M. (1996). Linking genome and proteome by mass spectrometry: large-scale identification of yeast proteins from two dimensional gels. *Proc. Natl. Acad. Sci. USA* 93:14440-14445.

255. Jiménez, C.R., Huang, L., Qiu, Y. and Burlingame, A.L. (1998). Searching sequence databases over the Internet: protein identification using MS-Fit. In: *Current Protocols in Protein Science*, Coligan, J.E., Dunn, B.M., Ploegh, H.L., Speicher, D.W., Wigfield, P.T. (Eds.). John Wiley & Sons, Inc., pp. 16.5.1-16.5.6.

256. Titorenko, V.I., Smith, J.J., Szilard, R.K. and Rachubinski, R.A. (1998). Pex20p of the yeast *Yarrowia lipolytica* is required for the oligomerization of thiolase in the cytosol and for its targeting to the peroxisome. *J. Cell Biol*. 142:403-420.

257. Kaufman, B.A., Newman, S.M., Perlman, P.S. and Butow, R.A. (2002). Crosslinking of proteins to mtDNA. *Methods Mol. Biol*. 197:377-389.

258. Szilard, R.K., Titorenko, V.I., Veenhuis, M. and Rachubinski, R.A. (1995). Pay32p of the yeast *Yarrowia lipolytica* is an intraperoxisomal component of the matrix protein translocation machinery. *J. Cell Biol*. 131:1453-1469.

259. Graham, J.M. (1999). Purification of a crude mitochondrial fraction by density-gradient centrifugation. In: *Current Protocols in Cell Biology*. Bonifacino, J.S., Dasso, M., Harford, J.B., Lippincott-Schwartz, J., Yamada, K.M. (Eds.). John Wiley & Sons, Inc., pp. 3.4.1-3.4.22.

260. Fabrizio, P., Liou, L.L., Moy, V.N., Diaspro, A., Valentine, J.S., Gralla, E.B. and Longo, V.D. (2003). SOD2 functions downstream of Sch9 to extend longevity in yeast. *Genetics* 163:35-46.

261. Lin, S.S., Manchester, J.K. and Gordon, J.I. (2001). Enhanced gluconeogenesis and increased energy storage as hallmarks of aging in *Saccharomyces cerevisiae*. *J. Biol. Chem*. 276: 36000-36007.

262. Masoro, E.J. (2006). Caloric restriction and aging: controversial issues. *J. Gerontol. Biol. Sci*. 61A:14-19.

263. Allen, C., Büttner, S., Aragon, A.D., Thomas, J.A., Meirelles, O., Jaetao, J.E., Benn, D., Ruby, S.W., Veenhuis, M., Madeo, F. and Werner-Washburne, M. (2006). Isolation of quiescent and nonquiescent cells from yeast stationary-phase cultures. *J. Cell Biol*. 174:89-100.

264. Aragon, A.D., Rodriguez, A.L., Meirelles, O., Roy, S., Davidson, G.S., Tapia, P.H., Allen, C., Joe, R., Benn, D. and Werner-Washburne, M. (2008). Characterization of

differentiated quiescent and nonquiescent cells in yeast stationary-phase cultures. *Mol. Biol. Cell* 19:1271-1280.

265. Minois, N., Lagona, F., Frajnt, M. and Vaupel, J.W. (2009). Plasticity of death rates in stationary phase in *Saccharomyces cerevisiae*. *Aging Cell* 8:36-44.

266. Fabrizio, P. and Longo, V.D. (2003). The chronological life span of *Saccharomyces cerevisiae*. *Aging Cell* 2:73-81.

267. Jenkins, G.W., Kemnitz, C.P. and Tortora, G.J. (2009). Anatomy and Physiology. From Science to Life, second ed. John Wiley & Sons, Inc., Hoboken, New Jersey.

268. Burtner, C.R., Murakami, C.J., Kennedy, B.K. and Kaeberlein, M. (2009). A molecular mechanism of chronological aging in yeast. *Cell Cycle* 8:1256-1270.

269. Bonawitz, N.D., Chatenay-Lapointe, M., Pan, Y. and Shadel, G.S. (2007). Reduced TOR signaling extends chronological life span via increased respiration and upregulation of mitochondrial gene expression. *Cell Metab*. 5:265-277.

270. Murakami, C.J., Burtner, C.R., Kennedy, B.K. and Kaeberlein, M. (2008). A method for high-throughput quantitative analysis of yeast chronological life span. *J. Gerontol. A Biol. Sci. Med. Sci*. 63:113-121.

271. Smith, D.L. Jr., McClure, J.M., Matecic, M. and Smith, J.S. (2007). Calorie restriction extends the chronological lifespan of *Saccharomyces cerevisiae* independently of the Sirtuins. *Aging Cell* 6:649-662.

272. François J. and Parrou, J.L. (2001). Reserve carbohydrates metabolism in the yeast *Saccharomyces cerevisiae*. *FEMS Microbiol. Rev*. 25:125-145.

273. Singer, M.A. and Lindquist, S. (1998a). Multiple effects of trehalose on protein folding *in vitro* and *in vivo*. *Mol. Cell* 1:639-648.

274. Benaroudj, N., Lee, D.H. and Goldberg, A.L. (2001). Trehalose accumulation during cellular stress protects cells and cellular proteins from damage by oxygen radicals. *J. Biol. Chem*. 276:24261-24267.

275. Singer, M.A. and Lindquist, S. (1998b). Thermotolerance in *Saccharomyces cerevisiae*: the Yin and Yang of trehalose. *Trends Biotechnol*. 16:460-468.

276. D'Autréaux, B. and Toledano, M.B. (2007). ROS as signalling molecules: mechanisms that generate specificity in ROS homeostasis. *Nat. Rev. Mol. Cell Biol*. 8:813-824.

277. Giorgio, M., Trinei, M., Migliaccio, E. and Pelicci, P.G. (2007). Hydrogen peroxide: a metabolic by-product or a common mediator of ageing signals? *Nat. Rev. Mol. Cell Biol*. 8:722-728.

278. Titorenko, V.I. and Terlecky, S.R. (2011). Peroxisome metabolism and cellular aging. *Traffic* 12:252-259.

279. Fabrizio, P., Pozza, F., Pletcher, S.D., Gendron, C.M. and Longo, V.D. (2001). Regulation of longevity and stress resistance by Sch9 in yeast. *Science* 292:288-290.

280. Chen, X.J. and Butow, R.A. (2005). The organization and inheritance of the mitochondrial genome. *Nat. Rev. Genet*. 6:815-825.

281. Chen, X.J., Wang, X., Kaufman, B.A. and Butow, R.A. (2005). Aconitase couples metabolic regulation to mitochondrial DNA maintenance. *Science* 307:714-717.

282. Butow, R.A. and Avadhani, N.G. (2004). Mitochondrial signaling: the retrograde response. *Mol Cell* 14:1-15.

283. Liu, Z. and Butow, R.A. (2006). Mitochondrial retrograde signaling. *Annu. Rev. Genet*. 40:159-185.

284. Okamoto, K. and Shaw, J.M. (2005). Mitochondrial morphology and dynamics in yeast and multicellular eukaryotes. *Annu. Rev. Genet*. 39:503-536.

285. Cerveny, K.L., Tamura, Y., Zhang, Z., Jensen, R.E. and Sesaki, H. (2007). Regulation of mitochondrial fusion and division. *Trends Cell Biol*. 17:563-569.

286. Hoppins, S., Lackner, L. and Nunnari, J. (2007). The machines that divide and fuse mitochondria. *Annu. Rev. Biochem*. 76:751-780.

287. Taylor, R.C., Cullen, S.P. and Martin, S.J. (2008). Apoptosis: controlled demolition at the cellular level. *Nat. Rev. Mol. Cell Biol*. 9:231-241.

288. Ludovico, P., Rodrigues, F., Almeida, A., Silva, M.T., Barrientos, A. and Côrte-Real, M. (2002). Cytochrome c release and mitochondria involvement in programmed cell death induced by acetic acid in *Saccharomyces cerevisiae*. *Mol. Biol. Cell* 13:2598-2606.

289. Severin, F.F. and Hyman, A.A. (2002). Pheromone induces programmed cell death in *S. cerevisiae*. *Curr. Biol*. 12:R233-R235.

290. Pozniakovsky, A.I., Knorre, D.A., Markova, O.V., Hyman, A.A., Skulachev, V.P. and Severin, F.F. (2005). Role of mitochondria in the pheromone- and amiodarone-induced programmed death of yeast. *J. Cell Biol*. 168:257-269.

291. Silva, R.D., Sotoca, R., Johansson, B., Ludovico, P., Sansonetty, F., Silva, M.T., Peinado, J.M. and Côrte-Real, M. (2005). Hyperosmotic stress induces metacaspase- and mitochondria-dependent apoptosis in *Saccharomyces cerevisiae*. *Mol. Microbiol*. 58:824-834.

292. Yang, H., Ren, Q. and Zhang, Z. (2008). Cleavage of Mcd1 by caspase-like protease Esp1 promotes apoptosis in budding yeast. *Mol. Biol. Cell* 19:2127-2134.

293. Roucou, X., Prescott, M., Devenish, R.J. and Nagley, P. (2000). A cytochrome c-GFP fusion is not released from mitochondria into the cytoplasm upon expression of Bax in yeast cells. *FEBS Lett*. 471:235-239.

294. Pereira, C., Camougrand, N., Manon, S., Sousa, M.J. and Côrte-Real, M. (2007). ADP/ATP carrier is required for mitochondrial outer membrane permeabilization and cytochrome c release in yeast apoptosis. *Mol. Microbiol*. 66:571-582.

295. Simola, M., Hänninen, A.L., Stranius, S.M. and Makarow, M. (2000). Trehalose is required for conformational repair of heat-denatured proteins in the yeast endoplasmic reticulum but not for maintenance of membrane traffic functions after severe heat stress. *Mol. Microbiol*. 37:42-53.

296. van der Klei, I.J., Yurimoto, H., Sakai, Y. and Veenhuis, M. (2006). The significance of peroxisomes in methanol metabolism in methylotrophic yeast. *Biochim. Biophys. Acta* 1763:1453-1462.

297. Hiltunen, J.K., Mursula, A.M., Rottensteiner, H., Wierenga, R.K., Kastaniotis, A.J. and Gurvitz, A. (2003). The biochemistry of peroxisomal β-oxidation in the yeast *Saccharomyces cerevisiae*. *FEMS Microbiol. Rev*. 27:35-64.

298. Veal, E.A., Day, A.M. and Morgan, B.A. (2007). Hydrogen peroxide sensing and signaling. *Mol. Cell* 26:1-14.

299. Schulz, T.J., Zarse, K., Voigt, A., Urban, N., Birringer, M. and Ristow, M. (2007). Glucose restriction extends *Caenorhabditis elegans* life span by inducing mitochondrial respiration and increasing oxidative stress. *Cell Metab*. 6:280-293.

300. Kaeberlein, M., Hu, D., Kerr, E.O., Tsuchiya, M., Westman, E.A., Dang, N., Fields, S. and Kennedy, B.K. (2005). Increased life span due to calorie restriction in respiratory-deficient yeast. *PLoS Genet*. 1:e69.

301. Wei, M., Fabrizio, P., Hu, J., Ge, H., Cheng, C., Li, L. and Longo, V.D. (2008). Life span extension by calorie restriction depends on Rim15 and transcription factors downstream of Ras/PKA, Tor, and Sch9. *PLoS Genet*. 4:e13.

302. Russell, S.J. and Kahn, C.R. (2007). Endocrine regulation of ageing. *Nat. Rev. Mol. Cell Biol*. 8:681-691.

303. Wang, M.C., O'Rourke, E.J. and Ruvkun, G. (2008). Fat metabolism links germline stem cells and longevity in *C. elegans*. *Science* 322:957-960.

304. Grönke, S., Mildner, A., Fellert, S., Tennagels, N., Petry, S., Müller, G., Jäckle, H. and Kühnlein, R.P. (2005). Brummer lipase is an evolutionary conserved fat storage regulator in *Drosophila*. *Cell Metab*. 1:323-330.

305. Blüher, M., Kahn, B.B. and Kahn, C.R. (2003). Extended longevity in mice lacking the insulin receptor in adipose tissue. *Science* 299:572-574.

306. Chiu, C.H., Lin, W.D., Huang, S.Y. and Lee, Y.H. (2004). Effect of a C/EBP gene replacement on mitochondrial biogenesis in fat cells. *Genes Dev*. 18:1970-1975.

307. Haemmerle, G., Lass, A., Zimmermann, R., Gorkiewicz, G., Meyer, C., Rozman, J., Heldmaier, G., Maier, R., Theussl, C., Eder, S., Kratky, D., Wagner, E.F. and Klingenspor, Ml. (2006). Defective lipolysis and altered energy metabolism in mice lacking adipose triglyceride lipase. *Science* 312:734-737.

308. Gerhart-Hines, Z., Rodgers, J.T., Bare, O., Lerin, C., Kim, S.H., Mostoslavsky, R., Alt, F.W., Wu, Z. and Puigserver, P. (2007). Metabolic control of muscle

mitochondrial function and fatty acid oxidation through SIRT1/PGC-1α. *EMBO J*. 26:1913-1923.

309. Léon, S., Goodman, J.M. and Subramani, S. (2006). Uniqueness of the mechanism of protein import into the peroxisome matrix: transport of folded, co-factor-bound and oligomeric proteins by shuttling receptors. *Biochim. Biophys. Acta* 1763:1552-1264.

310. Low, C.P., Liew, L.P., Pervaiz, S. and Yang, H. (2005). Apoptosis and lipoapoptosis in the fission yeast *Schizosaccharomyces pombe*. *FEMS Yeast Res*. 5:1199-1206.

311. Dirkx, R., Vanhorebeek, I., Martens, K., Schad, A., Grabenbauer, M., Fahimi, D., Declercq, P., Van Veldhoven, P.P. and Baes, M. (2005). Absence of peroxisomes in mouse hepatocytes causes mitochondrial and ER abnormalities. *Hepatology* 41:868-878.

312. Eisenberg, T., Büttner, S., Kroemer, G. and Madeo, F. (2007). The mitochondrial pathway in yeast apoptosis. *Apoptosis* 12:1011-1023.

313. Pereira, C., Silva, R.D., Saraiva, L., Johansson, B., Sousa, M.J. and Côrte-Real, M. (2008). Mitochondria-dependent apoptosis in yeast. *Biochim. Biophys. Acta* 1783:1286-1302.

314. Thomas, C., Pellicciari, R., Pruzanski, M., Auwerx, J. and Schoonjans, K. (2008). Targeting bile-acid signalling for metabolic diseases. *Nat. Rev. Drug Discov*. 7:678-693.

315. Stephan, J.S., Yeh, Y.Y., Ramachandran, V., Deminoff, S.J. and Herman, P.K. (2009). The Tor and PKA signaling pathways independently target the Atg1/Atg13

protein kinase complex to control autophagy. *Proc. Natl. Acad. Sci. USA* 106:17049-17054.

316. Kamada, Y., Yoshino, K., Kondo, C., Kawamata, T., Oshiro, N., Yonezawa, K. and Ohsumi, Y. (2010). Tor directly controls the Atg1 kinase complex to regulate autophagy. *Mol. Cell Biol*. 30:1049-1058.

317. Urban, J., Soulard, A., Huber, A., Lippman, S., Mukhopadhyay, D., Deloche, O., Wanke, V., Anrather, D., Ammerer, G., Riezman, H., Broach, J.R., De Virgilio, C. and Hall, M.N. (2007). Sch9 is a major target of TORC1 in *Saccharomyces cerevisiae*. *Mol. Cell* 26:663-674.

318. Yorimitsu, T., Zaman, S., Broach, J.R. and Klionsky, D.J. (2007). Protein kinase A and Sch9 cooperatively regulate induction of autophagy in *Saccharomyces cerevisiae*. *Mol. Biol. Cell* 18:4180-4189.

319. Lee, P., Cho, B.R., Joo, H.S. and Hahn, J.S. (2008). Yeast Yak1 kinase, a bridge between PKA and stress-responsive transcription factors, Hsf1 and Msn2/Msn4. *Mol. Microbiol*. 70:882-895.

320. Ptacek, J., Devgan, G., Michaud, G., Zhu, H., Zhu, X., Fasolo, J., Guo, H., Jona, G., Breitkreutz, A., Sopko, R., McCartney, R.R., Schmidt, M.C. and Rachidi, N. (2005). Global analysis of protein phosphorylation in yeast. *Nature* 438:679-684.

321. Fabrizio, P. and Longo, V.D. (2008). Chronological aging-induced apoptosis in yeast. *Biochim. Biophys. Acta* 1783:1280-1285.

322. Hamann, A., Brust, D. and Osiewacz, H.D. (2008). Apoptosis pathways in fungal growth, development and ageing. *Trends Microbiol*. 16:276-283.

323. Gems, D. and Partridge, L. (2008). Stress-response hormesis and aging: "that which does not kill us makes us stronger". *Cell Metab*. 7:200-203.

324. Pang, C.Y., Ma, Y.S. and Wei, Y.U. (2008). MtDNA mutations, functional decline and turnover of mitochondria in aging. *Front. Biosci*. 13:3661-3675.

325. Sinclair, D.A. and Oberdoerffer, P. (2009). The ageing epigenome: damaged beyond repair? *Ageing Res. Rev*. 8:189-198.

326. Lefebvre, P., Cariou, B., Lien, F., Kuipers, F. and Staels, B. (2009). Role of bile acids and bile acid receptors in metabolic regulation. *Physiol. Rev*. 89:147-191.

327. Hylemon, P.B., Zhou, H., Pandak, W.M., Ren, S., Gil, G. and Dent, P. (2009). Bile acids as regulatory molecules. *J. Lipid Res*. 50:1509-1520.

328. Vallim, T.Q. and Edwards, P.A. (2009). Bile acids have the gall to function as hormones. *Cell Metab*. 10:162-164.

329. Ramalho, R.M., Viana, R.J., Low, W.C., Steer, C.J. and Rodrigues, C.M. (2008). Bile acids and apoptosis modulation: an emerging role in experimental Alzheimer's disease. *Trends Mol. Med*. 14:54-62.

330. Amaral, J.D., Viana, R.J., Ramalho, R.M., Steer, C.J. and Rodrigues, C.M. (2009). Bile acids: regulation of apoptosis by ursodeoxycholic acid. *J. Lipid Res*. 50:1721-1734.

331. Amador-Noguez, D., Yagi, K., Venable, S. and Darlington, G. (2004). Gene expression profile of long-lived Ames dwarf mice and Little mice. *Aging Cell* 3:423-441.

332. Amador-Noguez, D., Dean, A., Huang, W., Setchell, K., Moore, D. and Darlington, G. (2007). Alterations in xenobiotic metabolism in the long-lived Little mice. *Aging Cell* 6:453-470.

333. Gems, D. (2007). Long-lived dwarf mice: are bile acids a longevity signal? *Aging Cell* 6:421-423.

334. Blagosklonny, M.V. and Hall, M.N. (2009). Growth and aging: a common molecular mechanism. *Aging* 1:357-362.

335. Hands, S.L., Proud, C.G. and Wyttenbach, A. (2009). mTOR's role in ageing: protein synthesis or autophagy? *Aging* 1:586-597.

336. Motola, D.L., Cummins, C.L., Rottiers, V., Sharma, K.K., Li, T., Li, Y., Suino-Powell, K., Xu, H.E., Auchus, R.J., Antebi, A. and Mangelsdorf, D.J. (2006). Identification of ligands for DAF-12 that govern dauer formation and reproduction in *C. elegans*. *Cell* 124:1209-1223.

337. Gerisch, B., Rottiers, V., Li, D., Motola, D.L., Cummins, C.L., Lehrach, H., Mangelsdorf, D.J. and Antebi, A. (2007). A bile acid-like steroid modulates *Caenorhabditis elegans* lifespan through nuclear receptor signaling. *Proc. Natl. Acad. Sci. USA* 104:5014-5019.

338. Dann, S.G. and Thomas, G. (2006). The amino acid sensitive TOR pathway from yeast to mammals. *FEBS Lett*. 580:2821-2829.

339. Heeren, G., Rinnerthaler, M., Laun, P., von Seyerl, P., Kössler, S., Klinger, H., Jarolim, S., Simon-Nobbe, B., Hager, M., Schüller, C., Carmona-Gutierrez, D., Breitenbach-Koller, L., Mück, C., Jansen-Dürr, P., Criollo, A., Kroemer, G., Madeo, F. and Breitenbach, M. (2009). The mitochondrial ribosomal protein of the

large subunit, Afo1p, determines cellular longevity through mitochondrial back-signaling via TOR1. *Aging* 1:622-636.

340. Ralser, M. and Lehrach, H. (2009). Building a new bridge between metabolism, free radicals and longevity. *Aging* 1:836-838.

341. Butow, R.A. and Avadhani, N.G. (2004). Mitochondrial signaling: the retrograde response. *Mol. Cell* 14:1-15.

342. Jazwinski, S.M. (2005). Rtg2 protein: at the nexus of yeast longevity and aging. *FEMS Yeast Res*. 5:1253-1259.

343. Howitz, K.T. and Sinclair, D.A. (2008). Xenohormesis: sensing the chemical cues of other species. *Cell* 133:387-391.

344. Lamming, D.W., Wood, J.G. and Sinclair, D.A. (2004). Small molecules that regulate lifespan: evidence for xenohormesis. *Mol. Microbiol*. 53:1003-1009.

345. Baur, J.A., Pearson, K.J., Price, N.L., Jamieson, H.A., Lerin, C., Kalra, A., Prabhu, V.V., Allard, J.S., Lopez-Lluch, G., Lewis, K., Pistell, P.J., Poosala, S., Becker, K.G., Boss, O., Gwinn, D., Wang, M., Ramaswamy, S., Fishbein, K.W., Spencer, R.G., Lakatta, E.G., Le Couteur, D., Shaw, R.J., Navas, P., Puigserver, P., Ingram, D.K., de Cabo, R. and Sinclair, D.A. (2006). Resveratrol improves health and survival of mice on a high-calorie diet. *Nature* 444:337-342.

346. Dasgupta, B. and Milbrandt, J. (2007). Resveratrol stimulates AMP kinase activity in neurons. *Proc. Natl. Acad. Sci. USA* 104:7217-7222.

347. Armour, S.M., Baur, J.A., Hsieh, S.N., Land-Bracha, A., Thomas, S.M. and Sinclair, D.A. (2009). Inhibition of mammalian S6 kinase by resveratrol suppresses autophagy. *Aging* 1:515-528.

348. Demidenko, Z.N. and Blagosklonny, M.V. (2009). At concentrations that inhibit mTOR, resveratrol suppresses cellular senescence. *Cell Cycle* 8:1901-1904.

349. Blagosklonny, M.V. (2009). Inhibition of S6K by resveratrol: in search of the purpose. *Aging* 1:511-514.

350. Morselli, E., Galluzzi, L., Kepp, O., Criollo, A., Maiuri, M.C., Tavernarakis, N., Madeo, F. and Kroemer, G. (2009). Autophagy mediates pharmacological lifespan extension by spermidine and resveratrol. *Aging* 1:961-970.

351. Shakibaei, M., Harikumar, K.B. and Aggarwal, B.B. (2009). Resveratrol addiction: to die or not to die. *Mol. Nutr. Food Res*. 53:115-128.

352. Morselli, E., Maiuri, M.C., Markaki, M., Megalou, E., Pasparaki, A., Palikaris, K., Galluzzi, L., Criollo, A., Malik, S.A., Madeo, F., Tavernarakis, N. and Kroemer, G. (2010). Caloric restriction and resveratrol prolong longevity via the sirtuin-1 dependent induction of autophagy. *Cell Death Disease* 1:e10.

353. Blagosklonny, M.V. (2006). Aging and immortality: quasi-programmed senescence and its pharmacologic inhibition. *Cell Cycle* 5:2087-2102.

354. Blagosklonny, M.V. (2010). Rapamycin and quasi-programmed aging: Four years later. *Cell Cycle* 9:1859-1862.

355. Vezina, C., Kudelski, A. and Sehgal, S.N. (1975). Rapamycin (AY-22,989), a new antifungal antibiotic. I. Taxonomy of the producing streptomycete and isolation of the active principle. *J. Antibiot*. 28:721-726.

356. Fabrizio, P., Battistella, L., Vardavas, R., Gattazzo, C., Liou, L.L., Diaspro, A., Dossen, J.W., Gralla, E.B. and Longo, V.D. (2004). Superoxide is a mediator of an altruistic aging program in *Saccharomyces cerevisiae*. *J. Cell Biol*. 166:1055-1067.

357. Herker, E., Jungwirth, H., Lehmann, K.A., Maldener, C., Frohlich, K.U., Wissing, S., Buttner, S., Fehr, M., Sigrist, S. and Madeo, F. (2004). Chronological aging leads to apoptosis in yeast. *J. Cell Biol*. 164:501-507.

358. Longo, V.D., Mitteldorf, J. and Skulachev, V.P. (2005). Programmed and altruistic ageing. *Nat. Rev. Genet*. 6:866-872.

359. Vachova, L. and Palkova, Z. (2005). Physiological regulation of yeast cell death in multicellular colonies is triggered by ammonia. *J. Cell Biol*. 169:711-717.

360. Büttner, S., Eisenberg, T., Herker, E., Carmona-Gutierrez, D., Kroemer, G. and Madeo, F. (2006). Why yeast cells can undergo apoptosis: death in times of peace, love, and war. *J. Cell Biol*. 175:521-525.

361. Severin, F.F., Meer, M.V., Smirnova, E.A., Knorre, D.A. and Skulachev, V.P. (2008). Natural causes of programmed death of yeast *Saccharomyces cerevisiae*. *Biochim. Biophys. Acta* 1783:1350-1353.

362. LeBlanc, A.C., Koutroumanis, M. and Goodyer, C.G. (1998). Protein kinase C activation increases release of secreted amyloid precursor protein without decreasing Aβ production in human primary neuron cultures. *J. Neurosci*. 18:2907-2913.

363. Bourque, S.D. and Titorenko, V.I. (2009). A quantitative assessment of the yeast lipidome using electrospray ionization mass spectrometry. *J. Vis. Exp*. 30:1-3, doi: 10.3791/1513.

364. Fleming, A., Noda, T., Yoshimori, T. and Rubinsztein, D.C. (2011). Chemical modulators of autophagy as biological probes and potential therapeutics. *Nat. Chem. Biol*. 7:9-17.

365. Corcelle, E.A., Puustinen, P. and Jäättelä, M. (2009). Apoptosis and autophagy: Targeting autophagy signalling in cancer cells – "trick or treats"? *FEBS J*. 276:6084-6096.

366. Høyer-Hansen, M. and Jäättelä, M. (2008). Autophagy: an emerging target for cancer therapy. *Autophagy* 4:574-580.

367. Turcotte, S. and Giaccia, A.J. (2010). Targeting cancer cells through autophagy for anticancer therapy. *Curr. Opin. Cell Biol*. 22:246-251.

368. Dalby, K.N., Tekedereli, I., Lopez-Berestein, G. and Ozpolat, B. (2010). Targeting the pro-death and pro-survival functions of autophagy as novel therapeutic strategies in cancer. *Autophagy* 6:322-329.

369. Levine, B. and Kroemer, G. (2008). Autophagy in the pathogenesis of disease. *Cell* 132:27-42.

370. He, C. and Klionsky, D.J. (2009). Regulation mechanisms and signaling pathways of autophagy. *Annu. Rev. Genet*. 43:67-93.

371. Moreau, K., Luo, S. and Rubinsztein, D.C. (2010). Cytoprotective roles for autophagy. *Curr. Opin. Cell Biol*. 22:206-211.

372. Eisenberg-Lerner, A. and Kimchi, A. (2009). The paradox of autophagy and its implication in cancer etiology and therapy. *Apoptosis* 14:376-391.

373. Liang, C., Jung, J.U. (2010). Autophagy genes as tumor suppressors. *Curr. Opin. Cell Biol*. 22:226-233.

374. Chen, N. and Karantza-Wadsworth, V. (2009). Role and regulation of autophagy in cancer. *Biochim. Biophys. Acta* 1793:1516-1523.

375. Brech, A., Ahlquist, T., Lothe, R.A. and Stenmark, H. (2009). Autophagy in tumour suppression and promotion. *Mol. Oncol*. 3:366-375.

376. Mizushima, N., Levine, B., Cuervo, A.M. and Klionsky, D.J. (2008). Autophagy fights disease through cellular self-digestion. *Nature* 451:1069-1075.

377. Kroemer, G., Mariño, G. and Levine, B. (2010). Autophagy and the integrated stress response. *Mol. Cell* 40:280-293.

378. Levine, B. (2007). Cell biology: autophagy and cancer. *Nature* 446:745-747.

379. Matoba, S., Kang, J.G., Patino, W.D., Wragg, A., Boehm, M., Gavrilova, O., Hurley, P.J., Bunz, F. and Hwang, P.M. (2006). p53 regulates mitochondrial respiration. *Science* 312:1650-1653.

380. Ma, W., Sung, H.J., Park, J.Y., Matoba, S. and Hwang, P.M. (2007). A pivotal role for p53: balancing aerobic respiration and glycolysis. *J. Bioenerg. Biomembr*. 39:243-246.

381. Schieke, S.M., Phillips, D., McCoy, J.P. Jr, Aponte, A.M., Shen, R.F., Balaban, R.S. and Finkel, T. (2006). The mammalian target of rapamycin (mTOR) pathway regulates mitochondrial oxygen consumption and oxidative capacity. *J. Biol. Chem*. 281:27643-27652.

382. Baysal, B.E., Ferrell, R.E., Willett-Brozick, J.E., Lawrence, E.C., Myssiorek, D., Bosch, A., van der Mey, A., Taschner, P.E., Rubinstein, W.S., Myers, E.N., Richard, C.W. 3rd, Cornelisse, C.J., Devilee, P. and Devlin, B. (2000). Mutations in SDHD, a mitochondrial complex II gene, in hereditary paraganglioma. *Science* 287:848-851.

383. King, A., Selak, M.A. and Gottlieb, E. (2006). Succinate dehydrogenase and fumarate hydratase: linking mitochondrial dysfunction and cancer. *Oncogene* 25:4675-4682.

384. Gottlieb, E. and Tomlinson, I.P. (2005). Mitochondrial tumour suppressors: a genetic and biochemical update. *Nat. Rev. Cancer* 5:857-866.

385. Bayley, J.P. and Devilee, P. (2010). Warburg tumours and the mechanisms of mitochondrial tumour suppressor genes. Barking up the right tree? *Curr. Opin. Genet. Dev*. 20:324-329.

386. Kaelin, W.G. Jr. (2009). SDH5 mutations and familial paraganglioma: somewhere Warburg is smiling. *Cancer Cell* 16:180-182.

387. Hao, H.X., Khalimonchuk, O., Schraders, M., Dephoure, N., Bayley, J.P., Kunst, H., Devilee, P., Cremers, C.W, Schiffman, J.D., Bentz, B.G., Gygi, S.P., Winge, D.R., Kremer, H. and Rutter, J. (2009). SDH5, a gene required for flavination of succinate dehydrogenase, is mutated in paraganglioma. *Science* 325:1139-1142.

388. Goffrini, P., Ercolino, T., Panizza, E., Giachè, V., Cavone, L., Chiarugi, A., Dima, V., Ferrero, I. and Mannelli, M. (2009). Functional study in a yeast model of a novel succinate dehydrogenase subunit B gene germline missense mutation

(C191Y) diagnosed in a patient affected by a glomus tumor. *Hum. Mol. Genet*. 18:1860-1868.

389. Huber, H.J., Dussmann, H., Kilbride, S.M., Rehm, M. and Prehn, J.H. (2011). Glucose metabolism determines resistance of cancer cells to bioenergetic crisis after cytochrome-c release. *Mol. Syst. Biol*. 7:470.

390. Pereira, C., Silva, R.D., Saraiva, L., Johansson, B., Sousa, M.J. and Côrte-Real, M. (2008). Mitochondria-dependent apoptosis in yeast. *Biochim. Biophys. Acta* 1783:1286-1302.

391. Cheng, W.C., Leach, K.M. and Hardwick, J.M. (2008). Mitochondrial death pathways in yeast and mammalian cells. *Biochim. Biophys. Acta* 1783:1272-1279.

392. Carmona-Gutierrez, D., Eisenberg, T., Büttner, S., Meisinger, C., Kroemer, G. and Madeo, F. (2010). Apoptosis in yeast: triggers, pathways, subroutines. *Cell Death Differ*. 17:763-773.

393. Ott, M., Gogvadze, V., Orrenius, S. and Zhivotovsky, B. (2007). Mitochondria, oxidative stress and cell death. *Apoptosis* 12:913-922.

394. Orrenius, S. (2007). Reactive oxygen species in mitochondria-mediated cell death. *Drug Metab. Rev*. 39:443-455.

395. Orrenius, S., Gogvadze, V. and Zhivotovsky, B. (2007). Mitochondrial oxidative stress: implications for cell death. *Annu. Rev. Pharmacol. Toxicol*. 47:143-183.

396. Portt, L., Norman, G., Clapp, C., Greenwood, M. and Greenwood, M.T. (2011). Anti-apoptosis and cell survival: a review. *Biochim. Biophys. Acta* 2011 1813:238-259.

397. Campling, B.G. et al. (1988). Use of the MTT assay for rapid determination of chemosensitivity of human leukemic blast cells. *Leuk. Res.* 12:823-831.

398. Jover, R. et al. (1994). Acute cytotoxicity of ten chemicals in human and rat cultured hepatocytes and in cell lines: Correlation between in vitro data and human lethal concentrations. *Toxic. In Vitro* 8:47-54.

399. Mosmann, T. (1983). Rapid colorimetric assay for cellular growth and survival: Application to proliferation and cytotoxicity assays. *J. Immunol. Methods* 65:55-63.

400. Tada, H. et al. (1986). An improved colorimetric assay for interleukin 2. *J. Immunol. Methods* 93:157-165.

401. Kerr, J. F. R., Wyllie, A. H. and Currie, A. R. (1972). Apoptosis: a basic biological phenomenon with wide-ranging implications in tissue kinetics. *Br. J. Cancer* 26:239-275.

402. Wyllie, A. H., Kerr, J. F. R. and Currie, A. R. (1980). Cell death: the significance of apoptosis. *Int. Rev. Cytol*. 68:251-305.

403. Taylor, R.C., Cullen, S.P. and Martin, S.J. (2008). Apoptosis: controlled demolition at the cellular level. *Nat. Rev. Mol. Cell Biol*. 9:231-241.

404. Tait, S.W. and Green, D.R. (2010). Mitochondria and cell death: outer membrane permeabilization and beyond. *Nat. Rev. Mol. Cell Biol*. 11:621-632.

405. Parsons, M.J. and Green, D.R. (2010). Mitochondria in cell death. *Essays Biochem*. 47:99-114.

406. Jourdain, A. and Martinou, J.C. (2009). Mitochondrial outer-membrane permeabilization and remodelling in apoptosis. *Int. J. Biochem. Cell Biol*. 41:1884-1889.

407. James, D., Parone, P.A., Terradillos, O., Lucken-Ardjomande, S., Montessuit, S. and Martinou, J.C. (2007). Mechanisms of mitochondrial outer membrane permeabilization. *Novartis Found. Symp*. 287:170-176; discussion 176-182.

408. Ow, Y.P., Green, D.R., Hao, Z. and Mak, T.W. (2008). Cytochrome c: functions beyond respiration. *Nat. Rev. Mol. Cell Biol*. 9:532-542.

409. Jiang, X. and Wang, X. (2004). Cytochrome C-mediated apoptosis. *Annu. Rev. Biochem*. 73:87-106.

410. Suen, D.F., Norris, K.L. and Youle, R.J. (2008). Mitochondrial dynamics and apoptosis. *Genes Dev*. 22:1577-1590.

411. Karbowski, M. (2010). Mitochondria on guard: role of mitochondrial fusion and fission in the regulation of apoptosis. *Adv. Exp. Med. Biol*. 687:131-142.

412. Lartigue, L., Kushnareva, Y., Seong, Y., Lin, H., Faustin, B. and Newmeyer, D.D. (2009). Caspase-independent mitochondrial cell death results from loss of respiration, not cytotoxic protein release. *Mol. Biol. Cell* 20:4871-4884.

413. Kushnareva, Y. and Newmeyer, D.D. (2010). Bioenergetics and cell death. *Ann. N.Y. Acad. Sci*. 1201:50-57.

414. Mootha, V.K., Wei, M.C., Buttle, K.F., Scorrano, L., Panoutsakopoulou, V., Mannella, C.A. and Korsmeyer, S.J. (2001). A reversible component of mitochondrial respiratory dysfunction in apoptosis can be rescued by exogenous cytochrome c. *EMBO J*. 20:661-671.

415. Waterhouse, N.J., Goldstein, J.C., von Ahsen, O., Schuler, M., Newmeyer, D.D. and Green, D.R. (2001). Cytochrome c maintains mitochondrial transmembrane

potential and ATP generation after outer mitochondrial membrane permeabilization during the apoptotic process. *J. Cell Biol*.153:319-328.

416. Slee, E.A., Adrain, C. and Martin, S.J. (1999). Serial killers: ordering caspase activation events in apoptosis. *Cell Death Differ*. 6:1067-1074.

417. Slee, E.A., Harte, M.T., Kluck, R.M., Wolf, B.B., Casiano, C.A., Newmeyer, D.D., Wang, H.G., Reed, J.C., Nicholson, D.W., Alnemri, E.S., Green, D.R. and Martin, S.J. (1999). Ordering the cytochrome c-initiated caspase cascade: hierarchical activation of caspases-2, -3, -6, -7, -8, and -10 in a caspase-9-dependent manner. *J. Cell Biol*. 144:281-292.

418. Luo, X., Budihardjo, I., Zou, H., Slaughter, C. and Wang, X. (1998). Bid, a Bcl2 interacting protein, mediates cytochrome c release from mitochondria in response to activation of cell surface death receptors. *Cell* 94:481-490.

419. Li, H., Zhu, H., Xu, C.J. and Yuan, J. (1998). Cleavage of BID by caspase 8 mediates the mitochondrial damage in the Fas pathway of apoptosis. *Cell* 944:491-501.

420. Yi, C.H. and Yuan, J. (2009). The Jekyll and Hyde functions of caspases. *Dev. Cell* 16:21-34.

421. Kersse, K., Vanden Berghe, T., Lamkanfi, M. and Vandenabeele, P. (2007). A phylogenetic and functional overview of inflammatory caspases and caspase-1-related CARD-only proteins. *Biochem. Soc. Trans*. 35:1508-1511.

422. Dinarello, C.A. (2009). Immunological and inflammatory functions of the interleukin-1 family. *Annu. Rev. Immunol*. 27:519-550.

423. Keller, M., Rüegg, A., Werner, S. and Beer, H.D. (2009). Active caspase-1 is a regulator of unconventional protein secretion. *Cell* 132:818-831.

424. Grivennikov, S.I. and Karin, M. (2011). Inflammatory cytokines in cancer: tumour necrosis factor and interleukin 6 take the stage. *Ann. Rheum. Dis*. 70, Suppl. 1:i104-108.

425. Donath, M.Y. and Shoelson, S.E. (2011). Type 2 diabetes as an inflammatory disease. *Nat. Rev. Immunol*. 11:98-107.

426. Feagins, L.A. (2010). Role of transforming growth factor-β in inflammatory bowel disease and colitis-associated colon cancer. *Inflamm. Bowel Dis*. 16:1963-1968.

427. Li, X., Jiang, S. and Tapping, R.I. (2010). Toll-like receptor signaling in cell proliferation and survival. *Cytokine* 49:1-9.

428. Guo, H., Pétrin, D., Zhang, Y., Bergeron, C., Goodyer, C.G. and LeBlanc, A.C. (2006). Caspase-1 activation of caspase-6 in human apoptotic neurons. *Cell Death Differ*. 13:285-292.

## 8 List of my publications and manuscripts in preparation (published papers are attached below)

**Published papers**

1. Guo, T., Gregg, C., Boukh-Viner, T., Kyryakov, P., **Goldberg, A.**, Bourque, S., Banu, F., Haile, S., Milijevic, S., Hung Yeung San, K., Solomon, J., Wong, V. and Titorenko, V.I. A signal from inside the peroxisome initiates its division by promoting the remodeling of the peroxisomal membrane. *J. Cell Biol.* (2007) 177:289-303.
   **This article was an Editors' Choice article in *Science* (2007) 316:801.**

2. **Goldberg, A.A.**, Bourque, S.D., Kyryakov, P., Boukh-Viner, T., Gregg, C., Beach, A., Burstein, M.T., Machkalyan, G., Richard, V., Rampersad, S. and Titorenko, V.I. A novel function of lipid droplets in regulating longevity. *Biochem. Soc. Trans.* (2009) 37:1050-1055.

3. **Goldberg, A.A.**, Bourque, S.D., Kyryakov, P., Gregg, C., Boukh-Viner, T., Beach, A., Burstein, M.T., Machkalyan, G., Richard, V., Rampersad, S., Cyr, D., Milijevic, S. and Titorenko, V.I. Effect of calorie restriction on the metabolic history of chronologically aging yeast. *Exp. Gerontol*. (2009) **44**:555-571.

4. **Goldberg, A.A.**, Richard, V.R., Kyryakov, P., Bourque, S.D., Beach, A., Burstein, M.T., Glebov, A., Koupaki, O., Boukh-Viner, T., Gregg, C., Juneau, M., English, A.M., Thomas, D.Y. and Titorenko, V.I. Chemical genetic screen identifies lithocholic acid as an anti-aging compound that extends yeast chronological life span in a TOR-independent manner, by modulating housekeeping longevity assurance processes. *Aging* (2010) 2:393-414.
   **This article was highlighted in the news media, including Radio-Canada** (http: //www.radio-canada.ca/nouvelles/science/2010/09/16/002-longevite-bile.shtml); **TFI News France** (http://lci.tf1.fr/science/sante/2010-09/la-bile-un-espoir-contre-le-vieillissement-6071272.html); **The McGill Daily** (http://hotink.

theorem.ca/system/ mcgilldaily/issues/000/004/689/ vol100iss7_screen_quality.pdf?1285709690); **Science Daily** (http://www.sciencedaily.com/releases/2010/09/100915100935.htm); **EurekAlert!** (http://www.eurekalert.org/pub_releases/2010-09/cu-foy091510.php); **Now Concordia** (http://now.concordia.ca/what-we-do/research/20100921/fountain-of-youth-in-bile-longevity-molecule-identified.php); **Media Relations Concordia** (http://mediarelations. concordia.ca/pressreleases/archives/2010/09/fountain_of_youth_in_bile_long.php?&print=1); **Bio Ethics Hawaii** (http://www.bioethicshawaii.org/s-science/the-key-to-human-longevity-in-yeast-could-be/); **Fight Aging!** (http://www.fightaging.org/archives/2010/09/bile-acids-and-yeast-longevity.php); **Xenophilia** (https://xenophilius.wordpress.com/2010/09/16/fountain-of-youth-in-bile-longevity-molecule-identified/); **Thaindian** (http:// www.thaindian.com/newsportal/health/bile-may-harbour-human-fountain-of-youth_ 100429315.html); **DNA India** (http://www.dnaindia.com/scitech/report_bile-may-harbour-human-fountain-of-youth_1438869); **India Vision** (http://www.indiavision.com/news/article/scitech/103189/); **REVLET** (http://www.revleft.com/vb/fountain-youth-bilei-t141779/index.html?s=1294a5663f51df1055ad3ff2b53db082&p=1865643); **Stop Aging Solutions** (http://stopagingsolutions.com/?p=704); **Longevity Medicine** (http://www.longevitymedicine.tv/longevity-as-housekeeping-and-a-role-for-bile-acids/); **News Guide US** (http://newsguide.us/education/science/Fountain-of-youth-in-bile-Longevity-molecule-identified/?date=2010-03-26); **Dallas News** (http://topics. dallasnews.com/quote/06AP1cA3HLa9j?q=Diabetes); **e! Science News** (http:// esciencenews.com/articles/2010/09/15/fountain.youth.bile.longevity.molecule.identified);**TENDENCIAS CIENTIFICAS** (http://www.tendencias21.net/La-clave-de-la-longevidad-humana-podria-estar-en-la-levadura_a4848.html?utm_source= feedburner& utm_medium=feed); **Canadian Health Reference Guide** (http://www.chrgonline.com/ news_detail. asp?ID=140067); **Techno-Science** (http://www.chrgonline.com/news_ detail.asp?ID=140067); **METRO** (http://www.journalmetro.com/plus/article/672613--la-bile-fontaine-de-jouvence) **and others.**

5. **Goldberg, A.A.**, Kyryakov, P., Bourque, S.D. and Titorenko, V.I. Xenohormetic, hormetic and cytostatic selective forces driving longevity at the ecosystemic level. *Aging* (2010) 2:361-370.

**Published book chapters**

1. **Goldberg, A.A.** and Titorenko, V.I. Peroxisomes and dimorphic transition in the yeast *Yarrowia lipolytica*. *In*: Emergent Functions of the Peroxisome. *Eds*. Titorenko, V.I. and Terlecky, S.R. Research Signpost, Kerala, India, pp. 87-96 (2009).

**Manuscripts in preparation**

1. Kyryakov, P., Goldberg, A.A., Beach, A., Burstein, M.T., Richard, V.R. and Titorenko, V.I. Caloric restriction extends longevity of chronologically aging yeast in part by remodeling trehalose and glycogen metabolism. *Aging*.

2. Kyryakov, P., Goldberg, A.A., Beach, A., Burstein, M.T., Richard, V.R. and Titorenko, V.I. Identification of novel gerontogenes reveals a complex signaling network regulating longevity in the chronologically aging yeast *Saccharomyces cerevisiae*. *PLoS Genetics*.

3. Kyryakov, P., Goldberg, A.A., Koupaki, o., Beach, A., Burstein, M.T., Richard, V.R. and Titorenko, V.I. Laboratory evolution of longevity regulation mechanisms by a lasting exposure of the yeast *Saccharomyces cerevisiae* to a bile acid. *Current Biology*.

4. Goldberg, A.A., Beach, A., Davies, G.F., Harkness, T.A.A., LeBlanc, A. and Titorenko, V.I. Lithocholic acid exhibits a potent and selective anti-tumor effect in human neuroblastoma cells by activating both intrinsic and extrinsic apoptotic death pathways and sensitizing these cells to hydrogen peroxide-induced death. *Oncotarget*.

5. Bourque, S.D., Richard, V.R., Beach, A., Burstein, M.T., Goldberg, A.A., Kyryakov, P. and Titorenko, V.I. A mechanism linking lipid metabolism and longevity in chronologically aging yeast. *Cell Metab*.

6. Bourque, S.D., Richard, V.R., Beach, A., Burstein, M.T., Goldberg, A.A., Kyryakov, P. and Titorenko, V.I. Lithocholic acid extends yeast longevity in part by targeting the longevity-defining aspects of lipid metabolism confined to the endoplasmic reticulum, lipid bodies and peroxisomes. *Dev. Cell*.